ADVANCES IN APPLIED MECHANICS

VOLUME III

ADVANCES IN APPLIED MECHANICS

EDITED BY

RICHARD VON MISES
Harvard University
Cambridge, Massachusetts

THEODORE VON KÁRMÁN
Columbia University
New York, New York

VOLUME III

1953

ACADEMIC PRESS INC., PUBLISHERS
NEW YORK, N.Y.

125 EAST 23RD STREET
NEW YORK 10, N. Y.

PRINTED IN THE UNITED STATES OF AMERICA

Contributors to Volume III

ALBERT I. BELLIN, *Harvard University, Cambridge, Massachusetts**

G. F. CARRIER, *Brown University, Providence, Rhode Island*†

F. N. FRENKIEL, *Applied Physics Laboratory, The Johns Hopkins University, Silver Spring, Maryland*

HILDA GEIRINGER, *Wheaton College, Norton, Massachusetts*

GOTTFRIED GUDERLEY, *Wright Air Development Center, Dayton, Ohio*

H. F. LUDLOFF, *Department of Aeronautical Engineering, New York University, New York, N. Y.*

L. ROSENHEAD, *University of Liverpool, Liverpool, England*

OTHAR ZALDASTANI, *Consulting Engineer, Boston, Massachusetts*

* Now with Office of Naval Research, Washington, D. C.
† Now at Harvard University, Cambridge, Massachusetts.

PREFACE

The publication of this volume was unduly delayed by the fact that the author of a 150-page article withdrew his paper when it was already set in type and when almost the whole volume was ready for print. The editors feel particularly indebted to the authors who had to accept the postponement and to those who on comparatively short notice furnished new contributions.

As in the previous volumes, the following articles reflect the various subjects of present-day research in applied mechanics.

During the last year while both editors were staying in Europe, Professor Gustav Kuerti, Case Institute of Technology, Cleveland, Ohio, has taken over most of their duties. His most valuable and devoted help is gratefully acknowledged.

TH. v. KÁRMÁN
R. v. MISES

CONTENTS

Boundary Layer Problems in Applied Mechanics

By G. F. CARRIER*

Brown University, Providence, Rhode Island

I. Introduction

In recent years, the term "boundary layer" has become most closely associated with the phenomena arising when a fluid flows past an obstacle at high Reynolds number. Despite this particular association, there is a large and interesting variety of physical problems whose analysis is most appropriately carried out by invoking the ideas that are associated with boundary layer problems.

In this article, we shall present a simple characterization of the boundary layer problem and shall give in varying detail the analysis of several isolated problems which fall into this category.

Since all our problems will be formulated as boundary value problems of certain differential equations, the characterization we present will be defined in terms of such boundary value problems. Our arguments will differ in form from those usually found in the literature associated with this field but, at the expense of preciseness, they give a clear account of the ideas which are involved.

It is easiest to associate these arguments with a specific problem, and we shall introduce them while treating one of the simplest boundary value problems of this type rather than attempt to give a general characterization immediately.

II. The Ocean Current Problem

One of the more straightforward applications of boundary layer theory arises in the study of ocean currents. It is possible to construct a boundary value problem which contains the essential features associated with

* Present address: Harvard University, Cambridge, Mass.

the long-time average motion of the fluid in ocean basins. Since, in this paper, we wish to introduce the boundary layer ideas as early as possible, we shall defer the derivation of this boundary value problem to the Appendix of this article. The differential equation which arises is:

$$\epsilon\Delta\Delta\psi - \psi_x = \sin y. \tag{2.1}$$

The boundary conditions are associated with the geometry of the problem and, for the Pacific Ocean, take the form

$$\begin{aligned} \psi &= \psi_x = 0 && \text{on } AB \text{ and } BC, \\ \psi &= \psi_{yy} = 0 && \text{on } CA, \end{aligned} \tag{2.2}$$

where the lines AB, BC, CA, are defined in Fig. 1. For this particular problem, the value of ϵ is 0.035. We note immediately that the problem

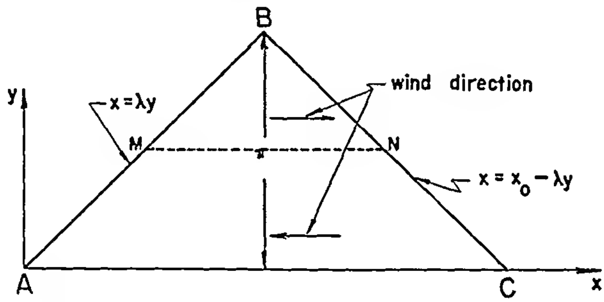

FIG. 1. Geometry of the ocean current problem. AB and BC are land boundaries, AC is a locus on which, observationally, $\partial u_x/\partial y = 0$.

is characterized by three essential features: (1) *the coefficient of the most highly differentiated terms is small compared to unity;* (2) *the other important terms have coefficients of order unity;* (3) *the size of the domain is characterized by lengths of order unity in the coordinate system chosen.* In the subsequent problems we shall indicate the "dimensional analysis" which as implied above is intrinsically part of the boundary layer analysis. However, that dimensional analysis has already been incorporated[1] in this problem.

We now find a solution of the problem posed by Eqs. (2.1) and (2.2) in the following manner. We first note that, for $\epsilon \ll 1$, a good approximation to *a* solution of Eq. (2.1) is available when the term with coefficient ϵ is ignored. Such a function is

$$\psi^{(0)} = -[x + a(y)] \sin y. \tag{2.3}$$

The difficulty, of course, is that we have only $a(y)$ at our disposal in order to satisfy the boundary conditions (2.2). The function $\psi^{(0)}$ obviously

[1] It is, of course, included in the Appendix.

cannot satisfy these conditions, and hence it is *not* a good approximation to a solution of the problem. Now consider any function ψ which has the property that the maximum values of ψ, ψ_x, ψ_{xxxx}, ψ_{yyyy}, etc., are all of the same order of magnitude.[2] Such a function can be a solution of (2.1) only if it is essentially of the form $\psi^{(0)} + O(\epsilon)$. Since we have established that a function of this form cannot be the required ψ, we must conclude that ψ will be "steep" somewhere in the domain. By this we mean that at least one of the higher derivatives of ψ is large compared to ψ. In particular, one of the contributions of $\Delta\Delta\psi$ must be of order ϵ^{-1} compared to ψ_x if ψ is to be different from $\psi^{(0)} + O(\epsilon)$. At this point we *hope* that the steep portion of the function ψ is confined to a region very close to the boundaries. If this turns out to be true, then the solution in the interior of the domain is represented very well by ψ^0, but we still need to find the behavior of ψ near the edge. The functional representation of the solution in this edge region is frequently called the boundary layer. We must note that one cannot always be sure that the steep part of the function is confined in this manner, but the investigation of any particular problem along the forthcoming lines will lead to contradictions if such is not the case.

In this particular problem it is convenient to represent the boundary layer solution as the sum of three functions, one for each portion of the boundary. Thus, we write

$$\psi = \psi^{(0)} + \varphi^{(1)} + \varphi^{(2)} + \varphi^{(3)}.$$

In accord with the foregoing wishful thinking, we anticipate that $\varphi^{(1)}$ will be steep near AB and will "fade out" very rapidly with increasing distance from AB. Similarly $\varphi^{(2)}$ is large near BC and small elsewhere; $\varphi^{(3)}$ is the boundary layer on CA. In order to determine $\varphi^{(1)}$, we shall find it convenient to adopt a new coordinate system. This system should be chosen so that one coordinate essentially measures distances from the boundary whereas the other measures distances along the boundary. The scale, i.e., units, to which these distances are measured should be such that $\varphi^{(1)}$ is a "smooth" function of its arguments. Hence, the coordinate stretching must depend on ϵ. In this case, the two coordinates can respectively be chosen as

$$\xi = (x - \lambda y)\epsilon^n, \quad \eta = y.$$

The number n must be determined by the criterion that $\epsilon\Delta\Delta\psi$ contribute in an amount which is of the same order in ϵ as the contribution of ψ_x. The lack of "stretching" of the y coordinate (or, effectively, of the dis-

[2] We shall henceforth refer to such a function as being "smooth."

tance along the boundary) comes about because of the boundary conditions on $\varphi^{(1)}$. These conditions are[3]

$$\psi^{(0)}(\lambda y,y) + \varphi^{(1)}(0,\eta) = \psi_x^{(0)}(\lambda y,y) + \epsilon^n \varphi_\xi^{(1)}(0,\eta) = 0.$$

The smoothness of $\psi^{(0)}$ implies the corresponding smoothness in η of φ. We now introduce these coordinates into (2.1), choose $n = -\frac{1}{3}$ in accord with our foregoing remarks, and obtain, simply,

$$(1 + \lambda^2)^2 \varphi_{\xi\xi\xi\xi}^{(1)} - \varphi_\xi^{(1)} + 0(\epsilon^{1/3}) = 0. \tag{2.4}$$

We may now decide to represent $\varphi^{(1)}$ formally as an asymptotic series in $\epsilon^{1/3}$ or equivalently, from a practical point of view, to drop the $0(\epsilon^{1/3})$ term from Eq. (2.4). When this is done, the first order solutions of (2.4) are

$$b(\eta), \quad C_m(\eta) \exp (S\xi e^{2m\pi i/3}),$$

where $S = (1 + \lambda^2)^{-2/3}$, m takes on the values 1, 2, 3, and $b(\eta)$, $C_m(\eta)$ must be determined by the boundary conditions. However, in view of our requirement that $\varphi^{(1)}$ decay rapidly as we leave the boundary, only the solution

$$\varphi^{(1)} = C_1(\eta) \exp (\xi S e^{2\pi i/3}) + C_2(\eta) \exp (\xi S e^{4\pi i/3}) \tag{2.5}$$

is acceptable.

We may now find the boundary layer solution associated with the boundary BC. Defining $\xi' = (x + x_0 - \lambda y)\epsilon^n$, $\eta' = y$, we again obtain Eq. (2.4) but we find this time that near $\xi' = 0$ (that is near BC), $\varphi^{(2)}$ behaves like

$$\varphi^{(2)} = C_3(\eta') \exp (S\xi'). \tag{2.6}$$

The parameters $C_j(y)$ and $a(y)$ now may be chosen so that the sum of the functions defined in Eqs. (2.3), (2.5), (2.6) can satisfy the requirements on AB and BC. We omit the algebra but note that these quantities (a,C_j) are such that, for example, at $y = \pi/2$, the function $\psi(x,\pi/2)$ is depicted in Fig. 2. The stream velocity profile at $y = \pi/2$ is also given there. Further comments concerning the physical problem can be found in (1), but here we shall only continue with remarks pertinent to the boundary layer analysis.

It is perhaps unfortunate that, in this first exemplary problem, we must dispose of a remaining difficulty in a manner which is physically satisfactory but seems a bit like cheating. However, at the boundary $y = 0$, we still must satisfy the conditions of Eqs. (2.2). Our model,

[3] The peculiar combination of arguments of ψ and φ arise merely because ψ is defined as a function of (x,y) and φ is defined as a function of (ξ,η).

i.e., Eq. (2.1), does not contain provision for this (the foregoing analysis would not give a decaying boundary layer solution for this edge), and hence we must either convince ourselves that this is of no consequence, or else we must refine our model. The former choice is easily taken and we merely note that if our function sin y, which is associated with the yearly average wind intensity, were replaced by a carefully chosen wind intensity representation which differs very little from sin y, the boundary condition would be satisfied by $\psi^{(0)}$ and no boundary layer (or other correction) would be required. That this is physically acceptable is clear. Certainly the wind intensity observations are not so accurate but that many alternative and similar functional forms could be adopted. Recalling then that our technique, as presented here and as frequently used, is

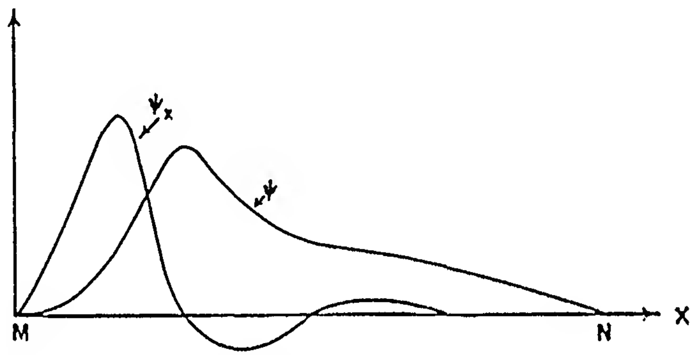

FIG. 2. Stream function and vertical velocity component at section $M - N$ of Fig. 1.

a crude one for getting physical information, we need not worry about this reconstruction of the problem to suit our needs. We must also note that further corrections would be needed in the corners where the boundary layer solution associated with one edge affects the values on the intersecting edge. However, it is again clear that since our ocean boundaries are not defined this accurately, a detailed analysis of the corner corrections is not justified.

Let us now summarize the situation as exemplified by this problem. A boundary value problem is considered which is characterized by a small coefficient on the most highly differentiated term of the differential equation. A function, $\psi^0 + \varphi$, is found such that ψ^0 is a smooth "solution" of the Eq. (2.1) and hence a solution of that equation with the ϵ term ignored. φ is a function which makes $\psi^{(0)} + \varphi$ a solution of an approximation to Eq. (2.1) and which contributes nontrivially only near the boundaries. Finally, one can readily check that the amount by which Eq. (2.1) fails to be satisfied by $\psi^{(0)} + \varphi$ is small compared to the contribution of say φ_x only. This last remark *proves nothing* about the

accuracy with which the true solution of the problem is approximated by $\psi^0 + \varphi$ but is *usually a reliable indication* of that accuracy. In (1) and (2), the observational verification of the analysis of this problem is noted.

III. A Heat Transfer Problem

In many physical processes (e.g., the manufacture of linoleum), a material having essentially the properties of a viscous fluid is "calendered" as shown in Fig. 3. When the quantity t_0/R as defined in Fig. 3

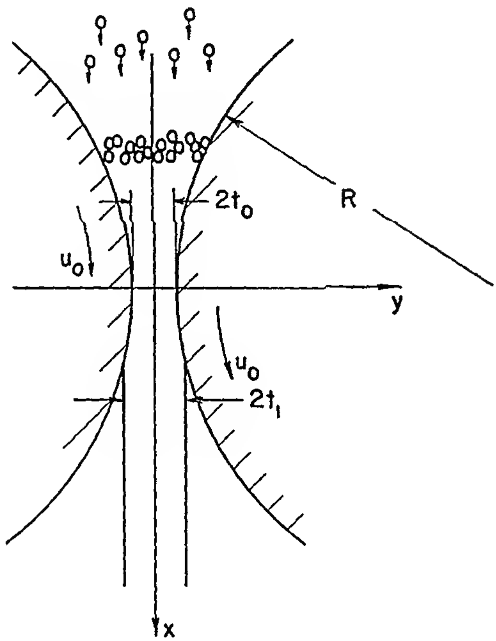

Fig. 3. The geometry of the calendering problem. The material enters as a collection of small pellets but soon is compressed into a continuum which behaves like a viscous fluid and emerges in sheet form.

is small compared to unity, the mechanical nature of the flow can be deduced from an analysis which is essentially classical lubrication theory. Thus the velocity and stress distributions are known throughout the flow field. However, an important industrial problem can arise which again invokes the boundary layer ideas. The difficulty which did arise is this. The peripheral speed of the rolls was increased above its nominal value in order to increase the production rate and the additional dissipation of heat caused a smearing of the sheet surface. When the rolls were cooled, this difficulty was partially alleviated. However, when the speed was excessive, blisters formed a short distance below the sheet surface, and the blister size was an increasing function of roll speed. Before a modification of the cooling facilities was attempted, it was

appropriate to attempt a detailed explanation of the blister formation and use it to evaluate the alleviation technique.

The problem we adopt here then[4] is that of finding the temperature distribution associated with an incompressible viscous fluid undergoing the motion indicated in Fig. 3. To the order of accuracy available and practical for such problems the particle velocity of the fluid is given by

$$u = u_0[1 + 3(1 - z^2)(t_1 - t)/2t], \tag{3.1}$$

the pressure by

$$p(\xi) = -3\mu u_0 L \int_{\xi}^{\xi_1} [(t_1 - t)/t^3] d\xi. \tag{3.2}$$

Here, μ is the fixed viscosity, $L = (2t_0 R)^{1/2}$, $z = y/t$, $\xi = x/L$, and the velocity, which is directed along the streamlines y/t = constant, has magnitude u.

The equation governing the conservation of energy is

$$k\Delta T - \rho C\bar{V} \cdot \operatorname{grad} T + \varphi = 0, \tag{3.3}$$

where $\bar{V}$ is the particle velocity, C the specific heat, k the conduction, Δ the Laplace operator in the x,y system, and φ the dissipation function. The latter has as its only important contribution the terms μu_y^2, all other contributions being of order $(t_0/R)^{1/2}$ or smaller as compared with this term. It is first essential to put this equation in a convenient dimensionless form. To do this, we first use the dimensionless variables ξ, η with $\eta = y/t_0$. We define $T = \tau(\mu u_0 L/\rho C t_0^2)$ and $\epsilon = kL/\rho C u_0 t_0^2$. A typical value for ϵ is 0.03. The equation then becomes

$$\epsilon[\tau_{\eta\eta} + (t_0/L)^2 \tau_{\xi\xi}] - (u/u_0)\tau_\xi + (u_\eta/u_0)^2 = 0. \tag{3.4}$$

This equation is valid only if τ is considered as $\tau(\xi,z)$ despite the fact that the indicated differentiations in the first term are taken with regard to ξ, η. In this equation u/u_0 is given by Eq. (3.1) and

$$(u_\eta/u_0)^2 = 9z^2 t_0(t_1 - t)/t^2. \tag{3.5}$$

It is now essential to decide on a specific boundary value problem. We are interested primarily in the temperature distribution across the passage but we have very little information on the "entrance" temperature. However, since we want to find how the temperature builds up as the material progresses through the passage, it is appropriate to choose arbitrarily the inlet temperature. In fact, a convenient problem whose solution answers all our questions is postulated by requiring that

$$\tau(\xi_0,z) = \tau(\xi,-1) = \tau(\xi,1) = 0. \tag{3.6}$$

[4] This problem was originally solved in a somewhat more general form in (3). The problem of finding the flow field was solved by Gaskell (4).

We again note that when the "ϵ term" is omitted from Eq. (3.4), the function $\tau^{(0)}$ which satisfies the remaining equation is easily found to be

(3.7) $$\tau^{(0)} = \int_{\xi_0}^{\xi} (u_\eta^2/uu_0)\,d\xi.$$

This, however, does not satisfy the boundary conditions on $z = \pm 1$, so we must *hope* that the steep portions of the functions, whose existence are now required, are confined to the regions near $z = \pm 1$. Accordingly,

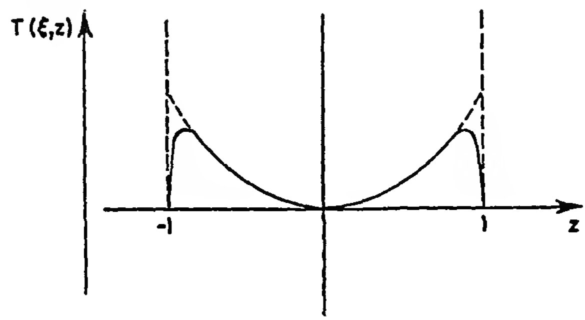

FIG. 4. Temperature distribution in fluid sheet at exit. Dotted lines indicate the "interior solution" without boundary layer correction.

we stretch the coordinate z (and also η) by the rule $z + 1 = \zeta\epsilon^{1/2}$. Replacing η by ζ in Eq. (3.4), letting $\tau = \tau^{(0)} + \psi(\xi,\zeta)$, and dropping terms of order $\epsilon^{1/2}$ or smaller from the resulting equation, we obtain[5]

$$\psi_{\zeta\zeta} - \psi_\xi = 0.$$

The line $\zeta = 0$ is, of course, the lower boundary of the passage and for this lower boundary layer we require that

(3.8) $$\begin{aligned}\psi(0,\zeta) &= \psi(\xi,+\infty) = 0\\ \psi(\xi,0) &= -\tau^{(0)}(\xi,-1).\end{aligned}$$

This is a classical problem whose solution is

(3.9) $$\psi = -\int_0^{\xi} \tau_\xi^{(0)}(S',-1)\ \mathrm{erfc}\ (\zeta/2\sqrt{S - S'})\ dS'.$$

A similar boundary layer must penetrate downward from the upper surface and, in fact, is represented by Eq. (3.9) when ζ is interpreted as $(1 - z)\epsilon^{-1/2}$. The temperature distribution is given in Fig. 4 for fixed ξ (i.e., $\xi = \xi_1$).

An important comment is now pertinent. First, with regard to the physical problem, it is clear that the cooling will "penetrate" to only a

[5] Note that the meaning of ψ_ξ in Eq. (3.4) was the derivative of ψ with fixed z, not fixed η.

distance of order $\epsilon^{1/2}t_0$; and more important *this is evident as soon as Eq. (3.4) is deduced and ϵ is found to be small!* That is to say, the dimensional analysis and boundary layer ideas give us almost all the necessary information without solving any differential equation at all! Only the *detailed* picture is enhanced by carrying out the detailed solution. We shall encounter this advantage again in a case where the detailed solution is very difficult. It is certainly one of the very valuable aspects of boundary layer ideas that such information can be gleaned at such a small expenditure of effort.

The engineering consequences of our problem were as follows. It became clear that for the speeds envisaged at that time a prohibitively low surface temperature was required to obtain interior peak temperatures consistent with satisfactory cohesive properties of the materials then in use.

IV. A Convection Problem

An interesting boundary layer problem arises when we consider the following situation. Suppose, as depicted in Fig. 5, a cylindrical container is filled with a gas and that the container surface is held at a given

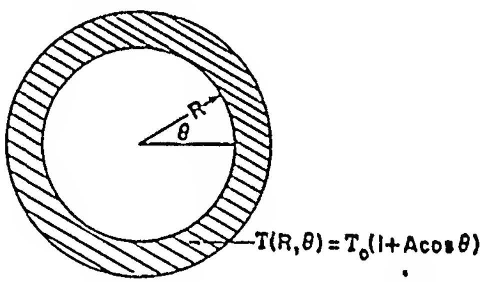

Fig. 5. Geometry of convection problem.

temperature distribution say $T = T_0(1 + A \cos \theta)$, with T the absolute temperature. Such problems arise when we consider heat transfer across cellular materials. It is of interest to determine the gas motion and the heat transfer rate. We will assume here that the radiation transfer does not interact with the gas to an appreciable extent. The laws governing the behavior of the gas are the familiar conservation of mass, momentum, and energy, an equation of state, and the usual thermodynamic information. We write then (for steady state phenomena)

$$
\begin{aligned}
&(\rho u_i)_{,i} = 0 \\
&\rho u_j u_{i,j} + p_{,i} + \rho g \delta_{2i} = (2\mu\epsilon_{ij})_{,j} + (\lambda\epsilon_{kk})_{,i} \\
&\rho u_j C_v T_{,j} + p u_{j,j} = (kT_{,j})_{,j} + 2\mu\epsilon_{ij}u_{i,j} + \lambda\epsilon_{kk}u_{j,j} \\
&p = \rho R T.
\end{aligned}
\tag{4.1}
$$

For maximum algebraic simplicity without loss of reasonable generality, we shall adopt the postulates that C_p, C_v, $C_p\mu/k$, R, are constants and that $\lambda = -\frac{2}{3}\mu$. We can then immediately refer all dimensional quantities to appropriate reference quantities in order to obtain the requisite dimensionless problem. We define then $\rho = \rho_0\varphi$, $T = T_0\tau$, $p = p_0 + \rho_0 gL\sigma$, $\xi_i = x_i/L$, $u_i = Cv_i$, $\mu = \mu_0\beta$, $\lambda = -2\mu_0\beta/3$, $k = k_0\beta$. Here ρ_0 and p_0 are the density and pressure which would prevail at the cylinder center when $T = T_0$, $u_i \equiv 0$. μ_0, k_0 are the viscosity and conductivity at this reference thermodynamic state. The reference velocity C is not yet known, but we can conveniently choose it to be such that the number C^2/gL becomes unity. As we shall see the boundary layer stretching will involve the size of the velocities so this choice is by no means a critical matter. With these substitutions, Eqs. (4.1) become

$$
\begin{aligned}
&(\varphi v_i)_{,i} = 0 \\
&\varphi v_j v_{i,j} + \sigma_{,i} + \varphi\delta_{2i} = 2\epsilon[(\beta E_{ij})_{,i} - (\beta E_{kk})_{,i}/3] \\
(4.2)\quad &\gamma^{-1}\rho v_j\tau_{,j} + [(\gamma - 1)/\gamma]\rho\tau v_{j,j} = P\epsilon(\beta\tau_{,j})_{,j} \\
&\qquad\qquad + 2[(\gamma - 1)/\gamma]\epsilon\alpha\beta[E_{ij}v_{i,j} - E_{kk}v_{i,i}/3] \\
&1 + \gamma\alpha\sigma = \varphi\tau.
\end{aligned}
$$

In these equations $\epsilon = \mu_0/\rho_0 CL$, $\alpha = C^2/\gamma RT_0$, $\gamma = C_p/C_v$, E_{ij} is the dimensionless ϵ_{ij} as implied by our reference quantities, $P = k_0/C_p\mu_0$ and is usually of order unity. The differentiations are now performed with regard to the ξ_j. We are interested here in that situation where $\epsilon \ll 1$. This occurs, for example, when L is a few centimeters or more, and T_0, p_0, ρ_0 correspond to sea-level atmospheric conditions. Under these conditions $\alpha \ll 1$ also. We are once more faced with the familiar situation where ϵ multiplies the highly differentiated term. Since many terms enter the equations, it is not at all clear yet that this is not occasioned by a poor choice for C. We may ascertain whether this is the case however by using the usual stretching technique, not only on the coordinates but on the magnitudes of σ and v_i. This is necessary because we do not know yet how they may be affected by the size of ϵ (or α). However, the boundary conditions fix the size of the variations in τ, and hence in ρ, so that

$$
\begin{aligned}
\tau &= 1 + \epsilon^b\chi \\
\varphi &= 1 - \epsilon^b\chi + \cdots .
\end{aligned}
$$

This will be consistent with $\tau(\theta,1) = 1 + A\cos\theta$ if $\epsilon^b = A$. It is also implied here that $A \ll 1$ and hence $b > 0$. Before performing the stretching of our other functions, however, we may anticipate that if we do have a boundary layer problem (in both temperature and velocity), the behavior in the interior consistent with all the equations is a rigid

body rotation. If we now introduce the stretching mentioned above, we must write

$$
(4.3)\qquad
\begin{aligned}
v &= \epsilon^{n}[\Omega r + \psi(r,\theta)] \\
u &= \epsilon^{m} w(r,\theta) \\
z &= \epsilon^{\nu}(1 - r) \\
\sigma &= \epsilon^{q} s - r \sin \theta.
\end{aligned}
$$

Here, of course, r and θ are the polar coordinates associated with the ξ_j. The numbers n, m, ν, q, must be chosen so that: (1) the most highly differentiated terms in each equation are retained when $\epsilon^{h}(h > 0)$ is neglected compared to unity, (2) the gravitational (or body force) term is also retained. These requirements lead to the choices $\nu = -\frac{1}{2} + b/4$, $n = b/2$, $m = \frac{1}{2} + b/4$, $q = 1 + b/2$. Note that unless $b < 2$ there is no stretching of the radial coordinate so only for $b < 2$ is the boundary layer approach appropriate. Thus for $0 < b < 2$, Eqs. (4.2) become

$$
(4.4)\qquad
\begin{aligned}
& w_z - \psi_\theta = 0 \\
& (\Omega + \psi)\psi_\theta - w\psi_z + \chi \cos \theta = \psi_{zz} \\
& (\Omega + \psi)\chi_\theta - w\chi_z = P\chi_{zz}.
\end{aligned}
$$

It is required that w, ψ, and χ, be periodic in θ, that $\chi(0,\theta) = \cos \theta$, $w(0,\theta) = 0$, and $\psi(0,\theta) = -\Omega$. Furthermore, each of these functions must vanish as $z \to \infty$. Since the system is only of fifth order in z, these conditions determine Ω as well as w, ψ, and χ.

Although this boundary value problem has not been solved with the appropriate accuracy,[6] certain conclusions can be drawn immediately. For example, the heat transfer (except for radiation transfer which can be studied separately) across the cell is given by

$$Q = \int_{-\pi/2}^{\pi/2} kT_n R\, d\theta = -kT_0 \epsilon^{\nu+1} \int_{-\pi/2}^{\pi/2} \chi_z\, d\theta.$$

That is, for the given geometry, gas, etc., the heat transfer per unit length (of cylinders) is proportional to $k\Delta T\epsilon^{\nu}$ where ΔT is the maximum temperature difference. That is

$$\frac{Q}{k\Delta T} \sim (\mu^2/\rho^2 g R^3)^{-1/4} \cdot \left(\frac{\Delta T}{T_0}\right)^{1/4}.$$

Thus, for example, the effect of changing the cell size in given cellular materials can easily be estimated without solving this complicated boundary value problem. We should note in passing that the situation where $k > 2$ has been dealt with in (6).

[6] To the author's knowledge the only (preliminary) results are to be found in (7).

V. The Relaxation Oscillations of the Van der Pol Oscillator

A fourth exemplary physical problem in which the boundary layer ideas are invoked is that of the relaxation oscillation phenomenon. This problem does not fall strictly into the classification we gave early in this paper, as we shall see, but the ideas will still provide a useful result. Specifically, we want the periodic solution of the nonlinear equation[7]

$$\epsilon y'' - (1 - y^2)y' + y = 0, \tag{5.1}$$

for small values of ϵ. In particular, we want to know the period. This problem arises in analysis of certain electrical circuit problems [see, e.g. (8)]. The asymptotic development with regard to ϵ of $y(t,\epsilon)$ has been given rigorously by Haag (9) and Dorodnitsyn (10). The solution we will find is essentially equivalent to the first two terms of this development. A comparison of our work[8] and that of Haag will indicate forcefully the power of the boundary layer ideas as a labor-saving device (whose operating expense is only a lack of rigor).

Our boundary value problem differs from those specified earlier in that the size of the domain (i.e., the period) is not specified. However, the differential equation is of the proper form and it has long been known that the period is of order unity and that $y(t,\epsilon)$ has the general appearanee shown in Fig. 1. Thus, we shall attempt to apply the boundary layer ideas in this analysis.

We note first that an "interior" solution of (5.1) can be found by omitting the term with coefficient ϵ. This leads to the result[9]

$$\ln y_1 - (y_1^2 - 1)/2 = t. \tag{5.2}$$

The only available constant of integration has been utilized to fix the (intrinsically arbitrary) origin of the time scale. This solution however is such that y_1'' behaves like $t^{-3/2}$ near $t = 0$, i.e., near $y = 1$. Thus, in the neighborhood of $t = 0, y_1$ is not a valid representation of y. In fact, we must anticipate that $\epsilon y''$ will produce a contribution of the same order as the other terms in this neighborhood. In our previous terminology (5.2) is valid only when y, as defined by (5.2), is "smooth" and hence when $\epsilon y_1''$ is negligible. This fact implies that we must use the stretching technique in the neighborhood of $t = 0$. In fact, we define

$$y = 1 + \epsilon^\alpha v(\xi), \quad t - t_0 = \epsilon^\beta \xi. \tag{5.3}$$

[7] $y' \equiv \partial[y(t,\epsilon)]/\partial t$.

[8] The material in this section is taken from an unpublished work by J. A. Lewis and the writer.

[9] y_1 merely denotes the approximation to y which is valid in this "interior region" whose location is to be determined.

We must choose α, β, so that $\epsilon y''$ is of the same order in ϵ as the other two terms. The only such choice is $\alpha = \frac{1}{3}$, $\beta = \frac{2}{3}$, and (5.3) becomes

$$v'' + 2vv' + 1 = 0(\epsilon^{1/3}). \tag{5.4}$$

We may integrate once explicitly (omitting the $\epsilon^{1/3}$ term) to obtain

$$v' + v^2 + \xi = 0.$$

Since this is a Ricatti equation, its solution appears in the form

$$v = z'(\xi)/z(\xi)$$

where $z = (-\xi)^{1/2}[K_{1/3}(s) + BK_{-1/3}(-s)]$, $s = (\frac{2}{3})(-\xi)^{3/2}$, and K_ν is the modified Hankel function. In order to evaluate t_0 and B we must match this portion of the boundary layer solution to the function y defined in (5.2). We note that there is a region in which $\xi \gg 1$ and $t \ll 1$, for example t of order $\epsilon^{1/3}$, ξ of order $\epsilon^{-1/3}$. In this region, the asymptotic behavior of z is appropriate whereas $y_1 \simeq 1 + (-t)^{1/2}$. However, the asymptotic behavior of v, i.e., its behavior for large $(-\xi)$, is $v \sim -(-\xi)^{1/2}$ if $B \neq 0$, whereas its behavior is $v \sim (-\xi)^{1/2}$ if B is zero. Thus, v and y_1 as approximated above are identical provided t_0 and B each vanish. Hence

$$z = (-\xi)^{1/2}K_{1/3}(s) \equiv (\pi\xi^{1/2}/\sqrt{3})[J_{1/3}(s') + J_{-1/3}(s')] \tag{5.5}$$

with

$$s' = (\tfrac{2}{3})\xi^{3/2}.$$

We must note that this representation of y, i.e., the function v, also is singular, in particular at the point ξ_1, which is associated with the smallest zero of the bracket in (5.5). Thus again our approximations must be invalid in this neighborhood.

In order to continue our solution we must anticipate the behavior of $y(t)$ for $y < 1$. In this neighborhood, the damping is negative, and furthermore as t becomes > 0 and approaches ξ_1, both y' and $\epsilon y''$ become large compared to y [as implied by (5.5)]. Thus, we must look for another streching which is appropriate as y proceeds through the origin. We define, $y = g(\eta)$, $\eta = (t - t_2)/\epsilon$, and obtain

$$g'' - (1 - g^2)g' = 0(\epsilon),$$

and one integration provides

$$g' - g + g^3/3 = C. \tag{5.6}$$

In order to determine C, we note that when g is near unity and ξ near ξ_1,

$$(g - 1)' + (g - 1)^2 = \tfrac{2}{3} + C + 0[(g - 1)^3].$$

However, this form for g must be consistent with $v' + v^2 = \xi$ in this same neighborhood. For this to be true we must choose $C = -\frac{2}{3} - \epsilon^{2/3}\xi_1 + 0(\epsilon)$. It may seem inconsistent to retain terms of order $\epsilon^{2/3}$ here (since previously we have not retained terms of order greater than zero in ϵ), but we shall see that it will produce a major effect in the answer. A careful study will show that other, superficially similar, retentions would produce less important effects. To see this one need merely follow the foregoing procedure keeping an extra contribution at each step where such a term has been dropped.

Equation (5.6) may now be integrated to give

$$(1 - g)^{-1} + (\tfrac{1}{3}) \ln [(g + 2 + \epsilon^{2/3}\xi_1/3)/(1 - g)] = -\eta. \tag{5.7}$$

Now, near $y = 1$ (with η large) we have $y \simeq g \simeq 1 + \epsilon(t - t_2)^{-1}$, $v \simeq (\xi - \xi_1)^{-1}$. These are consistent when $t_2 = \epsilon^{2/3}\xi_1$.

We must now observe that g goes to an asymptote at $-(2 + \epsilon^{2/3}\xi_1/3)$. However, the (neglected) effect of the third term of (5.1) would be to pull y down from the neighborhood of this asymptote into that portion defined by $y_1(t)$. Thus, we must add one more contribution to the boundary layer. This time we define

$$-y = 2 + \epsilon^{2/3}\xi_1/3 - \epsilon^k u(\sigma), \quad t - t_3 = \epsilon^\nu \sigma.$$

Equation (5.1) becomes (with $k = 1$, $\nu = 1$, and $a = 2 + \epsilon^{2/3}\xi_1/3$)

$$u''(a^2 - 1)u' - a = 0$$

and hence

$$u = a\sigma/(a^2 - 1) + Be^{-(a^2-1)\sigma}.$$

Matching u to g requires that $B = 3/e$ and $t_3 = t_2 - (\epsilon \ln \epsilon)/3$. For positive large σ, u, and y_1 will agree except that y is now on the negative half of the cycle and there is a time lapse of

$$T = (\tfrac{3}{2} - \ln 2) + (\tfrac{3}{2})\epsilon^{2/3}\xi_1. \tag{5.8}$$

Note that any intrinsically different choice for t_3 leads to a value of B of order ϵ^{-1}. This would invalidate our choice of the stretching parameter and hence is not permissible. In the equation for the half-period (5.8), we have not included this time lapse contribution of order $\epsilon \ln \epsilon$. This is only consistent because the earlier approximations can lead to errors of this order in the period. In particular, $u(\sigma)$ could include another constant term of order $\ln \epsilon$, but a determination of its magnitude requires a more careful analysis. For a result of that order of accuracy one can refer to (9). Thus, T is the half-period of the cycle to order $\epsilon \ln \epsilon$ and the functions y_1, v, g, and u define the motion.

It is convenient here to note that the contributions of order $\epsilon^{2/3}$ are

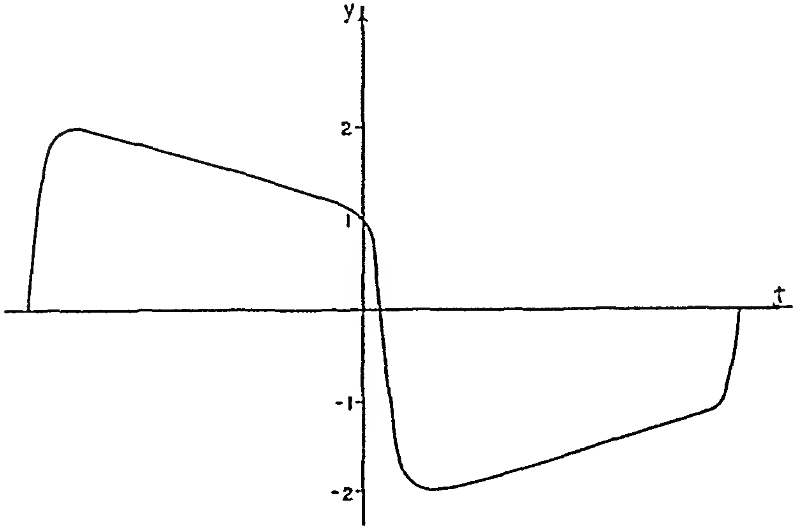

FIG. 6. The wave form associated with the periodic solution of Eq. (5.1) for $\epsilon \ll 1$.

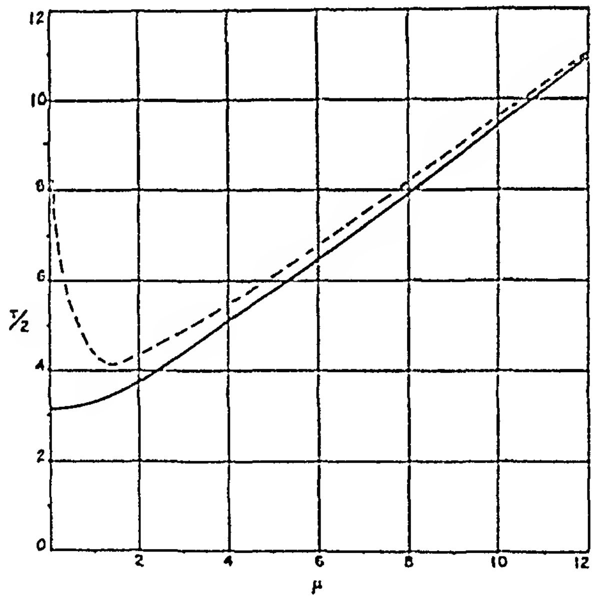

FIG. 7. Half-period associated with the periodic solution of Eq. (5.9) [or (5.1)]. The solid curve is the numerically obtained "exact" solution.

associated with the time required to turn the corner near $y = 1$, and the fact that the slow part of the cycle proceeds, not from $y = -2$ (the limit $\epsilon \to 0$ value) but rather from $-y_{max} \simeq 2 + \epsilon^{2/3}\xi_1/3$. The times required for the steepest part of the cycle and for the final corner are of higher order as we have seen.

In Fig. 7 we present a comparison between the values for the period as given by the boundary layer technique and those found by a careful

numerical integration. A more commonly presented form of (5.1) is

$$y'' - \mu(1 - y^2)y' + y = 0 \tag{5.9}$$

where $\mu^2 = \epsilon^{-1}$, and the argument of y is $\tau = \mu t$. In Fig. 7 the function plotted is $\tau(\mu)$ *vs* $\cdot\ \mu$. The values given by the asymptotic formula of Dorodnitsyn are not appreciably different from ours in the range where each representation is a good approximation.

VI. Other Boundary Layer Problems

There are, in particular, two groups of problems which we have deliberately not discussed in the foregoing work. One of these is that group of elasticity problems which falls into the boundary layer category. An excellent summary of that work has been given by Friedrichs (11), and in the individual contributions (12) to (16) one can find presentations of a more careful mathematical point of view in discussing these problems. The other very extensive group is that concerned with the flow of a viscous fluid past an obstacle. Most of the work on this important problem has been associated with the solution of the boundary layer equations rather than the formulation and recognition of the problem as a boundary layer problem in the foregoing sense. Compilations of this material can be found in (17) and (18).

VII. General Remarks

In closing this article, it seems desirable to stress the important features of the boundary layer analysis which we have attempted to exemplify. In a problem which can be recognized as a boundary layer problem, the solution can be subdivided into parts which are individually appropriate in different domains. The difficulties met in obtaining the solution for the individual domains are usually far smaller than those of obtaining a rigorous result (valid in the entire domain). Finally, it has been the writer's experience that, in many problems, the desired information (but not the detailed solution) may be obtained without proceeding beyond the point where the problem is *recognized* as a boundary layer problem. The process of recognition (as implied in the foregoing sections) usually consists of the following. One writes down the basic laws (differential equations) governing the behavior of the system under consideration. He then chooses dimensional reference parameters (a reference length, a reference temperature, etc.) in such a manner that the domain size, the magnitude of the nonhomogeneous terms, and as many of the dimensionless parameters entering the resulting differential equation as possible, are of order unity. Generally speaking, the parameters chosen as unity should be those associated with the terms which

contain lowest order derivatives. Then the characterization of boundary layer problem results when the coefficient of the highest derivative is small.

The solution of the boundary layer problem usually takes place in two steps. One first finds an interior solution by integrating the system of equations with the "ϵ terms" omitted. Then one changes the scale of the normal coordinate to the boundary and the scale of any other functions whose size is not known in such a manner that a system of equations of the appropriate order is retained. It must be emphasized again that one can only *hope* that the solution defined by this "scaled" system of equations and the associated boundary conditions is confined to a neighborhood of the boundary. Only when this has been verified, can one conclude that the problem is truly of the boundary layer variety. From this point on, one need only solve the equations appropriate to the subdivisions of the domain. In those cases where the simplifications achieved by the foregoing are sufficiently great, these final integrations can be carried out and the technique has been successful.

VIII. Appendix

Here we shall *indicate* the considerations leading to the boundary value problem defined by (2.1) and (2.2). We are concerned with a problem which involves the motion on a rotating sphere of a fluid. This motion is known to be of a turbulent nature, but with our limited understanding of such motions we adopt a simple model in which we introduce an eddy viscosity far greater than the usual "molecular viscosity." We then postulate that, using this eddy viscosity, the usual conservation of mass and momentum laws are applicable. In view (again) of our lack of understanding of the manner in which stress is transmitted to the surface of the (wavy) ocean by the wind, we adopt the empirical rule that the stress transmitted is proportional to the wind intensity. With this model we may further assume that the motion is essentially two-dimensional, that is, that the velocity vector lies always in a surface r = constant, where r is the radial spherical coordinate. Such an assumption implies that

$$\vec{V} = \operatorname{curl} \vec{k}\Psi(r,\theta,\varphi - \Omega t) + \vec{j}\Omega r \cos\theta$$

where $\vec{k}$ is the unit vector in the radial direction, θ and φ are the angular coordinates in a fixed reference system, and $\vec{V}$ is independent of the time in a system rotating at speed Ω, the angular velocity of the earth. This representation of $\vec{V}$ may be put in the equation

$$\operatorname{curl} [\vec{V}_t + (\vec{V}\cdot \operatorname{grad})\vec{V}] = \mu \operatorname{curl} \Delta\vec{V},$$

i.e., the curl of the momentum equation, and two results emerge. A differential equation for ψ which is the radial component of the above equation is the usable result. The other is the observation that the other components of this equation do not vanish. This implies that our representation for $\vec{V}$ cannot be rigorously appropriate even within the framework of our simplified model. Nevertheless, the approximation seems appropriate. The differential equation for ψ should now be integrated with regard to r, term by term, from a depth r_0 to the surface. The depth r_0 is sufficiently great that $\Psi(r_0,\theta,\varphi') \equiv 0$. This integration will yield two contributions. One of these is the radial component of the curl of the surface traction, i.e., the wind force; this is associated with the nonhomogeneous term of Eq. (2.1). The other contribution is a differential operator, operating on $\chi = \int_{r_0}^{r_1} \Psi dr$. We must now choose a reference length L which (conveniently) is such that the ocean height (in units of φ) divided by L is π. We then define $\psi = C\chi$. C is chosen so that when we replace $\cos\varphi$ by unity, Eq. (2.1) results with $\chi = \varphi'/L$. ϵ is a dimensionless combination of the physical parameters (2). One should note that the model is crude (after all, any "equivalent viscosity" tensor associated with the turbulence is certainly not homogeneous and probably not isotropic), and the subsequent approximations are somewhat rough. Thus the favorable comparison of the results obtained from this model and the actual observed behavior lend credence to this conception of the basic nature of the ocean current phenomenon.

References

1. Munk, W. H., "On the Wind-Driven Ocean Circulation," *J. Meterol.*, **7**, 79–93 (1950).
2. Munk, W. H., and Carrier, G. F., "The Wind-Driven Circulation in Ocean Basins of Various Shapes," *Tellus*, **2**, 158–167 (1950).
3. Finston, M., "Thermal Effects in Calendering Viscous Fluids," *J. Am. Meterol.*, **18**, 12 (1951).
4. Gaskell, R. E., "The Calendering of Plastic Materials," *Trans. Am. Soc. Mech. Engrs.*, **72**, 334 (1950).
5. Carrier, G. F., and Lewis, J. A., "On Heat Transfer Problems in Viscous Flow," *Quart. Applied Math.*, **VII**, 450 (1950).
6. Lewis, J. A., "Free Convection in Commercial Insulating Materials," A thesis, Brown University, 1950.
7. Ostrach, S., "A Boundary Layer Problem in the Theory of Free Convection," A thesis, Brown University, 1950.
8. McLachlan, N. W., "Ordinary Non-Linear Differential Equations," Oxford University Press, London, 1950.
9. Haag, J., "Etude Asymptotique des Oscillations de Relaxation," *Ann. Sci. Ecole Norm. Sup.*, **60** (1943).
10. Dorodnitsyn, A. A., "Asymptotic Solution of the van der Pol Equation" (Russian), *Inst. Mech. Acad. Sci. USSR*, **XI** (1947).

11. Friedrichs, K. O., "The Edge Effect in Bending and Buckling with Large Deflections," *Proc. Symposia* in *Applied Math.*, I, 1947.
12. Bromberg, E., and Stoker, J. J., "Non-Linear Theory of Curved Elastic Sheets," *Quart. Applied Math.*, 3, 246–265 (1945).
13. Friedrichs, K. O., "On the Minimum Buckling Load for Spherical Shells," *Applied Mech.*, Theodore von Kármán Anniversary Volume, 1941, pp. 258–272.
14. Friedrichs, K. O., and Stoker, J. J., "Buckling of the Circular Plate Beyond the Critical Thrust," *J. Applied Mech.*, 9, A7-A14 (1942); "The Non-Linear Boundary Value Problem of the Buckled Plate," *Am. J. Math.*, 63, 839–888 (1941).
15. von Kármán, T., "The Engineer Grapples with Non-Linear Problems," *Bull. Am. Math. Soc.*, 46, 615–683 (1940).
16. Reissner, H., "Spannungen in Kugelschalen (Kuppeln)," H. Mueller-Breslau Festschrift, 1912, pp. 181–193.
17. Kuerti, G., "The Laminar Boundary Layer in Compressible Flow," *Advances in Applied Mech.*, 2, 21–92 (1951). Academic Press, New York.
18. Lewis, J. A., "Boundary Layer in Compressible Fluid" (monograph V), *Wright-Field Tech. Rept.*, F-TR-1179, N.D. Feb. 1948.

The One-Dimensional Isentropic Fluid Flow

By OTHAR ZALDASTANI

Consulting Engineer, Boston, Massachusetts

I. Introduction

The field of research in nonlinear wave motion was inaugurated about a hundred and fifty years ago when Poisson (2) determined a simple wave solution of the differential equations for a one-dimensional flow of an isothermal perfect gas. The study of the rectilinear motion of an inviscid fluid was later systematically undertaken, but after a period of important discoveries, marked by Riemann's complete integration of the continuous flow problem, the investigations were mainly concentrated on the shock problems and the numerical and approximate treatments of interactions. Recently, few original papers have dealt again with the continuous motion, but definite advances have been made in this problem, and the following purports to show the present stage of the results achieved.

We are concerned with an inviscid fluid whose particles describe parallel straight lines and are in the same state over a plane perpendicular to the flow lines. We suppose further that the changes are adiabatic and that the resulting relation between the pressure, p, and

the density, ρ, holds throughout the fluid. In particular, special forms of this relation, which yield explicit solutions, are considered. The medium and the motion being thus defined, the governing equations form a system of two nonlinear first order partial differential equations.

The first attempt in the analysis of these equations was undertaken by Poisson (2) who, under the assumption of Boyle's law $p = a^2\rho$, with a = constant, described a wave propagation by the relation

$$u = f[x - (a + u)t],$$

in which u denotes a particle velocity, x its single space coordinate, t the time, and f an arbitrary function. The discussion of this solution was given by Stokes (4), who pointed out the formation of a discontinuity which ultimately arises from the motion. Airy (5) gave explicitly the relation connecting the velocity and the density in Poisson's solution, and this law became the basis of the investigations of Earnshaw (6) who determined all the properties of the compression and rarefaction waves of a polytropic fluid.[1]

The fundamental result was soon after reached by Riemann when he linearized the problem by interchanging the role of dependent and independent variables and gave a solution of the initial value problem.

Other ways of investigating the problem were considered by Bechert (18), Guderley (21), Sedov (27), and Staniukovitch (28). They consist of the search for particular solutions without the use of a contact transformation. Such integrals were found directly through the search for symmetric solutions and the method of separation of variables, and indirectly through inverse methods, see (36). However, the results so far obtained seem to be of limited interest.

In this survey only analytical solutions of the continuous motion are considered. They are obtained through two different approaches. Once the system of equations is linearized through the Legendre transformation and reduced to a second order differential equation, one can use either general integrals depending on two arbitrary functions or Riemann's procedure. Both methods have been recently simplified and successfully used in applications. For polytropic fluids, and a more general case suggested by Sauer (39), the results can be expressed in closed forms. They enable one to determine analytically, sufficient conditions for the occurrence of singularities within a continuous flow and to present a complete discussion of the motion in a closed tube.

[1] The geometrical interpretation of these simple integrals were given by Hugoniot (8) and Hadamard (9). A complete summary and discussion of all these classical results can be found in Rayleigh (10) and in Courant and Friedrichs (30).

II. The Basic Equations

1. Choice of Variables

We make use of the Eulerian representation and denote by x the abscissa of a particle and by t the time. A p,ρ-relation being assumed throughout the flow, the number of unknowns is reduced to two. One is the velocity, u; the other can be chosen as a function of the density ρ, defined by the integral

$$v = \int_{\rho_0}^{\rho} \frac{a}{\rho}\, d\rho, \tag{2.1}$$

where ρ_0 is an arbitrary lower limit of integration and a the velocity of sound, whose square is $dp/d\rho$. For later reference we introduce also the characteristic variables

$$r = \frac{\lambda}{2} = \frac{v+u}{2}, \quad s = \frac{\mu}{2} = \frac{v-u}{2}.$$

To each couple (x,t) corresponds a single value for u and v. The physical plane, (x,t), can therefore be mapped point by point into a plane (u,v) which may be called the speed plane inasmuch as v has, also, the dimension of a velocity. It is clear that the inverse correspondence will not be necessarily one-valued. This transformation, introduced by Schultz-Grunow (20,25) and von Mises, will be used below.

A similar correspondence exists obviously between the x,t-plane and the r,s-plane. In both cases the transformation will be denoted as the hodograph transformation, see (30), pp. 38–40.

For a polytropic fluid we have $p/\rho^\kappa = \text{const.} = C$, therefore

$$a^2 = \kappa \frac{p}{\rho} = \kappa C \rho^{\kappa - 1}.$$

Hence, with $\rho_0 = 0$,

$$v = \frac{2}{\kappa - 1} \sqrt{\kappa C}\, \rho^{\frac{\kappa-1}{2}} = \frac{2}{\kappa - 1}\, a. \tag{2.2}$$

In particular, in the case of a diatomic perfect gas $\kappa = \frac{7}{5}$ and therefore

$$v = 5a. \tag{2.3}$$

2. The Differential Equations

The equations of continuity and motion expressing Newton's second law are respectively

$$(\rho u)_x = -\rho_t \tag{2.4}$$

$$\rho(u_t + uu_x) = -p_x, \tag{2.5}$$

the subscripts indicating partial differentiation.

In terms of the specific enthalpy i, which, in isentropic flow, satisfies the relation $di = dp/\rho$, Eq. (2.5) takes the form

$$u_t = -\left(\frac{u^2}{2} + i\right)_x. \tag{2.6}$$

Equations (2.4) and (2.6) imply the existence of a stream function, $\psi = \psi(x,t)$, and a potential function, $\varphi = \varphi(x,t)$, such as

$$\psi_x = \rho, \quad \psi_t = -\rho u \tag{2.7}$$

and

$$\varphi_x = u, \quad \varphi_t = -\left(\frac{u^2}{2} + i\right). \tag{2.8}$$

It can be seen easily that ψ and φ will fulfil nonlinear second order differential equations.

The problem may be reduced, however, to a linear one by the hodograph transformation. We can use u and v as new independent variables and achieve this transformation simply by introducing the Legendre transforms U and V of the stream and potential functions

$$U = x\psi_x + t\psi_t - \psi \tag{2.9}$$

and

$$V = x\varphi_x + t\varphi_t - \varphi.$$

In view of (2.7) and (2.8) we obtain

$$U_u = -\rho t, \quad U_\rho = x - ut, \tag{2.10}$$

and

$$V_u = x - ut, \quad V_\rho = -\frac{a^2}{\rho} t. \tag{2.11}$$

These relations yield, by elimination of x and t, two equations between U and V,

$$V_u = U_\rho, \quad V_\rho = \frac{a^2}{\rho^2} U_u, \tag{2.12}$$

which take a form similar to the Cauchy-Riemann equations,

$$V_u = \frac{a}{\rho} U_v, \quad V_v = \frac{a}{\rho} U_u, \tag{2.13}$$

by the use of the variable v. This system, together with (2.1), provides then by elimination of U or V the linear second order differential equations

$$V_{vv} - V_{uu} = -\frac{1}{a}\left(1 - \frac{da}{dv}\right) V_v \tag{2.14}$$

and

$$U_{vv} - U_{uu} = \frac{1}{a}\left(1 - \frac{da}{dv}\right) U_v. \tag{2.15}$$

Once U or V is known x and t can be found by (2.10) or (2.11).

In the speed plane, $\varphi = \varphi(u,v)$ and $\psi = \psi(u,v)$ satisfy also linear differential equations. We can, for instance, solve Eq. (2.9) for ψ,

$$\psi = (x - ut)\rho - U = \rho U_\rho - U = aU_v - U,$$

and get its partial derivatives,

$$\psi_v = \left(\frac{da}{dv} - 1\right) U_v + aU_{vv} = aU_{uu},$$
$$\psi_u = aU_{vu} - U_u,$$

which in view of the first equation of (2.10) become

$$\psi_u = -a\rho t_v, \quad \psi_v = -a\rho t_u. \tag{2.16}$$

These relations enable one, by elimination of t or ψ, to get the linear equations

$$\psi_{vv} - \psi_{uu} = \frac{1}{a}\left(1 + \frac{da}{dv}\right) \psi_v, \tag{2.17}$$

$$t_{vv} - t_{uu} = -\frac{1}{a}\left(1 + \frac{da}{dv}\right) t_v. \tag{2.18}$$

Equation (2.17) is particularly noteworthy since it gives the particle lines in the speed plane. Once the function $\psi = \psi(u,v)$ is known, its transfer to the physical plane can be made analytically as follows. Along a particle line the relations

$$\psi_u\, du + \psi_v\, dv = 0 \tag{2.19}$$
$$t_u\, du + t_v\, dv = dt \tag{2.20}$$
$$dx = u\, dt \tag{2.21}$$

hold. Using now (2.16) and (2.19) Eq. (2.20) becomes

$$dt = \frac{1}{a\rho\psi_v}(\psi_{uu}{}^2 - \psi_{vv}{}^2)du$$

or

$$t = \int \frac{\psi_{uu}{}^2 - \psi_{vv}{}^2}{a\rho\psi_v}\, du, \tag{2.22}$$

and from (2.21) we get

$$x = \int \frac{u(\psi_{uu}^2 - \psi_{vv}^2)}{a\rho\psi_v}\, du, \tag{2.23}$$

v being obtained from the given relation $\psi(u,v) = \text{constant}$. Equations (2.22) and (2.23) furnish a parametric representation of the particle lines in the x,t-plane.

Equation (2.18), on the other hand, is most suitable for the discussion of the initial value problem. It will be used in Section IV,3 with r and s taken as independent variables.

The above transformation, which linearizes the problem and goes back to Riemann's original work, is possible, provided that the Jacobian

$$j = \frac{\partial(u,v)}{\partial(x,t)} = u_x v_t - u_t v_x$$

does not vanish. Solutions for which $j = 0$ cannot be obtained by this method; however, such a condition implies a relation between u and v and thus leads to the simple wave solutions introduced by Poisson.

For the general case the problem has therefore been reduced to solving a second order linear partial differential equation of the type

$$Z_{vv} - Z_{uu} = \theta(v) Z_v, \tag{2.24}$$

where $\theta(v)$ is a function of v depending on the assumed p,ρ-relation.

It is of interest here to determine the p,ρ-relations which convert (2.24) into Darboux's equation

$$Z_{vv} - Z_{uu} = \frac{2m}{v} Z_v, \tag{2.25}$$

where m is a constant. They are given, in view of (2.14), (2.15), (2.17), (2.18), and (2.25) by the equation

$$\frac{1}{a}\left(1 + \epsilon \frac{da}{dv}\right) = \frac{2m}{v}, \tag{2.26}$$

with $\epsilon = \pm 1$. Its general solution is

$$a = \frac{\epsilon}{1 + 2m} v + C v^{-\epsilon 2m} \tag{2.27}$$

with $C = \text{constant}$. The use of (2.1) determines ρ,

$$\rho = \bar{C}\left(C + \frac{\epsilon}{1 + 2m} v^{1+\epsilon 2m}\right)^{\frac{2m+1}{2m+\epsilon}}, \tag{2.28}$$

with $\bar{C}$ any constant, and thereby p through the relation $dp = a\rho\, dv$.

For $\epsilon = +1$ we obtain easily after integration,

$$p = p_0 + \bar{C}\left[\frac{v^{2m+3}}{(1+2m)^2(2m+3)} + \frac{C}{1+2m}v^2 + \frac{C^2}{1-2m}v^{-2m+1}\right], \tag{2.29}$$

with p_0 = constant; the elimination of v between (2.28) and (2.29) yields then

$$p = p_0 + \bar{C}\left[\frac{\rho^{*\kappa}}{(1+2m)^2(2m+3)} + \frac{C}{1+2m}\rho^{*\kappa-1} + \frac{C^2}{1-2m}\rho^{*\kappa-2}\right]$$

with

$$\kappa = \frac{2m+3}{2m+1}, \quad \rho^* = (1+2m)\left(\frac{\rho}{\bar{C}} - C\right). \tag{2.30}$$

This p,ρ-relation was recently determined by Sauer (39). The case of $\epsilon = -1$ provides a somewhat similar relation. It is clear that both cases contain the particular condition for polytropic fluids, obtained by setting $C = 0$.

All results presented in the following for polytropic fluids and based on the solutions of Darboux's equation will be valid for these new p,ρ-relations.

III. General Integrals of the Equation $Z_{vv} - Z_{uu} = \theta(v)Z_v$

A general method of integrating linear second order partial differential equations of hyperbolic type is provided by the classical Riemann approach to the initial problem. It can be applied to equations of the type (2.24) and the procedure supplies a general solution without the knowledge of the general integral.

General integrals of Eq. (2.24), leading to interesting applications, can also be obtained. In particular, we can make use of various integral operators given by Bergman in connection with his study of the two-dimensional steady supersonic flows, see (31,32). The results are much simplified when Eq. (2.24) has the form of the Darboux equation.

1. *Integral Operators for the General Case*

We first transform Eq. (2.24) by introducing

$$Z = Z^* \exp \tfrac{1}{2}\int^v \theta(v)dv. \tag{3.1}$$

Upon substituting into (2.24) we obtain

$$Z_{vv}{}^* - Z_{uu}{}^* = N(v)Z^*, \tag{3.2}$$

in which $N(v) = \dfrac{\theta^2 - 2\theta'}{4}$.

A solution of (3.2) is sought in the form

$$X = f_0 + \sum_{n=1}^{n=\infty} h_n f_n, \tag{3.3}$$

where $f_0, f_1, \cdots$ are functions of

$$\lambda = v + u$$

and $h_1, h_2, \cdots$ functions of v. After inserting (3.3) in (3.2) a formal computation yields

$$\sum_{n=1}^{n=\infty} (h_n'' - Nh_n)f_n + 2h_n'f_n' = Nf_0. \tag{3.4}$$

We now choose the functions $f_n(\lambda)$ so that

$$f_n' = f_{n-1}, \text{ i.e., } f_1 = \int^\lambda f_0 d\lambda, \quad f_2 = \int^\lambda f_1 d\lambda, \tag{3.5}$$

and the functions $h_n(v)$ so that

$$h_{n+1}' = -\tfrac{1}{2}(h_n'' - Nh_n) \quad \text{or} \quad h_n = -\tfrac{1}{2}h_{n-1}' + \tfrac{1}{2} \int^v Nh_{n-1} dv. \tag{3.6}$$

The n partial sum of (3.4) is then reduced to

$$-2h_{n+1}'f_n + 2h_1'f_0 = Nf_0.$$

Since the sum in (3.3) must be supposed to be convergent, $h_n f_n$ must go toward zero with $n \to \infty$. Let us assume that $h_n'f_n$ or $h_{n+1}'f_n$ has also the limit zero for infinite n. Consequently the simple condition

$$2h_1'f_0 = Nf_0 \quad \text{or} \quad h_1 = \tfrac{1}{2} \int^v N\, dv \tag{3.7}$$

holds for $n \to \infty$.

The functions $h_n(v)$ are thus completely determined by (3.6) and (3.7), or by (3.6) alone, if we introduce $h_0 = 1$; they only depend on $N(v)$, which is given by the p,ρ-relation.

The functions $f_n(\lambda)$ depend on f_0 only and can be expressed in terms of f_0 by various integrals.

We can use

$$f_n(\lambda) = \frac{1}{n!} \int_0^\lambda (\lambda - \xi)^n f_0'(\xi) d\xi, \tag{3.8}$$

which yields

$$X = \sum_{n=0}^{n=\infty} \frac{h_n(v)}{n!} \int_0^\lambda (\lambda - \xi)^n f_0'(\xi) d\xi,$$

or

$$X = \int_0^\lambda f_0'(\xi) \sum_{n=0}^{n=\infty} \left[\frac{h_n(v)}{n!} (\lambda - \xi)^n \right] d\xi.$$

If we introduce the function of three variables

$$E_1(u,v,\xi) = \sum_{n=0}^{n=\infty} \frac{1}{n!} (\lambda - \xi)^n h_n(v),$$

and write $W_1(\xi)$ for $f_0'(\xi)$, the solution can be put in the form

$$X = \int_0^\lambda E_1(u,v,\xi) W_1(\xi) d\xi.$$

In a quite similar way a solution Y can be constructed with a function of

$$\mu = v - u.$$

We have

$$Y = \int_0^\mu E_2(u,v,\xi) W_2(\xi) d\xi,$$

and the general solution Z of (2.24) reads finally

$$Z = (X + Y) \exp \tfrac{1}{2} \int^v \theta(v) dv.$$

The recurrence formula (3.5) is also satisfied by the expression

$$f_n(\lambda) = \frac{1}{\frac{1}{2} \cdot \frac{3}{2} \cdot \cdot \cdot (n - \frac{1}{2})} \int_0^\lambda (\lambda - \xi)^n K(\xi) \frac{d\xi}{(\lambda - \xi)^{1/2}}, \quad n = 1, 2 \cdot \cdot \cdot$$

with

$$f_0(\lambda) = \int_0^\lambda K(\xi) \frac{d\xi}{(\lambda - \xi)^{1/2}},$$

in which K is an arbitrary function. Making use of a new variable, s, defined by

$$\xi = \lambda(1 - s^2),$$

we can write after a short computation,

$$f_n(\lambda) = \frac{1}{\frac{1}{2} \cdot \frac{3}{2} \cdot \cdot \cdot (n - \frac{1}{2})} \int_{-1}^{+1} (\lambda s^2)^n K_1[\lambda(1 - s^2)] \frac{ds}{(1 - s^2)^{1/2}},$$

where K_1 is an arbitrary function. Consequently X is expressed in the form

$$X = \int_{-1}^{+1} F_1(u,v,s) K_1[\lambda(1 - s^2)] \frac{ds}{(1 - s^2)^{1/2}}, \tag{3.9}$$

with

$$F_1(u,v,s) = 1 + \sum_{n=1}^{n=\infty} \frac{(\lambda s^2)^n}{1 \cdot \frac{1}{2} \cdots (n - \frac{1}{2})} h_n(v).$$

A similar expression can be found for Y,

$$Y = \int_{-1}^{+1} F_2(u,v,s) K_2[\mu(1 - s^2)] \frac{ds}{(1 - s^2)^{1/2}} \tag{3.10}$$

with

$$F_2(u,v,s) = 1 + \sum_{n=1}^{n=\infty} \frac{(\mu s^2)^n}{1 \cdot \frac{1}{2} \cdots (n - \frac{1}{2})} h_n(v).$$

It remains to be shown that the infinite series included in these formulas are convergent. The reader is referred for this question to Bergman's work.

2. *Darboux's Equation*

It was shown that for the p,ρ-relations considered in Section II,2 Eq. (2.24) is reduced to the Darboux equation

$$Z_{vv} - Z_{uu} = \frac{2m}{v} Z_v. \tag{3.11}$$

This equation was first studied by Euler (1) and was later investigated by Poisson (3), Riemann (7), and Darboux (13).

We can apply the results presented in Section III,1 with the condition $\theta(v) = 2m/v$. We have

$$Z = v^m Z^* \tag{3.12}$$

and

$$N(v) = \frac{m(m+1)}{v^2}. \tag{3.13}$$

Equation (3.6), defining the functions $h_n(v)$, can then be satisfied by the relation

$$h_n(v) = \alpha_n v^{-n}, \tag{3.14}$$

in which the coefficients α_n are given by the recurrence formula

$$\alpha_n = \frac{n(n-1) - m(m+1)}{2n} \alpha_{n-1}$$

with $\alpha_0 = 1$. Writing $n(n-1) - m(m+1) = (n+m)(-m-1-n)$

we get

$$\alpha_n = \frac{(m+1)\cdots(m+n)(-m)\cdots(-m-1+n)}{2^n n!}.$$

The generating function $F_1(u,v,s)$ becomes

$$F_1(u,v,s) = 1 + \sum_{n=1}^{n=\infty} \frac{(m+1)\cdots(m+n)(-m)\cdots(-m-1+n)}{n!1\cdot\frac{1}{2}\cdots(n-\frac{1}{2})}\left(\frac{\lambda s^2}{2v}\right)^n,$$

and is therefore the hypergeometric function $F\left(m-1,-m,\frac{1}{2},\frac{\lambda s^2}{2v}\right)$. In view of (3.9), (3.10), and (3.12) the general solution may be written as

$$Z = v^m \int_{-1}^{+1} \left\{F\left(m+1,-m,\frac{1}{2},\frac{\lambda s^2}{2v}\right) f[\lambda(1-s^2)] + F\left(m+1,-m,\frac{1}{2},\frac{\mu s^2}{2v}\right) g[\mu(1-s^2)]\right\} \frac{ds}{(1-s^2)^{1/2}}, \tag{3.15}$$

in which f and g are arbitrary functions. This formula is an extension of the one given in (37), established for the special case of a diatomic perfect gas.

Other results can be reached in terms of derivatives of two arbitrary functions rather than integrals.

We attempt to find a solution in the form

$$X = \sum_{n=1}^{n=\infty} f_n(\lambda)h_n(v). \tag{3.16}$$

Upon substitution in (3.11) we find

$$\sum_{n=0}^{n=\infty}\left(h_n'' - \frac{2m}{v}h_n'\right)f_n + 2\left(h_n' - \frac{m}{v}h_n\right)f_n' = 0. \tag{3.17}$$

This relation can be satisfied by taking

$$f_n(\lambda) = f_{n-1}'(\lambda) \quad \text{and} \quad h_n(v) = \alpha_n v^{n+\gamma},$$

with γ a constant, provided α_n is chosen so that

$$\alpha_n[(n+\gamma) - m]v^{n+\gamma-1}f_n' \to 0 \quad \text{for} \quad n \to \infty,$$
$$\alpha_0\gamma(\gamma - 2m - 1) = 0$$

and

$$\alpha_n(n+\gamma)(n+\gamma-2m-1) + 2\alpha_{n-1}(n+\gamma-m-1) = 0. \tag{3.18}$$

The first condition may be assumed inasmuch as $\alpha_n v^\gamma f_n$ must go toward zero to have the series (3.16) convergent. The second requires (a)

$\gamma = 0$ or (b) $\gamma = 2m + 1$, to avoid $\alpha_0 = 0$, and thereby all coefficients vanishing. Taking $\alpha_0 = 1$, the recurrence formula (3.18) enables one to compute successively all the coefficients.

(a) $$\gamma = 0.$$

Relation (3.18) becomes

$$\alpha_n = -\frac{2}{n}\frac{m-n+1}{2m-n+1}\alpha_{n-1}$$

or with $\alpha_0 = 1$

$$\alpha_n = (-1)^n \frac{2^{n-1}}{n!}\frac{(m-1)\cdots(m-n+1)}{(2m-1)\cdots(2m-n+1)}$$
$$= (-1)^n \frac{2^{n-1}}{n!}\frac{\Gamma(m)\Gamma(2m-n+1)}{\Gamma(2m)\Gamma(m-n+1)}.$$

It is seen here that if m is a positive integer this series is reduced to a polynomial since $\alpha_n = 0$ for $n > m$.

(b) $$\gamma = 2m + 1$$

Hence

$$\alpha_n = -\frac{2}{n}\frac{m+n}{2m+n+1}\alpha_{n-1}$$

or

$$\alpha_n = (-1)^n \frac{2^{n-1}}{n!}\frac{(m+n)\cdots(m+2)}{(2m+n+1)\cdots(2m+3)}$$
$$= (-1)^n \frac{2^{n-1}}{n!}\frac{\Gamma(-m+1)\Gamma(-2m-n-1)}{\Gamma(-m-n)\Gamma(-2n-2)}.$$

This time, this series reduces to a polynomial for m a negative integer since now $\alpha_n = 0$ for $n > -m - 1$.

The same procedure can be followed to determine a solution of the type

$$Y = \sum_{n=0}^{n=\infty} g_n(\mu)h_n(v).$$

It follows that the general solution takes the form

$$\text{(3.19)} \quad Z = X + Y = Z_0 + \sum_{n=1}^{n=\infty} (-1)^n \frac{2^{n-1}}{n!}\frac{\Gamma(m)\Gamma(2m-n+1)}{\Gamma(2m)\Gamma(m-n+1)} v^n Z_0^{(n)}$$

in the case (a), and

$$\text{(3.20)} \quad Z = v^{1+2m}\left[Z_0 + \sum_{n=1}^{n=\infty} (-1)^n \frac{2^{n-1}}{n!}\frac{\Gamma(-m+1)\Gamma(-2m-n-1)}{\Gamma(-m-n)\Gamma(-2m-2)} v^n Z_0^{(n)}\right]$$

in the case (b), in which $Z_0^{(n)}$ denotes the expression

$$\frac{d^n f_n(\lambda)}{d\lambda^n} + \frac{d^n g_n(\mu)}{d\mu^n},$$

which could be expressed by Cauchy's integral formula, see (15).

The study of the convergence of these series would be similar to the one given by Bergman for the general case.

Formula (3.19) can be given in closed form by an integral operator if it is noticed that the X term represents actually a Taylor development of the function

$$F = \int_0^1 \varphi_0(\lambda - 2\nu t)t^{-(m+1)}(1 - t)^{-(m+1)}dt,$$

where

$$\varphi_0(\lambda) = \frac{\Gamma(-m)\Gamma(-m)}{\Gamma(-2m)} f_0(\lambda).$$

The general term of the development reads

$$(-1)^n \frac{2^n}{n!} \frac{d\varphi_0{}^n(\lambda)}{d\lambda^n} \int_0^1 t^{n-m-1}(1 - t)^{-m-1}dt$$
$$= \frac{(-1)^n 2^n}{n!} \nu^n \frac{\Gamma(n - m)\Gamma(-2m)}{\Gamma(n - 2m)\Gamma(-m)} \frac{df_0{}^n(\lambda)}{d\lambda^n}$$

or

$$(-1)^n \frac{2^{n-1}}{n!} \frac{(-m + 1) \cdots (-m + n - 1)}{(-2m + 1) \cdots (-2m + n - 1)} \nu^n \frac{df_0{}^n(\lambda)}{d\lambda^n},$$

which is seen to be the general term of the series X. Since similar considerations apply to Y, the general solution is finally given by the formula

$$(3.21) \qquad Z = \int_0^1 [\varphi(\lambda - 2\nu t) + \psi(\mu - 2\nu t)]t^{-(m+1)}(1 - t)^{-(m+1)}dt$$

where φ and ψ are arbitrary functions. The infinite series (3.20) would also lead to a simple integral formula.

IV. The Initial Value Problem

The velocity and the density, i.e., u and ν or r and s, being given over a certain range of x at time $t = 0$, the problem is to determine the subsequent motion of the fluid.

This problem can be transposed into the speed plane or the r,s-plane and the application of Riemann's method gives then a continuous solution, if some restrictive conditions are imposed to the initial values. In the general case, a continuous solution can still be constructed, after von Mises (38), by a proper patching of integrals. The introduction by Ludford (40) of an unfolding procedure extends the validity of Riemann's

formula to the general case and thereby provides a means to discuss the occurrence of singularities.

1. *Riemann's Method: Martin's Solution*

Taking r and s as independent variables, Eq. (2.14) reads

$$V_{rs} + \alpha(V_r + V_s) = 0 \tag{4.1}$$

in which

$$\alpha = \alpha(r + s) = \frac{1}{2a}\left(1 - \frac{da}{dv}\right), \tag{4.2}$$

and the relations (2.11) take the form

$$V_r = x - (u + a)t, \quad -V_s = x - (u - a)t. \tag{4.3}$$

The initial conditions determine a curve C in the r,s-plane along which, according to (4.3), the values of V_r and V_s are prescribed. Under the condition that C is a smooth curve nowhere tangent to a characteristic line of (4.1) one may obtain, see (33), the value of V at a point $P(r = \xi, s = \eta)$ by the Riemann formula

$$V(P) = \int_{P_1}^{P_2} [X \cos(n,r) + Y \cos(n,s)]d\sigma + \tfrac{1}{2}[(WY)_{P_1} + (WV)_{P_2}], \tag{4.4}$$

and determine x and t through (4.3). The points P_1 and P_2 denote here, respectively, the intersection of C with the lines $r = \xi$, $s = \eta$, and $(n,d\sigma)$

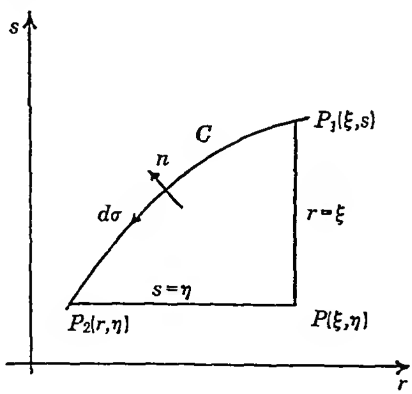

FIG. 1

is taken as a right-hand system, see Fig. 1; X and Y stand for

$$X = \tfrac{1}{2}(WV_s - VW_s) + \alpha VW,$$
$$Y = \tfrac{1}{2}(WV_r - VW_r) - \alpha VW;$$

and W is the Riemann function defined as a solution of the adjoint

equation,

$$W_{rs} - \alpha(W_r - W_s) - (\alpha_r - \alpha_s)W = 0,$$

satisfying the additional conditions

$$\begin{aligned} W(\xi,\eta) &= 1, \\ W_r &= \alpha W \quad \text{for } s = \eta, \\ W_s &= \alpha W \quad \text{for } r = \xi. \end{aligned}$$

Riemann's procedure was recently simplified by Martin (26) by introducing a function similar to the Riemann function but subject to simpler boundary conditions.

We consider, this time, together with (4.1) the conjugate equation

$$U_{rs} - \alpha(U_r + U_s) = 0. \tag{4.5}$$

It is easily verified that

$$(V_r U_r)_s = -(V_s U_s)_r$$

and therefore that the integral

$$\int (V_r U_r \, dr - V_s U_s \, ds) \tag{4.6}$$

taken around any closed path is equal to zero. Using for a closed path the contour P, P_1, P_2 of Fig. 1, (4.6) reads

$$-\int_P^{P_1} V_s U_s \, ds + \int_{P_1}^{P_2} V_r U_r \, dr - V_s U_s \, ds + \int_{P_2}^{P} V_r U_r \, dr = 0. \tag{4.7}$$

If a solution $U = U(r,s)$ of (4.5) satisfies furthermore the conditions

$$\begin{aligned} U &= r - \xi \quad \text{for } s = \eta, \\ U &= s - \eta \quad \text{for } r = \xi, \end{aligned}$$

the relation (4.7) becomes

$$V(P) = \tfrac{1}{2}[V(P_1) + V(P_2)] - \tfrac{1}{2} \int_{P_1}^{P_2} (V_r U_r \, dr - V_s U_s \, ds) \tag{4.8}$$

and hence gives the value of V at P in terms of its values at P_1 and P_2 and its partial derivatives along the monotone arc C. The problem is therefore reduced to the determination of the "resolvent" $U = U(r,s;\xi,\eta)$ which, like the Riemann function, depends on four variables r,s,ξ,η.

It can be proved, see (26), that the relations

$$U_r + U_\xi = 0, \quad U_s + U_\eta = 0 \tag{4.9}$$

hold respectively along the lines $r = \xi$ and $s = \eta$. We can also establish, by differentiating (4.8) partially with respect to ξ and η, the formulas

$$
(4.10)\qquad
\begin{aligned}
V_\xi(P) &= \tfrac{1}{2}V_r(P_1)[1 + U_r(P_1)] - \tfrac{1}{2}\int_{P_1}^{P_2} (V_r U_{r\xi} dr - V_s U_{s\xi} ds),\\
V_\eta(P) &= \tfrac{1}{2}V_s(P_2)[1 + U_s(P_2)] - \tfrac{1}{2}\int_{P_1}^{P_2} (V_r U_{r\eta} dr - V_s U_{s\eta} ds).
\end{aligned}
$$

We insert now in (4.10) the initial values

$$
(4.11)\qquad V_r = x, \quad -V_s = x
$$

obtained from (4.3) by setting $t = 0$. The result is

$$
(4.12)\qquad
\begin{aligned}
V_\xi(P) &= \tfrac{1}{2}x(P_1)[1 + U_r(P_1)] - \tfrac{1}{2}\int_{P_1}^{P_2} x d(U_\xi)\\
V_\eta(P) &= -\tfrac{1}{2}x(P_2)[1 + U_s(P_2)] - \tfrac{1}{2}\int_{P_1}^{P_2} x d(U_\eta).
\end{aligned}
$$

After integrating by parts and using relations (4.9) and the fact that $U_\eta(P_1) = -1$, $U_\xi(P_2) = -1$, we get

$$
(4.13)\qquad
\begin{aligned}
V_\xi(P) &= \tfrac{1}{2}[x(P_1) + x(P_2)] + \tfrac{1}{2}\int_{x(P_1)}^{x(P_2)} U_\xi dx\\
V_\eta(P) &= -\tfrac{1}{2}[x(P_1) + x(P_2)] + \tfrac{1}{2}\int_{(P_1)}^{x(P_2)} U_\eta dx.
\end{aligned}
$$

The prescribed initial conditions which determine the curve C can be expressed in the form

$$
(4.14)\qquad r = \varphi(x), \quad s = \psi(x)
$$

where, according to our restrictions, the functions $\varphi'(x)$ and $\psi'(x)$ are continuous and different from zero. In Eq. (4.13) $x(P_1)$ and $x(P_2)$ are, respectively, the inverse functions of $\xi = \varphi(x)$ and $\eta = \psi(x)$.

In view of (4.3) the initial problem is finally resolved by the relations

$$
(4.15)\qquad
\begin{aligned}
x - (u + a)t &= \tfrac{1}{2}[\varphi^{-1}(r) + \psi^{-1}(s)] + \tfrac{1}{2}\int_{\varphi^{-1}(r)}^{\psi^{-1}(s)} U_r dx,\\
x - (u - a)t &= \tfrac{1}{2}[\varphi^{-1}(r) + \psi^{-1}(s)] - \tfrac{1}{2}\int_{\varphi^{-1}(r)}^{\psi^{-1}(s)} U_s dx,
\end{aligned}
$$

in which ξ and η are now denoted by r and s and $U = U[\varphi(x),\psi(x);r,s]$.

The function U can be explicitly computed for polytropic fluids. Its determination leads to the generalized integral equation of Abel whose solution yields a formula for U involving Appell's hypergeometric function of two variables, see (26).

2. von Mises' Solution: Case of a Diatomic Perfect Gas

The fluid motion being governed by differential equations of hyperbolic type, the method of characteristics furnishes a step-by-step procedure for solving the general case. This method, initiated by Kobes (11), was developed by Sauer (22,23,24), Schultz-Grunow (20,25) and

von Mises (38). von Mises' approach stresses, in particular, the integration problems involved in the analytical treatment of the problem and leads to the construction of a continuous analytical solution.

We note first that, once u,v are taken as variables, Eqs. (2.4) and (2.5) become

$$au_x + uv_x + v_t = 0,$$
$$uu_x + av_x + u_t = 0,$$

and yield, after addition and subtraction,

$$(u + a)(v + u)_x + (v + u)_t = 0,$$
$$(u - a)(v - u)_x + (v - u)_t = 0.$$

These relations show that the curves, $dx/dt = u \pm a$, in the physical plane, are mapped, in the speed plane, into the lines: $v + u =$ constant,

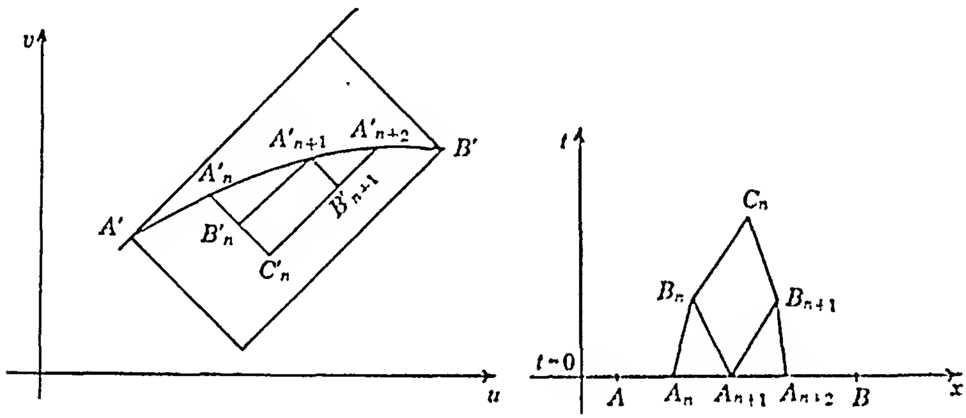

FIG. 2

i.e., straight lines of slope ∓45°. They are the characteristic curves in both planes.

The values of u and v being given for $t = 0$ over a certain range of x, a segment AB of the x-axis can be mapped, point by point, into a line $A'B'$ of the speed plane. We start with the assumption that at no points along $A'B'$ do the tangents have the directions ±45° and readily obtain the network of characteristics in the speed plane by choosing a sequence of points $A_1', A_2', \cdots$ on $A'B'$ and drawing through them the ±45° lines, see Fig. 2. To the points $A_1', A_2', \cdots$ correspond definite points $A_1, A_2, \cdots$ on the x-axis in the physical plane between A and B. For each such point, A_n, we have, by the use of the relation $dx/dt = u \pm a$, the two characteristic directions passing through it. The successive intersections of the characteristic elements through A_n and A_{n+1} supply a sequence of points B_n which are mapped into the intersections B_n' of the characteristics in the speed plane. The procedure can be repeated by

deriving, from the position B_n', the characteristic directions through B_n and thus getting a new sequence C_n, etc. The process ends obviously after a number of steps equal to the number of intermediate points $A_1', A_2', \cdots$ originally assumed. The result is a network whose nodal points are mapped into the cross points of the characteristic network in the speed plane from which we started. To each of these points $B_n, C_n, \cdots$ in the x,t-plane corresponding values of u and v are given by $B_n', C_n', \cdots$ and this gives the solution of the initial value problem.

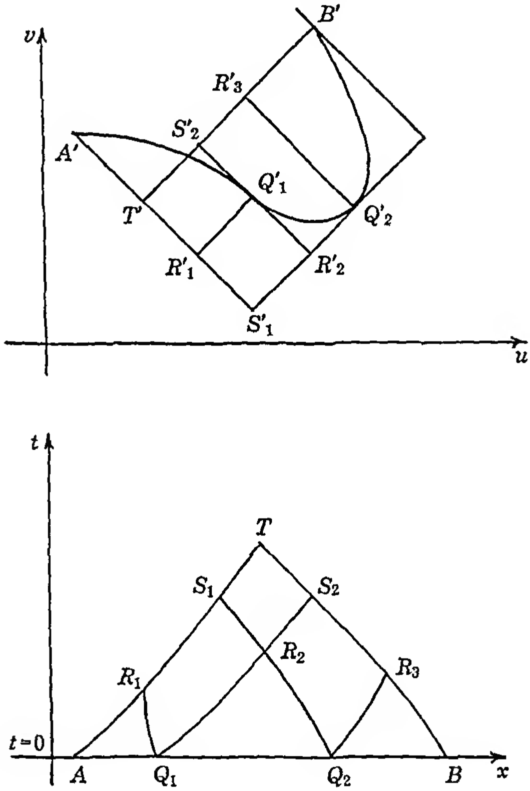

FIG. 3

We now consider the general case where the tangents along $A'B'$ take any direction; $A'B'$ consists then of a certain number of arcs along which the tangents have a slope different from $\pm 45°$. Let us take the case of Fig. 3 where the curve $A'B'$ has tangents in the characteristic directions at Q_1' and Q_2'. The former procedure supplies the solution in the triangular regions AQ_1R_1, $Q_1Q_2R_2$, and Q_2BR_3. The network of characteristics in the speed plane rectangle $Q_1'R_1'S_1'R_2'$ is also known and once it is transferred into the physical plane, the solution in the region Q_1R_1-S_1R_2 is obtained. The same holds for the rectangle $Q_2'R_2'S_2'R_3'$ in the

u,v-plane and the curvilinear quadrangle $Q_2R_2S_2R_3$ in the x,t-plane. Finally the speed plane rectangle $R_2'S_2'T'S_1'$ has to be considered and mapped into the quadrangle $R_2S_2TS_1$ of the physical plane.

From these considerations it is clear that a complete analytical solution involves two initial value problems defined by the following conditions: (a) u and v are given for $t = 0$ along a segment of the x-axis such that at no point within the segment, dv/du takes one of the values ± 1; (b) two characteristic curves are given in the x,t-plane with compatible values of u and v prescribed along them. Integrals of these two problems allow to construct, as shown above, a continuous solution which may, of course, be multiple valued in the speed plane.

It can happen that in the general case a solution does not exist. This will be the case, for instance, if the two characteristics Q_1R_1 and Q_1R_2 in the physical plane (which are independently determined, one by the data along AQ_1, the other by those along Q_1Q_2) intersect somewhere. Such occurrences will be discussed in Section IV,3.

The solution of problems (a) and (b) are now given for a diatomic perfect gas. For this special case we have, after (2.3) $v = 5a$ and Eqs. (2.11) and (2.14) become then

$$V_u = x - ut, \quad V_v = -\frac{v}{5}\,t, \tag{4.16}$$

and

$$V_{vv} - V_{uu} = -\frac{4}{v}\,V_v. \tag{4.17}$$

Instead of the Riemann method we shall make use in this example of a general integral of Eq. (4.17) and apply formula (3.20) with $m = -2$. The result is

$$V(u,v) = \frac{f(\lambda) + g(\mu)}{v^3} - \frac{f'(\lambda) + g'(\mu)}{v^2}, \tag{4.18}$$

where $f(\lambda)$ and $g(\mu)$ denote arbitrary functions.[2]

Solution of Problem (*a*). Two functions $u = u(x)$, $v = v(x)$ are given on a segment AB of the x-axis at $t = 0$. They map AB into an arc $A'B'$ in the speed plane which has at no point a tangent of slope $\pm 45°$. To each point P' inside the characteristic triangle $A'B'C'$, see Fig. 4, correspond in this case two distinct points P_1' and P_2', on $A'B'$, the first having the same λ value as P', the second the same μ value. The abscissas of the corresponding points P_1 and P_2 on AB may be called $x(\lambda)$ and $x(\mu)$. For points P' on $A'B'$, and only for those, $x(\lambda)$ coincides with

[2] Similar general integrals were also considered by Bechert (15) and Pfriem (19) who restricted, however, their applications almost exclusively to the trivial case of $m = 0$.

$x(\mu)$. It is to be noted that $x(\lambda)$ is a known function of λ, namely the inverse of $v(x) + u(x)$ and $x(\mu)$ a known function of μ, the inverse of $v(x) - u(x)$.

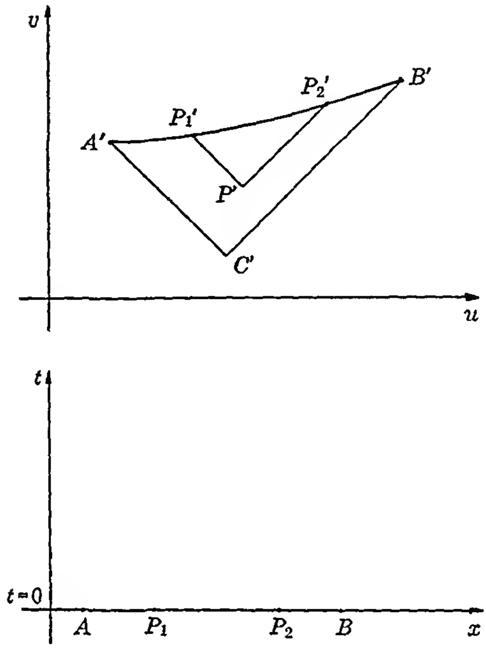

FIG. 4

The problem is to find an expression for $V(u,v)$ such that for u,v lying on $A'B'$, i.e., for $x(\lambda) = x(\mu) = x$,

$$V_u = x, \quad V_v = 0, \tag{4.19}$$

according to (4.16). In view of (4.18) the conditions (4.19) become

$$\begin{aligned} f' - g' - v(f'' - g'') &= v^3x, \\ 3(f + g) - 3v(f' + g') + v^2(f'' + g'') &= 0. \end{aligned} \tag{4.20}$$

We assume $f(\lambda)$ and $g(\mu)$ in the following form:

$$\begin{aligned} f(\lambda) &= A[x(\lambda)] + \lambda B[x(\lambda)] + \lambda^2 C[x(\lambda)], \\ g(\mu) &= -A[x(\mu)] + \mu B[x(\mu)] - \mu^2 C[x(\mu)], \end{aligned} \tag{4.21}$$

where $A(x)$, $B(x)$, $C(x)$ are three functions of one variable. By differentiation we find, with $x(\lambda) = x(\mu) = x$,

$$\begin{aligned} f' &= B + 2\lambda C + Y_1, & g' &= B - 2\mu C + Y_2, \\ f'' &= 2C + Z_1, & g'' &= -2C + Z_2, \end{aligned} \tag{4.22}$$

where the Y and Z are determined by

$$
(4.23)\qquad
\begin{aligned}
Y_1\frac{d\lambda}{dx} &= A' + \lambda B' + \lambda^2 C', & Y_2\frac{d\mu}{dx} &= -A' + \mu B' - \mu^2 C',\\
Z_1\frac{d\lambda}{dx} &= Y_1' + B' + 2\lambda C', & Z_2\frac{du}{dx} &= Y_2' + B' - 2\mu C'.
\end{aligned}
$$

If (4.21) and (4.22) are introduced in (4.20) these conditions become

$$
(4.24)\qquad
\begin{aligned}
Y_1 - Y_2 - v(Z_1 - Z_2) &= v^3 x\\
3(Y_1 + Y_2) - v(Z_1 + Z_2) &= 0.
\end{aligned}
$$

Equations (4.23) and (4.24) are six linear equations for the seven variables A', B', C', Y_1, Y_2, Z_1, Z_2. (Since we used three functions to represent f and g, we have one extra variable.) If we decide to make $Y_1 = Y_2$ a formal computation yields, see (38),

$$
(4.25)\qquad
\begin{aligned}
A' &= \frac{v}{4}\left[x(v^2 - u^2) + 2Vu\right]\frac{dv}{dx} + \frac{V}{4}(v^2 - 3u^2)\frac{du}{dx},\\
B' &= \frac{v}{2}\left[xu - V\right]\frac{dv}{dx} + \frac{3}{2}Vu\frac{du}{dx},\\
C' &= -\frac{v}{4}x\frac{dv}{dx} - \frac{3V}{4}\frac{du}{dx}.
\end{aligned}
$$

Here, the right-hand sides are functions of x, entirely determined by the two given functions $u(x)$, $v(x)$. Their indefinite integrals are $A(x)$, $B(x)$, $C(x)$. If we introduce for x first the value $x(\lambda)$ expressed in terms of λ and second $x(\mu)$ in terms of μ, we find $f(\lambda)$, $g(\mu)$ according to (4.21). $V(u,v)$ is then obtained by (4.18) and supplies x and t as functions of u and v through (4.16).

Solution of Problem (*b*). If a characteristic in the x,t-plane is represented in the form $x = \varphi(t)$, there hold two relations between the functions $\varphi(t)$, $u(t)$, $v(t)$ ($u(t)$ and $v(t)$ representing the u- and v-values along the characteristic curve). These relations are

$$
(4.26)\qquad \text{either}\begin{cases} v + u = \text{const.}\\ \dfrac{dx}{dt} = \varphi' = u + a,\end{cases}\qquad \text{or}\begin{cases} v - u = \text{const.}\\ \dfrac{dx}{dt} = \varphi' = u - a.\end{cases}
$$

Consequently, only one of the three functions can be chosen arbitrarily. We may also use the inverse of one of the function, say $t(v)$, assuming that both t and v are given as continuous functions of one monotonically changing parameter, e.g., of the arc length on the characteristic curve. This leads to the following formulation of the problem.

Two functions $t = \alpha(v)$ and $t = \beta(v)$ are given, the first holding along a $(u - a)$-characteristic, the latter along a $(u + a)$-characteristic. Both

curves pass through a point C for which $u = u_1$, $v = v_1$, $v + u = \lambda = \lambda_1$ and $v - u = \mu = \mu_1$. Without loss of generality we may assume $t = 0$ at this point, that is, $\alpha(v_1) = \beta(v_1) = 0$. The problem is to find the solution of (4.17) that fulfils the conditions

$$\begin{aligned} &t = \alpha(v) \text{ for } v - u = v_1 - u_1,\ v = \tfrac{1}{2}(\lambda + \mu_1), \quad \mu = \mu_1 \\ &t = \beta(v) \text{ for } v + u = v_1 + u_1,\ v = \tfrac{1}{2}(\lambda_1 + \mu), \quad \lambda = \lambda_1. \end{aligned} \tag{4.27}$$

Taking the derivatives of V expressed in terms of f and g by (4.18) and introducing them in (4.16), we find the general relation between t and the two functions $f(\lambda)$, $g(\mu)$ as follows

$$\tfrac{1}{5}v^5 t = 3f - 3vf' + v^2 f'' + 3g - 3vg' + v^2 g''.$$

It is clear that conditions (4.27) provide then one linear second order ordinary differential equation for $f(\lambda)$ and another for $g(\mu)$. They furnish the following particular integrals, see (38):

$$f(\lambda) = \tfrac{1}{20}(\lambda + \mu_1)^3 \int_{v_1}^{(\lambda+\mu_1)/2} (\lambda + \mu_1 - 2z)\alpha(z)dz, \tag{4.28}$$

and

$$g(\mu) = \tfrac{1}{20}(\lambda_1 + \mu)^3 \int_{v_1}^{(\lambda_1+\mu)/2} (\lambda_1 + \mu - 2z)\beta(z)dz,$$

which determine x and t through (4.18) and (4.16).

3. *Occurrence of Singularities in the Motion of a Polytropic Fluid: Ludford's Theorem*

It has been noted above that formula (4.4) was only valid if the curve C (Fig. 1) had nowhere a tangent parallel to the r- or s-axis. In most cases, however, the initial conditions do not meet this requirement and an analytical investigation of the subsequent motion can only be achieved by successive integrations of problems of type (a) and (b). This approach, although leading to the construction of a complete solution, does not provide any explicit analytical connection between the various integrals and the initial conditions. A new representation of the solution introduced by Ludford (40) allows such a relation to be found.

We consider the case where the curve C is tangent to a characteristic at some point, say at the point O of Fig. 5. We know from the considerations developed in Section IV,2 that the initial conditions along AB will determine a continuous solution composed of three integrals patched along the characteristics OD and OE. The first integral is defined in the triangular region AOD, the second in the rectangle $DOEB'$, and the third in the triangular region OBE. This solution which is multiple valued in the region OBE of the r,s-plane becomes one-valued if one unfolds

Fig. 5 so as to form Fig. 6. In this diagram the region OBE has been turned about the line OE and B and B' fall then on distinct points. Further, the value of s varies according to the graph at the right of the figure whereas the value of r varies as before.

Formula (4.4) can be applied in the usual way in the region AOD and may be used also in the region OBE provided the normal along OB has been reflected in OE. A slight modification of this formula yields an

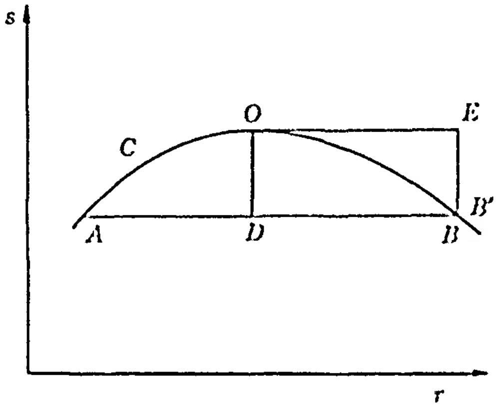

FIG. 5

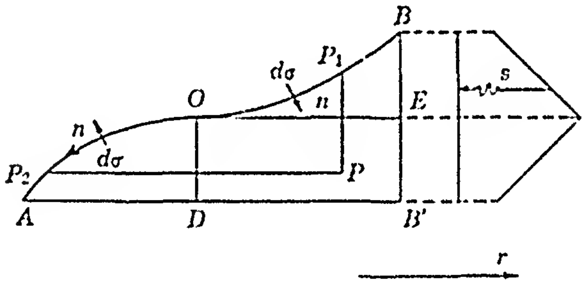

FIG. 6

expression valid throughout the entire region $AOBB'$ of the unfolded diagram. We express the curve C parametrically in the form

$$r = \varphi(x), \quad s = \psi(x);$$

X and Y become functions of x and (4.4) can be written

$$V(P) = \int_{x_1}^{x_2} [X\psi' - Y\varphi']dx + \tfrac{1}{2}[(WV)_{P_1} + (WV)_{P_2}], \tag{4.29}$$

where x_1 and x_2 are the values of the parameter x at the points P_1 and P_2 respectively. It can be easily seen, see (40), that this new relation holds throughout the region $AOBB'$ if P_1 and P_2 are respectively the intersections of the curve AOB with the $r = \xi$ and $s = \eta$ characteristics going through P, see Fig. 6.

The case in which either $\varphi'(x)$ or $\psi'(x)$ has a discontinuity at O may be treated similarly.

This procedure can be applied to discuss the occurrence of singularities in the motion of a polytropic fluid. We mentioned above the possibility of obtaining from given initial conditions solutions which at some time may become multiple valued in the physical plane. Such is the case if the Jacobian of the transformation $J = \partial(x,t)/\partial(r,s)$ vanishes along some curve in the speed plane. If we make use of the characteristic equations, see (30) p. 89,

$$x_r = (u - a)t_r, \quad x_s = (u + a)t_s, \tag{4.30}$$

which may be obtained through (2.4) and (2.5) by interchanging the role of variables, J takes the form

$$J = x_r t_s - x_s t_r = -2at_r t_s.$$

The breakdown of the solution will happen therefore when either t_r or t_s is zero along some curve in the speed plane.

In the following we assume that the initial values are such that (1) the functions $r = \varphi(x)$, $s = \psi(x)$ converge to finite limits as $x \to \mp\infty$; (2) $\varphi'(x)$, $\psi'(x)$ exist and are piecewise continuous; (3) $\varphi'(x)$, $\psi'(x)$ are zero at a finite number of points x, at most.

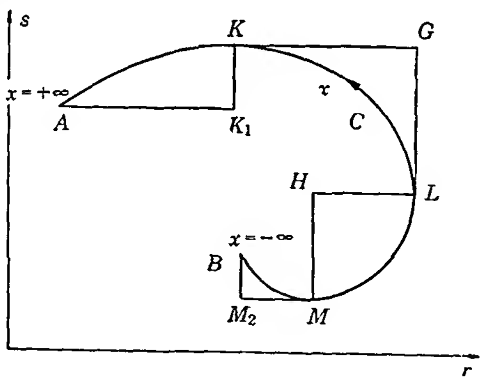

FIG. 7

For the convenience of the discussion we choose $\kappa > 1$ and consider the initial curve C of Fig. 7 and the corresponding unfolded diagram given in Fig. 8. The results can be easily extended to other cases.

Along C we have $t = 0$ and therefore

$$dt = (t_r\varphi' + t_s\psi')dx.$$

From relations (4.30) we get

$$dx = (u - a)t_r\varphi'dx + (u + a)t_s\psi'dx.$$

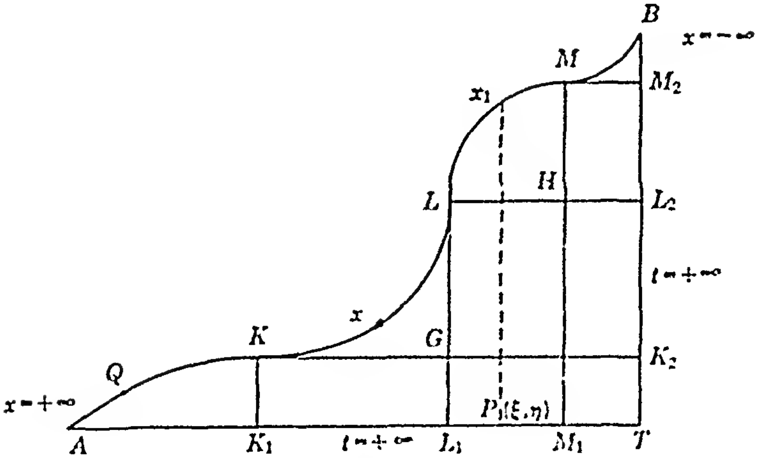

FIG. 8

Hence the initial values of t_r and t_s are

$$t_r = -\frac{1}{(\kappa - 1)\varphi'(\varphi + \psi)}, \tag{4.31}$$

$$t_s = \frac{1}{(\kappa - 1)\psi'(\varphi + \psi)}, \tag{4.32}$$

since $a = \dfrac{\kappa - 1}{2} v$ for polytropic fluids. The differential equation for t is given by (2.18) or can also be obtained by elimination of x in (4.30). In the case of a polytropic fluid and with the r,s-coordinates, it becomes

$$t_{rs} - \frac{m}{r + s}(t_r + t_s) = 0, \tag{4.33}$$

where $m = -\dfrac{\kappa + 1}{2(\kappa - 1)}$. The Riemann function of Eq. (4.33) is, see (33).

$$w(r,s;\xi,\eta) = \left(\frac{r + s}{\xi + \eta}\right)^{-m} F(1 + m, -m, 1; z) \tag{4.34}$$

where F denotes a hypergeometric function and $z = -\dfrac{(r - \xi)(s - \eta)}{(r + s)(\xi + \eta)}$. In view of the initial values (4.31) and (4.32), formula (4.29) becomes then

$$t(P) = \frac{1}{\kappa - 1}\int_{x_1}^{x_2} \frac{w(\varphi,\psi;\xi,\eta)}{(\varphi + \psi)}\,dx \tag{4.35}$$

and according to the previous paragraph is valid throughout the region ABT of Fig. 8. From this relation we can get by differentiation

$$t_\xi = \frac{1}{\kappa - 1}\left[\int_{x_1}^{x_2} \frac{1}{\varphi + \psi}\, w_\xi dx - \frac{\xi + \psi(x_2)^{-m-1}}{(\xi + \eta)^{-m}}\frac{dx_1}{d\xi}\right], \tag{4.36}$$

where w_ξ is obtained from (4.34),

$$w_\xi = m\frac{(r+s)^{-m}}{(\xi+\eta)^{-m+1}}F(1+m,-m,1;z) + \frac{-m(1+m)(s-\eta)(r+\eta)(r+s)^{-m-1}}{(\xi+\eta)^{-m+2}}F(2+m,1-m,2;z),$$

see (40).

We note that for points Q on C close to A the Riemann function, w, takes positive values since z is then small and F close to unity. It follows then from (4.35) that $t = +\infty$ at all points P of AT since $x_2 = +\infty$

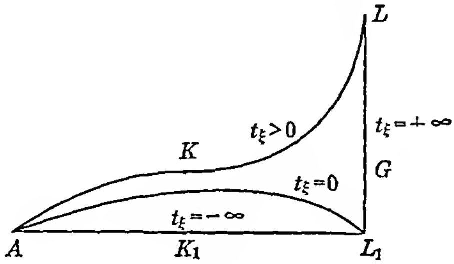

FIG. 9

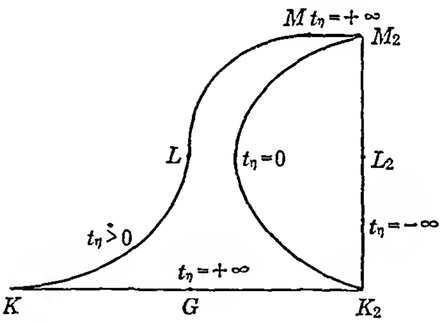

FIG. 10

and x_1 is finite. The same result applies to the points on BT and therefore the region ABT corresponds to the region $t > 0$ in the physical plane. By a similar argument it may be shown that $t_\xi = -\infty$ at every point of AT except L_1 (with the relation 4.36), and that $t_\eta = -\infty$ at every point of BT except K_2 and M_2. On LL_1, $t_\xi \to +\infty$ from the left and $-\infty$ from the right, on KK_2, $t_\eta \to -\infty$ from below and $+\infty$ from above; finally on $MM_2, t_\eta \to +\infty$ from below and $-\infty$ from above.

It can be seen from (4.36) that t_ξ is a continuous function of ξ,η in the region ALL_1. If we assume therefore that $\varphi'(x) < 0$, the relation (4.31) shows that t_ξ is positive on AL which, in view of the results given above, implies that it must vanish along some curve passing through A and L_1, see Fig. 9. Similarly it can be shown that if $\psi'(x) > 0$, t_η must vanish

along some curve in the region $KLMM_2L_2K_2$ passing through M_2 and K_2, see Fig. 10.

These results lead easily to a theorem established by Ludford (40) which states that, under the restrictions imposed on the initial values, it is sufficient to have $\varphi'(x) < 0$ or $\psi'(x) > 0$ for some range of x to insure that a discontinuity will arise in the subsequent motion.

V. Applications

Although a complete analytical solution of the one-dimensional flow has been available since Riemann, few problems related to this motion have been solved analytically. As Hugoniot (8) pointed out, the question consists always in building up a group of integrals compatible with each other and with the initial and boundary conditions. Considering only continuous solutions, the compatibility condition requires the integral surfaces to be tangent to each other along the characteristic lines. Incidently this implies, as shown above, Section IV,2, that the initial value problem reduces to problems (a) and (b).

The simplest cases, solutions compatible with rest (which are the simple waves) and those compatible with two simple waves, received an extensive study. The first problem was treated, with different approaches, by Earnshaw (6), Hugoniot (8), Kobes (11), Pfriem (16,17). The second was encountered by Gossot and Liouville (12) and later by Love and Pidduck (14) in their attempt to solve Lagrange's ballistic problem. The original Riemann's method was used throughout, and the analysis required an excessive number of calculations. von Mises' method provides a simple solution which is given below.[3]

1. *Interactions of Simple Waves*

As an application to the method outlined in Section IV,2 we consider the interaction of two centered simple waves for $\kappa = 1.4$. At $t = 0$ the fluid may be at rest in the interval $(-c,c)$ and its pressure and density be represented by $v = v_1$. The waves centered in $x = \pm c$, $t = 0$ meet at the point C, see Fig. 11, with coordinates

$$x = 0, \quad t = t_1 = \frac{c}{a_1} = \frac{5c}{v_1}.$$

Along the two cross characteristics starting at this point, t changes inversely proportional to the third power of v, according to the formulas for simple waves, see (30). To be in agreement with our assumptions

[3] The use in this problem of a general solution in terms of two arbitrary functions was also considered by Taub (29).

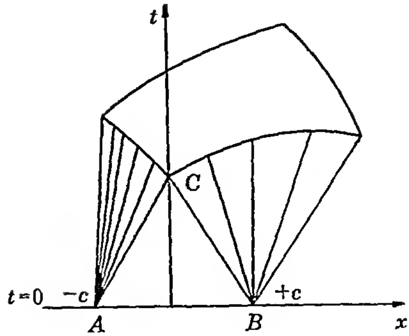

FIG. 11

we have to count the time as beginning in C. Thus we introduce

$$t' = t - t_1 = t - \frac{5c}{v_1}.$$

The functions $\alpha(v)$ and $\beta(v)$ are then

$$t' = \alpha(v) = \frac{5c}{v_1}\left(\frac{v_1^3}{v^3} - 1\right) = \beta(v).$$

Since in our case $u = 0$ at the point C, we have $\lambda_1 = \mu_1 = v_1$ and from (4.28)

$$f(\lambda) = \frac{c}{16v_1}(\lambda^2 - v_1^2)^2(v_1 - \lambda),$$
$$g(\mu) = \frac{c}{16v_1}(\mu^2 - v_1^2)^2(v_1 - \mu).$$

If these expressions are introduced in (4.18) and λ,μ replaced by $(v \pm u)$ we find

$$V(u,v) = \frac{c}{8v_1v^3}[(v_1^2 - v)(v_1 - v)(v_1^2 + v_1v + 4v^2) - 2u^2(v_1^3 + 3v_1v^2 - 10v^3) + u^4v_1].$$

The derivatives V_u and $-V_v$ give $x - ut'$ and $vt'/5$, respectively, and the result in terms of t, finally becomes

$$x - ut = \frac{cu}{2v^3}(u^2 - 3v^2 - v_1^2),$$
$$t = \frac{5c}{8v^5}[3v^4 + 2v^2v_1^2 + 3v_1^4 - 6u^2(v^2 + v_1^2) + 3u^4].$$

2. The Expansion of a Monatomic Perfect Gas into a Vacuum

The special case of $\kappa = \frac{5}{3}$ is considered and the motion is subject to the following initial conditions. At time $t = 0$ the medium is at rest,

$u = 0$, and the distribution of r and s along the x-axis is given as follows,

$$(5.1) \qquad 0 \le x < h \qquad r = s = r_0(x),$$
$$(5.2) \qquad x < 0 \qquad r = s = r_0(0) = b,$$
$$(5.3) \qquad x > 0 \qquad r = s = r_0(h) = 0.$$

It is assumed in addition that $r_0'(x) < 0$ so that each particle of the nonhomogeneous layer starts to move to the right. At time t the position of the face of the fluid will be $x = x_1(t)$ and on this face the density vanishes, i.e., $r + s = 0$.

This problem was formulated by McVittie (35) and Copson (34) in connection with the expansion of an interstellar gas cloud into a vacuum.

If we consider the initial conditions in the x,t-plane it is seen that in the vicinity of $t = 0$ a continuous solution can be constructed with four integrals, see Fig. 12. A state of rest is defined by (5.2) in the region

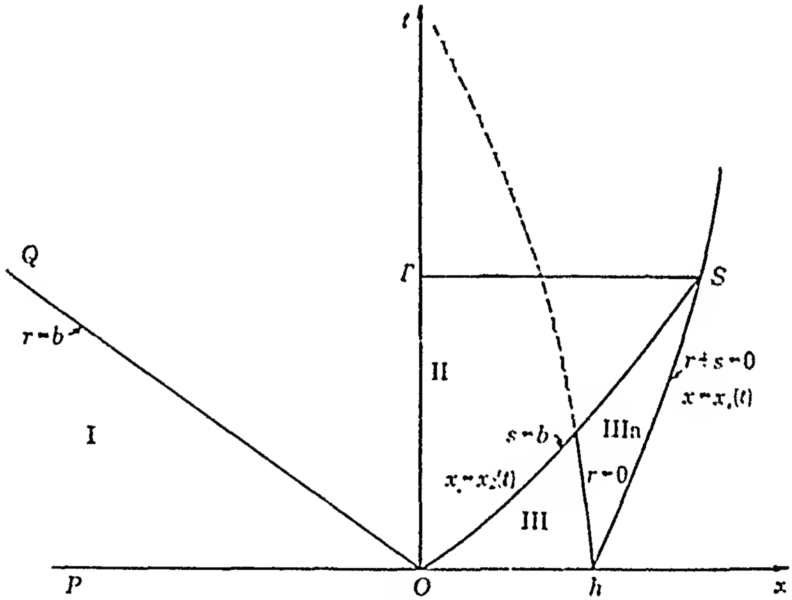

FIG. 12

I limited by the negative side of the x-axis and the characteristic $r = b$. The condition (5.1) determine a solution in the triangular region III bounded by the portion of the x-axis $0 \le x \le h$ and the two characteristics $x = x_2(t)$ $(s = b)$ and $r = 0$ passing respectively through O and h. A simple wave solution will be valid in region II since it must be compatible with a state of rest. The difficulty consists in finding an integral in region IIIa which is compatible with the solution in region III and also satisfies the condition $r + s = 0$ along the unknown boundary $x = x_1(t)$.

We start by looking for the analytical solution in region III. For $\kappa = \frac{5}{3}$ Eqs. (4.1) and (4.3) become

$$V_{rs} + \frac{1}{r+s}(V_r + V_s) = 0 \tag{5.4}$$

and

$$V_r = x - (u+a)t, \quad -V_s = x - (u-a)t. \tag{5.5}$$

The general solution

$$V = \frac{f(r) + g(s)}{r+s}$$

of (5.4) can easily be obtained through formula (3.20) and we can rewrite (5.5)

$$\begin{aligned} x - (u+a)t &= \frac{f'}{r+s} - \frac{f+g}{(r+s)^2}, \\ x - (u-a)t &= -\frac{g'}{r+s} + \frac{f+g}{(r+s)^2}. \end{aligned} \tag{5.6}$$

Equating the two values of x, at time $t = 0$, obtained from (5.6) we get the relation

$$\frac{f'(r_0) + g'(r_0)}{r_0} = \frac{f(r_0) + g(r_0)}{r_0^2}$$

which implies $f(r_0) + g(r_0) = 2Ar_0$, where A is a constant. We may therefore write

$$f(r) = Ar + \phi(r), \quad g(r) = Ar - \phi(r)$$

and the relations (5.6) become

$$x - (u+a)t = \frac{\phi'(r)}{r+s} - \frac{\phi(r) - \phi(s)}{(r+s)^2}, \tag{5.7}$$

$$x - (u-a)t = \frac{\phi'(s)}{r+s} + \frac{\phi(r) - \phi(s)}{(r+s)^2}. \tag{5.8}$$

Hence at $t = 0$.

$$x = \frac{\phi'(r_0)}{2r_0}.$$

By hypothesis $r_0(x)$ is a monotone function and has therefore a one-valued inverse function $x(r_0)$ defined in the range $0 \leq r_0 \leq b$. It follows that

$$\phi(r_0) = 2\int_0^{r_0} rx(r)\,dr.$$

Thus $\phi(r)$ is defined by the initial conditions in the range $0 \leq r \leq b$, and this completes the determination of the solution in region III.

We try now to extend the domain of definition of $\phi(r)$ in order to obtain from (5.7) a solution containing as a particle line the boundary line $x = x_1(t)$. Along this curve we have $r = r_1(t)$, $s = s_1(t)$ and the

relation $r_1(t) + s_1(t) = 0$. Subtracting (5.7) from (5.8) we get, with $a = \frac{r-s}{3}$,

$$\frac{2}{3}t = 2\frac{\phi(r) - \phi(s)}{(r+s)^3} - \frac{\phi'(r) - \phi'(s)}{(r+s)^2}.$$

The expression on the right hand must remain finite as $r \to r_1$, $s \to s_1$, which is only true if $\phi(r) = \phi(-r)$. Hence $\phi(r)$ has to be continued into negative values of r as an even function of r. Equation (5.7) becomes then

$$x - (u + a)t = \frac{(r+s)\phi'(r) - \phi(r) + \phi(-s)}{(r+s)^2},$$

and the limiting form of this relation as $r \to r_1$, $s \to -r_1$, is found to be

$$x_1 - 2r_1t = \tfrac{1}{2}\phi''(r_1). \tag{5.9}$$

Similarly from (5.8) we have D:1 J3.3

$$t = \tfrac{1}{4}\phi'''(r_1). \tag{5.10}$$

Relations (5.9) and (5.10) determine the curve $x = x_1(t)$.

It is clear that this method described by Copson (34) furnishes a solution in region IIIa, which is obviously compatible with the integrals in region III and II. If the curves $x = x_2(t)$ and $x = x_1(t)$ do not meet, these four integrals constitute the complete solution; if they have a common point S for $t = T$ the subsequent motion is reduced to the simple wave of region II. We have then the solution of the expansion into a vacuum of a homogeneous gas originally at rest, which was determined already by Hugoniot (8).

8. *Motion in a Closed Tube*

When in addition to the initial data some relations hold for $x = x_1$ and $x = x_2$ through an interval of time $(0,t)$, boundary value problems arise which in general cannot be solved by finite expressions.

In some cases, however, they can be reduced to initial value problems. If, for instance, the boundary conditions consist of having $u = 0$ at $x = x_2$ the reflected initial data can be introduced along the segment x_1x_3, such that $x_3 - x_2 = x_2 - x_1$, and by reason of symmetry $u = 0$ for $x = x_2$. The same procedure can be used if in addition u should vanish at $x = x_1$.

In the foregoing, the motion in a closed tube is considered for the case of $\kappa = 1.4$. The purpose of this investigation being essentially the study of the general trend of the gas behavior, no initial data are prescribed a priori; instead a rather simple solution, fitting the boundary

conditions is chosen from a "general" integral. The analytical approach does not lead therefore to the two problems of integration mentioned in Section IV,2, but requires the construction of a solution by patching along characteristics a series of particular solutions. The results stress the formation of singularities and raise the question of their occurrence when the motion is subject to arbitrary initial conditions.

We make use of the relations

$$-v^5t = U_u, \quad 5v^4(x - ut) = U_v, \tag{5.11}$$

and

$$U_{vv} - U_{uu} = \frac{4}{v} U_v, \tag{5.12}$$

which can easily be derived from (2.10) and (2.15), and we apply the procedure outlined in Section III,1 to obtain a general integral of (5.12). We choose here, however, for f_n the expression

$$f_n = \frac{1}{(n+1)!} \int^{\lambda} (\lambda - \xi)^{n+1} f(\xi) d\xi,$$

with an arbitrary lower limit of integration, and a similar one for g_n.

The solution of (5.12) will then read according to (3.3)

$$U = v^2 \left[\int^{\lambda} (\lambda - \xi) f(\xi) d\xi - \frac{3}{v}\frac{1}{2} \int^{\lambda} (\lambda - \xi)^2 f(\xi) d\xi + \frac{3}{v^2}\frac{1}{6} \int^{\lambda} (\lambda - \xi)^3 f(\xi) d\xi \right.$$
$$\left. + \int^{\mu} (\mu - \xi) g(\xi) d\xi - \frac{3}{v}\frac{1}{2} \int^{\mu} (\mu - \xi)^2 g(\xi) d\xi + \frac{3}{v^2}\frac{1}{6} \int^{\mu} (\mu - \xi)^3 g(\xi) d\xi \right].$$

If we take the derivatives of U with respect to u and v and introduce the resulting expressions in (5.11) we get

$$\begin{cases} 2v^5t = (v^2 - 2u^2)(\alpha - \alpha') + 6u(\beta + \beta') - 3(\gamma - \gamma'), \\ 5v^3(x - ut) = \beta + \beta' - u(\alpha - \alpha'), \end{cases} \tag{5.13}$$

where α, β, γ, α', β', γ' are defined by the following integrals

$$\alpha = \int^{\lambda} f(\xi) d\xi, \quad \beta = \int^{\lambda} \xi f(\xi) d\xi, \quad \gamma = \int^{\lambda} \xi^2 f(\xi) d\xi,$$
$$\alpha' = \int^{\mu} g(\xi) d\xi, \quad \beta' = \int^{\mu} \xi g(\xi) d\xi, \quad \gamma' = \int^{\mu} \xi^2 g(\xi) d\xi.$$

Incidentally we note that if $g(\xi) = -f(\xi)$, the second relation of (5.13) shows that we have, at any time, for $u = 0$, $x = 0$. Any such solution will thus give rise to a reflection at $x = 0$.

We also find easily the necessary and sufficient conditions to have $u = 0$ at any time at two fixed points. Substituting $u = 0$ in the second

equation of (5.13) we get with $\lambda = \mu = v$

$$5v^3x = \int^v \xi[f(\xi) + g(\xi)]d\xi \tag{5.14}$$

which should be an identity in v for two values of x. We write (5.14) for two different values x_i, $i = 1, 2$,

$$\frac{1}{5v^3}\int^v \xi f d\xi = -\frac{1}{5v^3}\int^v \xi g d\xi + x_i. \tag{5.15}$$

This relation is satisfied by taking for $\frac{1}{5v^3}\int^v \xi f d\xi$ some branches of the inverse of a periodic function and for $-\frac{1}{5v^3}\int^v \xi g d\xi$ other branches of the same function.

As an example this solution is completely studied below when a trigonometric function is chosen for the periodic function.

Let f and g be defined by

$$\frac{1}{5v^3}\int^v \xi f d\xi = \cos^{-1}(v - b) \tag{5.16}$$

and

$$\frac{1}{5v^3}\int^v \xi g d\xi = -\cos^{-1}(v - b)$$

where b is a constant. To each branch of $\cos^{-1}(v - b)$ correspond one-valued functions for f and g which generate through (5.13) a branch solution. x_i is here equal to $2n\pi$ (n being an integer) but we shall restrict our study to $0 \leq x \leq 2\pi$ and look in this interval for a continuous function u of x and t which vanishes at $x = 0$ and $x = 2\pi$. Our requirements can be fulfilled if three determinations of $\cos^{-1}(v - b)$ are considered, namely

$$-\cos^{-1}(v - b), \quad \cos^{-1}(v - b), \quad -\cos^{-1}(v - b) + 2\pi,$$

where $\cos^{-1}(v - b)$ denotes the principal determination. They provide respectively through (5.13) the following expressions for f and g,

$$f_1 = -5\xi\left[3\cos^{-1}(\xi - b) - \frac{\xi}{\sqrt{1 - (\xi - b)^2}}\right],$$
$$f_2 = -f_1$$
$$f_3 = f_1 + 30\pi\xi,$$

and the opposite ones for g_1, g_2, g_3. To each pair f_i, g_j ($i,j = 1,2,3$) there corresponds, according to (5.13), a system of two equations which determines u as a function of x at a given time. The relations being implicit, the difficulty lies in the patching of the branches in order to construct a

continuous solution satisfying our boundary conditions. It can be seen that the functions f and g are only defined in the interval,

$$b - 1 \leq \xi \leq b + 1,$$

which limits the values of u and v to the domain bounded by the limiting lines.

$$\lambda = b + 1, \quad \lambda = b - 1, \quad \mu = b + 1, \quad \mu = b - 1;$$

the transition of a branch solution to another occurs obviously along those lines which are the characteristic lines in the speed plane.

A first group of solutions can be constructed by taking for g a one-valued function equal to g_2 and for f the continuous function composed by f_1, f_2, f_3. It is clear that if they lead to branch solutions u_1, u_2, u_3 for u which are continuous, all the requirements will be satisfied. For this, two conditions must be fulfilled. (1) The lower limit of integration of the integrals α_1, β_1, γ_1; α_2, β_2, γ_2; α_3, β_3, γ_3 corresponding to f_1, f_2, f_3 should be chosen so as to maintain continuity at the transition points $\xi = b + 1$, between f_1 and f_2, and $\xi = b - 1$, between f_2 and f_3. (2) These transition points should occur in the solution for $\lambda = b + 1$, $\lambda = b - 1$, and not for $\mu = b + 1$, $\mu = b - 1$.

It is clear that the first condition can always be satisfied and still leave indeterminate the lower limit of integration of the integrals α_2', β_2', γ_2', corresponding to g_2 and those corresponding to one of the functions f. The second condition, as will be seen, limits the time t to a certain interval beyond which other determinations of g will have to be considered.

Finally, if the required solution has been determined, it remains to investigate whether such a solution represents a physically acceptable motion; such is the case if, for some range of t, u is obtained as a one-valued function of x. This last requirement can be fulfilled by giving convenient values to the remaining arbitrary constants.

For the numerical computation the lower limit of the integrals α_2, β_2, γ_2; α_2', β_2' were all chosen equal to 3, $b = 2$ and γ_2' was taken as

$$\gamma_2' = \int_3^\mu \xi^2 g_2 d\xi + \tfrac{40}{3}.$$

By a quadrature we get the expressions

$$\alpha_2 = \int_3^\lambda f_2 d\xi = \tfrac{15}{4}(2\lambda^2 - 3)\cos^{-1}(\lambda - 2) - \tfrac{5}{4}(\lambda + 6)[1 - (\lambda - 2)^2]^{1/2},$$

$$\beta_2 = \int_3^\lambda \xi f_2 d\xi = 5\lambda^3 \cos^{-1}(\lambda - 2),$$

$$\gamma_2 = \int_3^\lambda \xi^2 f_2 d\xi = \tfrac{5}{4}(3\lambda^4 + \tfrac{227}{8})\cos^{-1}(\lambda - 2) + \tfrac{5}{16}(\lambda^3 + \tfrac{14}{3}\lambda^2 + \tfrac{113}{6}\lambda + 85)[1 - (\lambda - 2)^2]^{1/2},$$

and the similar ones

$$\begin{aligned}
\alpha_2' &= \tfrac{15}{4}(2\mu^2 - 3)\cos^{-1}(\mu - 2) - \tfrac{5}{4}(\mu + 6)[1 - (\mu - 2)^2]^{1/2},\\
\beta_2' &= 5\mu^3 \cos^{-1}(\mu - 2),\\
\gamma_2' &= \tfrac{5}{4}(3\mu^4 + \tfrac{227}{8})\cos^{-1}(\mu - 2)\\
&\qquad + \tfrac{5}{16}(\mu^3 + \tfrac{14}{3}\mu^2 + \tfrac{113}{6}\mu + 85)[1 - (\mu - 2)^2]^{1/2} + \tfrac{40}{3}.
\end{aligned}$$

Now to maintain continuity at $\lambda = b + 1 = 3$ we must take

$$\alpha_1 = -\alpha_2, \quad \beta_1 = -\beta_2, \quad \gamma_1 = -\gamma_2. \tag{5.17}$$

Likewise, a simple computation gives

$$\begin{aligned}
\alpha_3 = -\alpha_2 + 15\pi\lambda^2 - \tfrac{45}{2}\pi, \quad \beta_3 &= -\beta_2 + 10\pi\lambda^3,\\
\gamma_3 &= -\gamma_2 + \tfrac{30}{4}\pi\lambda^4 + \tfrac{1135}{16}\pi,
\end{aligned} \tag{5.18}$$

in order to have continuity at $\lambda = b - 1 = 2$. In view of (5.17), (5.18) the system of Eqs. (5.13) becomes (S_1), (S_2), (S_3), respectively, for f_1, f_2, f_3.

$$(5.19)\ (S_1)\quad \left\{\begin{aligned}
2v^5 t &= -(v^2 - 3u^2)(\alpha_2 + \alpha_2') - 6u(\beta_2 - \beta_2')\\
&\qquad + 3(\gamma_2 + \gamma_2'),\\
5v^3(x - ut) &= -\beta_2 + \beta_2' + u(\alpha_2 + \alpha_2');
\end{aligned}\right.$$

$$(5.20)\ (S_2)\quad \left\{\begin{aligned}
2v^5 t &= (v^2 - 3u^2)(\alpha_2 - \alpha_2') + 6u(\beta_2 + \beta_2')\\
&\qquad - 3(\gamma_2 - \gamma_2'),\\
5v^3(x - ut) &= \beta_2 + \beta_2' - u(\alpha_2 - \alpha_2');
\end{aligned}\right.$$

$$(5.21)\ (S_3)\quad \left\{\begin{aligned}
2v^5 t &= -(v^2 - 3u^2)(\alpha_2 + \alpha_2') - 6u(\beta_2 - \beta_2')\\
&\qquad + 3(\gamma_2 + \gamma_2') + (15\pi\lambda^2 - \tfrac{45}{2}\pi)(v^2 - 3u^2)\\
&\qquad - \tfrac{45}{2}\pi\lambda^4 + 60\pi\lambda^3 u - \tfrac{3405}{16}\pi,\\
5v^3(x - ut) &= -\beta_2 + \beta_2' + u(\alpha_2 + \alpha_2') + 10\pi\lambda^3 - (15\pi\lambda^2 - \tfrac{45}{2}\pi)u.
\end{aligned}\right.$$

The speed plane is useful for discussing this solution, see Fig. 13. The straight lines $\lambda = 1$, $\lambda = 3$, $\mu = 1$, $\mu = 3$ are the limiting lines of the transformation and therefore the branches C_1, C_2, C_3 corresponding to S_1, S_2, S_3 are tangent to them at their limiting points. Since the solution was constructed with the assumption that the transition points occurred on the limiting lines $\lambda = 3$ and $\lambda = 1$, the arc C_2 must span between these lines and therefore must contain a point with velocity zero. This last requirement determines a certain interval for t. Upon substitution of $u = 0$ in S_2 we get $v^2 t = 0$ or, as $1 \leq v \leq 3$, $0.082 \leq t \leq 20$. It is clear that the solution obtained is defined in an interval within this time range. Beyond the interval the construction fails and determinations of g other than g_2 must then be considered.

The propagation of the point where $u = 0$ (the nodal point of the velocity wave in Fig. 14), which is a characteristic feature of nonlinear phenomena, and other properties, can be easily studied, see (37). They

help to plot C_1, C_2, C_3 for various values of t, see Fig. 13. In Fig. 14 corresponding curves in the u,x-plane are drawn. These curves show a time $t = t_0 = 1.7$ beyond which u becomes multiple valued, for which, therefore, the Jacobian J of the transformation vanishes. We obtain thus a time range, $0.082 \leq t \leq 1.7$, where a real flow exists.

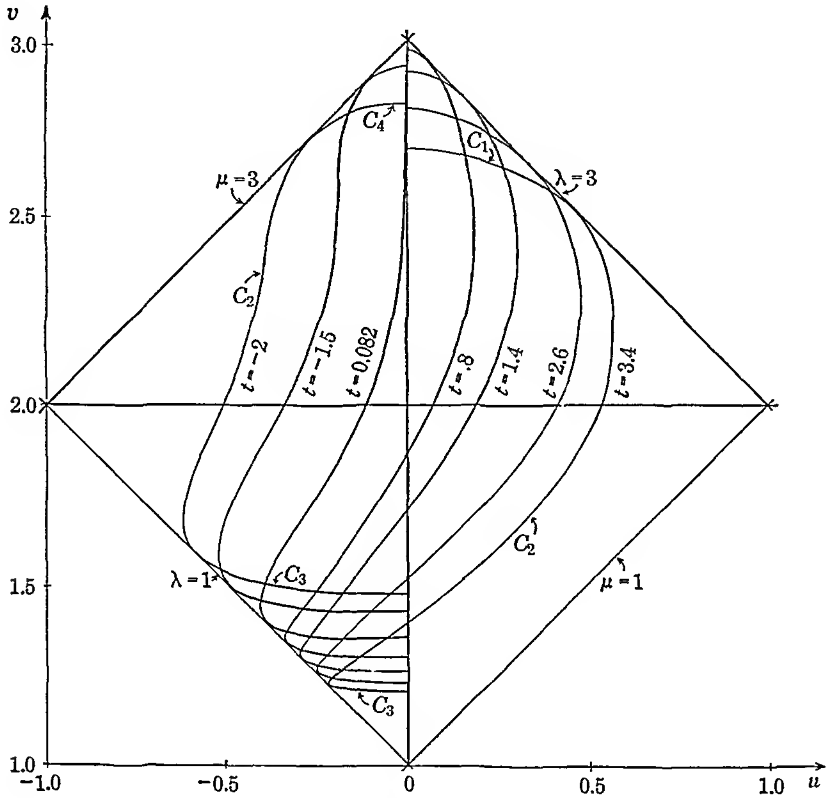

FIG. 13

For $t < 0.082$ the introduction of the function g_1 leads to the system S_4

$$\text{(5.22)}\ (S_4)\quad \begin{cases} 2v^5t = (v^2 - 3u^2)(\alpha_2 + \alpha_2') + 6u(\beta_2 + \beta_2') \\ \qquad\qquad - 3(\gamma_2 + \gamma_2'), \\ 5v^3(x - ut) = \beta_2 - \beta_2' - u(\alpha_2 + \alpha_2'), \end{cases}$$

which takes the place of (S_1) and enables one to obtain again a continuous curve composed in the speed plane of the branches C_2, C_3, C_4. The study of this new solution is particularly interesting for it describes the case of a reflection at $x = 0$. It may be seen in the u,v-plane that for $t < 0.082$ the moving nodal becomes imaginary and that the velocity is then everywhere negative, which indicates that the entire flow is moving to the left

in the u,x-plane. The reflection occurs for $t = 0.082$, and thereafter the solution describes interaction between the incoming and the reflected flow.

Investigations of the solution for more negative t-values led to the discovery of a new zero of the Jacobian. Thus a complete interval $-2.5 \leqq t \leqq 1.7$ is determined where the motion is real and continuous.

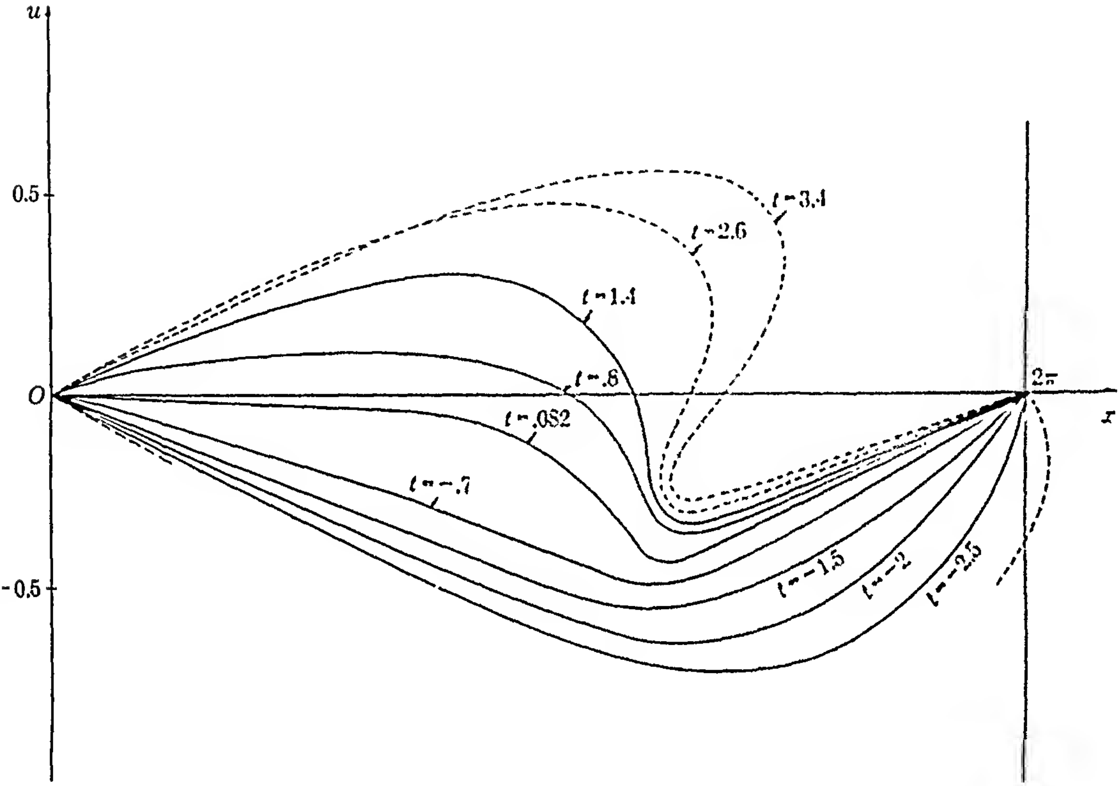

FIG. 14

The family of curves, shown on Fig. 14, which gives the state of flow for various values of t, shows how an initial discontinuity is smoothed out and how a discontinuity may develop from continuous initial conditions.

In fact, it can be established in the case of a polytropic fluid that, whatever the initial conditions are, singularities will necessarily occur in the motion. The proof was given by Ludford (40) using his unfolding procedure, outlined in Section IV,3, and formula (4.35). When the variations of the initial values $r = \varphi(x)$ and $s = \psi(x)$ are small, this approach yields an interesting estimate of the time, t_0, of first occurrence of a singularity. The result is

$$t_0 = \frac{2}{(\kappa + 1)M}$$

where M is the maximum value of $-\varphi'$ or ψ' on the initial curve.

References

1. Euler, L., *Institutiones calculi integralis*, Vol. III, Part II, Chaps. III, IV, V, Petropoli, 1770.
2. Poisson, S. D., Mémoire sur la théorie du son, *J. Ecole Polytech.*, **14**, 319–392 (1808).
3. Poisson, S. D., Mémoire sur l'intégration des équations linéaires aux derivées partielles, *J. Ecole Polytech.*, **19**, 215 (1821).
4. Stokes, E. E., On a difficulty in the theory of sound, *Phil. Mag.*, **33**, 349–356 (1848).
5. Airy, G. B., *Phil. Mag.* (June, 1849).
6. Earnshaw, S., On the mathematical theory of sound, *Phil. Trans. Roy. Soc.* (London), **150**, 133–148 (1860).
7. Riemann, B., Übcr die Fortpflangung ebener luftwellen von endlicher Schwingungsweite, *Gottingen Abhandl.*, **8** (1860).
8. Hugoniot, H., Sur la propagation du mouvement dans les corps, *J. Ecole Polytech.*, **57, 58** (1887).
9. Hadamard, J., *Leçons sur la propagation des ondes*, Hermann, Paris, 1903.
10. Rayleigh, J., Aerial plane waves of finite amplitude, *Proc. Roy. Soc.* (*London*), **84**, 247–284 (1910).
11. Kobes, K., *Z. d. österr. Ing. u. Architekt. Ver.*, **62**, 553 (1910).
12. Gossot, F., and Liouville, R., Effets ballistiques des poudres sans fumée, *Memorial des Poudres et Salpètres*, Vol. 17 (1914).
13. Darboux, G., *Leçons sur la théorie generale des surfaces*, Vol. II, Gauthier-Villars, Paris, 1915.
14. Love, A. E. H., and Pidduck, F. B., Lagrange's ballistic problem, *Phil. Trans. Roy. Soc.* (*London*), **A222**, 167–226 (1922).
15. Bechert, K., Zur Theorie ebener Stroemungen in reibungfreien Gasen, *Ann. Physik*, **37, 38** (1940).
16. Pfriem, H., Die ebene ungedämpfte Druckwelle grosser Schwingungsweite, *Forsch. Gebiete Ingenieurw.*, **12**, 51–64 (1941).
17. Pfriem, H., Reflexionsgesetze für ebene Druckwellen grosser Schwingungsweite, *Forsch. Gebiete Ingenieurw.*, **12**, 244–256 (1941).
18. Bechert, K., Differentialgleichungen der Wellenausbreitung in Gasen, *Ann. Physik*, **39** (1941).
19. Pfriem, H., Zur gegenseitigen Überlagerung ungedämpfter ebener Gaswellen grosser Schwingungsweite, *Akust. Z.*, **72**, 56–65 (1942).
20. Schultz-Grunow, F., Nichstationäre eindimensionale Gasbewegung, *Forsch. Gebiete Ingenieurw.*, **13**, 125–134 (1942).
21. Guderley, G., Starke Kugelige und zylindrische Verdichtungsstösse in der Nähe des Kugelmittelpunktes bzw. der Zylinderachse, *Luftfahrt-Forsch.*, **19**, No. 9 (1942).
22. Sauer, R., Charakteristikenverfahren für die eindimensionale instationäre Gasströmung, *Ing. Arch.*, **13**, 79–89 (1942).
23. Sauer, R., Theorie der nichstationären Gasströmung I, Ebene stetige Gaswellen, *Deut. Luftfahrtforsch.*, F.B. 1675/I (1942).
24. Sauer, R., Zur Theorie des nichstationären ebenen Verdichtungsstosses, *Ing. Arch.*, **14** (1943).
25. Schultz-Grunow, F., Nichstationäre kugelsymmetrische Gasbewegung, *Ing. Arch.*, **14** (1943).

26. MARTIN, H. M., The rectilinear motion of a gas, *Am. J. Math.*, 65, 391–407 (1943).
27. SEDOV, L. I., On unsteady motions of a compressible fluid, *Akademiia Nauk SSSR Doklady*, 47, 91–93 (1945).
28. STANIUKOVITCH, K. P., On automodel solutions of equations of hydrodynamics possessing central symmetry, *Akademiia Nauk SSSR Doklady*, 48, 310–312 (1945); 60, 1141–1144 (1948).
29. TAUB, A. H., Interaction of progressive rarefaction waves, *Annals of Math.*, 47, 811–828 (1946).
30. COURANT, R., and FRIEDRICHS, K. O. *Supersonic Flow and Shock Waves*, Interscience Publishers, New York, 1948.
31. BERGMAN, S., Two-dimensional transonic flow patterns, *Am. J. Math.*, 70, 856–891 (1948).
32. BERGMAN, S., On two dimensional supersonic flows, *NACA Tech. Note* No. 1875, 1949.
33. SOMMERFELD, A., *Partial Differential Equations in Physics*, Academic Press, New York, 1949, 52–54.
34. COPSON, E. T., The expansion of a gas cloud into a vacuum, *Monthly Notices Roy. Astron. Soc.*, 109, No. 3 (1949).
35. MCVITTIE, G. C., The expansion of an interstellar gas cloud into a vacuum, *Monthly Notices Roy. Astron. Soc.*, 110, No. 3 (1950).
36. BIRKHOFF, G., *Hydrodynamics*, Princeton University Press, 1950.
37. ZALDASTANI, O., The one-dimensional unsteady compressible fluid flow, *Sc. D. Thesis*, Harvard University, 1950.
38. VON MISES, R., One-dimensional adiabatic flow of an inviscous fluid, *Navord Report* 1710, 1951.
39. SAUER, R., Elementare Lösungen der Wellengleichung isentropischer Gasströmungen, *Z. angew. Math. Mech.*, 31 (1951).
40. LUDFORD, G. S. S., On an extension of Riemann's method of integration, with applications to one-dimensional gas dynamics, *Proc. Camb. phil. Soc.*, 48, 499–510 (1952).

Turbulent Diffusion: Mean Concentration Distribution in a Flow Field of Homogeneous Turbulence[1]

By F. N. FRENKIEL

Applied Physics Laboratory, The Johns Hopkins University, Silver Spring, Maryland

In the scientific literature of recent years one finds a large number of papers on theoretical and experimental investigations of turbulence phenomena. The theory of turbulence, and especially the statistical theory, is in full development and has already led to a better understanding of several aspects of the subject. Possible applications of the knowledge already acquired, to various fields of science and engineering, appear obvious although not always simple. In this paper we shall discuss one aspect of turbulent phenomena, turbulent diffusion, which has a particularly wide field of application in fluid dynamics, chemical engineering, heat transfer, meteorology, etc. It is possible that some readers interested in turbulent diffusion are not sufficiently familiar with the papers on the statistical theory of turbulence to determine easily the relation between turbulent diffusion and the general theory of turbulence. For such readers a discussion of the statistical description of a turbulent field is given. The main part of the paper is concerned with diffusion in a field of homogeneous and isotropic turbulence in which the decay of turbulence is neglected. In an Appendix, a brief summary is given of some further problems, including an extension of the results to a case of nonisotropic turbulence. The author plans to continue the discussion of this subject elsewhere, and also to extend it to more general cases of turbulent diffusion.

[1] This work was done under Contract NOrd 7386 with the U.S. Navy Bureau of Ordnance.

I. Introduction

When smoke puffs out of a chimney, solid particles of smoke, condensed water droplets and hot gases spread out in the atmosphere. In a smooth wind the spread of the dispersion wake is small and large smoke concentrations are observed far downstream of the chimney. But generally the wind blows in irregular gusts carrying puffs of smoke to and fro throughout a wide wake. At one moment the wind carries the aerosols speedily away and in the next throws them against the ground. The dispersion of smoke is clearly dependent on the character of the wind fluctuations, or the wind turbulence.

Less dramatic, but as important, is the influence of turbulence on an artificial flow such as in a wind tunnel, in a pipe, or in a precombustion chamber. While most instruments measure a constant velocity under these conditions, the effects of the existing turbulence can be, nevertheless, very appreciable.

As an example, let us consider the dispersion of a foreign gas emitted continuously from a point source placed in a laminar air stream. The

dispersion is, in this case, produced by molecular diffusion alone. We shall assume the pressure and temperature of the air to be normal and the constant stream velocity equal to, say, 20 meters per second. Figure 1a then shows the size of the wake in which 99.9 per cent of the emitted gas is collected. When the experiment is repeated in a turbulent air flow, the dispersion wake is broadened by the turbulent diffusion. As shown in Figs. 1b and 1c, the influence of turbulence on dispersion in

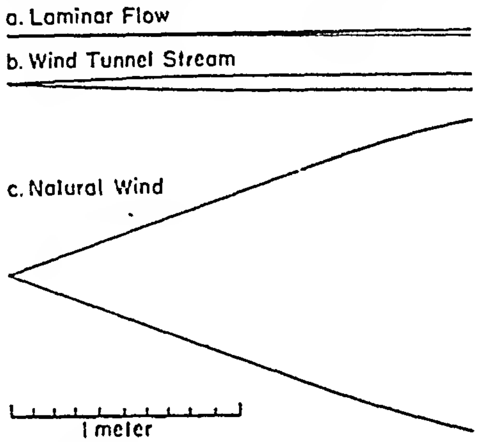

Fig. 1. Sizes of dispersion wakes for molecular and turbulent diffusion.

gases is quite important and varies with the character of the turbulent fluctuations.

1. *Turbulence and Molecular Agitation*

A characteristic feature of turbulent motion is that the turbulent fluctuations are, or at least can be regarded as, random. To describe completely a turbulent field, as well as to solve various turbulent problems, it is therefore necessary to apply statistical methods. At first glance there would appear to be a similarity between turbulence and the kinetic theory of gases; but such an analogy is only partly justified and may lead to incorrect conclusions. Let us try to examine how turbulent fluctuations differ in their nature from molecular agitation.

The *fluid dynamicist's viewpoint* is to consider the fluid as a continuum; the *molecular physicist's viewpoint* is to consider it as constituted of discrete particles. For the fluid dynamicist there exist instantaneous fluid velocities at each point of the fluid field; for the molecular physicist, at a geometrical point of the fluid field, a velocity exists only when a molecule is present at this point. In one case the velocity and its derivatives are assumed to be continuous in time and space; in the other the velocity is essentially discontinuous. Let us now try to establish a heuristic relation between the molecular velocities and the instantaneous velocity at a point of the fluid.

We consider first the case of a nonturbulent, homogeneous fluid at rest. At a certain instant t, we observe the simultaneous velocities of the n molecules which are present in an element of volume υ surrounding a point P. An average velocity can be computed from these velocities. When the size of υ increases, the value of the average varies irregularly but tends to a limit. In a fluid at rest this limit is equal to zero. For a certain volume υ_j, containing a sufficiently large number of molecules, this limit can be assumed to be reached. At any other point P' of the fluid field, we find the same average for a volume υ_j' surrounding the point (Fig. 2). We have, therefore, a physical relation between the *instantaneous fluid velocity at a point* and the *space average of molecular velocities* in a nonturbulent fluid at rest. The same description can also be used for a fluid flow having a uniformly distributed velocity.[2]

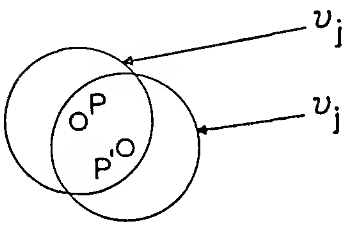

FIG 2

The situation is, however, quite different when the fluid field becomes turbulent. The fluid velocity varies from point to point and from time to time. Let us again take the space average of velocities of the molecules contained in continuously increasing volumes surrounding a point P. The space average will no longer reach a limit when the volume reaches υ_j and the simultaneous fluid velocities at the points P and P' may be different If a limit exists at all, before it is reached it may be necessary to increase the size of the averaging volume to magnitudes which can no longer be neglected by the fluid dynamicist, unless he decides to ignore the existence of turbulence altogether. Whether or not a limit is reached, we again define the instantaneous fluid velocity at a point P as the average velocity of the molecules in a volume about P of the order of magnitude of υ_j. The fluid velocity fluctuations are thus considered to be turbulent ones and molecular agitation is, by this definition, excluded from what we consider to be turbulence.

[2] This definition of an instantaneous fluid velocity at a point is acceptable as long as the number of molecules contained in a volume element υ_j is large enough to give a well-defined space average, and as long as the magnitude of υ_j is small compared to any dimensions with which the fluid dynamicist may be concerned

The smallest probe of a hot-wire anemometer used in the investigation of the microstructure of fluid flow is made of a wire with a diameter of about 1.25 microns and a length of about 350 microns. The number of molecules of a gas at normal pressure and temperature contained in a volume of 1 micron of length of such a wire is of the order of 35,000,000 Obviously a much smaller number of molecules is sufficient to determine a well-defined average.

2. *Fluid Continuum*

By defining an instantaneous fluid velocity at a given point the molecular velocities have been eliminated and the fluid is regarded as a continuum. In regarding the fluid as a continuum, however, consideration must be given to the physical effects of its molecular nature. To account for these effects, we consider, in addition to the vector field of fluid velocities, certain scalar fields which account for these physical effects at each instant and at each point. Some of these effects are represented by assigning to each point of the fluid a temperature, a pressure, and a density. These three scalar quantities are related by an equation of state. When a fluid in motion is considered, we include such conditions as the conservation of mass, which will be imposed by the equation of continuity. For each particular problem we can try to see whether some of the effects of the molecular nature of the fluid can be neglected. When fluid motion is studied, we can assume, in some cases, that the fluid is inviscid and use Euler's equation; in other cases the viscosity cannot be neglected, and the Navier-Stokes equations have to be applied. In problems of turbulent diffusion we must examine what property is diffused and how the molecular agitation will act on this property. In what follows, we are concerned with the diffusion of mass represented by the molecules themselves.

3. *Fluid Element*

Let us return to the question of the similarity between molecular agitation and turbulence. We can now visualize an instantaneous velocity referring to a point of a continuous fluid instead of the velocity of a molecule in a discontinuous fluid. But what about the analogues of the molecule itself and the molecular free path? What shall we mean by a particle of the fluid?

FIG. 3.

In our continuous fluid field a volume element v, surrounding a point P contains at a given moment t a group of molecules. This group of molecules moves with a general velocity equal to the fluid velocity at the point P, dispersing, at the same time, by molecular agitation. After a small interval of time the center of gravity of the group of molecules will be, say, at a point Q (Fig. 3). During the wandering through the fluid field, molecules leave and enter the volume element v; and several of those included in the original group of molecules will now be outside of the volume element

v_j surrounding the point Q. After a sufficiently long time, the fluid element exchanges practically all its molecules with the surrounding fluid. The average value of this interval of time can be called a mixing time. In the same way, we can represent a mixing length which in certain respects is similar to the Prandtl "mischungsweg" (1). In making analogies with the kinetic theory of gases the mixing length corresponds to the molecular free path.

While a molecule conserves its identity along its trajectory and while a molecular free path is unequivocally limited by two collisions, fluid elements penetrate and mix with one another, and the mixing length is not clearly defined by the character of the turbulent field.

4. Turbulent Diffusion and Dispersion of Particles

The size of a fluid element is a function of the number of molecules sufficient to average out the molecular agitation. This size depends, therefore, on the density of the fluid; it is independent of the character of the turbulent field. The trajectory of the fluid element will, on the contrary, be a function of the character of the turbulent fluctuations and will not depend on the molecular agitation.

The theory of turbulent diffusion investigates the motion of fluid elements that do not preserve an individual identity. Dispersion in fluids is concerned with the motion of material particles, which depends on the character of the turbulent field and on the nature of the particles themselves. We shall, however, neglect here the effects of gravity.

An essential factor in the behavior of a particle is its size as compared with the size of the fluid element. When we are concerned with diffusion of one gas in another, the particle is of molecular dimensions. The dispersion is, in this case, influenced by molecular agitation and by turbulence. Consider now the dispersion of particles such as colloids of a size larger than a gas molecule, but smaller than the magnitude of a fluid element. Since the size of a colloid is not large enough to average out the molecular agitation, we shall observe in a nonturbulent fluid at rest the Brownian motion. In a turbulent fluid, the effects of turbulent and mean fluid motions will be added to the Brownian motion. For a particle of the size of a fluid element the molecular agitation is averaged out. In a nonturbulent fluid at rest such particles will have no motion whatsoever. In a turbulent flow the dispersion of these particles will be determined exclusively by the character of the turbulence. When finally a particle is larger than a fluid element, the effect of high-frequency turbulent fluctuations is in part eliminated. The dispersion of particles is then a function not only of the character of the turbulence, but also of the size and shape of the particle.

II. Statistical Description of a Turbulent Field

1. Averaging Processes

Since turbulent velocities vary both in time and space and since this variation is considered to be random, one may be concerned with several kinds of average velocities. From the mathematical point of view a turbulent velocity field can be considered as a set of vector fields in space-time. Each vector field is a function of a parameter ω chosen at random in a measure space Ω whose measure is equal to 1. If $u(x,y,z,t,\omega)$ is a component of the instantaneous vector velocity at a point of the fluid field, for any specific ω, we can consider the following four major types of averages [cf. (2)]:

Ensemble average: $\bar{u}(x,y,z,t) = \int_\Omega u(x,y,z,t,\omega)d\omega;$

Space average:

$$<u>_s = \lim_{X,Y,Z\to\infty} \frac{1}{8XYZ} \int_{-X}^{X} \int_{-Y}^{Y} \int_{-Z}^{Z} u(x,y,z,t,\omega)dx\,dy\,dz;$$

Time average: $<u>_t = \lim_{T\to\infty} \frac{1}{2T} \int_{-T}^{T} u(x,y,z,t,\omega)dt;$

Space-time average:

$$<u>_{s,t} = \lim_{X,Y,Z,T\to\infty} \frac{1}{16XYZT} \int_{-X}^{X} \int_{-Y}^{Y} \int_{-Z}^{Z} \int_{-T}^{T} u(x,y,z,t,\omega)dx\,dy\,dz\,dt.$$

The relations between these various averages are not known. In a theoretical discussion it is most proper to use the ensemble average, which gives the mathematical expectation of the random function.[3] However, from experiments other averages are determined. We assume that for any random function $\Psi(x,y,z,t,\omega)$, we have

$$\bar{\Psi}(x,y,z,t) = <\Psi>_s = <\Psi>_t = <\Psi>_{s,t}. \tag{2.1}$$

This assumption is not necessarily equivalent to and may be stronger than the assumption that the turbulence is a homogeneous and stationary stochastic process. In fact, it is not always necessary to make such a strong assumption to apply the theoretical results. In what follows, a bar (such as in $\bar{u}$ or $\bar{\Psi}$) will be used to represent any of the averages. Whenever the bar refers to an average other than a statistical average, this will be mentioned explicitly in the text.

2. Mean and Turbulent Velocities

Figure 4 represents two examples of turbulent fluctuation recordings; the first was obtained in a wind tunnel with a hot-wire anemometer, the

[3] In the theory of mathematical probability the notation $E(u)$ would correspond to $\bar{u}$.

second in the natural wind with a pressure tube anemometer. Both represent fluctuations of instantaneous velocity as a function of the time. Let us consider the quantity

$$\mathfrak{M}_T = \frac{1}{2T}\int_{t-T}^{t+T} u_A(\alpha)d\alpha,$$

where $u_A(t)$ is the instantaneous value of the fluctuating fluid velocity at a point A and at an instant t, and where $2T$ is an interval of time. For the case of wind tunnel turbulence (Fig. 4a), $\mathfrak{M}_T$ becomes practically

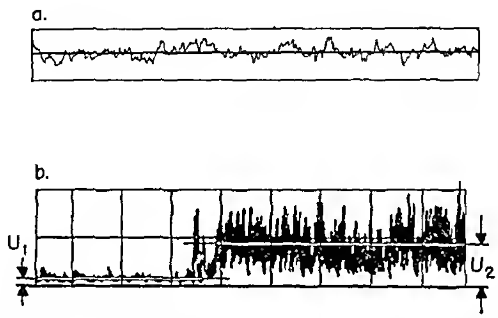

FIG. 4. Two typical turbulent velocity recordings: (a) in a wind tunnel stream, (b) in the natural wind.

constant when T reaches a certain interval of time T_1 and remains constant for $T > T_1$. We can then define

$$\bar{u}_A = \langle u_A \rangle_t = \lim_{T\to\infty} \frac{1}{2T}\int_{t-T}^{t+T} u_A(\alpha)d\alpha \tag{2.2}$$

as a mean velocity of the fluid at the point A. The *instantaneous velocity* $u_A(t)$ can be divided into two parts, the *mean velocity* $\bar{u}_A$ and the *turbulent velocity* $u_A'(t)$, such that

$$u_A(t) = \bar{u}_A + u_A'(t)$$

for all t.

Let us now consider the natural wind recording represented in Fig. 4b and assume that the length of the first part of the recording is sufficient to determine a practically constant value $\mathfrak{M}_T \approx \bar{u}_A = U_1$. We may then consider U_1 as a mean velocity for this part of the recording, and define as a turbulent velocity the difference $u_A(t) - U_1$. In a similar way, it may be possible to find a different mean velocity U_2 corresponding to the second part of the same recording. The definition of a mean velocity for the whole length of the recording would, however, be meaningless. If a much longer recording is used, it is possible that mean velocities such as U_1, U_2 can in their turn be regarded as "instantaneous" velocities and a new "mean" value $\bar{U}$ defined. Obviously the scale on

which the turbulent field is considered is of major importance in such cases. To define a turbulent velocity one must, however, be able to assume that a limit such as the one defined by Eq. (2.2) does exist.

3. *Intensity of Turbulence*

Consider in a turbulent field a set of orthogonal axes $Oxyz$ with the axis Ox parallel to the direction of a constant mean velocity (Fig. 5). Let $V(x_1,y_1,z_1,t)$ be the instantaneous vectorial velocity at a given point $P(x_1,y_1,z_1)$ and at a given instant t. Let us denote by u,v,w the projections of V on the three axes. Due to the choice of the direction of the axis Ox, we have $\bar{u}$ = constant, $\bar{v} = 0$, $\bar{w} = 0$, and the components of the turbulent velocity are $u' = u - \bar{u}$, $v' = v$, $w' = w$. For the averages of the turbulent components, we have $\overline{u'} = 0$, $\overline{v'} = 0$, $\overline{w'} = 0$, by definition.

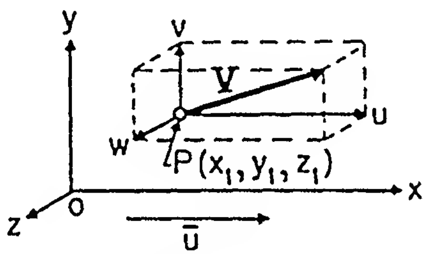

Fig. 5. Vector velocity at a point in a fluid flow having mean velocity $\bar{u}$ in the direction of the x-axis.

The spread of the fluctuating turbulent velocities u',v',w' can be measured by the values of the *variances* $\overline{u'^2} \neq 0$, $\overline{v'^2} \neq 0$, $\overline{w'^2} \neq 0$ or their square roots, the *standard deviations* $\sqrt{\overline{u'^2}}$, $\sqrt{\overline{v'^2}}$, $\sqrt{\overline{w'^2}}$. The ratio of such a standard deviation to the mean velocity (when $\bar{u} \neq 0$) is called the intensity of turbulence. We shall have a *longitudinal intensity of turbulence* $\sqrt{\overline{u'^2}}/\bar{u}$ and *transverse intensities of turbulence* $\sqrt{\overline{v'^2}}/\bar{u}$ and $\sqrt{\overline{w'^2}}/\bar{u}$.

4. *Eulerian Correlation Coefficients*

Let us consider now in the same field of turbulence (Fig. 6a) a second point $Q(x_2,y_1,z_1)$. The points P and Q are placed on a line parallel to the direction of the mean velocity and separated by a distance $x = x_2 - x_1$. At an instant t, the simultaneous longitudinal components of the turbulent velocities at the two points are $u_P'(t)$ and $u_Q'(t)$. The ratio[4]

$$R_x(x) = \frac{\overline{u_P'u_Q'}}{\sqrt{\overline{u_P'^2}}\sqrt{\overline{u_Q'^2}}}$$

[4] In the symbol $R_a(b)$, the subscript a refers to the direction of the line segment joining the two points, while b is the length of the line segment measured in this direction. The use of correlation coefficients was introduced by Taylor (3).

is called the *longitudinal correlation coefficient.* This coefficient is a function of the distance x. When $x = 0$, the two points coincide and there is complete correlation, hence $R_x(0) = 1$. When x is very large, there is practically no correlation between the components of the velocity at the two points, and $R_x(\infty) = 0$. Between these two limit values of x the correlation varies with the character of the turbulent fluctuations and determines a correlation curve $R_x(x)$.

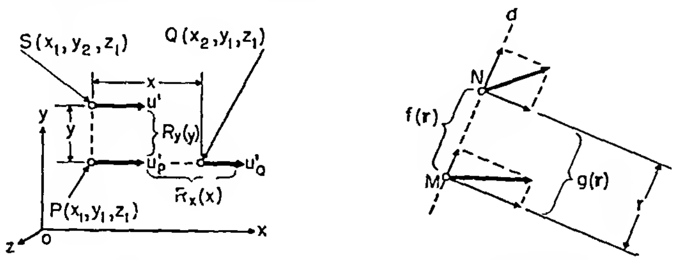

FIG. 6a. FIG. 6b.

FIG. 6. Diagram illustrating the orientation of the point velocities correlated by Eulerian correlation coefficients.

Consider now a third point $S(x_1,y_2,z_1)$ placed on the line through P in the y-direction (Fig. 6a) and at a distance $y = y_2 - y_1$ from P. The ratio

$$R_y(y) = \frac{\overline{u_P' u_S'}}{\sqrt{\overline{u_P'^2}}\sqrt{\overline{u_S'^2}}}$$

is called a *transverse correlation coefficient.*

In a similar way an *Eulerian time correlation coefficient* $R_t(h)$ can be defined, describing the correlation between the turbulent velocities at the same point, but at two instants separated by an interval of time h.

There is another notation frequently used in the literature. Let us consider (Fig. 6b) two points M and N, such that the line segment MN is a vector $\mathbf{r}$ in the direction d and of length r. The correlation coefficient between the simultaneous turbulent velocity components in the direction d at points M and N is now represented by the symbol $f(\mathbf{r},t)$. A correlation coefficient $g(\mathbf{r},t)$ is similarly defined in terms of components of the two velocities in a direction n normal to d. When d is parallel to the x-axis, we have obviously $f(x) = R_x(x)$ and when n is parallel to the y-axis, we have $g(y) = R_y(y)$.

5. *Homogeneous, Isotropic, and Stationary Turbulence*

Most of the theoretical work in turbulence concerns homogeneous and isotropic turbulence in an incompressible fluid at rest. In a *homogeneous* turbulent field the statistical characteristics are not changed by a transla-

tion of axes. Let us consider as an example (Fig. 7), the correlation between components of the simultaneous velocities at two points M and N taken in directions a and b respectively. If the configuration $aMNb$ is subjected to a translation in a field of homogeneous turbulence and

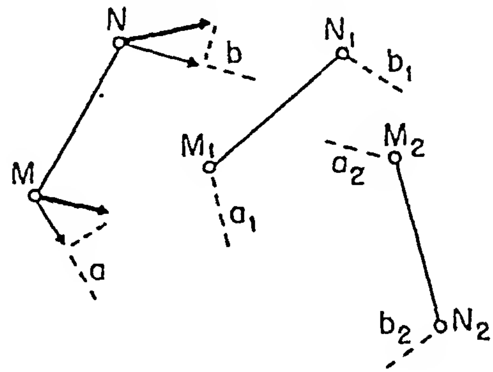

FIG. 7. Schematic diagram of the invariance of the statistical characteristics in homogeneous and in isotropic turbulence.

moves to $a_1M_1N_1b_1$, the correlation between the components of the simultaneous velocities at M_1 and N_1 projected respectively on a_1 and b_1 will be equal to the correlation at the initial location of the configuration. If the turbulence is, in addition, *isotropic*, the statistical characteristics

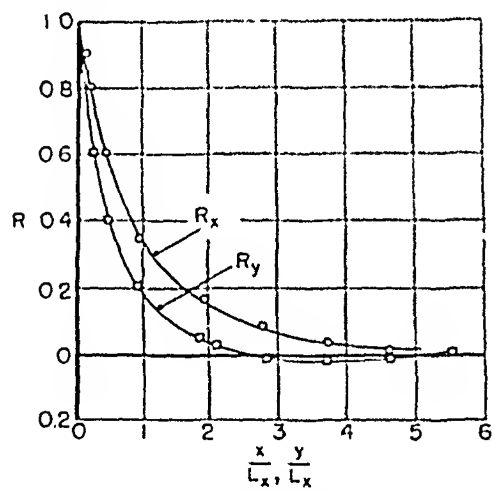

FIG. 8. Typical longitudinal and transverse correlation curves measured in a wind tunnel flow $\left[L_x = \int_0^\infty R_x(\alpha)d\alpha\right]$.

will also be invariant under a rotation or a reflection of the axes and the same correlation will be found for the configuration $a_2M_2N_2b_2$.

In a field of homogeneous turbulence $\overline{u_M'^2}(t) = \overline{u_N'^2}(t) = \overline{u'^2}(t)$, and if the turbulence is also isotropic $\overline{u'^2}(t) = \overline{v'^2}(t) = \overline{w'^2}(t)$. When the turbulence is homogeneous and isotropic $f(\mathbf{r},t) = f(r,t)$ and $g(\mathbf{r},t) = g(r,t)$,

and the longitudinal and transverse correlation coefficients are related by the equations (4,5):

$$R_y(y) = R_x(y) + \frac{1}{2} y \frac{dR_x(y)}{dy}, \tag{2.3}$$

$$R_x(x) = \frac{2}{x^2} \int_0^x \alpha R_y(\alpha) d\alpha. \tag{2.4}$$

Figure 8 represents a longitudinal and a transverse correlation curve, measured in a wind tunnel, which satisfy these two relations (6).

We have a *stationary* field of turbulence when the statistical characteristics of turbulence are independent of the time.

6. *Spectra of Turbulence*

Another way of describing the turbulent flow is to determine the spectrum which measures the relative contribution of various frequencies of velocity fluctuations to the turbulent energy (6). To the two spatial correlation curves discussed above will correspond two one-dimensional spectra of turbulence (5): the *longitudinal spectrum of turbulence* $F_x(k')$ and the *transverse spectrum of turbulence* $F_y(k'')$. Each of these functions represents the contribution to $\overline{u'^2}$ (proportional to the component of the turbulent energy $\frac{1}{2}\rho\overline{u'^2}$) at the wave number k' or k''. The longitudinal spectrum $F_x(k')$ can be determined by a harmonic analysis of the simultaneous u'-components along a line in the x-direction and is expressed as a function of the wavelength $2\pi/k'$ measured along this line. The transverse spectrum $F_y(k'')$ is derived similarly from the simultaneous u'-components along a line parallel to the y-direction, and the wavelength $2\pi/k''$ is measured along this transverse line.

The correlation coefficients and the one-dimensional spectra can be determined (6) from one another by Fourier transforms:

$$\begin{aligned} F_x(k') &= \frac{2}{\pi}\overline{u'^2} \int_0^\infty R_x(s) \cos(k's) ds, \\ F_y(k'') &= \frac{2}{\pi}\overline{u'^2} \int_0^\infty R_y(s) \cos(k''s) ds, \end{aligned} \tag{2.5}$$

$$\begin{aligned} \overline{u'^2}R_x(x) &= \int_0^\infty F_x(s) \cos(xs) ds, \\ \overline{u'^2}R_y(y) &= \int_0^\infty F_y(s) \cos(ys) ds. \end{aligned} \tag{2.6}$$

In the special case of homogeneous and isotropic turbulence, the longitudinal and transverse spectra at a given instant t are related by the equations (5):

$$F_y(k'') = \frac{1}{2} F_x(k'') - \frac{1}{2} k'' \frac{dF_x(k'')}{dk''}, \tag{2.7}$$

$$F_x(k') = 2k' \int_{k'}^{\infty} \frac{F_y(s)}{s^2}\, ds. \tag{2.8}$$

When the idea of a spectrum of turbulence was introduced by G. I. Taylor, reference was made to a spectrum at a fixed point of the fluid flow and not to a one-dimensional spectrum. Taylor's spectrum and the

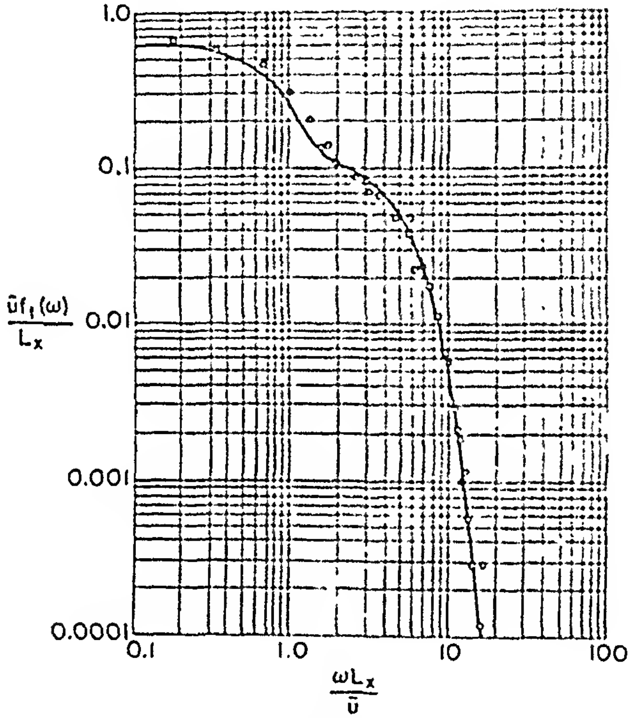

FIG. 9. Typical spectrum of turbulence at a fixed point in a wind tunnel stream 40 mesh lengths downstream of a grid.

Eulerian time correlation curve are related by equations similar to (2.5) and (2.6). Figure 9 represents such a spectrum as measured in a wind tunnel stream (7).

The three-dimensional spectrum of turbulence which is discussed in the preceding volume of the *Advances in Applied Mechanics* (8) can be expressed as a function of one-dimensional spectra by (9,10):

$$\begin{aligned} F(k) &= \frac{1}{3}\left[k^2 \frac{d^2F_x(k)}{dk^2} - k\frac{dF_x(k)}{dk}\right] \\ &= \frac{2}{3}\left[F_y(k) - k\frac{dF_y(k)}{dk} - k\int_k^{\infty}\frac{F_y(\alpha)}{\alpha^2}\,d\alpha\right]. \end{aligned} \tag{2.9}$$

7. Decay of Turbulence

A fluid in a turbulent state, left to itself, quiets down after a certain time, its turbulence decays, and the turbulent energy is transformed into heat. Most of the experimental investigations concern the decay of turbulence in wind tunnels downstream of a grid. Immediately behind the grid, vortices are shed at a frequency which depends on the dimensions of the grid. In the spectrum of turbulence the largest part of the turbulent energy will correspond to this frequency. At a small distance downstream of the grid the vortices which originate at the individual meshes mix in a more and more irregular pattern. The regular frequency of these vortices is slowly smeared out for increasing distances from the grid. A trace of this frequency may, however, appear in the form of a bump (cf. Fig. 9) in the spectrum of turbulence. At large distances downstream, say of more than 40 mesh lengths, the turbulence becomes nearly isotropic. Following the mean flow direction, one finds the character of the turbulence changing. Large eddies (low-frequency fluctuations) produce small ones, and turbulent energy is dissipated by viscosity. The viscous dissipation for large eddies is small compared with the rate of transformation of these eddies into small ones. The rate of dissipation by viscosity increases with decreasing eddy size.

Various assumptions are made about the mechanism of decay and lead to relations which give the variation of turbulent energy and of correlation curves as functions of the time of decay. Some of these solutions are treated extensively by several authors and are discussed in the preceding volume of this book series (8).

8. Local Isotropy

Kolmogoroff's theory of local isotropy (11) assumes that when a sufficiently small domain of a turbulent field is considered, the turbulence in this domain is homogeneous, isotropic, and stationary, irrespective of the source of the turbulent fluctuations, and even if the turbulence does not have these characteristics on a much larger scale.

In order to emphasize the contribution of small eddies, the statistical description of turbulence can be made in terms of differences between turbulent velocity components rather than in terms of the components themselves. Let us return, for instance, to Fig. 6a and consider point P as a reference point. One would now be concerned with differences such as $(u_Q' - u_P')$ and $(u_S' - u_P')$. The turbulence is said to be *locally isotropic* in a certain domain of space-time, when in this domain the statistical functions of such velocity differences are invariant under a translation, rotation or reflection of the coordinate axes. In this domain we

shall find, for instance, that the functions

$$B_{dd} = \overline{(u_Q' - u_P')^2} = \overline{u_Q'^2} - 2\overline{u_Q'u_P'} + \overline{u_P'^2}$$

and $B_{nn} = \overline{(u_S' - u_P')^2} = \overline{u_S'^2} - 2\overline{u_S'u_P'} + \overline{u_P'^2}$ are related to the correlation coefficients R_x and R_y in the following way:

$$B_{dd} = 2\overline{u'^2}(1 - R_x) \quad \text{and} \quad B_{nn} = 2\overline{u'^2}(1 - R_y). \tag{2.10}$$

When a turbulent field is not isotropic, and one assumes that there exists local isotropy in a small domain of this field, one implies that the scale of the existing turbulence is much larger than the magnitude of the domain of local isotropy. The theory of local isotropy, which has been discussed by several authors, and more particularly by Batchelor (12), always refers to very large Reynolds numbers of turbulence.

9. *Lagrangian Correlation Coefficient*

Let us consider a point $P_1(x_1,y_1,z_1)$ in a turbulent field. At an instant t, we find (Fig. 10) at this point a fluid element A. After an interval

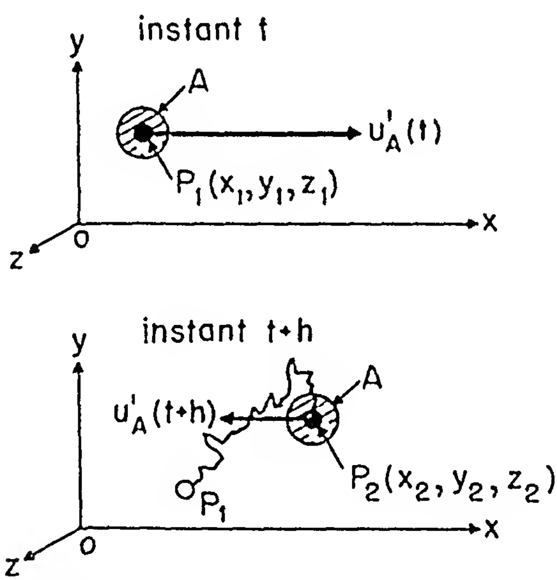

FIG. 10. Diagram illustrating the position of a fluid element at two different instants at which its velocities are correlated by a Lagrangian correlation coefficient.

of time h, A will have moved to a point $P_2(x_2,y_2,z_2)$. The components of the turbulent velocities of A at the two instants t and $t + h$ are, respectively, $u_A'(t)$, $v_A'(t)$, $w_A'(t)$, and $u_A'(t + h)$, $v_A'(t + h)$, $w_A'(t + h)$. We call *Lagrangian correlation coefficients* ratios such as

$$(2.11)\qquad \begin{aligned} R_{tL}{}^u(h) &= \frac{\overline{u_A'(t)\quad u_A'(t+h)}}{\sqrt{\overline{[u_A'(t)]^2}}\sqrt{\overline{[u_A'(t+h)]^2}}}, \\ R_{tL}{}^v(h) &= \frac{\overline{v_A'(t)\quad v_A'(t+h)}}{\sqrt{\overline{[v_A'(t)]^2}}\sqrt{\overline{[v_A'(t+h)]^2}}}. \end{aligned}$$

To these two correlation coefficients correspond two *Lagrangian time-scales of turbulence*

$$(2.12)\qquad L_{tL}{}^u = \int_0^\infty R_{tL}{}^u(\alpha)d\alpha \quad \text{and} \quad L_{tL}{}^v = \int_0^\infty R_{tL}{}^v(\alpha)d\alpha.$$

These scales of turbulence are measured in units of time. Lagrangian spectra of turbulence can be defined (13) as functions of the Lagrangian correlation coefficients by equations similar to (2.5) and (2.6).

In a field of turbulence which is homogeneous, isotropic, and stationary, $R_{tL}{}^u(h) = R_{tL}{}^v(h)$. To simplify the notation, we shall use in the following chapters, which refer to such a field of turbulence, the symbols

$$(2.13)\qquad R_h = R_{tL}{}^u(h) = R_{tL}{}^v(h) = R_{tL}{}^w(h) \text{ and } L_h = L_{tL}{}^u = L_{tL}{}^v = L_{tL}{}^w.$$

When a turbulent field at rest is considered, we shall use for the turbulent components u,v,w instead of u', v', w'. In fact, in this case $u = u'$, $v = v'$, and $w = w'$, since $\bar{u} = \bar{v} = \bar{w} = 0$. When turbulent diffusion in a fluid flow is discussed, where $\bar{u}$ = constant, $\bar{v} = 0$, and $\bar{w} = 0$, we shall represent the mean velocity $\bar{u}$ by the symbol U.

III. Fundamental Equation of Turbulent Diffusion

1. Derivation of the Fundamental Equation

Let us consider, within an incompressible turbulent fluid at rest, a fluid element A which at time 0 is placed at the origin of the coordinate axes (Fig. 11). We shall follow this fluid element as it wanders in a field of homogeneous, isotropic, and stationary turbulence. Let u, v, and w be the x-, y-, and z-components of the instantaneous velocity of the fluid element. Each of these components varies irregularly and shall be considered a random variable. The fluid element which at an initial time was at the origin will be found after a *dispersion time* t at a point $P(x,y,z)$, whose coordinates are equal to

$$(3.1)\qquad x = \int_0^t u(\alpha)d\alpha, \quad y = \int_0^t v(\alpha)d\alpha, \quad z = \int_0^t w(\alpha)d\alpha.$$

We shall investigate the variances of x, y, and z as functions of the dispersion time t. As in the case of the velocity components, we have

for the mean values of these coordinates $\bar{x} = \bar{y} = \bar{z} = 0$. Their variances are functions of the dispersion time, and since the turbulence is homogeneous, isotropic, and stationary, $\overline{x^2} = \overline{y^2} = \overline{z^2} = \Psi(t)$.

The function $\Psi(t)$ depends on the nature of the turbulent fluctuations. We shall determine here $\Psi(t)$ as a function of the turbulence characteristics described in the preceding section. We shall write the equations for the transverse diffusion in the y-direction. Since the turbulence is homogeneous and isotropic, the statistical characteristics will be

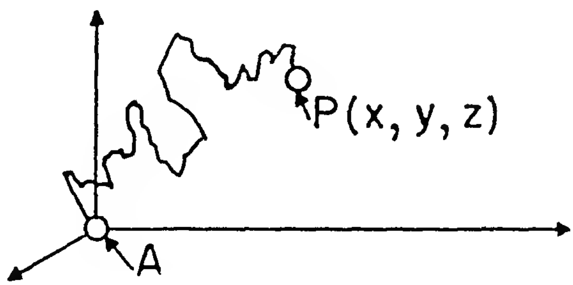

FIG. 11.

the same for the diffusion in the x- and z-directions. Computing the variance $\overline{y^2}$ with the value of y given in Eq. (3.1), we find

$$\overline{y^2} = \overline{\left[\int_0^t v(\alpha)d\alpha\right]^2} = \int_0^t \int_0^t \overline{v(\alpha_1)v(\alpha_2)}d\alpha_1 d\alpha_2. \tag{3.2}$$

Introducing the Lagrangian correlation coefficient $R_h(h)$, which has been defined in the preceding section, we find

$$\overline{y^2} = \overline{v^2} \int_0^t \int_0^t R_h(\alpha_2 - \alpha_1)d\alpha_1 d\alpha_2.$$

Writing $\alpha = \alpha_2 - \alpha_1$ and taking into account the fact that $R_h(h)$ is an even function, we get

$$\overline{y^2} = \overline{v^2} \int_0^t d\alpha_1 \int_{-\alpha_1}^{t-\alpha_1} R_h(\alpha)d\alpha = \overline{v^2}\left[\int_0^t d\alpha_1 \int^{\alpha_1} R_h(\alpha)d\alpha + \int_0^t d\alpha_1 \int_0^{t-\alpha_1} R_h(\alpha)d\alpha\right].$$

After inverting the order of integration and determining the new limits of integration, we find

$$\overline{y^2} = \overline{v^2}\left[\int_0^t d\alpha \int_\alpha^t R_h(\alpha)d\alpha_1 + \int_0^t d\alpha \int_0^{t-\alpha} R_h(\alpha)d\alpha_1\right],$$

which gives finally the fundamental equation of turbulent diffusion,

$$\overline{y^2} = 2\overline{v^2} \int_0^t (t - \alpha)R_h(\alpha)d\alpha. \tag{3.3}$$

This simple relation was first found by a different method by Kampé de Fériet (13). It seems easier to use this equation in applications than the equation

$$\overline{y^2} = 2\overline{v^2} \int_0^t d\alpha_2 \int_0^{\alpha_2} R_h(\alpha_1) d\alpha_1, \tag{3.4}$$

originally derived by Taylor (3).

Equation (3.3) or (3.4) gives the variance $\overline{y^2}(t)$, the expected value of the square of the y-coordinate of a fluid element, at the instant t as a function of the variance $\overline{v^2}$ of turbulent velocities and of the Lagrangian correlation curve $R_h(h)$.

Before discussing the general case, we shall consider two special cases: when the interval of time t is large, and when it is small, compared to the Lagrangian scale of turbulence $L_h = \int_0^\infty R_h(\alpha)d\alpha$.

2. Asymptotic Forms of the Fundamental Equation for Large Dispersion Time

When the dispersion time is large compared to the Lagrangian scale of turbulence L_h, we can write Eq. (3.3) as

$$\overline{y^2} \approx 2\overline{v^2}L_h t - 2\overline{v^2} \int_0^\infty \alpha R_h(\alpha) d\alpha \qquad (t \gg L_h). \tag{3.5}$$

In a turbulent field with a given variance $\overline{v^2}$ and a given Lagrangian correlation curve, the second term on the right is a constant. For very large dispersion times t, this constant becomes small as compared with the first term, and we then find (3)

$$\overline{y^2} \approx 2\overline{v^2}L_h t \qquad (t \gg L_h). \tag{3.6}$$

The variance $\overline{y^2}$ is, therefore, proportional to the dispersion time t when this time is very large compared to the Lagrangian scale of turbulence.

3. Asymptotic Forms for Small Dispersion Time

Consider now the case when the interval of time t is small compared to the Lagrangian scale of turbulence. The correlation coefficient $R_h(h)$ is then nearly equal to one in the integration interval of Eq. (3.3). Expanding the correlation function in a power series and taking into account its evenness, we find (3)

$$R_h(h) = 1 - \frac{h^2}{2}\frac{1}{\overline{v^2}}\overline{\left(\frac{dv}{dt}\right)^2} + \frac{h^4}{24}\frac{1}{(\overline{v^2})^2}\overline{\left(\frac{d^2v}{dt^2}\right)^2} \cdots$$

If we neglect the terms in h of an order higher than the second, we have

(3.7) $$R_h(h) \approx 1 - \frac{h^2}{\lambda_h^2},$$

where

(3.8) $$\frac{1}{\lambda_h^2} = \frac{1}{2\overline{v^2}}\overline{\left(\frac{dv}{dt}\right)^2} = -\frac{1}{2}\frac{d^2R_h(0)}{dh^2}.$$

λ_h is called the *Lagrangian microscale of turbulence.*

We can now substitute Eq. (3.7) in Eq. (3.3), and we find at small dispersion times t the relation

(3.9) $$\overline{y^2} \approx \left[1 - \frac{1}{6}\frac{t^2}{\lambda_h^2}\right]\overline{v^2}t^2 \qquad (t \ll L_h).$$

When t is not only small in comparison with L_h, but also in comparison with λ_h, the second term in the brackets becomes negligible compared to unity and (3)

(3.10) $$\overline{y^2} \approx \overline{v^2}t^2 \qquad (t \ll \lambda_h).$$

The variance $\overline{y^2}$ is, therefore, proportional to the square of the dispersion time t when this time is very small as compared with the Lagrangian scale of turbulence.

4. General Case

In the general case, when the dispersion time t cannot be considered small or large as compared with the Lagrangian scale of turbulence, the variance $\overline{y^2}$ as a function of t depends on the shape of the correlation curve. We consider in this section some examples of correlation functions.

To simplify the notation, we introduce the nondimensional factor ι, which is defined by the relation

(3.11) $$\iota = \frac{1}{L_h}\sqrt{\frac{\overline{y^2}}{\overline{v^2}}}$$

and is called the *dispersion factor.* This factor is proportional to the standard deviation $\sqrt{\overline{y^2}}$. The ratio

(3.12) $$\tau = \frac{t}{L_h}$$

is called the *relative dispersion time.*

In this nondimensional form, Eq. (3.3) becomes

(3.13) $$\iota^2 = 2\int_0^\tau (\tau - \alpha)\mathcal{R}_h(\alpha)d\alpha,$$

where the correlation coefficient $R_h(h)$ is represented as a function of the ratio h/L_h by $\mathcal{R}_h(h/L_h) = R_h(h)$.

In the preceding two sections we have shown that independently of the shape of the correlation curve the variance $\overline{y^2}$ (and, therefore, the dispersion factor ι) is given for large τ by Eq. (3.5) or (3.6), and for small τ by Eq. (3.9) or (3.10). To investigate the variation of ι as a function of τ when τ is not very large or very small compared to 1, we can try to represent the Lagrangian correlation curve by known functions, as is done in Fig. 12. The use of representative correlation functions is often convenient in the statistical analysis of random data, even if these functions do not satisfy all the theoretical requirements of a correlation

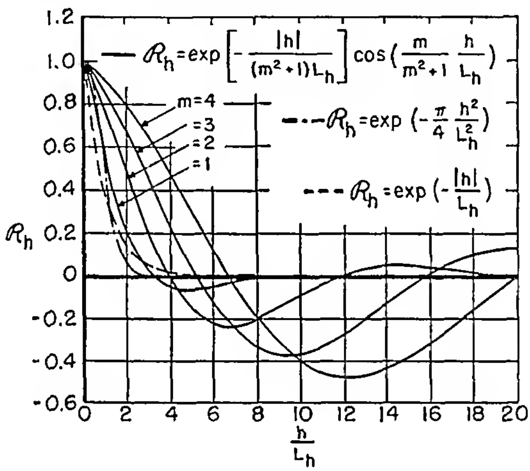

FIG. 12. Examples of representative correlation functions.

function of a continuous random variable (14). For instance, for some of the functions used here, the condition that the derivative at the origin be equal to zero (which follows from the differentiability and evenness of the correlation function) is not satisfied. We assume, in such a case, that the correlation function represents approximately the correct correlation curve for very small values of h/L_h.

We shall now determine, for two examples of correlation functions, analytical expressions approximating the dependence of the dispersion factor on τ and the limits of validity for the approximations. These limits are based on the assumption that the difference between the approximate value of ι^2 and the exact value obtained with the complete correlation function [using Eq. (3.3) or (3.13)] should be no more than 1 per cent of the correct value of ι^2.

When the correlation function is

$$\mathcal{R}_h = \exp\left[-\frac{\pi}{4}\left(\frac{h}{L_h}\right)^2\right], \tag{3.14}$$

we have the following solutions:

(3.15a) $\quad 0 < \tau \leq 0.28 \quad \iota^2 = \tau^2,$

(3.15b) $\quad 0.28 < \tau \leq 0.84 \quad \iota^2 = \left(1 - \frac{\pi}{24}\tau^2\right)\tau^2,$

(3.15c) $\quad 0.84 < \tau \leq 1.7 \quad \iota^2 = 2\tau \operatorname{erf}\left(\frac{\sqrt{\pi}}{2}\tau\right) + \frac{4}{\pi}\left[\exp\left(-\frac{\pi}{4}\tau^2\right) - 1\right],$

(3.15d) $\quad 1.7 < \tau \leq 64.4 \quad \iota^2 = 2\left(\tau - \frac{2}{\pi}\right),$

(3.15e) $\quad 64.4 < \tau \quad \iota^2 = 2\tau.$

The second correlation function we want to treat is [cf. (15)]

(3.16) $$\mathcal{R}_h = \exp\left(-\frac{|h|}{L_h}\right),$$

for which we have the solutions

(3.17a) $\quad 0 < \tau \leq 0.030 \quad \iota^2 = \tau^2,$

(3.17c) $\quad 0.030 < \tau \leq 3.63 \quad \iota^2 = 2[\exp(-\tau) + \tau - 1],$

(3.17d) $\quad 3.63 < \tau \leq 101 \quad \iota^2 = 2(\tau - 1),$

(3.17e) $\quad 101 < \tau \quad \iota^2 = 2\tau.$

Figures 13 and 14 represent the dispersion factor ι and its square ι^2 as functions of the relative dispersion time τ for these two correlation func-

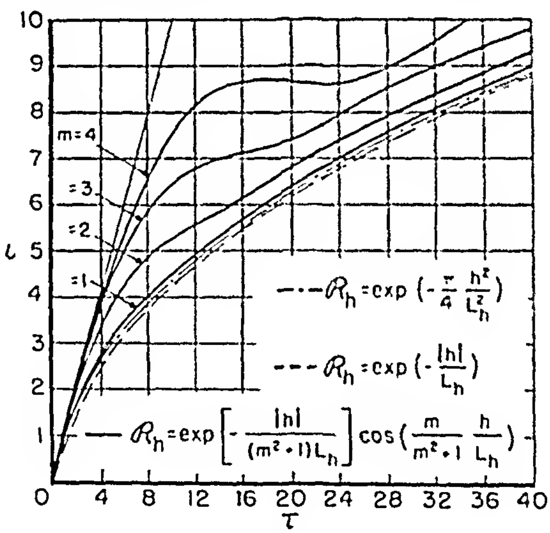

FIG. 13. Variation of the dispersion factor ι with the relative dispersion time τ for the correlation functions of Fig. 12.

tions as well as for the other correlation functions illustrated in Fig. 12. On the two figures, asymptotic values are traced with light lines. These asymptotes illustrate the fact that for τ small ι is linear in τ, as shown by Eq. (3.10), and for τ large ι^2 is linear in τ, as shown by Eq. (3.5).

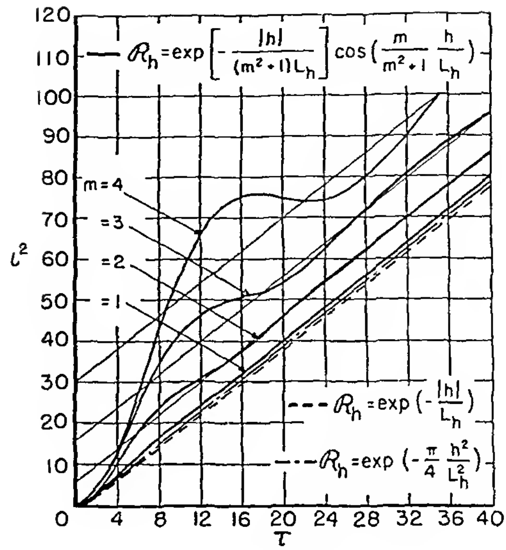

FIG. 14. Variation of ι^2 with the relative dispersion time τ for the correlation functions of Fig. 12.

5. *Measurement of Turbulence Characteristics Using Turbulent Diffusion*

In the preceding paragraphs we have determined the equations of turbulent diffusion when the characteristics of the turbulent field are, or can be assumed, known. Often we have the inverse problem: to determine the characteristics of the turbulent field from measurements of turbulent diffusion. We shall show here how this problem can be treated using the above equations. We are still concerned with homogeneous and isotropic turbulence, and we limit this problem here to the case of a stationary (nondecaying) turbulence in a fluid at rest. Since we refer to experimental measurements, we shall have to assume that the measured averages are equal to the ensemble averages used in the theory (cf. Section II,1).

The value of $\overline{v^2}$, which is proportional to the turbulent energy, can be determined from the measurements at very small dispersion times by the use of Eq. (3.10). We have (3)

$$\overline{v^2} = \lim_{t\to 0} \frac{\overline{y^2}}{t^2} \qquad (t \ll \lambda_h). \tag{3.18}$$

which shows that the standard deviation $\sqrt{\overline{v^2}}$ can be measured by the slope of $\sqrt{\overline{y^2}}\,(t)$ at small values of t.

From the measurements made at very large dispersion times, we find (3) with Eq. (3.6)

$$L_h = \lim_{t\to\infty} \frac{1}{2\overline{v^2}} \frac{\overline{y^2}}{t} \qquad (t \gg L_h) \tag{3.19}$$

in which $\overline{v^2}$ can be replaced by its value given by (3.18).

Both Eqs. (3.5) and (3.6) give (3)

$$L_h = \lim_{t\to\infty} \frac{1}{2\overline{v^2}} \frac{d\overline{y^2}}{dt} \qquad (t \gg L_h) \tag{3.20}$$

which shows that the Lagrangian scale of turbulence can be determined from the slope of $\overline{y^2}(t)$ at large values of t. The two equations (3.19) and (3.20) are valid only for $t \gg L_h$; however, the second one can be used for smaller dispersion times than the first. We also notice that if we trace the line asymptotic to the curve $\overline{y^2}(t)$ at large t, its t-intercept will be the quantity $-2\overline{v^2} \int_0^\infty \alpha R_h(\alpha)d\alpha$.

If we differentiate Eq. (3.3) twice, we find (3)

$$R_h(t) = -\frac{1}{2\overline{v^2}} \frac{d^2\overline{y^2}}{dt^2}. \tag{3.21}$$

The correlation curve can, therefore, be determined by double differentiation of the $\overline{y^2}(t)$ curve after $\overline{v^2}$ has been found from Eq. (3.18).

In practical applications the value of $\overline{v^2}$ can be found without too much difficulty by Eq. (3.18). The application of Eq. (3.21) is, however, much more difficult since calculating the second derivative from a graph is not as easy as reading off the slope.

When the correlation function is known or is assumed in advance, graphic methods can be used to find $\overline{v^2}$ and L_h by applying Eq. (3.13). One can represent sets of curves giving the ratio $\overline{y^2}/\overline{v^2} = \iota^2 L_h^2$ as a function of t for various values of L_h. After $\overline{v^2}$ is computed with Eq. (3.18), the experimental curve for $\overline{y^2}/\overline{v^2}$ can be superimposed on these sets of curves and L_h can be evaluated. Another graphic method would be to represent the curves $\iota(\tau)$ in logarithmic coordinates and superimpose on these curves the experimental $\sqrt{\overline{y^2}}(t)$. A comparison of these curves would give the values of $\overline{v^2}$ and L_h.

IV. Mean Concentration Distribution Produced by a Point Source of Diffusion

1. *Turbulent Fluid at Rest*

Let us consider a turbulent fluid at rest, the turbulence being homogeneous, isotropic and stationary, and let us assume that a large number

of fluid elements are concentrated at time $t = 0$ at the origin of a set of rectangular axes. After an interval of time t these fluid elements are dispersed in a cloud by the influence of the turbulent fluctuations. If the turbulence is homogeneous and isotropic, the cloud is spherically symmetrical. In the preceding sections we have given the variance of the y-coordinates at time t, $\overline{y^2}(t)$, for such a cloud of fluid elements as a function of the characteristics of turbulence. The size of the cloud at any time t is described just by the value of this variance, or rather of its square root, the standard deviation $\sqrt{\overline{y^2}}$. We shall now investigate the distribution of fluid elements within the cloud.

This distribution, assumed to be continuous, can be characterized at any given instant t by the probability of finding a fluid element at some point α,β,γ inside the small parallelepiped dx, dy, dz with one corner at the point x,y,z. Then the relative number of fluid elements in the volume $dx\,dy\,dz$ at time t is Prob $[x < \alpha < x + dx,\ y < \beta < y + dy,\ z < \gamma < z + dz] = \Psi(x,y,z,t)dx\,dy\,dz$. The function $\Psi(x,y,z,t)$, called the probability density function, completely determines the distribution at time t. Obviously, $\iiint_{-\infty}^{+\infty} \Psi(x,y,z,t)dx\,dy\,dz = 1$ for all t. We assume at all times a three-dimensional Gaussian distribution and, therefore, a probability density function of the form $\Psi(x,y,z,t) = (k^3/\pi^{3/2}) \exp [-k^2(x^2 + y^2 + z^2)]$, where k depends on t.

In order to determine k, we compute the variance $\overline{y^2}$ for this distribution. We find

$$\overline{y^2} = \frac{\iiint_{-\infty}^{+\infty} y^2\Psi(x,y,z,t)dx\,dy\,dz}{\iiint_{-\infty}^{+\infty} \Psi(x,y,z,t)dx\,dy\,dz} = \frac{1}{2k^2},$$

and therefore

$$\Psi(x,y,z,t) = [1/(2\pi\overline{y^2})^{3/2}] \exp [-(x^2 + y^2 + z^2)/(2\overline{y^2})]. \tag{4.1}$$

The last equation presents the assumed probability density function at time t in terms of the coordinates x,y,z, and the variance $\overline{y^2}(t)$.

The number (or mass) of fluid elements emitted at the initial moment is denoted by Q_0. $\bar{s}_0(x,y,z,t)$ is the density or mean concentration of such elements at the point x,y,z and time t, measured in number (or mass) of fluid elements per unit of volume. Apparently when $t = 0$, $\bar{s}_0(x,y,z,0) = 0$ for any point x,y,z other than the origin, and $\bar{s}_0(0,0,0,0) = \infty$. The number of fluid elements to be found in a volume element $dx\,dy\,dz$, after

dispersion time t, is $\bar{s}_0(x,y,z,t)dx\,dy\,dz$. Using Eq. (4.1), we have

$$\frac{\bar{s}_0(x,y,z,t)}{Q_0}\,dx\,dy\,dz = \frac{dx\,dy\,dz}{(2\pi\overline{y^2})^{3/2}} \exp\left[-\frac{1}{2\overline{y^2}}(x^2+y^2+z^2)\right]. \tag{4.2}$$

In this equation $\overline{y^2}$ is to be regarded as a function of $\overline{v^2}$, $R_h(h)$ and t as given by Eq. (3.3).

2. Instantaneous Point Source of Dispersion in a Fluid Flow

We shall now examine the case of dispersion of fluid elements from a point source in a turbulent flow. If the axis Ox is taken parallel to the direction of the mean velocity U of the flow, the coordinate x in Eq. (4.2) should be replaced by $(x - Ut)$.

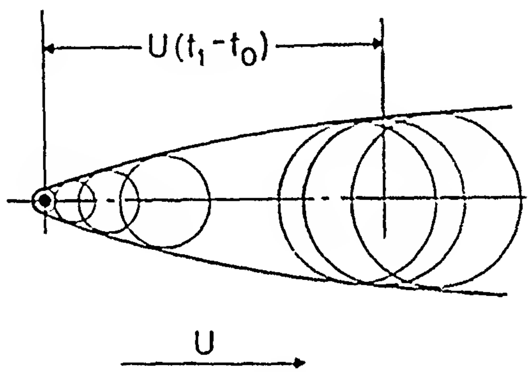

FIG. 15. Sketch of the dispersion wake of a continuous point source showing the superposition of the diffusing spherical clouds.

To facilitate the treatment of the continuous point source of dispersion, in the next section, let us now assume that instead of an instantaneous point source, we have one which emits Q fluid elements per unit of time. Then $\bar{S}(x,y,z,t_1 - t_0)dt_0$, the mean concentration distribution at time t_1 due to the emission of fluid elements during the interval of time $(t_0, t_0 + dt_0)$, is given by

$$\bar{S}(x,y,z,t_1 - t_0)dt_0 = \frac{Q\,dt_0}{(2\pi\overline{y^2})^{3/2}} \exp\left\{-\frac{1}{2\overline{y^2}}\{[x - U(t_1 - t_0)]^2 + y^2 + z^2\}\right\}. \tag{4.3}$$

3. Continuous Point Source of Dispersion in a Fluid Flow

Consider now the dispersion from a continuous source emitting steadily Q fluid elements per unit of time (16). The dispersion wake of the continuous source can be considered the result of the superposition of an infinite number of diffusing spherical clouds which move with the mean velocity U (Fig. 15). The mean concentration at a point x,y,z and time

t_1 is equal to the sum of the effects of the emission from $-\infty$ till t_1, or

$$(4.4)\quad \int_{-\infty}^{t_1} \bar{S}(x,y,z,t_1-\alpha)d\alpha = \int_{-\infty}^{t_1} \frac{Q}{(2\pi\overline{y^2})^{3/2}} \exp\left\{-\frac{1}{2\overline{y^2}}\{[x-U(t_1-\alpha)]^2+y^2+z^2\}\right\} d\alpha.$$

After introducing the variable dispersion time $\beta = t_1 - \alpha$, one finds

$$(4.5)\quad \int_{-\infty}^{t_1} \bar{S}(x,y,z,t_1-\alpha)d\alpha = \int_0^{\infty} \frac{Q}{(2\pi\overline{y^2})^{3/2}} \exp\left[-\frac{(x-U\beta)^2+y^2+z^2}{2\overline{y^2}}\right] d\beta,$$

where

$$\overline{y^2} = 2\overline{v^2}\int_0^{\beta}(\beta-\gamma)R_h(\gamma)d\gamma.$$

Since the right-hand member of (4.5) does not contain t_1, the mean concentration

$$(4.6)\quad \bar{s}(x,y,z) = \int_{-\infty}^{t_1} \bar{S}(x,y,z,t_1-\alpha)d\alpha$$

is independent of the time t_1.

Let us consider a plane perpendicular to the direction of the mean velocity U and placed at a distance x downstream of the point source. The average number of fluid elements which pass through an element of area $dy\,dz$ of this plane during a unit of time is given by $\bar{s}(x,y,z)U\,dy\,dz$. During this unit of time the source emits Q fluid elements. The quantity

$$(4.7)\quad \frac{\bar{s}(x,y,z)U}{Q} = \frac{1}{(2\pi)^{3/2}}U\int_0^{\infty}\frac{1}{(\overline{y^2})^{3/2}}\exp\left[-\frac{(x-U\alpha)^2+y^2+z^2}{2\overline{y^2}}\right]d\alpha$$

is the (relative) mean concentration flux distribution at the point x,y,z in the plane x.

4. Nondimensional Distribution Function

We shall now represent Eq. (4.7) in a nondimensional form. With this representation it will be easier to examine the dependence of the mean concentration flux on the various parameters. We introduce new coordinates

$$\xi = x/UL_h, \quad \eta = y/UL_h, \quad \zeta = z/UL_h,$$

in which L_h is the Lagrangian scale of turbulence. The Lagrangian correlation function is again represented as a function of h/L_h by

$$\mathcal{R}_h(h/L_h) = R_h(h),$$

and the intensity of turbulence is given by

$$T = \sqrt{\overline{v'^2}}/U.$$

The distribution function is represented as a function of the above coordinates by

$$\sigma_U(\xi,\eta,\zeta) = U^2L_h^2[\bar{s}(x,y,z)U/Q].$$

With the nondimensional notation, Eq. (4.7) becomes

(4.8) $\sigma_U(\xi,\eta,\zeta)$

$$= \frac{1}{(2\pi)^{3/2}T'^3}\int_0^\infty \frac{1}{\iota^3(\beta)}\exp\left\{-\frac{1}{2T'^2\iota^2(\beta)}[(\xi-\beta)^2+\eta^2+\zeta^2]\right\}d\beta,$$

where
$$\iota^2(\beta) = 2\int_0^\beta (\beta-\gamma)\mathcal{R}_h(\gamma)d\gamma.$$

We see immediately that the mean concentration distribution, besides depending on the coordinates, is a function of

(a) the shape of the Lagrangian correlation curve determined by the function $\mathcal{R}_h(h/L_h)$,

(b) the intensity of turbulence T', and

(c) the product UL_h of the mean velocity by the Lagrangian scale of turbulence.

The mean concentration is independent of the time at which it is observed.

In Eq. (4.8) ξ represents the distance downstream from the continuous source. We shall consider two cases: when the distance is large and when it is small, i.e., when ξ is respectively large and small compared to unity.[5] In the first case the time available for the dispersion is large; in the second case the dispersion time is small. The relative magnitudes of these times depend on the shape of the Lagrangian correlation curve, as we have shown in Section III,4.

5. *Large Distances from a Continuous Point Source*

When the dispersion time is large

(4.9) $$\iota^2(\tau) = 2\tau$$

and $\iota^2(\beta) = 2\beta$. Replacing $\iota^2(\beta)$ in Eq. (4.8) by 2β, we find after integration

(4.10) $$\sigma_U(\xi,\eta,\zeta) = \frac{1}{4\pi T'^2\rho}\exp\left(\frac{\xi-\rho}{2T'^2}\right),$$

where $\rho = \sqrt{\xi^2+\eta^2+\zeta^2}$.

[5] The validity of the small distance approximation (3.10) seems more limited than that of the large distance one (3.6) because $\iint\sigma_U d\eta d\zeta$, over any plane ξ = const., diverges in the small distance case, but not in the large distance case.

The dispersion factor ι was determined neglecting the diffusion in the direction of the mean flow. The value of ι corresponds to a one-dimensional case of diffusion. We now recompute ι taking into account the three-dimensionality of the dispersion wake. The new dispersion factor ι_d corresponds to the standard deviation $\sqrt{\overline{y_d^2}}$ for the mean concentration flux measured in a plane perpendicular to the direction of the mean velocity along a diameter passing through the dispersion axis OX. We have

$$\iota_d^2 = \frac{1}{L_h^2}\frac{\overline{y_d^2}}{\overline{v^2}} = \frac{\int_0^\infty \eta^2 \sigma_U(\xi,\eta,0)d\eta}{T^2\int_0^\infty \sigma_U(\xi,\eta,0)d\eta}. \tag{4.11}$$

We now replace σ_U in the above equation by its value given in Eq. (4.10). Replacing the ratio η/ξ in the two integrals by a hyperbolic sine and using the Schläfli transformation for the modified Bessel functions of the second kind, $K_n(a) = \int_0^\infty \exp(-a \cosh \alpha) \cosh (n\alpha) d\alpha$, we find

$$\iota_d^2 = 2\xi \frac{K_1\left(\frac{\xi}{2T^2}\right)}{K_0\left(\frac{\xi}{2T^2}\right)}. \tag{4.12}$$

Figure 16 represents ι_d^2 as a function of ξ/T^2. Since the ratio of the first order Bessel function K_1 to the zero order Bessel function K_0 tends to one

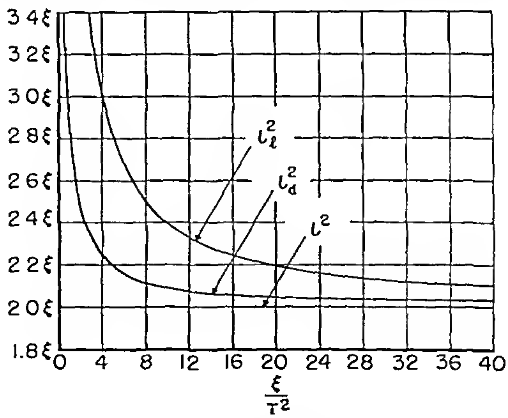

Fig. 16. Variation of the square of the dispersion factor (in units of ξ) with ξ/T^2 for an instantaneous point source (ι^2), a continuous point source (ι_d^2), and for a continuous line source (ι_l^2).

when their common argument tends to infinity, we have

$$\lim_{\xi/T^2\to\infty} \iota_d^2 = \iota^2 = 2\xi. \tag{4.13}$$

In the limit, therefore, we have a relation corresponding to the equation which Taylor has given (cf. Eq. 3.6) for the one-dimensional case.

It should be noted that Eq. (4.12) is valid only when ξ is much larger than unity. On the other hand, when ξ/T^2 is very large Eq. (4.12) is well represented by its asymptotic form (4.13). Equation (4.12) will, therefore be most useful when both ξ and T are large.

An approximate formula can be given for $\sigma v(\xi,\eta,\zeta)$ for the case when η and ζ are small compared with ξ. Developing $(\xi - r)$ in a series and neglecting the high order terms, we find from (4.10) the approximate relation of Roberts [cf. (17)]

$$\sigma v(\xi,\eta,\zeta) \approx \frac{1}{4\pi T^2}\frac{1}{\xi}\exp\left(-\frac{\eta^2+\zeta^2}{4T^2\xi}\right), \tag{4.14}$$

which in any plane ξ = constant represents a Gaussian mean concentration distribution.

6. *Small Distances from a Continuous Point Source*

When the distance from the source is sufficiently small,

$$\iota(\tau) = \tau. \tag{4.15}$$

After replacing $\iota(\beta)$ by β in Eq. (4.8) and performing the integration, we find

$$\sigma v(\xi,\eta,\zeta) = \frac{1}{(2\pi)^{3/2}}\frac{1}{\rho^2 T}\exp\left(-\frac{1}{2T^2}\right) \left[1+\sqrt{\frac{\pi}{2}}\frac{\xi}{T\rho}\exp\left(\frac{1}{2T^2}\frac{\xi^2}{\rho^2}\right)\operatorname{erfc}\left(-\frac{1}{\sqrt{2}\,T}\frac{\xi}{\rho}\right)\right], \tag{4.16}$$

where $\rho^2 = \xi^2 + \eta^2 + \zeta^2$ and $\operatorname{erfc}(a) = 1 - (2/\sqrt{\pi})\int_0^a \exp(-\alpha^2)d\alpha$.

Equation (4.16) can be simplified in some special cases. For instance, when the intensity of turbulence is small, the first term in the brackets may be neglected in comparison with the second term. If, in addition, T is small compared to the ratio ξ/ρ (the cosine of the angle between the dispersion axis and the line joining the point (ξ,η,ζ) to the source), we can simplify further by noting that $\operatorname{erfc}(a)$ approaches 2 for positive ξ. Finally, for small values of η and ζ as compared to ξ (and for small T), we find the simple relation

$$\sigma v(\xi,\eta,\zeta) \approx \frac{1}{2\pi T^2}\frac{1}{\xi^2}\exp\left(-\frac{1}{2T^2}\frac{\eta^2+\zeta^2}{\xi^2}\right), \tag{4.17}$$

which gives an approximate solution for positive ξ.

A numerical application of Eq. (4.16) is shown in Fig. 17 for the case when the turbulent intensity is $T = 0.5$. Mean concentrations in the

planes containing the dispersion axis ξ, are given by representing several iso-concentration curves (σ_U = const.) using as coordinates ξ and $\delta = \sqrt{\eta^2 + \zeta^2}$. It should be noticed that with Eq. (4.16), we find upstream of the dispersion origin finite mean concentrations.

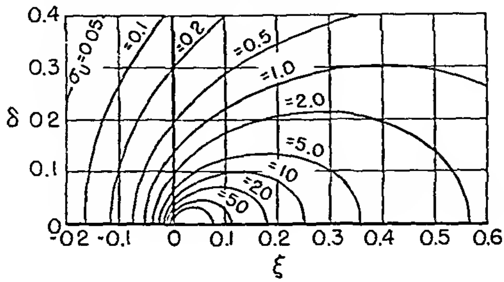

FIG. 17. Mean concentration distribution in a plane containing the dispersion axis for small distances from a continuous point source and for an intensity of turbulence $T = 0.5$.

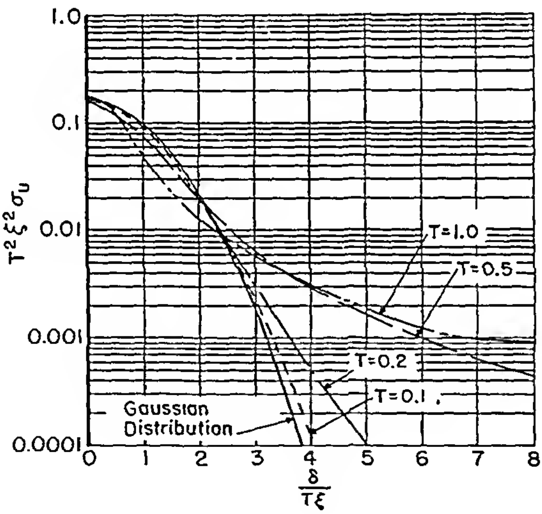

FIG. 18. Mean concentration distributions in planes perpendicular to the mean velocity direction at small distances from a continuous point source. Comparison between an approximate Gaussian distribution (for $T \ll 1$) and the distributions obtained with Eq. (4.16).

While the approximate equation (4.17) yields a Gaussian distribution of mean concentrations in any plane ξ = constant, the Eq. (4.16) gives a non-Gaussian distribution.

A comparison is made in Fig. 18 between the Gaussian mean concentration distribution in planes ξ = constant corresponding to the approximate Eq. (4.17) and the distributions found using Eq. (4.16). The product $T^2\xi^2\sigma_U$ is presented as a function of $\delta/T\xi$ for both equations.

These distributions are represented for several values of the intensity of turbulence for positive ξ. As we see, the difference between the results obtained using the two equations become very large when the intensity of turbulence or the transverse distance δ is large.

7. *Approximate Solution for the Continuous Point Source*

When the turbulent velocities are small compared with the mean velocity, it may be possible to neglect the diffusion in the mean velocity direction. We shall use this assumption, for a continuous point source emitting Q fluid elements per unit of time in a fluid flow with mean velocity U, to find approximate expressions for the mean concentration

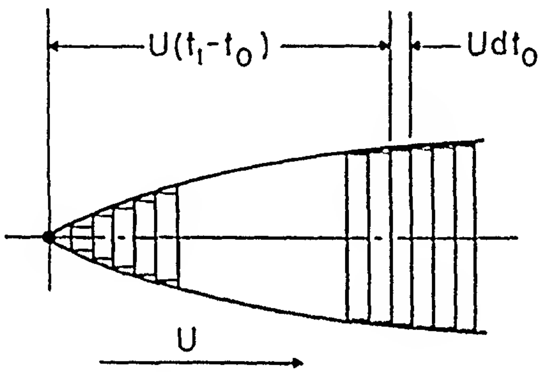

FIG. 19. Sketch of the dispersion wake of a continuous point source showing the wake formed by disk elements assuming no diffusion in the mean velocity direction (for $T \ll 1$).

distribution. All the fluid elements emitted during an interval of time $(t_0, t_0 + dt_0)$ will be found within a disk limited by two planes perpendicular to the mean velocity direction and placed at any moment t_1 at distances $U(t_1 - t_0)$ and $U(t_1 - t_0) + U dt_0$ downstream of the source. The dispersion wake of the continuous source is now assumed to be formed by an infinite number of such disk elements placed one against another downstream of the source (Fig. 19). In Section IV,3 the dispersion wake was found as a result of the superposition of an infinite number of spherical clouds. The mean concentration distribution in a disk element can be found using Eq. (4.2), which corresponds to one such spherical cloud, by performing an integration from $-\infty$ to $+\infty$ with respect to x. We find as a result of this integration

$$\sigma_U(\xi,\eta,\zeta) \approx \frac{1}{2\pi\iota^2(\xi)T^2} \exp\left[-\frac{\eta^2 + \zeta^2}{2\iota^2(\xi)T^2}\right], \tag{4.18}$$

where
$$\iota^2(\xi) = 2\int_0^\xi (\xi - \alpha)\mathfrak{R}_h(\alpha)d\alpha.$$

This approximate equation is useful for the whole range of positive ξ and represents a Gaussian mean concentration distribution in any plane ξ = constant. For the two cases of large and small distances from the source Eq. (4.18) leads to (4.14) and (4.17), respectively. For intermediate distances, the mean concentration distribution is a function of

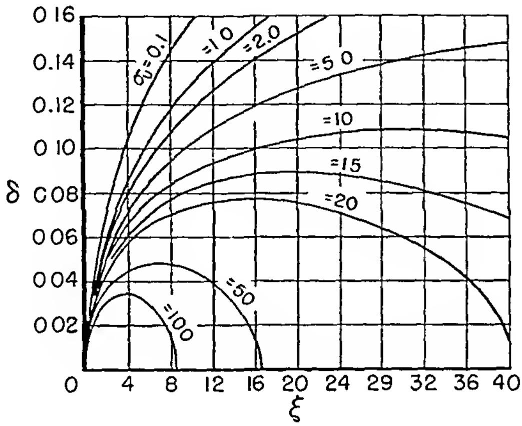

FIG. 20. Mean concentration distribution for a continuous point source in a plane containing the dispersion axis. Approximate solution for the case when the Lagrangian correlation function is $\mathfrak{R}_h = \exp [-\pi h^2/(4L_h^2)]$.

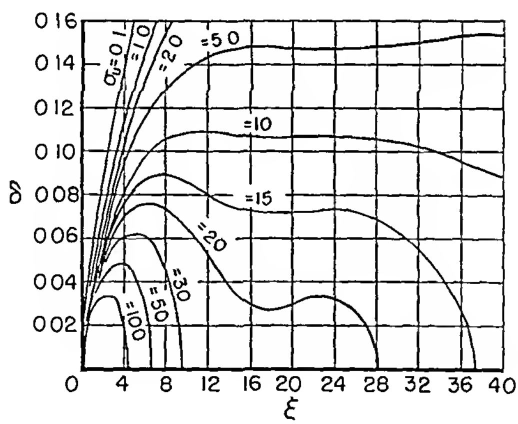

FIG. 21. Mean concentration distribution for a continuous point source in a plane containing the dispersion axis. Approximate solutions for the case when $\mathfrak{R}_h = \cos\{[m/(m^2 + 1)](h/L_h)\}\exp\{-|h|/[L_h(m^2 + 1)]\}$ with $m = 4$.

the shape of the Lagrangian correlation curve. Figures 20 and 21 represent mean concentration distributions for two particular correlation functions. Iso-concentration curves (σ_U = const.) are given for the plane containing the dispersion axis. Some of the curves traced on Fig. 21 present humps. This particular kind of iso-concentration curve

is obtained because this figure corresponds to the case when the correlation curve $\mathcal{R}_h(h)$ presents large negative values (cf. Fig. 12).

8. *Mean Concentration Distribution along the Dispersion Axis*

Expressions for the mean concentration distribution along the ξ-axis can be found by setting $\eta = \zeta = 0$ in the expression for σ_U given in the preceding sections. At large distances from the source ($\xi \gg 1$) Eq. (4.10) can be used. For small distances from the source ($\xi \ll 1$) Eqs. (4.16) and (4.17) may be applied, the latter being an approximate solution for

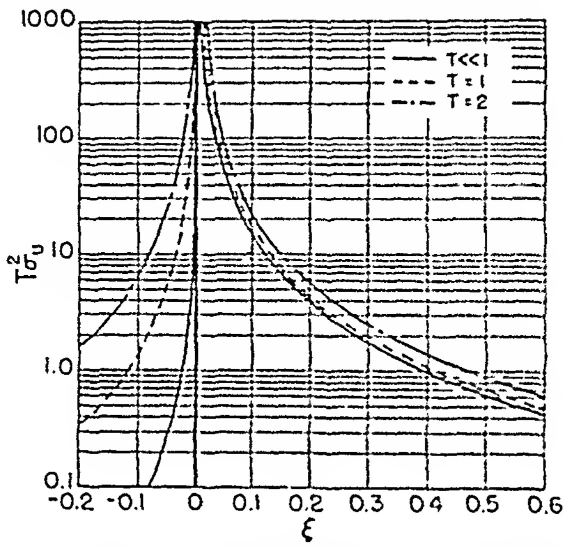

FIG. 22. Mean concentration distribution along the dispersion axis at small distances from a continuous point source. Comparison of the approximate and the exact solutions.

small intensities of turbulence T. Figure 22 represents $T^2\sigma_U(\xi,0,0)$ as a function of ξ for the case of small ξ. The correct solution (4.16) is represented by several curves, corresponding to different values of T, while the approximate Eq. (4.17) is represented by the single light curve.

An approximate solution for the whole range of positive values is obtained from (4.18) with $\eta = \zeta = 0$. The mean concentration distribution along the dispersion axis corresponding to this approximate equation is shown on Fig. 23. Curves representing $T^2\sigma_U(\xi,0,0)$ for several shapes of the Lagrangian correlation curve are traced as functions of ξ. It may be interesting to remark that for several experimental measurements made in the natural wind (17) the mean concentration along the dispersion axis of a continuous point source is proportional to the distance from the source raised to the power -1.76. Some of the curves represented on Fig. 23 have, for small ξ, a slope corresponding closely to such an

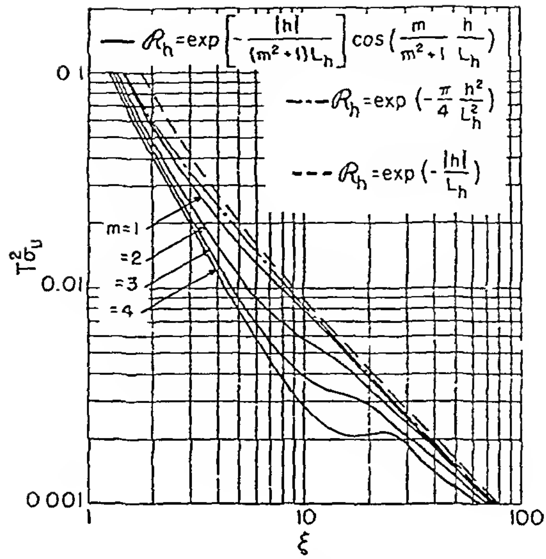

FIG. 23. Mean concentration distribution along the dispersion axis as a function of the distance from a continuous point source. Approximate solutions for several Lagrangian correlation functions.

experimental result. We shall not, however, at this time try to attach any particular significance to this result.

9. *Mean Opacity*

In many experimental investigations one is concerned with the measurement of the outline of a dispersing cloud by a distant observer. We shall define as the *mean opacity* (18) the mean concentration integrated along the line of sight of the observer. For the case of an instantaneous point source, if one looks along a line in the z-direction, the mean opacity is just

$$\bar{N}_0(x,y,t) = \int_{-\infty}^{+\infty} \bar{s}_0(x,y,z,t)dz.$$

Using Eq. (4.3), we find

$$\bar{N}_0(x,y,t) = \frac{Q_0}{2\pi\overline{y^2}} \exp\left[-\frac{1}{2\overline{y^2}}(x^2+y^2)\right]. \tag{4.19}$$

For the same line of sight, the mean opacity of the turbulent wake of a continuous point source placed in a fluid flow is

$$\bar{N}(x,y) = \int_{-\infty}^{+\infty} \bar{s}(x,y,z)dz.$$

It can easily be seen that the calculation of the mean opacity for a continuous point source is the same as the calculation of the mean concentration for an infinite linear source. We can, therefore, apply the results

for the infinite linear source, which will be found in the next chapter, to obtain the mean opacity for a continuous point source. To simplify the application of these results, we rewrite the last equation as follows:

$$UL_h\left(\frac{\bar{N}(x,y)U}{Q}\right) = \int_{-\infty}^{+\infty} \sigma_U(\xi,\eta,\zeta)d\zeta = \sigma_{U,l}, \tag{4.20}$$

referring to the next section for the expressions represented by $\sigma_{U,l}$.

V. Mean Concentration Distribution Produced by an Infinite Line Source of Diffusion

1. Nondimensional Distribution Function

Let us now consider the turbulent diffusion from a continuous linear source of infinite length emitting Q_l fluid elements per unit of time and unit of length of the source. The x-axis is chosen parallel to the direction of the mean velocity U, and the z-axis is aligned with the linear source. We shall first consider the diffusion of those elements which are emitted during an interval of time $(t_0,t_0 + dt_0)$ from an element of length of the source $(z_0,z_0 + dz_0)$. Then $\bar{S}_l(x,y,z - z_0,t_1 - t_0)dt_0dz_0$, the mean concentration distribution at a point (x,y,z) and at the time t_1 due to these fluid elements, is given by (cf. Section IV,2)

$$\bar{S}_l(x,y,z - z_0,t_1 - t_0)dt_0dz_0 = \frac{Q_l dt_0 dz_0}{(2\pi\overline{y^2})^{3/2}} \exp \left\{-\frac{1}{2\overline{y^2}}\{[x - U(t_1 - t_0)]^2 + y^2 + (z - z_0)^2\}\right\}. \tag{5.1}$$

The mean concentration distribution due to the continuous emission of the infinitely long line source is obtained by integrating from $-\infty$ to t_1 for t_0 and from $-\infty$ to $+\infty$ for z_0. After performing this double integration (cf. Section IV,3), we find that

$$\begin{aligned} \bar{s}_l(x,y) &= \int_{-\infty}^{+\infty}\int_{-\infty}^{t_1} \bar{S}_l(x,y,z - z_0,t_1 - t_0)dt_0dz_0 \\ &= \frac{Q_l}{2\pi}\int_0^{\infty} \frac{1}{\overline{y^2}} \exp\left[-\frac{(x - U\alpha)^2 + y^2}{2\overline{y^2}}\right] d\alpha \end{aligned}$$

is independent of z and of t_1. Let us consider a plane perpendicular to the mean velocity direction placed at a distance x downstream of the linear source. The average number of fluid elements per unit of time which pass through a rectangular element of area of unit length in the z-direction, and of length dy in the y-direction, is given by $\bar{s}_l(x,y)Udy$.

The mean concentration distribution function, represented by

$$\sigma_{U,l}(\xi,\eta) = UL_h[\bar{s}_l(x,y)U/Q_l],$$

is found to be

$$(5.2)\quad \sigma_{U,l}(\xi,\eta) = \frac{1}{2\pi T^2}\int_0^\infty \frac{1}{\iota^2(\beta)}\exp\left\{-\frac{1}{2T^2\iota^2(\beta)}[(\xi-\beta)^2+\eta^2]\right\}d\beta,$$

where $\iota^2(\beta) = 2\int_0^\beta (\beta-\gamma)\Re_h(\gamma)d\gamma$.

We note that $\sigma_{U,l}$ is directly related to the σ_U given in Eq. (4.8):

$$(5.3)\qquad \sigma_{U,l}(\xi,\eta) = \int_{-\infty}^{+\infty}\sigma_U(\xi,\eta,\zeta)d\zeta.$$

2. Large Distances from a Continuous Linear Source

When the distance from the source is very large, we find, using Eqs. (4.10) and (5.3),

$$\sigma_{U,l}(\xi,\eta) = \frac{1}{4\pi T^2}\int_{-\infty}^{+\infty}\frac{1}{\sqrt{(\xi^2+\eta^2+\zeta^2)}}\exp\left[\frac{1}{2T^2}(\xi-\sqrt{\xi^2+\eta^2+\zeta^2})\right]d\zeta.$$

Changing the variables by introducing $\sinh^2\varphi = \zeta^2/(\xi^2+\eta^2)$, and using the Schläfli transformation, we find after integration

$$(5.4)\qquad \sigma_{U,l}(\xi,\eta) = \frac{1}{2\pi T^2}\exp\left(\frac{\xi}{2T^2}\right)K_0\left(\frac{\sqrt{\xi^2+\eta^2}}{2T^2}\right).$$

We shall now determine the dispersion factor ι_l, defined by

$$\iota_l^2 = \frac{1}{L_h^2}\frac{\overline{y_l^2}}{\overline{v^2}} = \frac{\int_0^\infty \eta^2\sigma_{U,l}(\xi,\eta)d\eta}{T^2\int_0^\infty \sigma_{U,l}(\xi,\eta)d\eta}$$

just as the dispersion factor ι_d was given in Eq. (4.11). ι_l represents the standard deviation $\sqrt{\overline{y_l^2}}$ for the mean concentration measured along a line in the y-direction.

After replacing $\sigma_{U,l}$ in the last equation by the use of (5.4) and changing the variables in the two integrals by setting $\eta/\xi = \sinh\varphi$, we apply a Sonine transformation for Bessel functions of the second kind which can be written as

$$K_{n+1}(ab) = \{a^{n+1}/[2^n b^{n+1}\Gamma(n+1)]\}\int_0^\infty K_0(a\sqrt{\alpha^2+b^2})\alpha^{2n+1}d\alpha$$

and we find

$$\iota_l^2 = 2\xi\frac{K_{3/2}\left(\frac{\xi}{2T^2}\right)}{K_{1/2}\left(\frac{\xi}{2T^2}\right)}.$$

The last relation can be easily reduced to

(5.5) $$\iota_l^2 = 2\xi\left(1 + \frac{2T^2}{\xi}\right).$$

The dispersion factor ι_l for the linear source can now be compared to the dispersion factor ι_d for the point source as well as to ι corresponding to the one-dimensional case of Taylor. These three dispersion factors are represented in Fig. 16 as functions of the ratio ξ/T^2. It should be again noted that the results given on this figure are valid only at large distances from the source.

When η/ξ and T are both small, then Eq. (5.4) can be approximated by

(5.6) $$\sigma_{U,l}(\xi,\eta) \approx \frac{1}{2\sqrt{\pi\xi}\,T} \exp\left[-\frac{\eta^2}{4\xi T^2}\right],$$

which is a Gaussian distribution in η.

3. *Small Distances from a Continuous Linear Source*

When the distance from a continuous linear source is sufficiently small, the mean concentration distribution is found with Eqs. (4.8), (4.15), and (5.3), which give, after introduction of polar coordinates,

$$\sigma_{U,l}(\xi,\eta) = \frac{1}{(2\pi)^{3/2}T^3} \exp\left(-\frac{1}{2T^2}\right) \int_0^\pi \csc^3\varphi \exp\left(-\frac{\operatorname{ctg}^2\varphi}{2T^2}\right)$$
$$\int_0^\infty \frac{1}{\alpha^2} \exp\left[-\frac{1}{2T^2}\left(\frac{\xi^2+\eta^2}{\alpha^2}\csc^2\varphi - 2\frac{\xi}{\alpha}\csc\varphi\right)\right] d\varphi\, d\alpha.$$

When the integration is performed, we find[6]

(5.7) $$\sigma_{U,l}(\xi,\eta) = \frac{1}{2\sqrt{2\pi}\,T} \frac{1}{\sqrt{\xi^2+\eta^2}} \exp$$
$$\left(-\frac{1}{2T^2}\frac{\eta^2}{\xi^2+\eta^2}\right) \operatorname{erfc}\left(-\frac{1}{\sqrt{2}\,T}\frac{\xi}{\sqrt{\xi^2+\eta^2}}\right).$$

If η/ξ and T are small, this equation can be simplified for positive ξ, to give

(5.8) $$\sigma_{U,l}(\xi,\eta) \approx \frac{1}{\sqrt{2\pi}\,T\xi} \exp\left(-\frac{1}{2T^2}\frac{\eta^2}{\xi^2}\right).$$

[6] The restricted validity of this formula, and of others referring to small distances was mentioned in a footnote on page 87. Successive integrations of $\sigma_U(\xi,\eta,\zeta)$ in (4.8) first with respect to ζ, and then η, seem to aggravate the difficulty, because numerical calculations of $\sigma_{U,l}(\xi,\eta) = \int \sigma_U(\xi,\eta,\zeta)d\zeta$ are less satisfactory than those of $\sigma_U(\xi,\eta,\zeta)$ and, as noted on page 87, $\int\int \sigma_U(\xi,\eta,\zeta)d\zeta d\eta$ is infinite. This point will be discussed further in a forthcoming paper by the author and B. A. Fleishman.

4. Approximate Solution for the Whole Range of Distances from a Continuous Linear Source

An approximate solution found for the mean concentration distribution with Eqs. (4.18) and (5.3) is given by

$$\sigma_{U,l}(\xi,\eta) \approx \frac{1}{\sqrt{2\pi}\, \iota(\xi) T} \exp\left[- \frac{\eta^2}{2\iota^2(\xi) T^2} \right]. \tag{5.9}$$

This relation can be used for the whole range of positive values of ξ when both η/ξ and T are small compared to unity. For the two cases of large and small ξ (5.9) leads to (5.6) and (5.8), which have been already given.

VI. Differential Equations of Diffusion and Statistical Theory of Turbulence

1. Molecular Diffusion

The law of molecular diffusion was first stated in 1855 by Fick (19). For the three-dimensional case of molecular diffusion this law is given as a partial differential equation

$$\frac{\partial \bar{s}_0}{\partial t} = D\nabla^2 \bar{s}_0 \tag{6.1}$$

$\left(\nabla^2 = \frac{\partial^2}{\partial x^2} + \frac{\partial^2}{\partial y^2} + \frac{\partial^2}{\partial z^2}\right)$, in which $\bar{s}_0$ is the mean concentration for the diffusing molecules at a point (x,y,z) and time t and D is the *coefficient of molecular diffusion.*

In the case of an instantaneous point source of diffusion placed at the origin of the coordinates, the solution of (6.1) is given by

$$\bar{s}_0 = \text{const.} \frac{1}{(Dt)^{3/2}} \exp\left[- \frac{x^2 + y^2 + z^2}{4Dt} \right]. \tag{6.2}$$

The numerical value of the coefficient D depends on the nature of the diffusing fluid and on the nature of the fluid in which the process of diffusion takes place. When the differences between the two fluids can be neglected, the coefficient of molecular diffusion D can be related to the coefficient of kinematic viscosity ν by the relation [cf. (20)]

$$D = \epsilon\nu, \tag{6.3}$$

where ϵ is a numerical coefficient. A simplified relation

$$D \approx \nu \tag{6.4}$$

is also often used. The variance (cf. Section IV,1) $\overline{y^2}_{\text{mol}}$ for the molecular diffusion is readily found from Eq. (6.2) to be

$$\overline{y^2}_{\text{mol}} = 2Dt. \tag{6.5}$$

This variance is proportional to the dispersion time t. (In the above discussion the scale on which the diffusion process takes place is much larger than the molecular magnitudes.)

In the preceding chapters we have neglected the effects of the molecular agitation in comparison with the effects of turbulence. We shall now compare these effects for the case of an instantaneous point source. We call $\overline{y^2}_{tot}$ the variance of the dispersing cloud produced by both turbulence

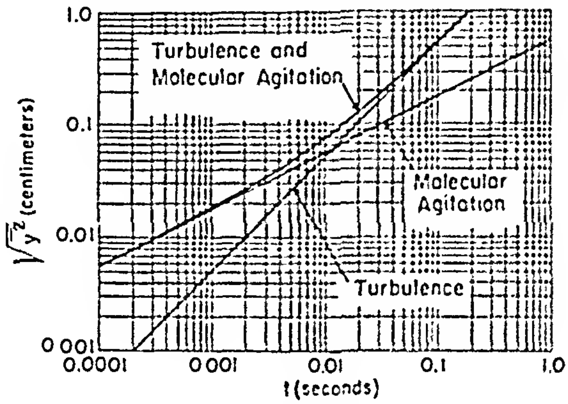

FIG. 24. Comparison of the variances $\sqrt{\overline{y^2}}$ produced by: molecular agitation alone, turbulence alone, and by molecular agitation and turbulence simultaneously. This example corresponds to the case of small dispersion time ($t \ll L_h$) and when $\sqrt{\overline{v^2}} = 5$ cm./sec.

and molecular agitation. Assuming that there is no correlation between the molecular agitation and the turbulent fluctuations, one finds (21,22)

$$\overline{y^2}_{tot} = \overline{y^2}_{turb} + \overline{y^2}_{mol}. \tag{6.6}$$

While $\overline{y^2}_{mol}$ is proportional to t, $\overline{y^2}_{turb}$ is expressed as a function of t by Eq. (3.3). When the dispersion time is very small compared to the Lagrangian scale of turbulence (but large as compared to molecular magnitudes) then $\overline{y^2}_{turb} \approx \overline{v^2}t^2$ and, therefore, $\overline{y^2}_{mol} > \overline{y^2}_{turb}$ as long as $t < 2D/\overline{v^2}$. A numerical comparison between $\overline{y^2}_{mol}$ and $\overline{y^2}_{turb}$ is made in Fig. 24. In this figure a coefficient of molecular diffusion

$$D \approx \nu = 0.15 \text{ cm.}^2/\text{sec.}$$

is used and a standard deviation of turbulent velocities $\sqrt{\overline{v^2}} = 5$ cm./sec. As we see, the effects of molecular agitation on the dispersion are not always negligible as compared to the effects of turbulence; indeed, when the dispersion process starts, the former effect is greater than the latter.

Similar relations can be written for the dispersion of Brownian particles in a turbulent fluid. The variance for the Brownian movement is expressed by Einstein's equation (23), which is analogous to Eq. (6.5)

except that the coefficient of molecular diffusion is replaced by an appropriate coefficient for the Brownian diffusion.

2. Fickian Law of Turbulent Diffusion and the Coefficient of Eddy Diffusion

Extensive use is made, especially in the scientific literature on atmospheric turbulence, of differential equations to describe the process of turbulent diffusion. Let us, for instance, consider the instantaneous point source in a field of homogeneous and isotropic turbulence in a fluid at rest. It is rather widely believed that in this case the turbulent diffusion obeys the *Fickian law of diffusion*

$$\frac{\partial \bar{s}_0(x,y,z,t)}{\partial t} = K\nabla^2 \bar{s}_0(x,y,z,t), \tag{6.7}$$

in which $\bar{s}_0(x,y,z,t)$ is again the mean concentration at a point (x,y,z) and at an instant t, and K is a *coefficient of eddy diffusion* independent of the dispersion time. The character of the turbulent flow is often described in the literature by the value of the coefficient K. Since (cf. Section IV,1) at $t = 0$, $\bar{s}_0(0,0,0,0) = \infty$ and $\bar{s}_0(x,y,z,0) = 0$, and since

$$\int_{-\infty}^{+\infty} \int_{-\infty}^{+\infty} \int_{-\infty}^{+\infty} \bar{s}_0(x,y,z,t)dx\,dy\,dz = Q_0,$$

one finds for the solution of (6.7)

$$\bar{s}_0(x,y,z,t) = \frac{Q_0}{(4\pi K t)^{3/2}} \exp\left[-\frac{x^2+y^2+z^2}{4Kt}\right]. \tag{6.8}$$

A similar equation was obtained using the statistical theory of turbulent diffusion [cf. (4.2)] and is rewritten here for comparison:

$$\bar{s}_0(x,y,z,t) = \frac{Q_0}{(2\pi \overline{y^2})^{3/2}} \exp\left[-\frac{x^2+y^2+z^2}{2\overline{y^2}}\right]. \tag{6.9}$$

In this equation $\overline{y^2}$ is a function of t expressed by

$$\overline{y^2} = 2\overline{v^2}\int_0^t (t-\alpha)R_h(\alpha)d\alpha.$$

The two expressions on the right in (6.8) and (6.9) are identical when $\overline{y^2} = 2Kt$. This functional relation between $\overline{y^2}$ and t exists only when the dispersion time t is very large compared to the Lagrangian scale of turbulence, in which case [cf. (3.6)]

$$\overline{y^2} \approx 2\nu^* t, \qquad (t \gg L_h) \tag{6.10}$$

with $\nu^* = \overline{v^2}L_h$. We call ν^* the *turbulent viscosity*. The Fickian law of diffusion (6.7) and its solution (6.8) are, therefore, valid for turbulent diffusion only for very large dispersion times ($t \gg L_h$).

We shall consider the turbulent viscosity ν^* as a characteristic of the turbulence, while in the value of the coefficient of eddy diffusion K we shall include the effects of both turbulence and molecular agitation. Thus,

$$K = \nu^* + D, \tag{6.11}$$

which becomes $K \approx \nu^* + \nu$ if Eq. (6.4) is applied.

3. Factor of Turbulent Diffusion

We define as the *factor of turbulent diffusion* (24) the quantity

$$n^* = \frac{1}{2}\frac{d\overline{y^2}}{dt} = \overline{v^2}\int_0^t R_h(\alpha)d\alpha, \tag{6.12}$$

a function of the dispersion time t. When t becomes very large compared to the Lagrangian scale of turbulence

$$\lim_{t\to\infty} n^*(t) = \overline{v^2}L_h = \nu^*. \tag{6.13}$$

Upon differentiation of the equation for the mean concentration distribution (6.9), we find that it satisfies the differential equation

$$\frac{\partial \bar{s}_0(x,y,z,t)}{\partial t} = n^*(t)\nabla^2\bar{s}_0(x,y,z,t) \tag{6.14}$$

under the conditions that $\bar{s}_0(0,0,0,0) = \infty$, $\bar{s}_0(x,y,z,0) = 0$ and

$$\int_{-\infty}^{+\infty}\int_{-\infty}^{+\infty}\int_{-\infty}^{+\infty} \bar{s}_0(x,y,z,t)dx\,dy\,dz = Q_0$$

[cf. (25)]. While the Fickian law of diffusion (6.7) is valid only for $t \gg L_h$, Eq. (6.14), in which the constant K is replaced by the factor of turbulent diffusion $n^*(t)$, holds for the whole range of t values.

4. Apparent Coefficient of Eddy Diffusion

The Fickian law of diffusion has been, and still is, used to determine coefficients of eddy diffusion K from experimental measurements, and numerical data for K are often quoted in the literature. In many experiments, for instance, in some meteorological investigations, the turbulent field cannot be considered homogeneous and isotropic and various laws are often given [cf. (17)] for the distribution of K in space. However, even for a homogeneous and isotropic turbulent field for which the characteristics of turbulence are stationary in time, the values of K determined with Eqs. (6.7) and (6.8) will vary with the dispersion time at which the measurement is made, unless $t \gg L_h$. This variation has indeed been

noticed in some experimental investigations (17). Richardson (26,27) attributed this variation to the effects of eddies of increasing sizes when the dispersion time increases, using a differential equation which presents certain similarities with Eq. (6.14).

The significance of those experimental values of K, quoted in the literature, which have been obtained assuming the validity of Eq. (6.7), can be clarified by comparing again (6.8) with (6.9). An experimental determination of K in a field of homogeneous, isotropic, and stationary turbulence, using Eq. (6.8), will be incorrect unless the dispersion time t is much larger than the quantity L_h. Such an incorrect value measures, in fact, an *apparent coefficient of eddy diffusion*

$$K_t = \frac{\overline{y^2}_{\text{tot}}}{2t}. \tag{6.15}$$

We call the *apparent turbulent viscosity* the quantity

$$\nu_t^* = \frac{\overline{y^2}_{\text{turb}}}{2t} = \frac{\overline{v^2}}{t}\int_0^t (t - \alpha)R_h(\alpha)d\alpha, \tag{6.16}$$

which gives, with (6.5) and (6.6),

$$K_t = \nu_t^* + D, \tag{6.17}$$

or $K_t \approx \nu_t^* + \nu$ if the approximate relation (6.4) can be applied.

When the effects of the molecular diffusion are neglected in comparison with the effects of the turbulent diffusion, we shall have

$$\frac{K_t}{K} \approx \frac{\nu_t^*}{\nu^*} = \frac{1}{L_h t}\int_0^t (t - \alpha)R_h(\alpha)d\alpha, \tag{6.18}$$

which can also be written as

$$\frac{K_t}{K} \approx \frac{\nu_t^*}{\nu^*} = \frac{\iota^2}{2\tau}. \tag{6.19}$$

The ratio ν_t^*/ν^* is a function of the relative dispersion time $\tau = t/L_h$ and of the shape of the Lagrangian correlation curve to which ι^2 is related through Eq. (3.13). Figure 25 represents this ratio as a function of τ for several correlation functions. When the dispersion time tends to infinity, the apparent turbulent viscosity ν_t^* tends to $\nu^* = \overline{v^2}L_h$. For some correlation curves ν_t^* may become larger than ν^*. In such a case, the apparent coefficient of eddy diffusion K_t [as found by applying (6.7) or (6.8) under the assumption that K is independent of t] is larger than the real coefficient of eddy diffusion K.

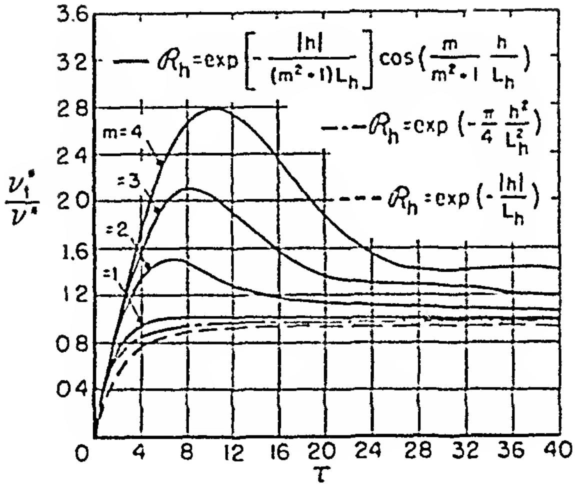

FIG. 25. Ratio of the apparent turbulent viscosity to the real turbulent viscosity. When the kinematic viscosity is neglected, $\nu_t^*/\nu^* = K_t/K$ with K_t apparent, and K real, coefficients of eddy diffusion.

APPENDIX

A. The study of mean concentration distributions can be extended to the case of sources other than a point or line source. In another paper (28) the author discusses the dispersion of a spherical cloud in a field of homogeneous and isotropic turbulence. At an initial time the dispersing fluid elements are uniformly distributed in the cloud and a time history of mean concentration distribution along a radius of the cloud is then determined.

B. We have investigated in this paper the turbulent diffusion in relation to coordinates which are moving with a known mean velocity, whether this mean velocity is zero or not. We shall now briefly discuss the turbulent diffusion in relation to coordinates which are themselves carried by the turbulent motion.

Let us consider at time 0 two fluid elements placed respectively at the origin of the coordinate axes and at the end of a vector $\mathbf{l}_0$ from the origin. The vectorial distance $\mathbf{l}(t)$ is a function of the dispersion time t. One can try to find the variances of the components of $\mathbf{l}(t)$ by a similar method as the one used in Section III,1. However, instead of a simple Lagrangian correlation coefficient between velocities of the same fluid element, one is now concerned with a correlation coefficient between velocities of two fluid elements. This problem is investigated by Brier (29) for a one-dimensional diffusion problem. Brier studies the relation between the Lagrangian correlation for successive velocities of two fluid elements and the Eulerian correlation for successive velocities at two points. In a discussion of Kolmogoroff's similarity theory Batchelor (30) uses the

diffusion relative to axes moving with the turbulent motion to extend the similarity theory to turbulent diffusion. The similarity theory for diffusion processes is also the subject of a paper by Inoue (31).

C. The results found for mean concentration distributions in fields of homogeneous and isotropic turbulence can be extended to cases of homogeneous nonisotropic turbulence. Let us consider the diffusion process when $R_{tL}^u \neq R_{tL}^v \neq R_{tL}^w$, $\overline{u^2} \neq \overline{v^2} \neq \overline{w^2}$ and, therefore, $\overline{x^2} \neq \overline{y^2} \neq \overline{z^2}$. Assuming that the probability density function referred to in Section IV,1 is at all times of the form

$$\psi(x,y,z,t) = (k_1k_2k_3/\pi^{3/2}) \exp\left[-(k_1^2x^2 + k_2^2y^2 + k_3^2z^2)\right],$$

we find easily that the function of x,y,z in Eq. (4.7) representing the mean concentration distribution due to a continuous point source should now be

$$\text{(A.1)} \quad \frac{\bar{s}(x,y,z)U}{Q} = \frac{U}{(2\pi)^{3/2}} \int_0^\infty \frac{AB}{(\overline{x^2})^{3/2}} \exp\left[-\frac{1}{2\overline{x^2}}\{(x - U\alpha)^2 + A^2y^2 + B^2z^2\}\right] d\alpha$$

where

$$\frac{1}{A^2} = \frac{\overline{y^2}}{\overline{x^2}} \quad \text{and} \quad \frac{1}{B^2} = \frac{\overline{z^2}}{\overline{x^2}}.$$

Recalling the relation $\overline{x^2}(\alpha) = 2\overline{u^2} \int_0^\alpha (\alpha - \gamma)R_{tL}^u(\gamma)d\gamma$ and the corresponding ones for $\overline{y^2}$ and $\overline{z^2}$ [cf. Eq. (3.3)], we see that, in general, A and B depend on α, and the integration with respect to α in Eq. (A.1) can be quite complicated, depending on how the correlation functions $R_{tL}^i(t)$, $i = u,v,w$, depend on t. In the two cases of very large and very small distances from the dispersion source, however, A and B are constants and the integrand in (A.1) can be considerably simplified. One can, in fact, use for each of these cases the distribution functions, in terms of dimensionless variables, already given for the corresponding isotropic case, as well as the figures which represent these functions, provided the dimensionless variables are defined somewhat differently.

For small distances from the source, i.e., when the distance is much smaller than each of the three component Lagrangian scales of turbulence multiplied by the mean velocity: $x = Ut \ll L_{tL}^iU$, $i = u,v,w$, we recall that $\overline{x^2}(t) \approx \overline{u^2}t^2$ and there are similar expressions for $\overline{y^2}$ and $\overline{z^2}$. It follows then that

$$A^2 = \frac{\overline{u^2}}{\overline{v^2}} = \frac{T_u{}^2}{T_v{}^2} \quad \text{and} \quad B^2 = \frac{\overline{u^2}}{\overline{w^2}} = \frac{T_u{}^2}{T_w{}^2},$$

where $T_i^2 = \sqrt{\overline{i^2}}/U$, $i = u,v,w$, are the component intensities of turbulence, and it is easily seen, after setting $\beta = \alpha/L_{tL}{}^u$ in Eq. (A.1), that Eqs. (4.16) and (4.17), as well as Figs. 17, 18, and 22, are applicable to the nonisotropic case if we define ξ, η, ζ as follows:

$$\xi = \frac{x}{UL_{tL}{}^u}, \quad \eta = \frac{T_u y}{UT_v L_{tL}{}^u}, \quad \zeta = \frac{T_u z}{UT_w L_{tL}{}^u},$$

and we substitute T_u for T.

When we consider large distances from the source, i.e., when

$$x = Ut \gg UL_{tL}{}^i,$$

$i = u,v,w$, we have $\overline{x^2}(t) \approx 2\overline{u^2}L_{tL}{}^u t$,

$$A^2 = \frac{\overline{u^2}L_{tL}{}^u}{\overline{v^2}L_{tL}{}^v} \quad \text{and} \quad B^2 = \frac{\overline{u^2}L_{tL}{}^u}{\overline{w^2}L_{tL}{}^w},$$

and Eqs. (4.10) and (4.14) are valid for the nonisotropic case provided

$$\xi = \frac{x}{UL_{tL}{}^u},$$

$$\eta = \frac{T_u y}{T_v U \sqrt{L_{tL}{}^u L_{tL}{}^v}}, \quad \zeta = \frac{T_u z}{T_w U \sqrt{L_{tL}{}^u L_{tL}{}^w}},$$

and T_u is substituted for T. In both cases σ_U is defined in the natural way; i.e., $\sigma_U d\eta d\zeta = \dfrac{\bar{s}U}{Q}\, dy dz$. This means that the relation between σ_U and $\bar{s}$ varies, depending in each case on the definitions of η and ζ in terms of y and z.

D. Numerous theoretical investigations of turbulent diffusion in a nonhomogeneous field of flow have been made in connection with applications to meteorology and are summarized in a monograph by Sutton (32). These studies are, in general, based on the Fickian law of diffusion with a diffusion coefficient whose value may vary in space, but is independent of the dispersion time. For this reason the strict application of the results is somewhat limited. In many cases, however, it may be possible to find more general solutions for a nonhomogeneous field of turbulence.

Acknowledgments

The author is indebted to Dr. B. A. Fleishman for several suggestions. He wishes to express his appreciation to Miss Doris Rubenfeld for the preparation of the figures and to Mr. O. J. Deters for his assistance during the preparation of the manuscript.

References

1. *Modern Developments in Fluid Dynamics,* S. Goldstein, Editor, Oxford, Clarendon Press, 1938.
2. Kampé de Fériet, J., Spectral Tensor of Homogeneous Turbulence, Symposium on Turbulence, *U. S. Naval Ordnance Laboratory, Rept. NOLR* **1136,** 1–31 (1949).
3. Taylor, G. I., Diffusion by Continuous Movements, *Proc. London Math. Soc.,* **A20,** 196–211 (1921).
4. von Kármán, T., and Howarth, L., On the Statistical Theory of Isotropic Turbulence, *Proc. Roy. Soc.* (*London*), **A164,** 192–215 (1938).
5. Frenkiel, F. N., Corrélations et spectres dans un écoulement homogène, *Compt. rend.,* **222,** 367–369; 473–475 (1946).
6. Taylor, G. I., The Spectrum of Turbulence, *Proc. Roy. Soc.* (*London*), **A164,** 476–490 (1938).
7. Simmons, L. F. G., and Salter, C., An Experimental Determination of the Spectrum of Turbulence, *Proc. Roy. Soc.* (*London*), **A165,** 73–89 (1938).
8. von Kármán, T., and Lin, C. C., On the Statistical Theory of Isotropic Turbulence, *Advances in Applied Mechanics,* II, 1–19. (1951). Academic Press, New York.
9. Heisenberg, W., Zur statistischen Theorie der Turbulenz, *Z. Physik,* **124,** 628–657 (1948).
10. Lin, C. C., Remarks on the Spectrum of Turbulence, *Proc. Symp. Applied Math.,* Am. Math. Soc., New York, 1949, pp. 81–86.
11. Kolmogoroff, A. N., The Local Structure of Turbulence in Incompressible Fluid for Very Large Reynolds Number, *Compt. rend. acad. sci. U.R.S.S.,* **30,** 301–305 (1941).
12. Batchelor, G. K., Kolmogoroff's Theory of Locally Isotropic Turbulence, *Proc. Cambridge Phil. Soc.,* **43,** 533–559 (1947).
13. Kampé de Fériet, J., Les fonctions aléatoires stationnaires et la théorie de la turbulence homogène, *Ann. soc. sci. Bruxelles,* **I-59,** 145–194 (1939).
14. Frenkiel, F. N., Etude statistique de la turbulence: Spectres et corrélations, *O.N.E.R.A.* (*Paris*), *Rapport Tech.* No. **34,** 1948 (Report completed in 1942).
15. Dryden, H. L., Turbulence Investigations of the National Bureau of Standards, *Proc. Fifth Intern. Congr. Applied Mech.,* Cambridge, Mass., 1938, pp. 362–368.
16. Frenkiel, F. N., On Turbulent Diffusion, Symposium on Turbulence, *U. S. Naval Ordnance Laboratory, Rept. NOLR* **1136,** 67–86 (1949).
17. Sutton, O. G., Atmospheric Turbulence and Diffusion, *Compendium of Meteorology, Am. Meteorol. Soc.,* Boston, 1951, pp. 492–509.
18. Roberts, O. F. T., The Theoretical Scattering of Smoke in a Turbulent Atmosphere, *Proc. Roy. Soc.* (*London*), **A104,** 640–654 (1923).
19. Fick, A., Ueber Diffusion, *Ann. Physik Chemie,* **94,** 59–86 (1855).
20. Jeans, Sir James, *An Introduction to the Kinetic Theory of Gases,* University Press, Cambridge, 1940.
21. Taylor, G. I., Statistical Theory of Turbulence, *Proc. Roy. Soc.* (*London*), **A151,** 421–478 (1935).
22. Schubauer, G. B., A Turbulence Indicator Utilizing the Diffusion of Heat, *N.A.C.A. Tech. Rept.,* No. **524,** 1935.
23. Einstein, A., Ueber die von molekularkinetischen Theorie der Warme geforderte Bewegung von in ruhenden Flussigkeiten suspendierten Teilchen, *Ann. Physik,* **17,** 549–560 (1905).

24. Frenkiel, F. N., Mesure de la diffusion turbulente du vent naturel dans le voisinage du sol, *Compt. rend.*, **224**, 98–100 (1947).
25. Batchelor, G. K., Diffusion in a Field of Homogeneous Turbulence: I. Eulerian Analysis, *Australian J. Sci. Research*, **A2**, 437–450 (1949).
26. Richardson, L. F., Atmospheric Diffusion Shown on a Distance-Neighbour Graph, *Proc. Roy. Soc. (London)*, **A110**, 709–737 (1926).
27. Richardson, L. F., and Stommel, H., Note on Eddy Diffusion in the Sea, *J. Meteorol.*, **5**, 238–240 (1948).
28. Frenkiel, F. N., Turbulent Diffusion from a Non-punctual Source, *Proc. First U. S. Natl. Congr. Applied Mech.*, Chicago, 1950 (in press).
29. Brier, G. W., The Statistical Theory of Turbulence and the Problem of Diffusion in the Atmosphere, *J. Meteorol.*, **7**, 283–290 (1950), also the Statistical Theory of Diffusion by Turbulent Eddies, *Meteorol. Monographs*, **1**, 15–19 (1951).
30. Batchelor, G. K., The Application of the Similarity Theory of Turbulence to Atmospheric Diffusion, *Quart. J. Roy. Meteorol. Soc.*, **76**, 133–146 (1950).
31. Inoue, E., On the Turbulent Diffusion in the Atmosphere, *J. Meteorol. Soc. Japan*, **28**, 441–456 (1950).
32. Sutton, O. G., *Atmospheric Turbulence*, Methuen and Co., London, 1949.

On Aerodynamics of Blasts

By H. F. LUDLOFF

*New York University**

Page

I. Introduction

The influence of a structure on the form and pressure field of a passing blast can be elucidated by the following simplified model. Suppose a

* The investigations of the author and his collaborators, reported in this survey, were supported by O. N. R., Mechanics Branch, and by N. O. L.

plane shock advances into still air with a velocity parallel to a plane wall and strikes a bend of contour $y = f(x')$ in the wall (Fig. 1). As a consequence, the flow behind the shock will be disturbed and, in general, rotational, while the air in front remains at rest (with respect to the

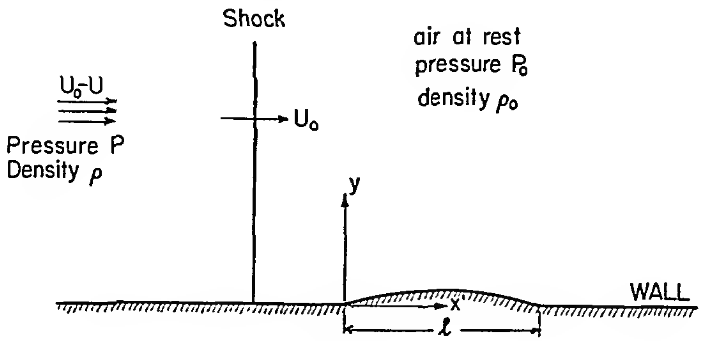

FIG. 1

wall). To find the general solution of such a nonlinear problem has not yet been possible, although many interesting shock tube experiments are available.

It is well known that the shock reflection due to the presence of the bend may be either a regular reflection (Fig. 2) or a Mach reflection (Fig. 3), with the presence of a three-shock configuration and a discontinuity surface known as slipstream.

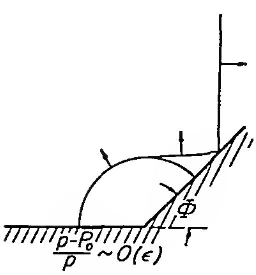

FIG. 2

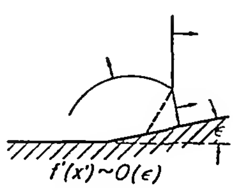

FIG. 3

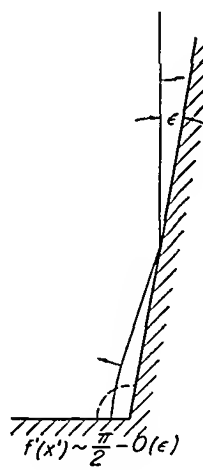

FIG. 4

When the angle of incidence ω_0 is less than a certain "extreme angle" ω_*, regular reflection is possible. If $\omega_0 > \omega_*$, Mach reflection occurs. The value of the extreme angle ω_* depends on the pressure ratio P_0/p across the shock (1), as indicated in Fig. 5.

To simplify the blast problem, assumptions can be made that permit the introduction of a small parameter ϵ and make it possible to form a linearized theory. This can be achieved by making any one of the following three assumptions:

1. The shock is very weak, i.e., $\dfrac{p - P_0}{p} = 0(\epsilon)$, while the bend may be arbitrary. From Fig. 5 it is clear that regular reflection is possible for any angle of incidence. In first approximation the flow is irrotational.

2. The bend (or the protuberance) is very shallow, i.e., the slope $f'(x') = 0(\epsilon)$, while the shock strength may be arbitrary. Then, in general, Mach reflection will occur, because ω_0 is nearly 90° (to start

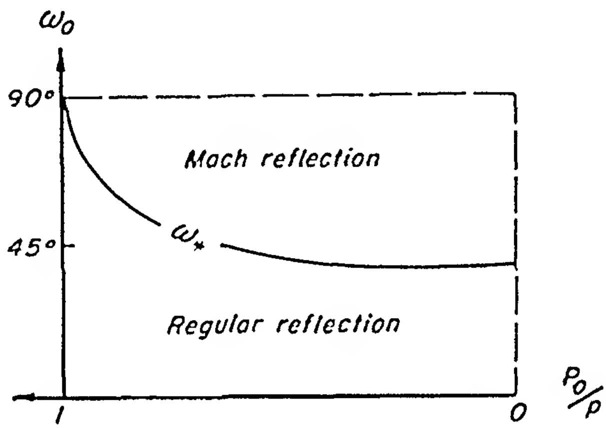

FIG. 5

with). A detailed theory shows that the reflected shock is very weak and a slipstream exists, although not in a mathematical, nevertheless in a physical sense.

3. The bend forms an almost vertical wall, i.e., the slope

$$f'(x') = \frac{\pi}{2} - 0(\epsilon).$$

Again the shock strength may be arbitrary. Then ω_0 is very small, and it can be seen that a regular reflection approaching a head-on reflection occurs.

These three cases can be illustrated by Figs. 2, 3, and 4.

The problem of a weak shock passing over a corner of finite angle has been solved by Keller and Blank (2), who applied the principles of optics.

Case 2 has first been treated by Bargmann (3) who used the simplification of irrotational flow which is not valid for strong shocks.

Cases 2 and 3 have been treated by Lighthill (4,5), and by Ting and Ludloff (6). Lighthill's derivations are restricted to wedges because the

conical field transformation is used which is an essential element of his method. Furthermore, his procedure leads to final results which are not obtained in closed analytic form and are represented in a coordinate space whose relation to the physical space is quite complicated. Therefore, a different approach developed by Gardner, Ludloff, and Ting (6,7) will be presented in the following considerations. This approach, in which hyperbolic equations are used throughout, is more direct, and the results obtained are more general. Shocks passing over flat surfaces of arbitrary shape can be dealt with in such a manner that closed analytic expressions result for the pressure and density fields in the whole domain behind the advancing shock front. Comparisons with shock tube experiments can be readily carried out, and interesting details about the nature of the "slipstream" occurring with the Mach reflection of the shock can be determined.

II. The Diffraction of Very Weak Shocks around Wedges of Arbitrary Angle

1. Statement of the Problem

If a weak, plane compression wave advances into still air, the whole velocity and pressure field behind the advancing front may be considered a small perturbation away from the state of rest. Therefore the velocity potential φ, the pressure p and the density ρ may be written:

$$\varphi = \epsilon \cdot \varphi^{(1)}, \quad p = P_0 + \epsilon \cdot p^{(1)} \quad \text{and} \quad \rho = \rho_0 + \epsilon \cdot \rho^{(1)},$$

wherein $p^{(1)} = -\rho_0 \cdot \varphi_t^{(1)}$, following from Euler's equations.

φ as well as p obey the wave equation, which is the linearized approximation of the time dependent equation of motion. Thus, for two dimensional flow:

$$p_{xx}^{(1)} + p_{yy}^{(1)} - \frac{1}{c^2} p_{tt}^{(1)} = 0. \tag{1.1}$$

Assume that a plane front approaches a wedge of arbitrary vertex angle 2Φ and is parallel to its edge, as indicated in Fig. 6.

By introducing the polar angle $\theta = \arg(x + iy)$, the boundary condition on the walls of the wedge $\theta = \pm\Phi$ is $\varphi_n^{(1)} = 0$ for all times t; thus:

$$p_n^{(1)} = 0. \tag{1.2}$$

Since weak waves are being considered, it is implied that the form of the wave front at any time can be constructed by Huyghens' principle as the envelope of circular wavelets which originate from the configuration at a prior instant, in particular at the instant of contact with any

wall or corner which may be in the path of the advancing wave. Hence plane fronts move with sound velocity c along their normal ("ray") and are reflected by infinite plane walls according to the law of reflection. At the instant, say $t = 0$, the front strikes the edge of the wedge, a diffracted cylindrical surface is produced, the axis of the cylinder being the edge. At all later times, the configuration of surfaces is similar to that in Fig. 6, and the scale is determined by the radius of the cylinder $r = ct$.

As a supplement to Huyghens' principle it must be required that the total energy concentrated in the whole wave front remain constant and

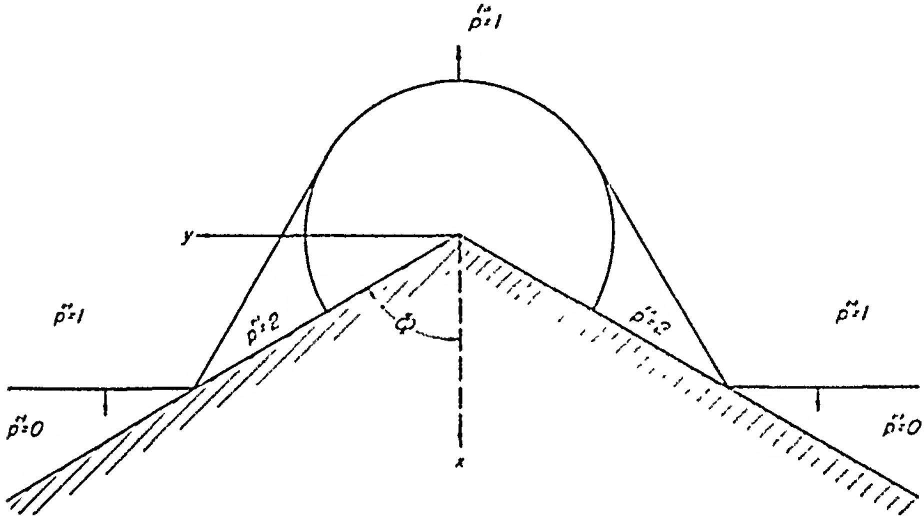

Fig. 6

independent of time. Our wave fronts are pressure pulses with a discontinuity $[p] = \epsilon \cdot [p^{(1)}]$ across the moving surface. Suppose that $dS_0(t_0)$ and $dS(t)$ are corresponding small elements of this surface at subsequent instants, which are cut out by a set of rays passing through a small closed curve forming the boundary of dS_0 or dS. Correspondingly, let $[p(0)]$ and $[p]$ be the values of the discontinuity on dS_0 and on dS. Then the above stated energy requirement stipulates:

$$\frac{[p(0)]}{[p]} = \left(\frac{dS}{dS_0}\right)^{1/2}. \tag{1.3}$$

Equation (1.3) permits $[p]$ to be computed from $[p(0)]$ on the same ray, once the motion of the discontinuity surface is known. From this it follows that the discontinuity $[p]$ does not change, so long as the plane discontinuity surface moves parallel to itself. $[p]$ also stays the same when the discontinuity surface is reflected from a plane wall; it is easily seen that the reflected wave must be a compression wave of the same

intensity to make the particle velocity behind the reflected front parallel to the wall. When a cylindrical surface arises, the magnitude of $[p]$ follows again from Eq. (1.3). Since all the rays reaching the cylinder come from the axis, where $dS_0 = 0$, $[p]$ on the cylinder must be zero.

Therefore, assuming the pressure discontinuity across the incident shock to be $[p] = \epsilon \cdot 1$, the boundary conditions for the domain of diffraction are as follows: Behind the incident shock $p^{(1)} = 1$, behind the reflected shock, i.e., in the "triangular" regions $p^{(1)} = 2$, on the wedge surface $p_n{}^{(1)} = 0$. From these values, $p^{(1)}$ inside the circular sector can be determined.

2. *The Conical Flow Method*

Consider the configuration of Fig. 6 in an xyt-space. The circle of that figure describes a cone, and the lines describe planes. Clearly, the boundary values of p on the cone are constant along each generator. The boundary condition is also constant on the wedge surface. Since the vertex of the cone coincides with the coordinate origin, the desired solution of (1.1) can depend only on $\sigma = x/ct$ and $\eta = y/ct$.

The conical character of this field suggests a reduction of the number of dimensions of the problem. Introducing the conical coordinates σ and η, Eq. (1.1) may be reduced by means of Busemann's transformation (8)

$$\bar{\rho} = \frac{(\sigma^2 + \eta^2)^{1/2}}{1 + (1 - \sigma^2 - \eta^2)^{1/2}}, \quad \theta = \tan^{-1}\frac{\eta}{\sigma} \tag{2.1}$$

so that (1.1) becomes Laplace's equation in the "polar coordinates" $\bar{\rho}$, θ:

$$\bar{\rho}\frac{\partial}{\partial \bar{\rho}}\left(\bar{\rho}\,\frac{\partial p^{(1)}}{\partial \bar{\rho}}\right) + \frac{\partial^2 p^{(1)}}{\partial \theta^2} = 0, \tag{2.2}$$

with the solution

$$p^{(1)} = Im\{f(z)\} \tag{2.3}$$

where $f(z)$ is an analytic function of $z = \bar{\rho} \cdot e^{i\theta}$.

Thus, the cone $(x^2 + y^2)^{1/2} \leq ct$ is mapped into the unit circle $\bar{\rho} \leq 1$. The problem is reduced to that of finding a function f, analytic in an appropriate sector of the unit circle with prescribed boundary values of the imaginary part of f or its derivative. To be more specific, the boundary conditions are:

$$\begin{aligned} &p_n{}^{(1)} = 0 \text{ on } 0 \leq \bar{\rho} \leq 1, \quad \theta = \Phi \text{ and } \theta = 2\pi - \Phi; \\ &p^{(1)} = 2 \text{ on } \bar{\rho} = 1, \quad \Phi \leq \theta \leq 2\Phi \text{ and } 2\pi - 2\Phi \leq \theta \leq 2\pi - \Phi; \\ &p^{(1)} = 1 \text{ on } \bar{\rho} = 1, \quad 2\Phi \leq \theta \leq 2\pi - 2\Phi. \end{aligned} \tag{2.4}$$

To solve for p, the exterior of the wedge in the z-plane is mapped into the upper half of the w-plane by the transformation:

$$w = \bar{r} \cdot e^{i\omega} = (e^{-i\Phi} \cdot z)^{\lambda}, \quad \text{where } \lambda = \pi/(2\pi - 2\Phi).$$

In this way, the circular sector in which p is to be determined becomes a semicircle in the w-plane with $p_n^{(1)} = 0$ on the diameter (into which the sides of the wedge transform). By the reflection principle, p may be extended into the whole circle so that a boundary value problem defined in the unit circle results.

3. *The Solution*

Thus, a harmonic function p with piecewise constant boundary values has to be determined. The solution may be obtained as the sum of expressions which take on a specified constant value, say 1, on one arc of the circle, the value zero on the rest of the circumference. The solution of this latter problem can be readily given in geometrical terms, as indicated in Fig. 7.

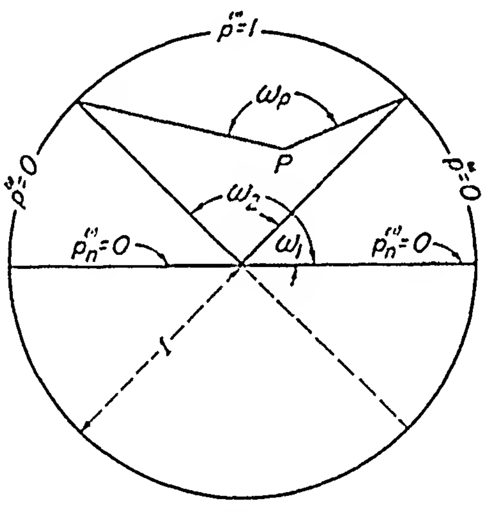

FIG. 7

Suppose the points $e^{i\omega_1}$ and $e^{i\omega_2}$ in the w-plane correspond to the points $e^{i\cdot 2\Phi}$ and $e^{i(2\pi - 2\Phi)}$ in the z-plane, at which the prescribed boundary values of p change discontinuously. Then, the expression $\frac{1}{\pi}\left[\omega_P - \frac{\omega_2 - \omega_1}{2}\right]$ satisfies obviously the required boundary conditions, because when the field point P moves on the circumference, ω_P becomes $\frac{\omega_2 - \omega_1}{2}$ or $\pi + \frac{\omega_2 - \omega_1}{2}$ depending on whether P lies on the upper or lower arc AB

respectively. It is not hard to show that

$$(3.1) \quad p^{(1)} = \frac{1}{\pi}\left[\omega_P - \frac{\omega_2 - \omega_1}{2}\right] = \frac{1}{\pi}\left[\arg\left\{\frac{w - \exp(i\omega_2)}{\omega - \exp(i\omega_1)}\right\} - \frac{\omega_2 - \omega_1}{2}\right],$$

which is clearly the imaginary part of an analytic function of w and z, and thus fulfils also the Laplace equation.

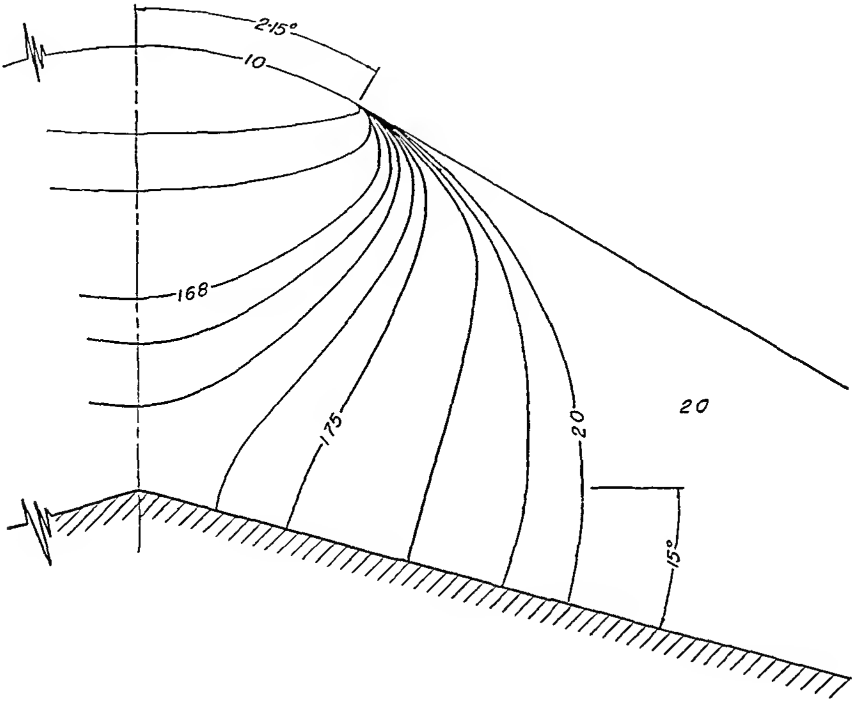

FIG. 8

By composing two expressions of the type (3.1) in an appropriate manner, all the boundary conditions (2.4) can be fulfilled. In the real variables $\bar{\rho}$ and θ the final solution may be written:

$$(3.2) \quad p^{(1)} = 1 + \frac{1}{\pi}\, tg^{-1}\left\{\frac{(1 - \bar{\rho}^{2\lambda})\cos\lambda\pi}{-(1 + \bar{\rho}^{2\lambda})\sin\lambda\pi - 2\bar{\rho}^{\lambda}\sin\lambda(\theta - \pi)}\right\}$$
$$+ \frac{1}{\pi}\, tg^{-1}\left\{\frac{-(1 - \bar{\rho}^{2\lambda})\cos\lambda\pi}{(1 + \bar{\rho}^{2\lambda})\sin\lambda\pi - 2\bar{\rho}^{\lambda}\cdot\sin\lambda(\theta - \pi)}\right\}.$$

The constant pressure curves in the domain behind the diffracted front, which follow from (3.2), are plotted in Fig. 8. Satisfactory agreement with shock tube interferograms has been obtained.

III. Pressure and Density Fields behind Blasts Advancing over Arbitrary Flat Surfaces (6,7)

1. *Analytic Formulation of the Problem*

Assume that an originally plane shock front of given intensity (strong or weak) advances over the surface $f(x')$ of a given flat structure (or a given thin airfoil) into still air of density ρ_0 and pressure P_0 (see Fig. 1). The velocity of the shock may be U_0, and the speed of the air behind the shock $(U_0 - U)$, its density and pressure there ρ and p. The length of the wall disturbance (or the chord of the air foil) may be l. At the time $t = 0$, the shock may strike the leading edge $x' = 0$. If the inclination of the body surface $f'(x')$ with regard to the direction of propagation of the shock is small, the shock front will end perpendicularly on the surface at any instant so that a curved shock front results and a shock configuration which may be interpreted as Mach reflection. Due to the curvature of the shock, the flow behind the diffracted part of the shock will be rotational, and, for sufficiently strong blasts, supersonic with regard to the body surface. Figures 9(a) and 9(b) represent conditions behind the advancing shock front depending on whether the air flow behind the shock is subsonic or supersonic relative to the obstacle. In either case, the time history of the diffraction is depicted in an xyt-space, so that every cross section of the figure represents the domain of disturbance at a given instant t, after the incident shock hit the leading edge of the obstacle, and a disturbance has spread with sound speed throughout domain II up to the circular reflected shock. The *coordinate system, x,y,t, is to be fixed in the undisturbed flow behind the shock*, i.e., in the flow occurring in domain I. With regard to this system, the leading edge and the whole body surface $f(x')$ is moving to the left,[1] the shock is moving to the right. In the subsonic case (a), the leading edge of the disturbance moves more slowly, in the supersonic case (b) faster than the perturbation produced by the shock diffraction. Therefore, in the latter case, domain III has been disturbed by the leading edge only, but has not been reached by the shock disturbance. Hence, here Ackeret's formulas of stationary, supersonic flow apply.

The field in domain II is clearly nonstationary and may be treated as a time dependent perturbation away from the state of (relative) rest existing in domain I. The basic system is the pressure field due to the advancing plane shock front (strong or weak). Upon this field a perturbation produced by the slight inclination of the structure (or of the airfoil) and by the changing small shock diffraction is superposed. A linearized

[1] Note that the system x',y,t is fixed in the wall.

theory can be derived, based upon an expansion in terms of a parameter ϵ, which can be interpreted as the thickness ratio of the wall disturbance (or of the airfoil).

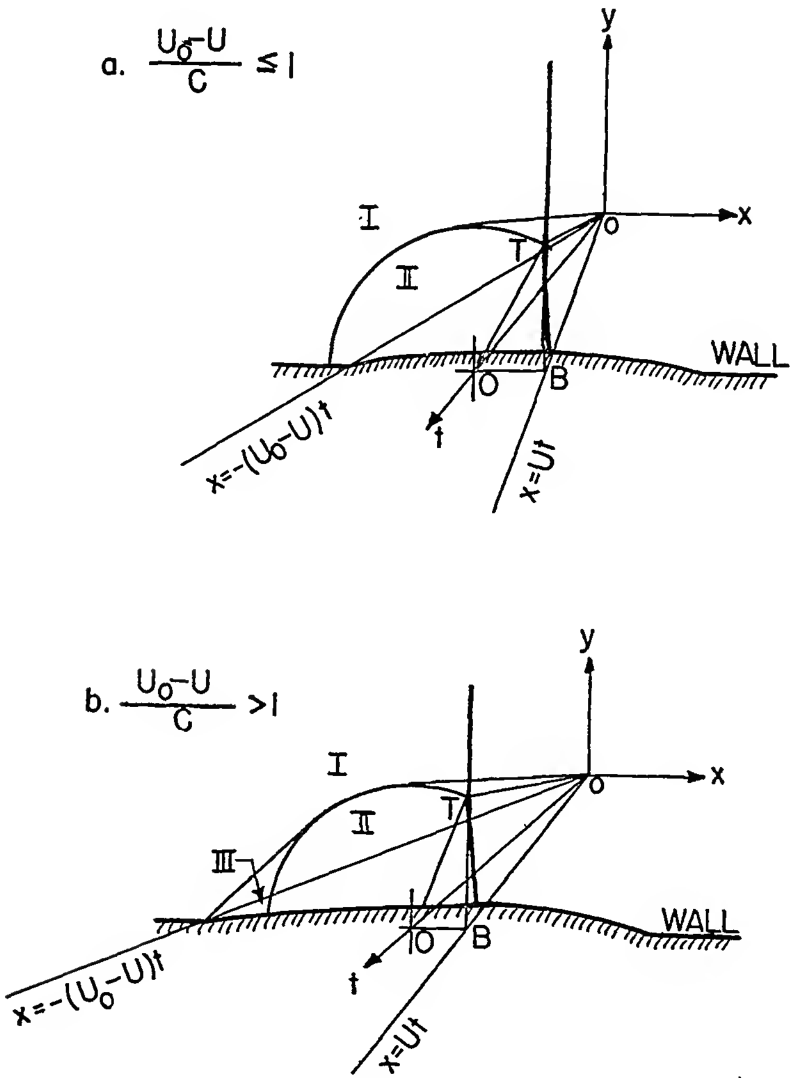

FIG. 9

a. The Linearized Differential Equations. The differential equations determining the two-dimensional, unsteady, rotational flow behind the shock in domain II are:

The continuity equation:

$$\rho_t + (\rho u)_x + (\rho v)_y = 0,$$

the equations of motion:

$$\frac{Du}{Dt} = -\frac{1}{\rho} p_x; \quad \frac{Dv}{Dt} = -\frac{1}{\rho} p_y \tag{1.1}$$

and the adiabatic relation:

$$\frac{D}{Dt}\left(\frac{p}{\rho^\gamma}\right) = 0,$$

resulting from the assumption that both viscosity and heat conduction are negligible.

Now expand p, ρ, u, and v in terms of ϵ:

$$\begin{aligned} p &= P + \epsilon \cdot p^{(1)}(x,y,t) + \epsilon^2 \cdot p^{(2)}(x,y,t) + \cdots \\ \rho &= R + \epsilon \cdot \rho^{(1)}(x,y,t) + \epsilon^2 \cdot \rho^{(2)}(x,y,t) + \cdots \\ u &= \quad\; \epsilon \cdot u^{(1)}(x,y,t) + \epsilon^2 \cdot u^{(2)}(x,y,t) + \cdots \\ v &= \quad\; \epsilon \cdot v^{(1)}(x,y,t) + \epsilon^2 \cdot v^{(2)}(x,y,t) + \cdots \end{aligned} \tag{1.2}$$

If (1.2) is inserted in (1.1) and the coefficients of like powers of ϵ are equated, Eqs. (1.1) become, in first approximation:

$$\rho_t^{(1)} + R \cdot u_x^{(1)} + R \cdot v_y^{(1)} = 0, \tag{1.3}$$

$$R \cdot u_t^{(1)} = -p_x^{(1)}, \tag{1.4}$$

$$R \cdot v_t^{(1)} = -p_y^{(1)}, \tag{1.5}$$

$$p_t^{(1)} = c^2 \cdot \rho_t^{(1)}. \tag{1.6}$$

Elimination of three out of the four unknown functions yields

$$\Box p^{(1)} \equiv \left(\frac{\partial^2}{\partial x^2} + \frac{\partial^2}{\partial y^2} - \frac{1}{c^2}\frac{\partial^2}{\partial t^2}\right) p^{(1)} = 0 \tag{1.7}$$

and

$$\frac{\partial}{\partial t}(\Box g) = 0 \tag{1.8}$$

where g denotes either $u^{(1)}$, $v^{(1)}$, or $\rho^{(1)}$.

It is now necessary to find two initial conditions and one boundary condition for $p^{(1)}$ to single out a unique solution satisfying the wave equation (1.7).

b. The Boundary and Initial Conditions. On the incident shock front: Relative to the undisturbed flow behind the shock, the air in front of the shock and the wall are moving with the constant velocity $-(U_0 - U)$, while the undisturbed shock front moves with the velocity $+U$.

The disturbed shock front may be expressed by the equation:

$$x = Ut + \epsilon \cdot \psi^{(1)}(y,t) + 0(\epsilon^2). \tag{1.9}$$

Then, in order ϵ^1, the conservation of mass, momentum, and energy across the shock requires

$$U^2 \cdot \rho^{(1)} - RUu^{(1)} = -RU\left(\frac{U_0 - U}{U_0}\right)\psi_t^{(1)}, \tag{1.10}$$

$$p^{(1)} + U^2 \cdot \rho^{(1)} - 2RUu^{(1)} = 0, \tag{1.11}$$

$$v^{(1)} = -U_0\left(\frac{U_0 - U}{U_0}\right)\psi_y^{(1)}, \tag{1.12}$$

$$\frac{\gamma}{\gamma - 1} \cdot p^{(1)} - \frac{c^2}{\gamma - 1} \cdot \rho^{(1)} - RUu^{(1)} = RU_0\left(\frac{U_0 - U}{U_0}\right)\psi_t^{(1)}. \tag{1.13}$$

By the use of the equations of motion for eliminating $u^{(1)}$, $v^{(1)}$, $\rho^{(1)}$, and $\psi^{(1)}$ a boundary condition for p alone can be formulated. At $x = Ut$,

$$D_{x,t}^{(2)}\{p^{(1)}(x = Ut,\ y \geq 0,\ t)\} = 0, \tag{1.14)*}$$

where $D_{x,t}^{(2)}$ is a linear, second order differential operator in x and t with known coefficients in terms of $M = U/c$ and γ.

The boundary condition on the wall is, in first approximation,

$$v(x \leq Ut,\ y = 0,\ t) = (U_0 - U)f'(x + [U_0 - U]t), \tag{1.15}$$

where $'$ means differentiation with respect to the whole argument. By combining Eq. (1.5) with the preceding equation, a boundary condition for $p^{(1)}$ can be derived

$$p_y^{(1)}(x \leq Ut,\ y = 0,\ t) = -R(U_0 - U)^2 \cdot f''(x + [U_0 - U]t). \tag{1.16)*}$$

At the point of intersection of the shock front and the wall, i.e., at $x = Ut$, $y = 0$, both (1.14) and (1.16) hold. By combining (1.16) with the shock relations, there results

$$\lim_{y \to 0^+} p_y^{(1)}(x = Ut,\ y \geq 0,\ t) = -\frac{4}{\gamma + 1} RUU_0 \cdot f''(U_0 t), \tag{1.17)*}$$

while (1.16) implies:

$$\lim_{x \to Ut^-} p_y^{(1)}(x \leq Ut,\ y = 0,\ t) = -R(U_0 - U)^2 \cdot f''(U_0 t). \tag{1.16a)*}$$

This indicates that in general $p_y^{(1)}$ has a singularity at this point; but $p^{(1)}$ itself turns out to be regular. In the case of a wedge ($f'' = 0$), this singularity does not come into play.

Since the disturbance which spreads, after the shock strikes the leading edge, is small, the boundary line separating the disturbed region II from the undisturbed region I (or from III, in case this region exists) is, except for terms of $0(\epsilon)$, the Mach circle. Hence it must be required that on the outer side of the Mach circle, i.e., at $r = (ct)^+$, $p^{(1)} = 0$ along

domain II, and $p^{(1)} = p^{(1)}{}_{\text{Ackeret}}$ along domain III. It can be shown that this is equivalent to prescribing:

(1.18)* $$p^{(1)} \to 0, \text{ as } \sqrt{x^2 + y^2} \to \infty.$$

Then the form of the solution of the wave equation, as assumed in III, 2 and III, 3 can be shown automatically to vanish in the whole domain I, i.e., to fulfil the original conditions and, moreover, to represent a pressure distribution which is continuous across the Mach circle, so that the reflected shock is of $0(\epsilon^2)$.

Obviously, the two initial conditions are:

(1.19)* $$p^{(1)}(x \leq Ut, y \geq 0, t \geq 0) = 0,$$
(1.20)* $$p_t^{(1)}(x \leq Ut, y \geq 0, t \geq 0) = 0.$$

The equations with asterisks summarize the analytical formulation of the problem.

2. *The Solution Procedure, Explained for the Case of Medium Shock Strength*

a. Restatement of the Problem. Although the solution of the problem stated in the previous section will be given later on for *any* shock strength, it is instructive to outline the solution procedure first for shocks of medium strength, based on an ONR report by Gardner and Ludloff, written in 1948 (7). This method, which contains the main idea in a simple fashion, was afterwards extended to the case of strong shocks in the thesis of Ting (6), and to the case of head-on collision of shocks in the thesis of Friedman (9).

Assume that the incident shock is sufficiently weak so that the velocity field downstream of the curved part (i.e., the Mach stem) of the shock may be considered irrotational. Then, the time dependent flow in domain II can be represented by a disturbance velocity potential $\varphi^{(1)}$, which obeys the wave equation.

(2.1) $$\varphi_{xx}^{(1)} + \varphi_{yy}^{(1)} - \frac{1}{c^2}\varphi_{tt}^{(1)} = 0,$$

the derivation being analogous to that of Eq. (1.7).

Now the boundary conditions have to be formulated in terms of $\varphi^{(1)}$.

Along the incident shock front, the conservation laws (1.10) to (1.13) can be simplified and degenerate. Since for shocks which are not strong, $\dfrac{U_0 - U}{U} = m \ll 1$, the right-hand terms of Eqs. (1.10) and (1.13) are, obviously, of $0(m \cdot \epsilon)$, and can be neglected in comparison with the left-hand terms which can be shown to be all of the same $0(\epsilon)$. Similarly,

either term in Eq. (1.12) is of $0(m \cdot \epsilon)$ and can be disregarded. Thus the conservation laws can be written as follows:

$$
\begin{aligned}
U^2\rho^{(1)} - RUu^{(1)} &= 0, \\
(c^2 + U^2)\rho^{(1)} - 2RUu^{(1)} &= 0, \\
c^2 \cdot \rho^{(1)} \left(\frac{\gamma}{\gamma - 1} - \frac{1}{\gamma - 1}\right) - RUu^{(1)} &= 0.
\end{aligned} \tag{2.2}
$$

If now also on the left-hand sides terms of $0(m \cdot \epsilon)$ are neglected, the three equations turn out to be identical; hence, after introducing $\varphi^{(1)}$,

$$\varphi_t^{(1)} + K \cdot c \cdot \varphi_x^{(1)} = 0 \tag{2.3}$$

where $K = 2M/1 + M^2$ and $M = U/c$, the Mach number of the shock.

The first order Eq. (2.3) corresponds to the second-order Eq. (1.14) of the general problem.[2]

On the surface of the body the condition prescribing the direction of the velocity is, in accordance with (1.15)

$$\varphi_y^{(1)}(x \leq Ut,0,t) = M_W \cdot c \cdot f'(x + M_W \cdot ct) \tag{2.4}$$

here $M_W = \dfrac{U_0 - U}{c}$ is the Mach number of the wall relative to the air behind the shock.

It is convenient to restate the problem, in terms of the function

$$\chi = \varphi_t^{(1)} + Kc\varphi_x^{(1)}. \tag{2.5}$$

Then

$$D.E.\colon \Box\chi = 0, \tag{2.6}$$

$$B.C.\colon \text{On } x = Ut,\ y \geq 0,\ \chi = 0, \tag{2.7}$$

$$\text{On } y = 0,\ x \leq Ut,$$

$$\chi_y = M_W c^2(K + M_W) \cdot f''(x + M_W \cdot ct). \tag{2.8}$$

b. The Lorentz Transformation and "Reflection." The boundary conditions may be better visualized, if the problem is represented in an xyt-space. As shown in Fig. 10(A), condition (2.8) is prescribed on the plane $y = 0$, while condition (2.7) is stipulated on the plane $x = Ut$ which is perpendicular to the first plane.

This situation suggests the application of a Lorentz transformation of the coordinates which is known to leave the wave equation invariant and amounts to a rotation of the coordinate system about the y-axis, as in Fig. 10(B).

[2] It will be shown in Section IV, Eq. (2.11) that the boundary condition (1.14) is equivalent to two relations of the first order, one of which is (2.3). The other relation is disregarded in the present simplified scheme.

If

(2.9) $$\bar{x} = \frac{x - M \cdot ct}{(1 - M^2)^{1/2}}, \quad \bar{t} = \frac{ct - M \cdot x}{(1 - M^2)^{1/2}}, \quad \bar{y} = y.$$

Then

(2.10) $$D.E: \Box\chi = 0.$$

(2.11) $B.C.$: On $\bar{x} = 0$, $\bar{y} \geq 0$, $\chi = 0$.

(2.12) On $\bar{y} = 0$, $\bar{x} \leq 0$, $\chi_{\bar{y}} = M_W c^2(\bar{K} + M_W) f''(a \cdot \bar{x} + b \cdot \bar{t})$,

where

(2.13) $$a = \frac{1 + M \cdot M_W}{(1 - M^2)^{1/2}} \quad \text{and} \quad b = \frac{M + M_W}{(1 - M^2)^{1/2}}; \quad \bar{K} = M.$$

The condition $\chi = 0$ on $\bar{x} = 0$ suggests a "reflection of the boundary condition" in such a manner that $\chi_{\bar{y}}$ be prescribed in the whole $\bar{x}\bar{t}$-plane,

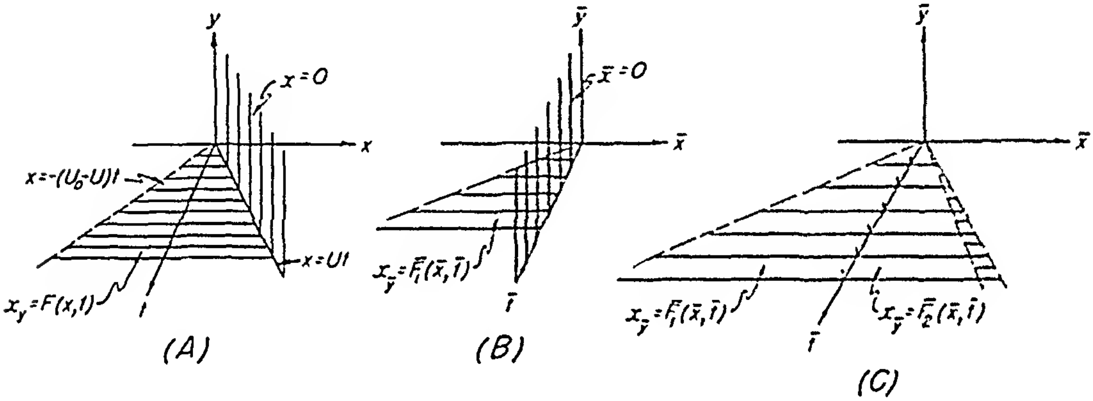

FIG. 10

i.e., also for $\bar{x} \geq 0$. See Fig. 10(C). This extension of the definition of $\chi_{\bar{y}}$ into the domain of positive $\bar{x}$ must be chosen in a way that guarantees the fulfillment of $B.C.$ (2.11). This is achieved by requiring for $\bar{x} \geq 0$

(2.14) $$\chi(\bar{x},\bar{y},\bar{t}) = -\chi(-\bar{x},\bar{y},\bar{t})$$

which contains (2.11) as a special case.

Needless to say, the extension of χ into the domain of positive $\bar{x}$ has as little physical meaning as any image method, but serves merely the purpose that both $B.C.$'s are prescribed in *one* plane, which is a prerequisite for the solution procedure outlined in the next section (2,c). Thus:

(2.15) For $\bar{y} = 0$, $\bar{x} \leq 0$: $\chi_{\bar{y}} = M_W c^2(\bar{K} + M_W) f''(a\bar{x} + b\bar{t})$,

(2.16) for $\bar{y} = 0$, $\bar{x} \geq 0$: $\chi_{\bar{y}} = -M_W c^2(\bar{K} + M_W) f''(-a\bar{x} + b\bar{t})$.

Note that the singularity of $\chi_{\bar{y}}$ at $\bar{x} = 0$, $\bar{y} = 0$ corresponds to the singularity of $p_{\bar{y}}$ expressed in Eqs. (1.16a) and (1.17).

c. The Possio Integral.[3] A solution of the wave equation fulfilling (2.15) and (2.16) can be expressed as the potential of what have been called "temporary sources," distributed over the $\bar{x},\bar{t}$-plane. Since the potential at $\bar{x},\bar{y},\bar{t}$ of a "source" of intensity g located at (ξ,o,τ) is

$$g(\xi,\tau)/[(\bar{t} - \tau)^2 - (\bar{x} - \xi)^2 - \bar{y}^2]^{1/2},$$

the potential of a "source distribution" becomes:

$$\chi(\bar{x},\bar{y},\bar{t}) = -\frac{1}{\pi}\int\int_H d\xi d\tau \frac{g(\xi,\tau)}{[(\bar{t} - \tau)^2 - (\bar{x} - \xi)^2 - \bar{y}^2]^{1/2}}. \tag{2.17}$$

It has been shown by many authors that if χ is represented in this manner, then

$$\lim_{y\to 0^+} \chi_{\bar{y}}(\bar{x},\bar{y},\bar{t}) = -\pi \cdot g(\bar{x},\bar{t}). \tag{2.17a}$$

The domain of integration H is that region of the ξ,τ-plane, in which the denominator is real. This is the hyperbolic area $(\bar{t} - \tau) \geq [(\bar{x} - \xi)^2 + \bar{y}^2]^{1/2}$, which is obtained by intersecting the fore cone whose vertex is

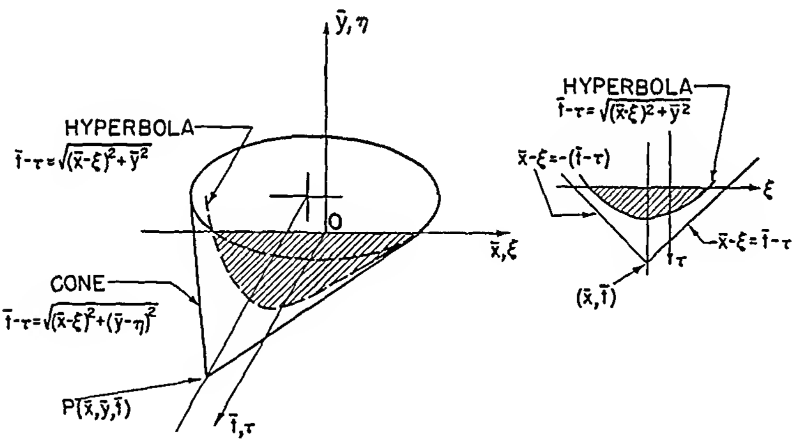

FIG. 11

at $\bar{x}$, $\bar{y}$, $\bar{t}$ with the ξ,τ-plane (see Fig. 11). It is readily seen that only points inside the so defined ξ,τ-domain may contribute to a disturbance at the point $(\bar{x},\bar{y},\bar{t})$. On the other hand, the contributing points are limited to the area, in which g, i.e., $f''(\pm a\bar{x} + b\bar{t})$ is different from zero. Thus, a sector of the hyperbolic area is cut out.

As the value of the "source strength" $\chi_{\bar{y}}$ assumes a different form for positive and negative $\bar{x}$, the integral may be split into two parts to be evaluated separately:

[3] Possio, C., *Acta Pont. Acad. Sci.*, 1, 93–105 (1937); also refs. 10 and 11.

$$(2.18)\quad \chi(\bar{x},\bar{y},\bar{t}) = -R\int d\tau \int_{\xi<0} d\xi \frac{f''(a\cdot\xi + b\cdot c\tau)}{[(\bar{t}-\tau)^2 - (\bar{x}-\xi)^2 - \bar{y}^2]^{1/2}} + R\int d\tau \int_{\xi>0} d\xi \frac{f''(-a\cdot\xi + b\cdot c\tau)}{[(\bar{t}-\tau)^2 - (\bar{x}-\xi)^2 - \bar{y}^2]^{1/2}}$$

here $R = \frac{1}{\pi} M_W c^2(\bar{K} + M_W)$.

d. Solution for $\varphi^{(1)}$. The preceding considerations demonstrate how solutions can be obtained by means of the Possio representation. Actually not χ, but $\varphi^{(1)}$ is desired. But the boundary value problem for $\varphi^{(1)}$ can be immediately deduced from that for χ. Returning to physical coordinates, (2.1), (2.3), and (2.16) imply:

$$(2.1)\qquad D.E.\colon \Box\varphi^{(1)} = 0.$$

B.C.: For $y = 0$, $x \leq Ut$,

$$(2.4)\qquad \varphi_y^{(1)} = M_W \cdot c\cdot f'(x + M_W\cdot ct).$$

For $y = 0$, $x \geq Ut$,

$$(2.19)\qquad (\varphi_y^{(1)})_t + K\cdot c(\varphi_y)_x = -M_W c^2(K + M_W)f''(d[\beta\cdot ct - x]),$$

where $d = \dfrac{1 + 2MM_W + M^2}{1 - M^2}$ and $\beta = \dfrac{2M + M_W + M^2M_W}{1 + 2MM_W + M^2}$.

Condition (2.19) is given as a differential equation of the first order in x and t for $\varphi_y^{(1)}$, which has to be supplemented by a boundary condition expressing the continuity of $\varphi_y^{(1)}$ at $x = Ut$:

$$(2.20)\qquad \lim_{x = Ut^-} \varphi_y^{(1)} = \lim_{x = Ut^+} \varphi_y^{(1)}.$$

This yields finally the condition for $y = 0$, $x \geq Ut$:

$$(2.21)\quad \varphi_y^{(1)} = B\cdot cf'(d[\beta\cdot ct - x]) + (M_W - B)cf'(D[K\cdot ct - x]).$$

Here B and D are simple linear combinations of M and M_W. Furthermore, for weak shocks $M_W \ll 1$ and $M < K < \beta < 1$.

From the preceding information $\varphi^{(1)}$ can be expressed as a Possio integral with a distribution of "source intensities" $\varphi_y^{(1)}$ over the plane $y = 0$, given by (2.4) and (2.21). It will be seen that three domains exist in which $(\varphi_y^{(1)})_{y=0}$ is different from zero. Note that, since $f(u)$ describes the wall contour, $u = 0$ fixes the leading edge (whatever the meaning of u may be), and for negative u, $f \equiv 0$. While $x = -M_W\cdot ct$ describes the motion of the real leading edge (of the wall disturbance), $x = K\cdot ct$ and $x = \beta\cdot ct$ indicate the motions of two "fictitious leading edges" which are obtained from the real one by the "reflection procedure." These three lines in the x,t-plane, separate three domains in which $(\varphi_y)_{y=0}$ assumes the following values

$$
\begin{aligned}
-M_W \cdot ct < x < M \cdot ct&: (\varphi_y{}^{(1)})_{y=0} = M_W \cdot c \cdot f'(x + M_W \cdot ct), \\
M \cdot ct < x < K \cdot ct&: (\varphi_y{}^{(1)})_{y=0} = B \cdot c \cdot f'(d[\beta \cdot ct - x]) \\
&\qquad + (M_W - B)c \cdot f'(D[K \cdot ct - x]), \\
K \cdot ct < x < \beta \cdot ct&: (\varphi_y{}^{(1)})_{y=0} = B \cdot c \cdot f'(d[\beta \cdot ct - x]).
\end{aligned} \tag{2.22}
$$

Upon substitution of these values into the Possio integral, $\varphi^{(1)}(x,y,t)$ can be considered derived for any wall contour $f(u)$.

In the special case of a shock passing over a wedge, the expression for the pressure becomes identical with Bargmann's well-known result (3) derived by the use of the conical field transformation.

3. *The Analytic Solution for Arbitrary Shock Strength*

a. The Lorentz Transformation. As pointed out before, the moving plane $x = Ut$, at which the complicated boundary condition (1.14) is prescribed, can be reduced to rest at the origin by application of the Lorentz transformation (2.9). In Lorentz coordinates $\bar{x},\bar{y},\bar{t}$ the general problem of Section III,1 can be restated as follows:

$$D.E.: p_{\bar{x}\bar{x}}{}^{(1)} + p_{\bar{y}\bar{y}}{}^{(1)} - p_{\bar{t}\bar{t}} = 0. \tag{3.1}$$

B.C.:

(3.2) Reflected shock: $p^{(1)} \to 0$, as $\sqrt{\bar{x}^2 + \bar{y}^2} \to \infty$.
(3.3) Surface: At $\bar{y} = 0$, $\bar{x} < 0$, $\bar{t} > 0$: $p_{\bar{y}} = Rc^2 A_0 \cdot f''(\bar{a}[\bar{\lambda}_0 x + \bar{t}])$.
(3.4) Mach shock: At $\bar{x} = 0$, $\bar{y} \geq 0$, $\bar{t} \geq 0$: $\bar{D}_{\bar{x},\bar{t}}{}^{(2)}[p^{(1)}] = 0$.
(3.5) Intersection: $\lim\limits_{\bar{x} \to 0^+} p_{\bar{y}}{}^{(1)}(\bar{x},0,\bar{t}) = Rc^2 A_0 \cdot f''(\bar{a}\bar{t})$,

$$\lim_{\bar{y} \to 0^+} p_{\bar{y}}{}^{(1)}(0,\bar{y},\bar{t}) = Rc^2\mu \cdot f''(\bar{a}\bar{t}). \tag{3.6}$$

Here

$$
\begin{aligned}
\bar{a} &= \frac{U_0}{c(1 - M^2)^{1/2}}, \quad \bar{\lambda}_0 = \left(1 - M^2 + \frac{MU_0}{c}\right)\frac{c}{U_0}, \\
A_0 &= -M_W{}^2, \quad \mu = -\frac{4}{\gamma + 1}\frac{U_0}{c}M,
\end{aligned} \tag{3.7}
$$

and
$$\bar{D}_{\bar{x},\bar{t}}{}^{(2)} = \frac{\partial^2}{\partial \bar{x}^2} + 2M\frac{\partial^2}{\partial \bar{x}\partial \bar{t}} + \frac{1}{M_0{}^2}\frac{\partial^2}{\partial \bar{t}^2}; \; M_0 = \frac{U_0}{c_0}.$$

I.C.:

(3.8) The initial conditions are: $p^{(1)} = p_{\bar{t}}{}^{(1)} = 0$ for $\bar{t} \leq 0$.

b. The Possio Integral. The similarity of the initial boundary value problem defined by (3.1)–(3.8) to that in Section III,2 suggests that the solution be assumed in form of a Possio integral:

$$p^{(1)}(\bar{x},\bar{y},\bar{t}) = -\frac{1}{\pi}\int\int_H d\tau d\xi \frac{p_{\bar{y}}{}^{(1)}(\xi,o,\tau)}{[(\bar{t} - \tau)^2 - (\bar{x} - \xi)^2 - \bar{y}^2]^{1/2}}. \tag{3.9}$$

Looking at Fig. 11, it is obvious that the method is applicable only if the "source intensity" $p_{\bar{y}}^{(1)}$ is prescribed on the entire plane $\bar{y} = 0$, in particular inside the area H, which is bounded by the hyperbola $\bar{t} - \tau = [(\bar{x} - \xi)^2 + \bar{y}^2]^{1/2}$ and the straight line $\tau = 0$.

Actually, however, $p_{\bar{y}}^{(1)}$ is given for the left half of the plane

$$\bar{y} = 0(\bar{x} < 0)$$

while it is unknown in the right half plane $\bar{x} > 0$. Hence, the next step is to find an equation for $p_{\bar{y}}^{(1)}(\bar{x} > 0,0,\bar{t})$ which will replace condition (3.4) prescribed on the plane $\bar{x} = 0$, and also produce the correct type of singularity for $p_{\bar{y}}^{(1)}$ at the origin as defined by Eqs. (3.5) and (3.6).

By the use of condition (3.3), (3.9) may be split into two parts:

$$\text{(3.10)}\quad p^{(1)}(\bar{x} \leq 0,\bar{y},\bar{t}) = -\frac{Rc^2A_0}{\pi}\iint_{H_1} d\tau d\xi \frac{f''(\bar{a}[\tau + \bar{\lambda}_0\xi])}{[(\bar{t} - \tau)^2 - (\bar{x} - \xi)^2 - \bar{y}^2]^{1/2}} - \frac{1}{\pi}\iint_{H_2} d\tau d\xi \frac{p_{\bar{y}}^{(1)}(\xi > 0,0,\tau)}{[(\bar{t} - \tau)^2 - (\bar{x} - \xi)^2 - \bar{y}^2]^{1/2}}$$

where H_1 and H_2 are the two parts of the total integration area in which ξ assumes positive or negative values respectively.

c. Determination of $p_{\bar{y}}^{(1)}(\xi > 0)$. Substitution of (3.10) in (3.4) will provide the desired equation for the unknown function $p_{\bar{y}}^{(1)}(\xi > 0,0,\tau)$. Upon carrying out the proper differentiations with regard to $\bar{x}$ and $\bar{t}$, $\bar{D}_{\bar{x},\bar{t}}^{(2)}\{p^{(1)}(\bar{x} = 0, \bar{y} > 0, \bar{t})\}$ is obtained in form of two surface integrals (over ξ and τ) and one line integral (over τ alone), the latter resulting from differentiations with regard to the integration limits. The whole expression is zero, if both the double integral as well as the line integral vanish separately. This yields the two conditions

$$\text{(3.11)}\quad \bar{D}_{\bar{x},\bar{t}}\{p_{\bar{y}}^{(1)}(\bar{x} > 0,0,\bar{t})\} = -Rc^2A_0 \cdot \bar{a}^2G(-\bar{\lambda}_0) \cdot f^{(\text{iv})}(\bar{a}[\bar{t} - \bar{\lambda}_0\bar{x}]),$$

where

$$\text{(3.12)}\quad G(\bar{\lambda}) = \frac{1}{M_0^2} - 2M\lambda + \bar{\lambda}^2,$$

and

$$\text{(3.13)}\quad p_{\bar{y}\bar{x}}^{(1)}(0^+,0,\bar{t}) = \bar{a}Rc^2[A_0(\bar{\lambda}_0 + 2M) - 4M\mu]f'''(\bar{a}\bar{t}).$$

The missing, second boundary condition at $\bar{x} = 0^+$, $\bar{y} = 0$, $\bar{t}$ is supplied by a kind of "mean value theorem" around this singular point:

$$\tfrac{1}{2}[p_{\bar{y}}^{(1)}(0^+,0,\bar{t}) + p_{\bar{y}}^{(1)}(0^-,0,\bar{t})] = p_{\bar{y}}^{(1)}(0,0^+,\bar{t});$$

it yields

$$\text{(3.14)}\quad p_{\bar{y}}^{(1)}(\bar{x} = 0^+, \bar{y} = 0, \bar{t}) = Rc^2(2\mu - A_0)f''(\bar{a}\bar{t}).$$

Since it can be shown that the differential Eq. (3.11) is hyperbolic, the

solution of the boundary value problem (3.11), (3.13), (3.14) is

$$(3.15)\quad p_{\bar{y}}^{(1)}(\bar{x} > 0,0,\bar{t}) = Rc^2\{A_1 f''(\bar{a}[\bar{t} - \bar{\lambda}_1\bar{x}]) + A_2 f''(\bar{a}[\bar{t} - \bar{\lambda}_2\bar{x}]) + A_3 \cdot f''(\bar{a}[\bar{t} - \bar{\lambda}_3\bar{x}])\},$$

where $\bar{\lambda}_1 = \bar{\lambda}_0$, and $\bar{\lambda}_2$ and $\bar{\lambda}_3$ are the roots of the quadratic equation $G(\bar{\lambda}) = 0$;

$$(3.16)\quad A_1 = -A_0 \frac{\bar{\lambda}_0^2 + 2M\bar{\lambda}_0 + 1/M_0^2}{\bar{\lambda}_0^2 - 2M\bar{\lambda}_0 + 1/M_0^2};$$

A_2 and A_3 are the solutions of the two simultaneous linear equations:

$$(3.17)\quad \begin{aligned} A_2 + A_3 + A_1 + A_0 &= -\frac{8}{\gamma + 1}\frac{MU_0}{c}, \\ \bar{\lambda}_2 A_2 + \bar{\lambda}_3 A_3 + \bar{\lambda}_1 A_1 + \bar{\lambda}_0 A_0 &= 2M\left[\frac{8}{\gamma+1}\cdot\frac{MU_0}{c} - A_0\right]. \end{aligned}$$

d. The Final Results. Therefore the final results can be written in the form:

$$(3.18)\quad p^{(1)}(\bar{x},\bar{y},\bar{t}) = -\frac{Rc^2A_0}{\pi}\iint_{H_1} d\tau d\xi \frac{f''(\bar{a}[\tau + \bar{\lambda}_0\xi])}{[(\bar{t} - \tau)^2 - (\bar{x} - \xi)^2 - \bar{y}^2]^{1/2}} - \sum_{i=1}^{3}\frac{Rc^2A_i}{\pi}\iint_{H_2} d\tau d\xi \frac{f''(\bar{a}[\tau - \bar{\lambda}_i\xi])}{[(\bar{t} - \tau)^2 - (\bar{x} - \xi)^2 - \bar{y}^2]^{1/2}}.$$

By using the transformation (2.9), the disturbance pressure $p^{(1)}(x,y,t)$ can be obtained from (3.18).

From the differential Eq. (1.6) and a combination of the shock relations (1.10) to (1.13), the density variation may be computed:

$$\rho^{(1)}(x,y,t) = \frac{1}{c^2}p^{(1)}(x,y,t) + \frac{1}{c^2}\Omega_0 \cdot p^{(1)}\left(x,y,\frac{x}{U}\right),$$

where

$$(3.19)\quad \Omega_0 = \frac{(\gamma - 1)(M^2 - 1)}{M^2[2 + (\gamma - 1)M^2]}.$$

e. The Separation Line between Rotational and Irrotational Flow and Its Physical Significance. Since the reflected shock is of $0(\epsilon^2)$, it follows that

$$p^{(1)}(x,y,t) = 0 \text{ for } x^2 + y^2 - c^2t^2 \geq 0^-.$$

In particular, along the incident shock:

$$(3.20)\quad p^{(1)}\left(x,y,t = \frac{x}{U}\right) = 0 \text{ for } x^2 + y^2 \geq x^2/M^2,$$

$$\text{i.e., for } x\sqrt{1 - M^2} \leq M \cdot y.$$

Taking this into account, it follows from Eq. (3.19) that the lines of constant density (isopycnics) coincide with the lines of constant pressure (isobars) for $x/y \leq M/\sqrt{1 - M^2}$, but deviate from the latter for $x/y > M/\sqrt{1 - M^2}$, i.e., inside the area OTB of Fig. 12.

In other words, looking at Fig. 12, the flow inside OTB is rotational, outside it is irrotational. This is in accordance with Kelvin's theorem, since no particles cross the separation line OT. As the reflected circular shock is of $0(\epsilon^2)$, in a first order theory particles can acquire vorticity not by crossing the reflected shock but only by crossing the curved portion of the incident shock TB. These particles stay inside the area swept over by TB, i.e. inside the area OTB.

Since, moreover,

$$(3.21) \qquad \lim_{x\sqrt{1-M^2}-My=0^+} p^{(1)}(x,y,x/U) = 0,$$

there is no discontinuity of density in $0(\epsilon)$, i.e., no slipstream in the mathematical sense. However, it will be seen from Fig. 12 that in a physical sense there is a slipstream of finite width.

f. Application of the Theory. Equations (3.18) and (3.19) have been applied to the cases of a wedge and of a circular arc airfoil (12). For a blast passing over a wedge of vertex angle ϵ the following simple result is obtained:

$$p^{(1)}(\sigma,\eta) = \frac{Rc^2}{\pi U_0/c} \cdot \sum_{i=0}^{3} \frac{\lambda_i M - 1}{(1 - \lambda_i^2)^{1/2}} \cdot A_i \cos^{-1} \frac{|\lambda_i - \sigma|}{[(1 - \lambda_i\sigma)^2 + (\lambda_i^2 - 1)\eta^2]^{1/2}},$$

where

$$(3.22) \quad \lambda_0 = \frac{M - \bar{\lambda}_0}{1 - \bar{\lambda}_0 M}, \quad \lambda_i = \frac{\bar{\lambda}_i + M}{1 + \bar{\lambda}_i M}, \quad i = 1,2,3; \quad \sigma = \frac{x}{ct}, \quad \eta = \frac{y}{ct}.$$

$$\rho^{(1)}(\sigma,\eta) = \frac{1}{c^2} p^{(1)}(\sigma,\eta) + \frac{\Omega_0}{c^2} p^{(1)}(M,\eta).$$

Equations (3.22) apply, if $M_W > 1$, as in Fig. 12. In the event that $M_W < 1$ two of the $\cos^{-1}$ terms have to be replaced by corresponding $\cosh^{-1}$ terms.

As a numerical example, the pressure and density fields have been computed for $P/P_0 = 7.3076$ or $M_W = 1.21$ and $M = 0.51$. The isopycnics and isobars, as well as the curved shock front, are plotted as shown in Fig. 12. It is interesting to note how *strongly and suddenly each isopycnic splits off from the corresponding isobar* after traversing the separation line OT between rotational and irrotational flow. Within a thin strip along OT, there is a steep density gradient, while there is no appreciable pressure gradient. This may be interpreted as a *slipstream*

of finite width. This slipstream which must be expected with every Mach reflection can be clearly seen in W. Bleakney's (13) interferograms; also the characteristic shape of the isopycnics in the vicinity of OT has been recently verified experimentally in all details (14).

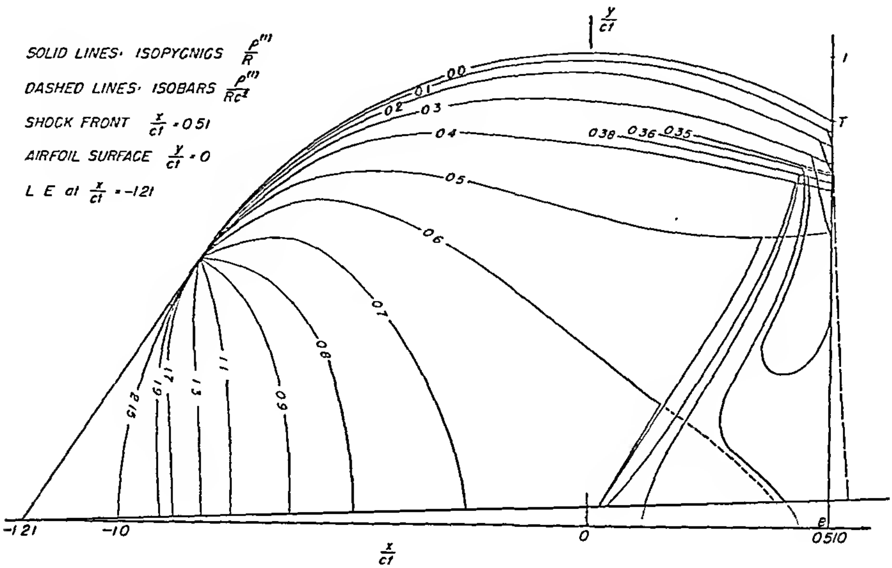

FIG. 12

4. Diffraction of Blasts by Slender Axisymmetric Bodies (15)

The preceding considerations can be modified to be applicable to the diffraction of strong blasts advancing over axisymmetric bodies of arbitrary profile $f(z)$. Computations of this kind, besides serving a practical purpose, shed some light on the Mach effect and the "slipstream" of spatial shock configurations. The geometrical setup may be the same as in the two-dimensional case except that the reflected shock in the Mach configuration is now spherical and the blast struck object is a slender body of revolution. The problem is treated as a time-dependent perturbation, using the method of Lorentz transformation and "reflection," developed in the preceding section. But since conditions in the present problem are axisymmetrical, the solutions of the wave equation have to be assumed in the form of "retarded potentials." A system of cylindrical Lorentz coordinates $(\bar{x},\bar{r},\bar{t})$ may be fixed in the undisturbed air downstream of the shock; at $\bar{t} = 0$ the coordinate origin may coincide with the tip of the body, $\bar{x}$ lying along the axis. The problem must be formulated in terms of the pressure, which has to be expanded in powers of ϵ^2:

$$p = P + \epsilon^2 \cdot p^{(1)} + \epsilon^4 \cdot p^{(2)} + \cdots .$$

Thus, the differential equation is

$$p_{\bar{x}\bar{x}}^{(1)} + p_{\bar{r}\bar{r}}^{(1)} + \frac{1}{\bar{r}} p_{\bar{r}}^{(1)} - p_{\bar{t}\bar{t}} = 0. \tag{4.1}$$

The boundary conditions are,

on the body surface: At $\bar{r} = 0$, $\bar{x} \leq 0$, $\bar{t} > 0$,

$$\bar{r} p_{\bar{r}}^{(1)} = -A_0[f'^2(u) + f(u)f''(u)], \tag{4.2}$$

where

$$u = \bar{a}(\bar{t} + \bar{\lambda}_0 \bar{x}).$$

Note that the form of (4.2) is different from the condition in the two-dimensional case, due to the singularity of $p_{\bar{r}}$ on the axis.

At the shock front: At $\bar{x} = 0$, $\bar{r} \geq 0$, $\bar{t} > 0$:

$$\bar{D}_{\bar{x},\bar{t}}^{(2)}[p^{(1)}] = 0, \tag{4.3}$$

where $\bar{D}_{\bar{x},\bar{t}}^{(2)}$ is a differential operator of the second order in $\bar{x}$ and $\bar{t}$. The parameters A_0, $\bar{a}$, and $\bar{\lambda}$ are the same expressions as in III,3.

It is necessary to note that at the intersection point of shock and body surface there is a singularity in the derivative, even for a conical body, characterized by:

$$\lim_{\bar{r}=0,\, \bar{x}\to 0^-} (\bar{r} p_{\bar{r}}^{(1)}) = -A_0[f'^2(\bar{a}\bar{t}) + f(\bar{a}\bar{t}) \cdot f''(\bar{a}\bar{t})];$$

however

$$\lim_{\bar{x}=0,\, \bar{r}\to 0^+} (\bar{r} p_{\bar{r}}^{(1)}) = -B_0[f'^2(\bar{a}\bar{t}) + f(\bar{a}\bar{t}) \cdot f''(\bar{a}\bar{t})]. \tag{4.4}$$

In accordance with the "reflection principle," (4.3) can be replaced by a condition on the "extended axis" of the body.

At $\bar{r} = 0$, $\bar{x} \geq 0$, $\bar{t} > 0$:

$$\bar{r} p_{\bar{r}}^{(1)} = \sum_{i=1}^{3} A_i[f'^2(u_i) + f(u_i) \cdot f''(u_i)], \tag{4.5}$$

where $u_i = \bar{a}(\bar{t} - \bar{\lambda}_i \bar{x})$. Also B_0, A_i, and $\bar{\lambda}_i$, are simple functions of U_0, U, and M.

It is now essential that due to the properties of the wave equation the solution be assumed in the form of a "retarded potential"—integral:

$$p^{(1)}(x,r,t) = \frac{1}{2}\left\{\int_{-\infty}^{0} d\xi \, \frac{g_1(\xi, t - R/c)}{R} + \int_{0}^{+\infty} d\xi \, \frac{g_2(\xi, t - R/c)}{R}\right\} \tag{4.6}$$

where $R = [(\bar{x} - \xi)^2 + \bar{r}^2]^{1/2}$ is the real distance between source point $(\xi,0)$ and field point $(\bar{x},\bar{r})$. It turns out that the "retarded temporary

source strengths" g_1 and g_2 are equal to expressions (4.2) and (4.5) respectively, after $\bar{x}$ and $\bar{t}$ have been replaced by ξ and $\tau = \bar{t} - R(\xi)/c$. Note that now only one integration is involved.

After substituting (4.2) and (4.5), (4.6) represents the solution for a general profile form $f(z)$.

For the particular case of a blast passing over the conical nose of a missile, the solution in physical (conical) coordinates $\sigma = x/ct$ and $\eta = r/ct$ reduces to:

$$(4.7)\quad p^{(1)}(\sigma,\eta) = K \cdot \sinh^{-1}\left[\frac{1}{(1-M^2)^{1/2}} \cdot \frac{\sigma - M}{\eta}\right] + \sum_{i=0}^{3} A_i \sinh^{-1}\left\{\frac{1}{(1-M^2)^{1/2}}\left[\frac{\sigma - M - \omega_i}{\eta}\right]\right\}$$

where the ω_i are simple functions of σ and η.

The density field is given by:

$$(4.8)\qquad \rho^{(1)} = \frac{1}{c^2}\,[p^{(1)}(\sigma,\eta) - \Omega p^{(1)}(M,\eta)].$$

Also, K and Ω are simple expressions in U_0, U, and M.

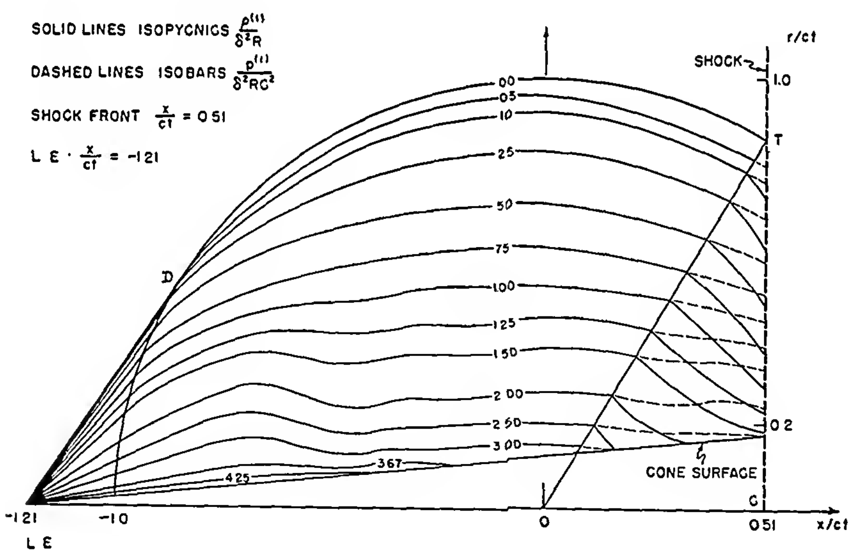

FIG. 13

In Fig. 13 the surfaces of constant pressure and density are plotted for a blast passing over a cone of half vertex angle $\epsilon = 10^{-1}$. The shock strength is characterized by $(U_0 - U)/c = 1.21$, so that this plot can be compared with the two-dimensional plot of Fig. 12. The following

features emerge: The rotationality of the flow is again restricted to the domain TOC, since the reflected shock, in general, is of $O(\epsilon^4)$; at T its strength is of even higher order. It is seen that in the present case the splitting off of corresponding isopycnics and isobars is far less strong, and the density gradient along any isobar is weak. There are no longer singularities at O and D: in neither point do several isopycnics end. Clearly, the difference of the entropy changes across the incident and Mach shocks is here not supplied by a narrow slipstream, but by an entropy gradient spread uniformly over the domain TOC.

IV. Head-on Encounter of a Shock with an Almost Perpendicular Wall

The head-on collision of a blast will first be represented, following Lighthill's ingenious method (5). In Section IV,3 a generalization of the hyperbolic approach will be attempted (9).

A plane shock advancing into still air may encounter the corner of a building whose two faces each make the small angle ϵ with the shock (see Fig. 14). For this two-dimensional flow problem, choose a coordinate system whose origin is fixed in the corner, the direction of motion of the shock being the negative x-axis. For reasons of symmetry, the considerations can be restricted to a half plane, representing a shock advancing into an almost rectangular corner. Conditions are defined by the incident shock velocity U_0, the pressure and density in still air p_0, ρ_0 and by the angle ϵ. Lighthill's treatment of this problem is based on the fact that no fundamental length or time scale exists so that the pressure and velocity fields depend only on x/ct and y/ct. Since ϵ is small, the corner may be considered as a small disturbance of the reflected shock, and a perturbation theory may be developed which makes use of the fact that the flow field is conical. The curved portion of the reflected shock (where it is inside the circle with center at the corner; see Fig. 14) is found to be weaker than the rest and may be regarded as the product of reflection followed by diffraction.

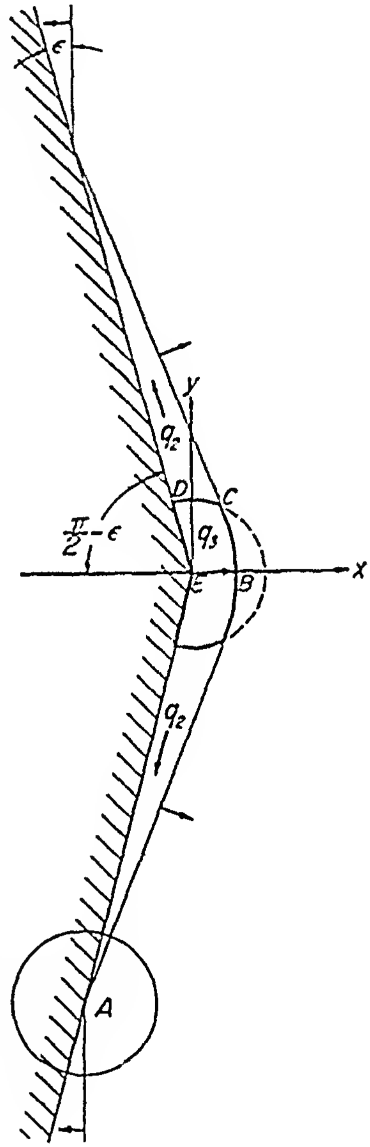

FIG. 14

At first, the theory of reflection of a shock by an infinite plane wall is recalled. Then the boundary value problem in the region of nonuniform flow is formulated and solved by use of the Busemann transformation and a conformal mapping. Finally, the pressure distribution along the wall is discussed.

1. Regular Reflection at an Infinite Plane Wall

Let suffix 0 denote the values of quantities in still air; suffix unity may be reserved for pressure p, density ρ, velocity q, and local sound speed c behind the incident shock and thus also in front of the reflected shock, while suffix 2 applies to the corresponding quantities behind the reflected shock, when reflection takes place at an infinite plane wall, so that p_2, ρ_2, q_2, and c_2 are constants. Let the velocity and angle of incidence of the shock be U_0,ϵ; let the velocity and angle of reflection be V,ϵ' (see Fig. 15). Since the shocks always meet at the wall,

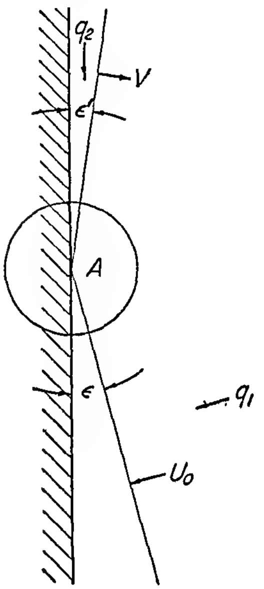

FIG. 15

$$V \cdot \operatorname{cosec} \epsilon' = U_0 \cdot \operatorname{cosec} \epsilon.$$

The rules for conservation of mass, momentum, and energy, at the incident shock, yield

$$(1.1)\quad q_1 = \frac{5}{6}\, U_0 \left(1 - \frac{c_0^2}{U_0^2}\right);$$

$$p_1 = \frac{5}{6}\, \rho_0 \left(U_0^2 - \frac{1}{7}\, c_0^2\right);\ \rho_1 = 6\rho_0 \Big/ \left(1 + 5\, \frac{c_0^2}{U_0^2}\right)$$

if $\gamma - 1 = \frac{2}{5}$ is assumed.

The conservation laws, applied across the reflected shock, yield corresponding relations between quantities with subscripts 2 and 1. If afterwards the quantities of subscript 1 are replaced by quantities of subscript 0 by means of (1.1), the desired relations result:

$$V = \tfrac{1}{3}U_0(1 + 2M_0^{-2});\ \epsilon' = \tfrac{1}{3}\epsilon(1 + 2M_0^{-2});\ q_2 = \epsilon q_1(\tfrac{4}{3} + \tfrac{2}{3}M_0^{-2}).$$

$$(1.2)\quad p_2 = \frac{5(7M_0^2 - 1)(4M_0^2 - 1)}{21M_0^2(M_0^2 + 5)}\, \rho_0 U_0^2;\ \rho_2 = \frac{3M_0^2(7M_0^2 - 1)}{(M_0^2 + 5)(M_0^2 + 2)}\, \rho_0$$

$$c_2 = \tfrac{1}{3}U_0(4M_0^2 - 1)^{1/2}(M_0^2 + 2)^{1/2} \cdot M_0^{-2}.$$

Here $M_0 = U_0/c_0$ is the Mach number of the incident shock. It may be noted that V,p_2,ρ_2, and c_2 are independent of ϵ, if ϵ^2 is neglected.

2. Conditions in the Region of Nonuniform Flow: Lighthill's Method

a. The Equations of Motion. Let $\bar{q}_3$ (components u, v), p_3, ρ_3 denote velocity, pressure, and density in the region of nonuniform flow, which

adjoins the region of uniform flow behind the reflected shock on two circular arcs, the latter marking the boundary up to which the circular disturbance wave produced by the small corner ϵ has spread (see Fig. 14). The radius of the circle is c_3t or, if quantities of $0(\epsilon)$ are neglected in fixing the nonuniform domain, c_2t. Since shallow corners spread small disturbances, the velocity $\bar{q}_3 - \bar{q}_2$ will be of $0(\epsilon)$ and, since from (1.2) $\bar{q}_2$ is seen to be of $0(\epsilon)$, also $\bar{q}_3 = 0(\epsilon)$. Furthermore, by the application of Huyghens' principle, the conditions on the circular arcs are: $p_3 = p_2$, $\rho_3 = \rho_2$ and on one side $u = 0$, $v = \epsilon q_1(\frac{4}{3} + \frac{2}{3}M_0^{-2})$ (on the other side $u = 0$, $v = -\epsilon q_1(\frac{4}{3} + \frac{2}{3}M_0^{-2})$), if ϵ^2 is neglected. These conditions suggest that the coordinate system be fixed in the corner of the wall and perturbation theory be applied to find the solution for $\bar{q}_3$, $p_3 - p_2$ and $\rho_3 - \rho_2$ small throughout the field. If $0\ (\epsilon^2)$ is consistently neglected, the equations of motion become

(2.1) $$(\rho_3)_t + \rho_2(u_x + v_y) = 0,$$
(2.2) $$\rho_2 \cdot u_t = -(p_3)_x; \quad \rho_2 \cdot v_t = -(p_3)_y,$$

and

(2.3) $$(p_3)_t = c_2^2(\rho_3)_t;$$

the last equation specifies that there is no heat transfer between fluid elements.

Now Lighthill makes use of the simplifying fact that u, v, and p_3 depend only on the conical coordinates $\sigma = x/c_2t$ and $\eta = y/c_2t$, in this way reducing the number of dimensions of the problem from three to two. Introducing, moreover, the pressure variation $p = (p_3 - p_2)/c_2\rho_2$ which has the dimension of a velocity, Eqs. (2.1) and (2.2) may be written as follows:

(2.4) $$\sigma \cdot p_\sigma + \eta \cdot p_\eta = u_\sigma + v_\eta,$$
(2.5) $$\sigma \cdot u_\sigma + \eta \cdot u_\eta = p_\sigma, \quad \sigma \cdot v_\sigma + \eta \cdot v_\eta = p_\eta.$$

If u and v are eliminated, the following differential equation for p alone is obtained:

(2.6)* $$\Delta p - \left(\sigma \frac{\partial}{\partial \sigma} + \eta \frac{\partial}{\partial \eta} + 1\right)\left(\sigma \frac{\partial p}{\partial \sigma} + \eta \frac{\partial p}{\partial \eta}\right) = 0,$$

a second order equation which is elliptic inside the unit circle.

When the condition of irrotationality holds, the same equation is satisfied by u and v. But in its absence u and v satisfy third order equations. This indicates that also the present problem should be formulated in terms of p alone.

b. The Boundary Conditions. In the σ,η-plane, the region of nonuniform flow is that part of the unit circle which lies between wall and shock. On

both wall and shock change in σ is slow compared with change in η; hence both may be approximated by straight segments. In the case of the wall clearly $\sigma = 0$. The approximate value of σ on the shock where it is curved, is the distance $U_0 t/\epsilon$ so far traveled along the wall surface by the

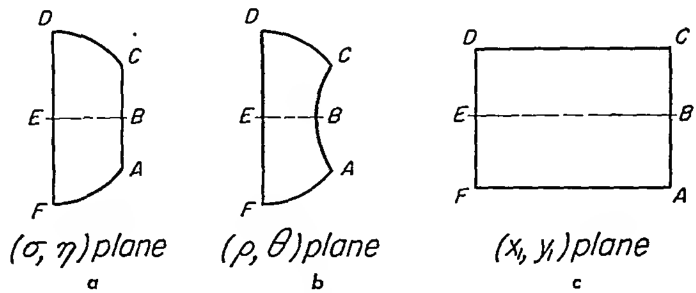

FIG. 16

incident shock, multiplied by the angle of reflection ϵ'. This gives, by use of (1.2)

$$\sigma = \frac{x}{c_2 t} = \frac{U_0}{c_2}\frac{\epsilon'}{\epsilon} = \left(\frac{M_0^2 + 2}{4M_0^2 - 1}\right)^{1/2} = M_2 < 1. \tag{2.7}$$

Thus, the region of nonuniform flow in the σ,η-plane is approximately

$$0 < \sigma < M_2, \quad \sigma^2 + \eta^2 < 1. \quad \text{(See Fig. 16a.)}$$

The boundary condition at the wall is $u/v = -\epsilon$. But, since $v = 0(\epsilon)$, it follows that $u = 0(\epsilon^2) = 0$ on $\sigma = 0$ for any η. Therefore for $\sigma = 0$, $u_\eta = 0$ and, according to Eq. (2.5)

(2.8)* $\quad p_\sigma = 0.$

(2.9)* $\quad$ On the circular *arc boundary* $p = 0$.

To get the boundary condition on $\sigma = M_2$, let the shock (inside the circle) be, up to $0(\epsilon)$, $\sigma = M_2 + \epsilon \cdot \Psi(\eta)$. Applying the conservation laws across the curved portion of the reflected shock one obtains:

$$\begin{aligned} p &= \epsilon \frac{5(M_0^2 + 2)}{9M_0^2} U_0(\Psi - \eta \cdot \Psi'); \quad v = -\epsilon \frac{5(M_0^2 - 1)}{6M_0^2} U_0\Psi' \\ u &= \epsilon \frac{5(4M_0^2 + 2)[(4M_0^2 - 1)(M_0^2 + 2)]^{1/2}}{9M_0^2(7M_0^2 - 1)} U_0(\Psi - \eta \cdot \Psi'), \end{aligned} \tag{2.10}$$

from which Ψ can be eliminated, so that

$$u = A_0 \cdot p, \quad \eta \cdot v_\eta = B_0 \cdot p_\eta \quad \text{on } \sigma = M_2, \tag{2.11}$$

where

$$A_0 = \frac{4M_0^2 + 2}{7M_0^2 - 1}\left(\frac{4M_0^2 - 1}{M_0^2 + 2}\right)^{1/2}, \quad B_0 = \frac{3(M_0^2 - 1)}{M_0^2 + 2}.$$

u and v can be eliminated from (2.11) by use of the equations of motion so that a shock condition for p alone results:

$$\text{(2.12)*} \qquad \frac{\partial p/\partial \sigma}{\partial p/\partial \eta} = \frac{(A_0 + M_2)\eta - B_0 M_2 \cdot \eta^{-1}}{1 - M_2^2}.$$

In addition to (2.12),* there is the condition that the change in v along the shock from the center to the top be:

$$\text{(2.13)*} \qquad \int \frac{B_0}{\eta} p_\eta d_\eta = \int v_\eta d_\eta = \epsilon \cdot q_1 \left(\frac{4}{3} + \frac{2}{3} M_0^{-2}\right),$$

which may be interpreted as normalization, determining the front factor of p.

The equations with asterisks complete the formulation of the boundary value problem in terms of p alone.

c. Computation of the Wall Pressure Distribution. To facilitate solving the problem, the differential Eq. (2.6) as well as the boundary conditions are subjected to two subsequent transformations. Since the flow field is conical, Eq. (2.6) can again be reduced to the Laplace equation by means of the Busemann transformation, stated in Section II, Eq. (2.1). Hence

$$\text{(2.14)} \qquad \bar{\rho} \frac{\partial}{\partial \bar{\rho}} \left(\bar{\rho} \frac{\partial p}{\partial \bar{\rho}}\right) + \frac{\partial^2 p}{\partial \theta^2} = 0.$$

Since in the $\bar{\rho},\theta$-plane, the boundary conditions become inconvenient, an additional conformal transformation $(\bar{\rho},\theta) \rightarrow z_1$, is applied which maps the domain in which p is defined, into a rectangle (see Fig. 16b,c). In this final $z_1(x_1,y_1)$-plane, the problem can be formulated as follows: An analytic function $w(z_1) = \dfrac{\partial p}{\partial x_1} - i \dfrac{\partial p}{\partial y_1}$ is to be determined, which is purely imaginary on three sides of the rectangle and on the fourth side, say $x_1 = \lambda$, becomes a prescribed function of y_1. The solution is finally obtained in the form:

$$\text{(2.15)} \qquad w(z_1) = iK \frac{\vartheta_2(-iz_1)}{\vartheta_4(-iz_1)} \cdot W(z_1)$$

where K is a normalization factor determined by numerical integration, ϑ_2 and ϑ_4 are theta functions, and

$$\text{(2.16)} \qquad W(z_1) = \exp \left\{- \sum_n (2 - a^n - b^n) n^{-1} \cdot \operatorname{cosech} 2n\lambda \cdot \cosh 2nz_1\right\}$$

where a and b are given functions of M_0, and λ a simple expression in M_2. Hence, the wall pressure distribution becomes:

$$\left(\frac{\partial p}{\partial y_1}\right)_{x_1=0} = -K\frac{\vartheta_2(y_1)}{\vartheta_4(y_1)}W(iy_1). \tag{2.17}$$

By plotting an especially chosen dimensionless quantity

$$\bar{p} = \frac{(p_2 - p_3)}{\epsilon(p_2 - p_0)},$$

Lighthill has shown that the pressure distribution along the wall is practically independent of the incident shock strength (see Fig. 17). It is

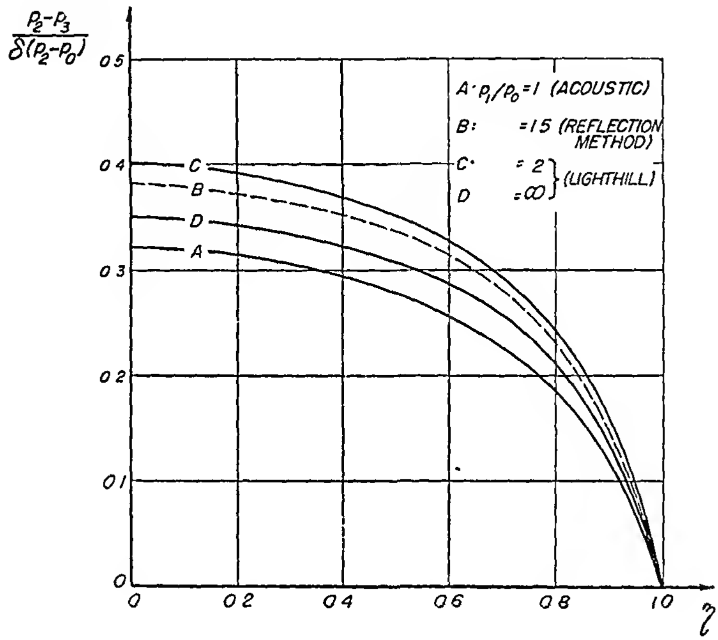

FIG. 17

perhaps interesting to note that qualitatively the same conclusion can be reached directly from the problem statement, by using the following simple reasoning.

At the wall the equations of motion assume the following form.

For $\sigma = 0,\ 0 < \eta < 1$: $\quad p_\sigma = 0$ and $p_\eta = \eta \cdot v_\eta$.
Furthermore, at $\sigma = 0,\ \eta = 1$: $\quad v = \epsilon q_1(\frac{4}{3} + \frac{2}{3}M_0^{-2}),\quad p = 0$
and at $\sigma = 0,\ \eta = 0$: $\quad v = 0$, for reasons of symmetry.

Therefore

$$\int_1^\eta p_\eta d\eta = \int_1^\eta \eta v_\eta d\eta,$$

and

$$p(\eta) = \eta \cdot v(\eta) - v(1) + \int^1 v(\eta)d\eta.$$

In particular:

$$p(0) = -\epsilon(\tfrac{4}{3} + \tfrac{2}{3}M_0^{-2}) + \int_0^1 v(\eta)d\eta = -\epsilon(\tfrac{4}{3} + \tfrac{2}{3}M_0^{-2})\left[1 - \int_0^1 \bar{v}(\eta)d\eta\right]$$

where $\bar{v}(\eta)$ is a normalized positive function with the values $\bar{v}(0) = 0$ and $\bar{v}(1) = 1$. If, for simplicity, $\bar{v} = \eta$ is assumed, then

$$p(\eta) = \epsilon q_1(\tfrac{2}{3} + \tfrac{1}{3}M_0^{-2})(\eta^2 - 1),$$

which agrees qualitatively with the form of Lighthill's curves. To compare the *absolute values* of the wall pressure for different incident shock strengths, $\bar{p}(0)$ can be computed as follows.

By definition:

$$p_2 - p_3 = \epsilon \cdot c_2\rho_2 q_1\left(\frac{2}{3} + \frac{1}{3}M_0^{-2}\right) = \gamma p_2 \cdot \epsilon \cdot \frac{q_1}{c_2}\left(\frac{2}{3} + \frac{1}{3}M_0^{-2}\right).$$

From (1.2)

$$p_2 - p_0 = p_2[1 - g(M_0)],$$

where

$$g(M_0) = \frac{21(M_0^2 + 5)}{5\gamma(7M_0^2 - 1)(4M_0^2 - 1)}.$$

Hence

$$\bar{p} = \gamma \frac{q_1}{c_2}\left(\frac{2}{3} + \frac{1}{3}M_0^{-2}\right)[1 - g(M_0)]^{-1}. \tag{2.18}$$

Now, q_1/c_2 as well as $g(M_0)$ can be computed by means of (1.2). Upon substitution into (2.18), it turns out that

for weak shocks $(M_0 = 1 + \epsilon)$ $\quad \bar{p} \sim 0.50 + 0(\epsilon)$,

for strong shocks $(M_0 \to \infty)$ $\quad \bar{p} \sim 1.2 + 0\left(\frac{1}{M}\right)$.

Thus it is seen that in the two limiting cases, $\bar{p}$ is independent of the shock strength, and the absolute values of $\bar{p}$ are of the same order.

3. Attempt at a Generalization of the Approach of Section III,2 (9)

Since Lighthill's results are represented in a coordinate space whose relation to the physical space is quite complicated, his final formulas for the pressure field are difficult to evaluate; moreover his method is restricted to wedges. Therefore, it might be of interest to generalize the approach developed in Section III,2 to make it applicable to the present problem. As before, the procedure may be explained for shocks of medium strength.

The denotation may be the same as in Section IV,2, except that the contour of the "corner" may now be, more generally, $x = f(y)$ where $f(y)$ may be defined for $-l/2 < y < + l/2$; for $|y| > l/2$ the faces of the corner may be plane, each forming the small angle ϵ with the incident shock front. If $f'(y)$ is small, it will act as a small disturbance of the reflected shock.

The results pertaining to the reflection of a shock from an infinite plane wall can be applied exactly as before. However, the boundary value problem in the region of nonuniform flow is to be formulated as a *hyperbolic* problem, similarly as in Section III,2; moreover the formalism defining the "reflection of the boundary condition" has to be modified and extended. The solution will be indicated in a symbolic manner.

a. Restatement of the Problem in the Region of Nonuniform Flow. If the incident shock is not too strong, it is permissible to treat the region of nonuniform flow as irrotational. Introducing a velocity potential φ, from which the velocity field $\bar{q}_3(u,v)$ may be derived, the equations of motion simplify to

$$\varphi_{xx} + \varphi_{yy} - \frac{1}{c^2}\varphi_{tt} = 0. \tag{3.1}$$

The domain of nonuniform flow extends from the wall to the shock, i.e., $0 < x < M_2c_2t$, between the two circular arcs $\left[x^2 + \left(y \pm \frac{l}{2}\right)^2\right]^{1/2} < c_2t$.

The boundary condition at the wall, for $-l/2 < y < + l/2$ is $u/v = \epsilon \cdot f'(y)$. Since, according to Section IV,1, $v = 0(\epsilon)$,

$$\varphi_x = 0(\epsilon^2) = 0 \quad \text{on } x = 0. \tag{3.2}$$

On the circular arcs

$$p_3 - p_2 = 0; \quad \varphi_x = 0; \quad \varphi_y = \epsilon q_1(\tfrac{4}{3} + \tfrac{2}{3}M_0^{-2}). \tag{3.3}$$

The boundary condition on the shock degenerates, as in Section III,2. Application of the conservation laws yields the simple relation[4]

$$\varphi_t + Kc_2\varphi_x = 0 \quad \text{on } x = M_2c_2t, \tag{3.4}$$

where

$$K = \frac{2M_2}{1 + M_2^2}.$$

In order to represent the solution of this hyperbolic problem in form of a Possio integral, it must be kept in mind that boundary conditions may be prescribed only in *one* plane. This is more difficult to accomplish in the present problem than in Section III,2, since the geometrical

[4] Note that Eq. (3.4) has the same form as the first Eq. (2.11).

arrangement and the type of the boundary conditions is different; compare Figs. 14, 18, and 10(A). The conditions on the wall as well as on the shock front are homogeneous so that no stipulation of "source intensities" can be derived from it. On the other hand, the conditions on the circular arc, although they are inhomogeneous, are not appropriate for this purpose either. Therefore, the latter shall be replaced by an initial condition at the wall which furnishes the equivalent information, namely:

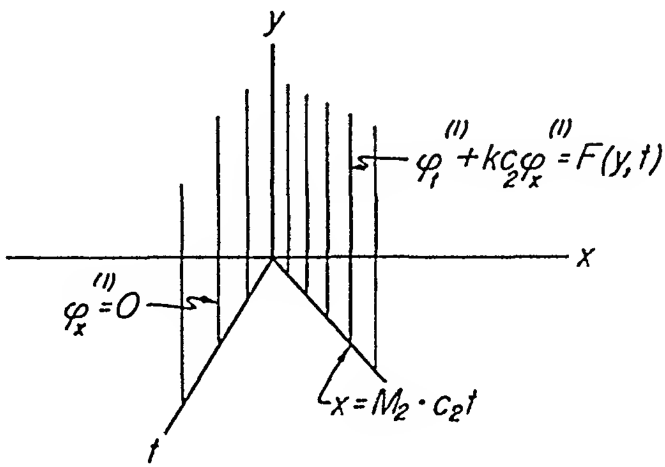

FIG. 18

For $t = 0^+$, $x = 0$, $y \geq 0$:

$$\varphi_y = -\epsilon \cdot f'(y) q_1(\tfrac{4}{3} + \tfrac{2}{3} M_0^{-2}), \qquad \text{(3.5)}$$
$$\varphi_x = 0, \quad \varphi_t = 0.$$

This means that immediately after reflection, the region near the wall may be treated similarly as the homogeneous flow field behind the reflected shock, the disturbance waves originating from each point of the wall having had no time to spread and interfere with each other. Thus, the problem may be formulated as follows:

(3.1) *D.E*: $\square\varphi = 0.$

I.C.: For $t = 0$, $x = 0$, $y \geq 0$,

(3.5) $\varphi_y = -\epsilon \cdot f'(y) q_1(\tfrac{4}{3} + \tfrac{2}{3} M_0^{-2})$; $\varphi_x = 0$; $\varphi_t = 0.$

(3.2) *B.C.*: For $t > 0$, $x = 0$, $y \geq 0$, $\varphi_x = 0.$

(3.4) For $t > 0$, $x = M_2 c_2 t$, $y \geq 0$, $\varphi_t + Kc_2\varphi_x = 0.$

b. The First Step of the Solution. The geometrical arrangement of these conditions is shown in Fig. 18, which should be compared with Fig. 10(A) to appreciate the different setup of the two problems. The formulation of the boundary conditions can be improved, by subtracting from the desired function φ a solution φ_0 of the wave equation which

fulfils conditions (3.2) and (3.5). This is accomplished by making

$$\varphi^{(0)} = -\epsilon q_1(\tfrac{4}{3} + \tfrac{2}{3}M_0^{-2})^{1/2}\{f(y + ct) + f(y - ct)\} \tag{3.6}$$

and setting .

$$\varphi^{(1)} = \varphi - \varphi^{(0)}.$$

Then $\varphi^{(1)}$ is to be determined from the following problem

(3.7) *D.E*: $\Box\varphi^{(1)} = 0.$

(3.8) *I.C.*: For $t = 0,\ x = 0,\ y \geq 0,\quad \varphi_x^{(1)} = \varphi_y^{(1)} = \varphi_t^{(1)} = 0.$

(3.9) *B.C.*: For $t \geq 0,\ x = 0,\ y \geq 0,\quad \varphi_x^{(1)} = 0.$

For $x = M_2c_2t,\ y \geq 0,\ t > 0,$

(3.10) $\varphi_t^{(1)} + K \cdot c_2 \cdot \varphi_x^{(1)} = \epsilon[\tfrac{2}{3} + \tfrac{1}{3}M_0^{-2}]q_1c_2\{f'(y + ct) - f'(y - ct)\}$

$= F(y,t)$, which is given.

In the present formulation the condition on the plane $x = M_2c_2t$ is inhomogeneous, while the conditions on the plane $x = 0$ as well as on the intersection line $x = t = 0$ are homogeneous. This situation permits the use of a Possio solution, provided that the homogeneous condition (3.9) is first disregarded and subsequently taken into account by a "multiple reflection" procedure which may be considered as an extension of the procedure explained in Section III,2. Obviously both boundary conditions (3.9) and (3.10) cannot be satisfied simultaneously by a single Possio integral. This state of affairs is reminiscent of the problem of the wall correction to be applied to the flow through a tunnel of rectangular section. In the latter case, the wall conditions can be singly, but not simultaneously, satisfied by placing a virtual "image solution" on either side of the true model. It is not until after a whole series of reflections is set up that both wall conditions are fulfilled. The analogous procedure will also here generate a solution. Before this is explained more explicitly, the derivation of $\varphi^{(1)}$ may be indicated.

First, problem (3.7–3.10) is reformulated in terms of

$$\chi = \varphi_t^{(1)} + Kc_2\varphi_x^{(1)}. \tag{3.11}$$

If the wall condition (3.9) is disregarded, χ can be readily expressed as Possio integral with the "source intensity" $F(y,t)$.

After $\chi(x,y,t)$ has been determined, $\varphi^{(1)}$ can be computed from Eq. (3.11). The boundary condition, by which this first order differential equation is to be supplemented, is the requirement that $\varphi^{(1)}$ vanish at and beyond $x = -ct$, a characteristic of the wave equation which $\varphi^{(1)}$ must also obey, in accordance with (3.7).

c. The "Multiple Reflection" Formalism. The last objective is to fulfil the boundary condition at the wall

$$\text{At } x = 0, \quad y \geq 0, \quad t > 0: \varphi_x = 0.$$

As $\varphi^{(1)}$ is completely determined by the preceding procedure, $\varphi_x^{(1)}$ at $x = 0$ is fixed and, in general, different from zero. However, $\varphi^{(1)}$ does fulfil the condition on the shock $x = M_2c_2t$

$$\text{(A)} \qquad \varphi_t^{(1)} + Kc_2\varphi_x^{(1)} = F(y,t).$$

To account for the wall condition one may require an equivalent relation which is derived from (A) by "reflection." At $x = -M_2c_2t$ (reflected shock)

$$\text{(B)} \qquad \varphi_t - Kc_2\varphi_x = F(y,t).$$

If (B) could be fulfilled by the same function φ as (A), then the prescribed condition at $x = 0$ would be automatically satisfied.

Actually, only (A) can be satisfied by $\varphi^{(1)}$. To satisfy (B) a correction function $\varphi^{(2)}$ may be added to $\varphi^{(1)}$ such that at $x = -M_2c_2t$

$$\varphi_t^{(1)} + \varphi_t^{(2)} - Kc_2(\varphi_x^{(1)} + \varphi_x^{(2)}) = F(y,t).$$

This determines $\varphi^{(2)}$. At this stage, the condition (B) on the "reflected shock" is taken care of by $\varphi^{(1)} + \varphi^{(2)}$, while the requirement (A) on the real shock is spoiled by the addition of $\varphi^{(2)}$ which gives an undesired contribution at $x = M_2c_2t$. Therefore, another correction function $\varphi^{(3)}$ is added, so that at $x = M_2c_2t$

$$\varphi_t^{(1)} + \varphi_t^{(2)} + \varphi_t^{(3)} + Kc_2[\varphi_x^{(1)} + \varphi_x^{(2)} + \varphi_x^{(3)}] = F(y,t)$$

or by use of (A)

$$\varphi_t^{(3)} + Kc_2\varphi_x^{(3)} = -[\varphi_t^{(2)} + Kc_2\varphi_x^{(2)}],$$

and the original situation on the real shock is restored.

Continuing in this manner, correction functions $\varphi^{(k)}$ may be added which, alternately, take care of conditions (A) and (B). Since it can be shown that this process converges (as in the wind tunnel problem), the resulting series solution will assume the correct values on both the real and reflected shocks, which insures that all the required conditions are satisfied.

In the limit of a weak compression wave, the above series solution goes over into the acoustic approximation described in Section II, and the wall condition is automatically satisfied by the first term of the series. If a slightly stronger shock is selected, the first two terms of the series are a sufficient approximation. Numerical computations of the wall pressure

distribution, for $p_1/p_0 = 1.5$, show satisfactory agreement with Lighthill's result. It is hoped that the method outlined above is also amenable for evaluation, if the pressure field in the whole domain is desired (as in shock tube interferograms).

References

1. Courant, R., and Friedrichs, K. O., *Supersonic Flow and Shock Waves*, Interscience Publishers, 1948, p. 326.
2. Keller, J. B., and Blank, A., *Commun. Pure Applied Math.*, **4**, 75–94 (1951).
3. Bargmann, V., AMP Report 108.2 R NDRC (1945).
4. Lighthill, M. J., *Proc. Roy. Soc. (London)*, **A198**, 454–470 (1949).
5. Lighthill, M. J., *Proc. Roy. Soc. (London)*, **A201**, 554–565 (1950).
6. Ting, L., and Ludloff, H. F., *J. Aeronaut. Sci.*, **18**, 143 (1951); **19**, 317–329 (1952).
7. Gardner, C. S., and Ludloff, H. F., Tech. Rept. to ONR, 1948.
8. Busemann, A., *Deut. Akad. Luftfahrtforsch.*, **7B**, 105–122 (1943).
9. Ludloff, H. F., and Friedman, M. B., to be published in *J. Aeronaut. Sci.*
10. Garrick, I. E., and Rubinow, S. I., NACA, Tech. No. 1383, 1947.
11. Gardner, C. S., and Ludloff, H. F., *J. Aeronaut. Sci.*, **17**, 47–59 (1950).
12. Ferdman, S., M.A. Thesis, New York University, 1951.
13. Fletcher, C. H., Taub, A. H., and Bleakney, Walker, *Revs. Modern Phys.*, **23**, 271–286 (1951).
14. White, D. R., *J. Aeronaut. Sci.*, **18**, 633–634 (1951).
15. Ludloff, H. F., and Friedman, M. B., *J. Aeronaut. Sci.*, **19**, 425–426 (1952).

On the Presence of Shocks in Mixed Subsonic-Supersonic Flow Patterns

By GOTTFRIED GUDERLEY

Wright Air Development Center, Dayton, Ohio

Introduction

Experiments indicate that in supersonic regions embedded in a subsonic flow, shocks occur quite frequently. The present article is concerned with the explanation of this phenomenon.

From a mathematical point of view this explanation is very simple; we shall find that in general the boundary value problem which one obtains, does not have a solution in the form of a potential flow. It is

true that many examples of transonic potential flows are known; these flows, however, will be recognized as exceptions.

If the theory of mixed elliptic-hyperbolic boundary value problems were sufficiently developed, the above proposition would appear as a simple consequence. In the present state of knowledge, one is forced to approach the question in a less general way, i.e., by means of examples which can be discussed with the mathematical tools available at present. Fortunately the investigation of counter examples is sufficient, since we propose to show the non-existence (rather than the existence) of solutions of boundary value problems of a certain kind.

A physicist will naturally not be satisfied with the curt result, that a potential flow does not exist. Especially in view of the numerous examples of possible potential flows, he will ask in which manner an arbitrarily small change of the contour of a flow can make a potential flow impossible. This question will be answered by a physical interpretation of some examples. In one respect the arguments cannot be quite satisfactory. The fact that a potential flow is not possible does not necessarily mean that a flow pattern which fulfils the boundary conditions, can be found if shocks *are* admitted.

The method of presentation adopted here may need a word of explanation. The nonexistence of the potential flow is a mathematical fact which follows without further physical argument from the properties of the boundary value problem. In general the author prefers to show first the underlying physical idea and then to bring the necessary mathematical developments. In the present case, however, he feels that the introduction of physical surmises at the beginning will detract the attention from the underlying mathematical problem, especially since the physicist is in general not accustomed to ask whether the solution of a boundary value problem exists, if the problem has been formulated in a "reasonable" manner. Therefore the present article starts with the mathematical discussion and brings the physical considerations afterwards.

Only planar flows will be considered throughout this paper.

I. The Nonexistence of Solutions for Certain Boundary Value Problems of the Mixed Type

1. A General Property of a Supersonic Region Embedded in a Subsonic Flow

In the present section it will be shown by relatively simple means that even slight changes of the contour in an embedded supersonic region will make the flow incompatible with a potential flow. The mathematical basis is a discussion of the sign of the Jacobian for the mapping from the physical to the hodograph plane [cf. (1) and (2)]. The following deriva-

tion, which is due to Busemann (3,4), shows the physical essence in a particularly simple manner.

Let us consider a supersonic region adjacent to a subsonic flow field. One can immediately exclude flow fields in which the sonic line is normal to the stream lines (except at isolated points), for then the sonic line will coincide with a limiting line [cf. (5)], and the supersonic region will fold back over the subsonic region as in the example of the source flow (Fig. 1). Where the sonic line runs obliquely to the stream lines, one will obtain a flow field which corresponds to Fig. 2; the Mach wave which runs toward a point of the sonic line and the Mach wave which leaves this point, will lie on the same side of the stream line through this point, since at the sonic line the Mach waves are normal to the stream lines. If one moves in the downstream direction along a Mach wave which runs toward the sonic line (say BC in Fig. 2), then in the vicinity of the sonic line, the

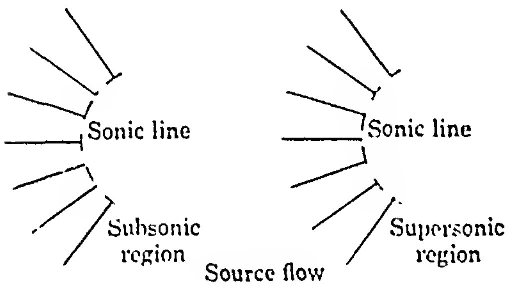

FIG. 1

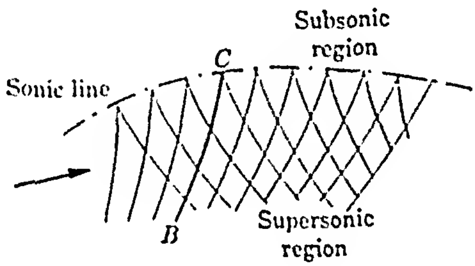

FIG. 2

pressure will change from supersonic to sonic, i.e., the pressure will increase. Therefore the Mach waves that cross the path BC will be compression waves. Thus it follows that all Mach waves starting at the sonic line are compression waves. Since the sonic line is a line of constant pressure, all Mach waves running toward the sonic line are rarefaction waves. This structure of the flow field is characteristic for every potential flow with an embedded supersonic region.

As one of the numerous applications we mention here that a Mach wave which leaves the sonic line will never reach it again, for it cannot change from a compression to a rarefaction wave. This implies that a subsonic flow over a body in which a supersonic region extends behind the body, cannot be a potential flow, for the Mach waves that pass behind the body would otherwise start at the sonic line and also end there.

As important to our present question we note that the body contour adjacent to a supersonic region which is embedded in a subsonic flow, must always be convex, since all waves which run from the sonic line toward the body are compression waves, and all waves starting there must be rarefaction waves. If one flattens the contour locally, such that the

waves starting at the contour are compression waves, then one has a contradiction to a necessary property of a potential flow. This will certainly happen if a section of the contour is straight, but actually it is only necessary that the local curvature of the boundary stream line becomes smaller by a finite amount. An example of this kind has been worked out by Schaefer (6).

One can conclude that an embedded supersonic flow field will not be a potential flow, if certain relatively small changes of the contour are made. This has been shown so far only if the surface curvature is changed at least by a certain finite amount. That the flow is actually still more sensitive will be seen subsequently by considerations which are due to Frankl, Busemann, and Guderley.

2. Tricomi's Boundary Value Problem and Analogous Flow Patterns

As a preparation to the investigations of Frankl (8) let us show the analogy between Tricomi's boundary value problem (7) and certain flow fields. This analogy will lead to a plausible generalization of Tricomi's theorem, which is the basis of Frankl's argument.

Tricomi considers the differential equation

$$z_{xx} + xz_{yy} = 0,$$

where x and y are the independent variables and z is the dependent variable. For $x > 0$ the differential equation is elliptic, for $x < 0$, it is hyperbolic. The region for which Tricomi solves the boundary value problem is shown in Fig. 3. In the elliptic domain the boundary is an

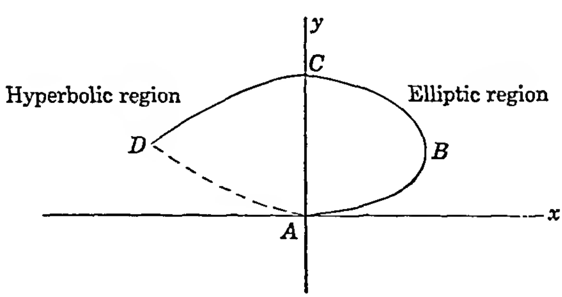

FIG. 3

arbitrary curve (with the usual restrictions made in proofs of uniqueness and existence). In the hyperbolic domain the contour is formed by the two characteristics CD and AD which run through the points of intersection A and C of the contour in the elliptic domain with the line $x = 0$. Tricomi prescribes the values of z along the entire elliptic contour and along one of the characteristics of the hyperbolic contour, say CD, and

then shows that the solution exists and is unique, if one imposes certain requirements of continuity for z and its derivatives.

With regard to the way in which the boundary conditions are prescribed, this problem shows a strong analogy to some boundary value problems for transonic gas flow.

We consider the flow through a Laval nozzle with a sharp corner at the throat (Fig. 4). The flow at the left is subsonic (i.e., its differential equation is elliptic). The sonic line starts at the corner H of the throat and proceeds toward the middle of the nozzle (line HKE). The flow past the corner at point H occurs in the form of a Meyer expansion. Point H may denote the point within the Meyer expansion at which the sonic state prevails, point L may be the point of the Meyer expansion from which the Mach wave LME starts. The points H and L coincide in space, but the conditions at these points are different. Some of the

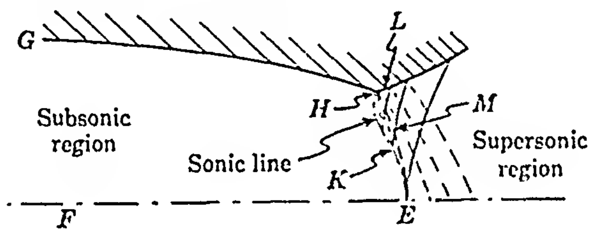

FIG. 4

Mach waves of the Meyer expansion end at the sonic line; one of them, the Mach wave LME will reach the sonic line in the middle of the tunnel. Mach waves which lie farther downstream will not reach the sonic line. In Fig. 4 some Mach waves which cross the Mach waves of the Meyer expansion have been drawn (e.g., KM). One of these Mach waves intersects the Mach waves of the Meyer expansion right at the corner of the contour. One can consider it as a Mach wave which runs through the points H and L and denote it accordingly. The length of this Mach waves between the points H and L is naturally zero.

Let ψ be the stream function. One has as boundary conditions along the subsonic (elliptic) contour: $\psi = 0$ along the line of symmetry EF, ψ arbitrarily prescribed along the entrance cross section FG, and $\psi =$ constant along the nozzle contour GH. With regard to the supersonic region we restrict our attention to that part which influences the subsonic region. This portion is limited by the sonic line HKE and the Mach wave LME. As another boundary of this region one can consider the Mach wave HL. Along this Mach wave HL one has the condition $\psi =$ constant.

The similarity of the boundary conditions between this and Tricomi's problem is obvious. Along the subsonic part (elliptic part) of the con-

tour and along one characteristic of the supersonic part, the values of the function (ψ or z) are given. Clearly, in the nozzle flow no boundary values can be imposed along the Mach wave LME, which corresponds in Tricomi's boundary value problem to the characteristic AD.

This analogy between physical flows and Tricomi's problem suggests certain extensions of Tricomi's theorem. If one considers the flow in

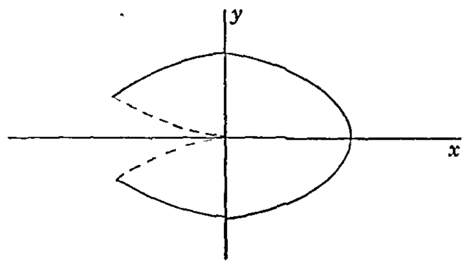

FIG. 5

the entire nozzle instead of in its upper half, then a form of Tricomi's boundary value problem according to Fig. 5 is suggested. The contour in this case is symmetrical to a horizontal axis. The Tricomi contour which corresponds to the flow through an unsymmetrical nozzle (Fig. 6) is shown in Fig. 7. Finally, it is quite unusual that the nozzle has a sharp corner in the throat. But also for a nozzle with a smooth throat one will have characteristics which correspond to the characteristics

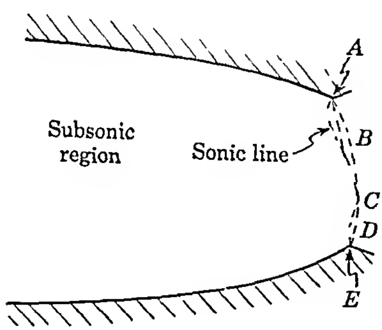

FIG. 6

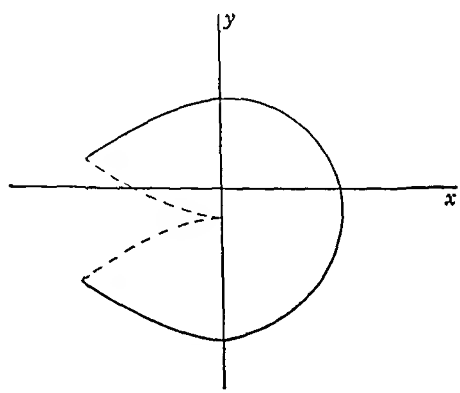

FIG. 7

ABC and EDC in Fig. 6, along which no boundary values can be prescribed. The Tricomi problem which corresponds to a Laval nozzle with a smooth contour in the throat is shown in Fig. 8. There the supersonic contour has a gap DE; aside from this it is arbitrary, but it must not have more than one point of intersection with each characteristic. This restriction is imposed since simple examples of hyperbolic boundary

value problems indicate that otherwise one obtains either boundary value problems which are obviously undetermined or boundary value problems for which the data in the supersonic regime are contradictory and will not allow a solution to exist.

The contour of Fig. 8 can be obtained in the following manner. One starts with a contour which is closed also in the hyperbolic region and which obeys the above restrictions. From one interior point F of the line $x = 0$ one then draws the two characteristics FE and FD. Guided by the analogy to physical flow patterns one would then expect that the solution exists and is unique, if the value of z is prescribed along the entire contour with the exception of the portion DE.

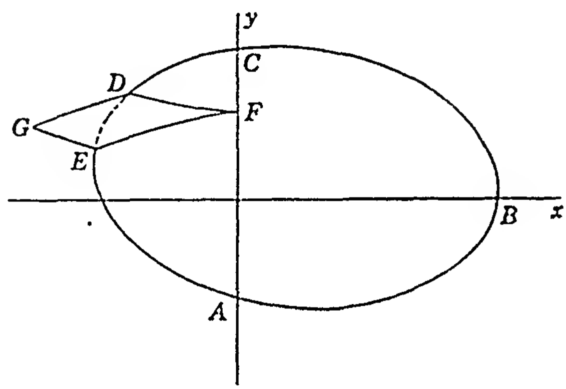

FIG. 8

A general proof for this extension of Tricomi's problem has not been given. A uniqueness proof for a contour which fulfils the restriction that no line $x/y^{2/3}$ = constant intersects it more than once, is shown in Guderley (12).

3. The Nonexistence of Solutions of Tricomi's Problem for a Contour Which Is Closed in the Supersonic Region

If for the contour of Fig. 8 the uniqueness of the solution for the boundary value problem with the gap EDF has been established, then one can readily show the nonexistence of a solution for which the values of z have been prescribed along the entire contour.

For the boundary value problem with a "gap," the solution may either exist or it may not exist. If it does not exist, then the solution with boundary values prescribed along the entire contour will not exist either, since along the gap additional conditions are imposed.

In the other case, one may first disregard the boundary values along ED, then the solution will be uniquely determined in the region $ABCDFE$. This solution determines the values of z along the characteristics DF and EF. One can construct by means of the method of characteristics a

solution which assumes along *DF* and *EF* the values of z which were previously obtained from the boundary value problem for the region *ABCDFE*. This solution is unique. It can be considered as the continuation of the solution of the boundary value problem for the region *ABCDFE* through the region *DGEF*. In general there will be a discontinuity in one of the derivatives as one passes over the characteristics *DF* and *EF*; however, such a discontinuity does not constitute a violation of the differential equation (Courant and Hilbert, 9).

Now, if the solution obtained in the area *EFDG* agrees along *DE* with the values originally prescribed, then a solution of the original boundary value problem exists. For arbitrarily prescribed data such an agreement cannot be expected, and it follows that in general a solution of the boundary value problem does not exist if the boundary values are prescribed along a contour which is closed also in the supersonic region.

4. Frankl's Argument

In applying the previous result to the flow past a body, one can proceed in two ways. Each approach involves an unproven assumption at a decisive point.

One can carry out the discussion in the physical plane and assume that the previous result holds true not only for the Tricomi equation but also for the more complicated equation of a compressible flow. The other possibility is to make first the hodograph transformation. One thus obtains a differential equation which is very similar to Tricomi's equation (if one carries out considerations of transonic similarity, the equations become even identical). By this transformation the boundary conditions assume a very inconvenient nonlinear form. Here one must make the assumption that the above result about the nonexistence of the solution of the boundary value problem with a closed contour will be correct also for the present boundary conditions.

The second approach is the one originally used by Frankl. The author prefers the first one because of its simplicity. Because of the assumptions involved, either approach constitutes only a very plausible but not completely conclusive argument.

Figure 9 represents a symmetric body in a subsonic flow parallel to its plane of symmetry. Only the upper half of the flow field will be considered. Adjacent to the profile there may be an embedded supersonic region. We enclose the subsonic flow field by a circle with a large radius. Then the elliptic contour of the boundary value problem is given by this circle, the line of symmetry upstream and downstream of the body, and the portions of the contour of the body for which the

velocity is subsonic. The supersonic contour consists of the portions of the body boundary for which the velocity is supersonic. Obviously one has here a boundary value problem for which the boundary conditions are prescribed along a contour which is closed as well in the subsonic as in the supersonic region. According to the considerations of the previous paragraph such a contour will in general not have a solution.

Repeating the argument of the previous section one may try to create a gap in the supersonic region artificially by two characteristics which start at the same point of the sonic line (curves AB and AC). One would expect to have a boundary value problem which possesses a solution, if one disregards the contour between B and C. This solution would determine the flow field except in the triangle ABC. One can then

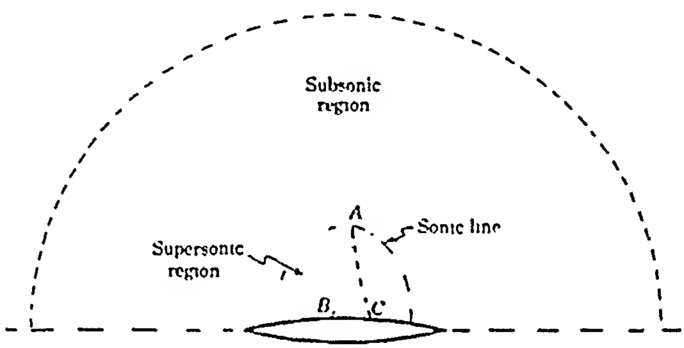

FIG. 9

construct the flow field in this triangle by means of the method of characteristics. If the stream line of the flow field so constructed which connects points B and C agrees with the original contour, then a potential flow exists. If it does not agree, then a potential flow is impossible.

It is in general not possible to carry out this procedure, since it is extremely difficult to solve the boundary value problem. Furthermore, the location of the characteristics in the physical plane is not predetermined (since the differential equation is not linear), and therefore one does not know where the gap in the contour must be left. At high supersonic Mach numbers, the supersonic region will extend behind the body, and then the supersonic contour can never have the right shape, since it will contain concave parts. (This argument is actually the same as that of Section I,1.)

Really clear-cut are those examples for which the flow with which one starts is a potential flow, e.g., a flow obtained by the hodograph method. If one introduces in such a flow a gap (e.g., the gap ABC indicated in Fig. 9), then it is plausible that the flow in the region outside

of the gap is uniquely determined. With the flow along the characteristics BA and CA known, one can then determine the flow field in the region ABC. This flow field agrees naturally with the one found originally by the hodograph method. If one chooses within the gap a contour which differs from the original one, then this contour will not be compatible with a potential flow.

Accordingly, if one changes in a potential flow part of the contour which is cut out by two characteristics which start at the same point of the sonic line, then the potential flow is no longer possible, even if the changes are much milder than those described in the first section of this article.

The meaning of the statement, that *in general* no potential flow exists is now clear. Only for one shape of the contour within the "gap" is a potential flow possible; for every other form one will have a deviation from the potential flow.

5. General Remarks on the Investigations of Busemann and Guderley

Frankl's argument shows the nonexistence of a potential flow for a general contour in a very simple and concise form. Some questions, however, have been left unanswered. The first one has been mentioned previously, namely that the mathematical theorems, which show the nonexistence of the solutions are not proved for the problems which are encountered in Frankl's analysis.

One is led to the other question by the following consideration: in Frankl's argument it seems irrelevant where the gap in the contour is introduced. If one would shift it into one of the corners of the supersonic region, then the area covered by the gap is zero. One would obtain a solution of the boundary value problem for which the boundary conditions are fulfilled along the entire contour. What happens in this case?

There is no way known to treat the first question in full generality. Busemann and Guderley use the following artifice. One starts with a known potential flow (such flow patterns can be determined by means of the hodograph method). Then one asks how such a flow pattern changes if the boundaries or the free stream Mach number are changed by a small amount. For small changes one can linearize the boundary conditions and thus obtain a linear boundary value problem, which can then be investigated. Incidentally, the boundary condition thus obtained is not identical with that in Tricomi's problem. In the original papers of Busemann and Guderley the linearization of the boundary conditions was carried out for the exact hodograph equation. In the present article we shall restrict ourselves to the hodograph equation simplified by the transonic similarity law; this equation is identical with Tricomi's equa-

tion. Strictly speaking the replacement of the exact hodograph equation by Tricomi's equation requires also a justification.

Regarding the second question one can say: If one shifts the "gap" into one of the corners of the supersonic region, its influence cannot vanish, since in this way one would obtain a hodograph solution in which the boundary conditions are fulfilled everywhere. Thus one is led to expect that the gap will be replaced by a singularity of the flow field which occurs at that point of intersection between sonic line and contour into which the gap has been shifted.

In the following these ideas will be carried out in detail.

6. *Hodograph*

Let x and y be the Cartesian coordinates in the physical plane, Φ the velocity potential, κ the ratio of the specific heats, "a" the local velocity of sound, u and v the velocity components in the x and y direction, a^* the critical velocity.

The potential equation in the physical plane

$$\Phi_{xx}\left(1-\frac{u^2}{a^2}\right) - 2\Phi_{xy}\cdot\frac{uv}{a^2} + \Phi_{yy}\left(1-\frac{v^2}{a^2}\right) = 0 \tag{1.1}$$

can be transformed into the hodograph plane by means of Legendre's transformation

$$\phi(u,v) = ux + vy - \Phi \tag{1.2}$$

with

$$u = \Phi_x, \quad v = \Phi_y \tag{1.3a,b}$$

(see e.g., Liepmann and Puckett, 5). Inversely one has

$$x = \phi_u, \quad y = \phi_v. \tag{1.4a,b}$$

Introducing as independent variables the absolute value of the velocity vector w and its direction θ, one obtains the following equation for the transformed potential

$$\phi_{ww} + \frac{1}{w}\left(1-\frac{w^2}{a^2}\right)\phi_w + \frac{1}{w^2}\left(1-\frac{w^2}{a^2}\right)\phi_{\theta\theta} = 0 \tag{1.5}$$

or more explicitly

$$\phi_{ww}\left(a^{*2} - \frac{\kappa-1}{\kappa+1}w^2\right) + \frac{1}{w}\phi_w(a^{*2}-w^2) + \frac{1}{w^2}\phi_{\theta\theta}(a^{*2}-w^2) = 0. \tag{1.5a}$$

This equation is linear. By a limiting process used in the derivation of the transonic similarity law (10), the last differential equation is simplified to

$$\phi_{\eta\eta} - \eta\phi_{\theta\theta} = 0 \tag{1.6}$$

with

$$\eta = (\kappa + 1)^{1/3} \frac{w - a^*}{a^*}. \tag{1.7}$$

Except for an unessential difference in sign Eq. (1.6) agrees with Tricomi's equation.

In some of the future examples θ need not be bounded; then one obtains from Eq. (4), using the transonic approximations

$$x = \frac{(\kappa + 1)^{1/3}}{a^*} \cdot \phi_\eta \cdot \cos\theta - \frac{\phi_\theta}{a^*} \cdot \sin\theta, \tag{1.8a}$$

$$y = \frac{(\kappa + 1)^{1/3}}{a^*} \cdot \phi_\eta \cdot \sin\theta + \frac{\phi_\theta}{a^*} \cdot \cos\theta. \tag{1.8b}$$

If one studies flow patterns which lie in the vicinity of a sonic parallel flow, then θ is close to zero throughout the flow field and one obtains

$$x = \frac{(\kappa + 1)^{1/3}}{a^*} \cdot \phi_\eta, \quad y = \frac{\phi_\theta}{a^*}. \tag{1.9a,b}$$

The deviation of the stream lines from lines y = constant can be obtained in this approximation as

$$\tilde{y} = \int \theta dx, \tag{1.10}$$

taken along the line y = constant.

The equation of the stream function simplified in a similar manner is given by

$$\psi_{\eta\eta} - \eta\psi_{\theta\theta} = 0. \tag{1.11}$$

The relation between ϕ and ψ is given by

$$\psi = \rho^*\phi_\theta, \tag{1.12}$$

where ρ^* is the density at the sonic velocity. (The last equation can be derived from Eqs. (46a) and (46b) of Guderley (10); the assumption that the flow lies in the vicinity of a parallel sonic flow is not necessary.)

7. *Linearization of the Boundary Conditions in the Hodograph Plane*

To arrive at a linear boundary value problem in the hodograph plane one can proceed in the following manner. Assume that a shock-free flow in the physical plane is known. One stream line may correspond to the

contour of a body. This flow field may be transformed into the hodograph. We ask now what happens if the boundary in the physical plane is changed by such a small amount that one can linearize the boundary conditions in the hodograph plane.

The contour of the body is given by a stream line, i.e., in the present approximation according to Eq. (1.12) by

$$\phi_\theta = \text{const.} \tag{1.13}$$

The map of the boundary of the flow in the hodograph plane may be given by $\eta = \bar{\eta}(\theta)$. The shape of the boundary stream line in the physical plane can be described either by $x = \bar{f}_1(\theta)$ or by $y = \bar{f}_2(\theta)$ where $\bar{f}_1$ and $\bar{f}_2$ are known functions. Since along a stream line

$$\frac{dy}{dx} = \tan\theta,$$

$\bar{f}_1$ and $\bar{f}_2$ are not independent from each other. By means of Eq. (1.8), one can then determine ϕ_η; one thus obtains

$$\phi_\eta = f(\theta),$$

where $f(\theta)$ is a known function. Thus one has as boundary conditions in the original flow

$$\phi_\theta(\bar{\eta},\theta) = \text{const.} \tag{1.14a}$$

and

$$\phi_\eta(\bar{\eta},\theta) = f(\theta). \tag{1.14b}$$

If the contour in the physical plane is changed by a small amount, this will express itself by a change of the function $f(\theta)$. Let the changed function be given by $f(\theta) + F(\theta)$. Naturally in this case the contour in the hodograph plane will also be changed, the new contour may be given by

$$\eta = \bar{\eta}(\theta) + \mathrm{H}(\theta).$$

The function $\mathrm{H}(\theta)$ is unknown. Also the transformed potential will change. It may now be expressed by $\phi(\eta,\theta) + \Omega(\eta,\theta)$.

From Eq. (1.14) one then obtains as the boundary conditions for the changed flow

$$\begin{aligned}\phi_\theta(\bar{\eta} + \mathrm{H},\ \theta) + \Omega_\theta(\bar{\eta} + \mathrm{H},\ \theta) &= \text{const.},\\ \phi_\eta(\bar{\eta} + \mathrm{H},\ \theta) + \Omega_\eta(\bar{\eta} + \mathrm{H},\ \theta) &= f(\theta) + F(\theta).\end{aligned}$$

If one linearizes these conditions assuming that H, Ω, and F are small and if, furthermore, one eliminates H, then one obtains

$$\Omega_\eta(\bar{\eta},\theta) - \frac{\phi_{\eta\eta}(\bar{\eta},\theta)}{\phi_{\eta\theta}(\bar{\eta},\theta)} \cdot \Omega_\theta(\bar{\eta},\theta) = F(\theta). \tag{1.15}$$

If one differentiates Eq. (1.13), which is valid along the map of the original contour in the direction of this line, one obtains

$$\phi_{\eta\theta} \frac{d\bar{\eta}}{d\theta} + \phi_{\theta\theta} = 0.$$

With Eq. (1.6) and this result, one obtains from Eq. (1.15) as the final boundary condition for the perturbation potential

$$\Omega_\eta(\bar{\eta},\theta) + \bar{\eta} \frac{d\bar{\eta}}{d\theta} \Omega_\theta(\bar{\eta},\theta) = F(\theta). \tag{1.16}$$

Naturally Ω fulfils the differential Eq. (1.6)

$$\Omega_{\eta\eta} - \eta\Omega_{\theta\theta} = 0. \tag{1.17}$$

A derivation of the corresponding boundary condition for the exact hodograph equation can be found in Guderley (11).

8. Some Remarks about This Boundary Value Problem

In potential theory one distinguishes between boundary value problems of the first and of the second kind. Tricomi prescribes along the boundary the value of the function z; this problem corresponds to a boundary value problem of the first kind. The problem with the boundary condition (1.15) can be considered as the generalization of the boundary value problem of the second kind.

For Tricomi's contour (Fig. 3) the uniqueness proof can be carried out also for boundary value problems of the second kind in exactly the same manner as for boundary value problems of the first kind (Guderley, 12, p. 28).

In potential theory an integral condition must be fulfilled in order for the solution of the inner boundary value problem of the second kind to exist. The present case is quite similar.

If one considers a closed domain D with a contour C in which Eq. (1.16) is fulfilled, one has $\iint_D (\Omega_{\eta\eta} - \eta\Omega_{\theta\theta})d\eta d\theta = 0$. Integrating the first expression in the integral with respect to η, the second with respect to θ, one obtains the integral condition $\int_C \Omega_\eta d\theta + \eta\Omega_\theta d\eta = 0$. Hence one obtains from Eq. (1.16)

$$\int_C F(\theta)d\theta = 0. \tag{1.18}$$

Some considerations of plausibility regarding this condition in the case that the contour is open in the supersonic region are given in Guderley

(12, Appendix III). In the application to the flow past a body this condition does not represent a restriction with regard to the deformations which are admissible. A closer study would show that in those problems one will always have a free parameter whose choice is determined by the condition (1.18). Therefore we shall assume in the following that the condition (1.18) is fulfilled.

One can transform a boundary value problem of the second kind into one of the first kind. Equation (1.17) can be written as

$$\Omega_\eta = X_\theta, \quad \eta\Omega_\theta = X_\eta, \tag{1.19}$$

where X is a suitable function of η and θ. The boundary condition (1.15) can be written as a condition for X:

$$X_\theta + \frac{d\bar{\eta}}{d\theta} X_\eta = F(\theta).$$

Hence

$$X = \int F(\theta) d\theta, \tag{1.20}$$

where the integration is carried out along the original contour. The differential equation for X is obtained by eliminating Ω from Eq. (1.17). One then obtains

$$X_{\eta\eta} - \frac{1}{\eta} X_\eta - \eta X_{\theta\theta} = 0. \tag{1.21}$$

9. *Particular Solutions of Eq. (1.17)*

By the restriction to small changes of the boundary in the physical plane a linear boundary value problem of the second kind has been obtained in the hodograph. If a general theory of the boundary value problem existed, this theory would give immediately the conditions for the existence of a solution. Actually less is known for boundary conditions of the second kind than for boundary conditions of the first kind. Even the extension of Tricomi's boundary value problem given in Guderley (12) cannot be carried out for boundary value problems of the second kind.

The main question is whether a solution of a boundary value problem of the second kind exists when the boundary is closed in the supersonic region as well as in the subsonic region. The integral conditions (1.18) may be fulfilled. We shall show the nonexistence by examples, which can be discussed by means of the particular solutions derived in the following.

Let us introduce in Eq. (1.17) the following transformation of the independent variables

(1.22a,b) $$\xi = \frac{\eta}{(\frac{3}{2}\theta)^{2/3}}, \quad \rho = -\eta^3 + (\tfrac{3}{2}\theta)^2.$$

The ξ,ρ-system is shown in Fig. 10. A corresponding transformation is found in Tricomi's memoir (7). One then obtains the following dif-

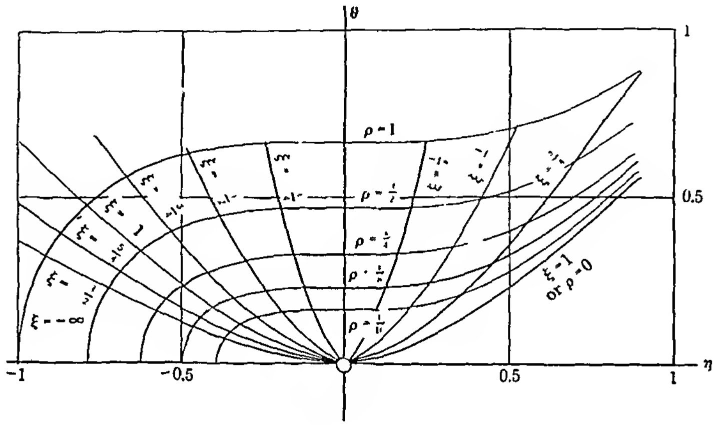

Fig. 10

ferential equation for Ω

(1.23) $$\Omega_{\xi\xi}\frac{(1-\xi^3)^2}{\xi} - \frac{5}{2}\Omega_\xi\xi(1-\xi^3) + \frac{1}{16}\Omega = 9\rho^2\Omega_{\rho\rho} + \frac{21}{2}\rho\Omega_\rho + \frac{1}{16}\Omega.$$

Particular solutions of this differential equation are found by the product hypothesis

(1.24) $$\Omega = g(\rho)\cdot G(\xi)$$

which leads to the ordinary differential equations

(1.25a) $$G''\frac{(1-\xi^3)^2}{\xi} - \frac{5}{2}\xi(1-\xi^3)G' + \left(-\lambda + \frac{1}{16}\right)G = 0$$

and

(1.26) $$9\rho^2 g'' + \tfrac{21}{2}\rho g' + (-\lambda + \tfrac{1}{16})g = 0.$$

Here λ is an arbitrary constant. Equation (1.25a) can be written in its self-adjoint form

(1.25b) $$\frac{d}{d\xi}\left((1-\xi^3)^{5/6}\frac{dG}{d\xi}\right) + \left(-\lambda + \frac{1}{16}\right)\frac{\xi}{(1-\xi^3)^{7/6}}\cdot G = 0.$$

Equation (1.26) is solved by

(1.27) $$g = \rho^{-1/12 \pm 1/6\sqrt{\lambda}}.$$

If one carries out the transformation (1.22) with respect to the boundary condition (1.16) one obtains

$$\Omega_\xi \frac{d\bar{\rho}}{d\xi} + \Omega_\rho \cdot 9\bar{\rho}^2 \frac{\xi}{(1-\xi^3)^2} = F^*(\xi), \tag{1.28}$$

where along the contour

$$\rho = \bar{\rho}(\xi), \quad \theta = \bar{\theta}(\xi),$$

and

$$F^*(\xi) = F(\bar{\theta}(\xi)) \frac{\bar{\rho}^{5/3}}{(1-\xi^3)^{5/3}} \left(\frac{d \log \bar{\rho}}{d\xi} + \frac{3\xi^2}{1-\xi^3}\right). \tag{1.28a}$$

If the contour coincides with a line ξ = constant, condition (1.28) prescribes the values of Ω_ξ; if it coincides with a line ρ = constant, Eq. (1.28) gives Ω_ρ.

The contours which we shall discuss in future examples will be formed by two lines ξ = constant = c_1 and ξ = constant = c_2 and one line ρ = constant. The regions thus obtained will not have a gap (Figs. 11, 12, 13). Depending upon the choice of the constants c_1 and c_2 the regions will be either entirely subsonic (Fig. 11), entirely supersonic (Fig. 12), or a mixed supersonic-subsonic regime (Fig. 13). For simplicity, we assume that along $\xi = c_1$ and $\xi = c_2$ the condition $\Omega_\xi = 0$ is prescribed. (Other examples will be discussed later.) Thus one obtains the boundary condition for G

$$G'(c_1) = 0, \quad G'(c_2) = 0. \tag{1.29}$$

Naturally boundary conditions of the first kind can also be treated this way and the procedure is exactly the same (Guderley, 12).

The boundary conditions (1.29) together with the differential Eq. (1.25b) form an eigenvalue problem for the functions G. Therefore for the particular examples which will be discussed here, one can base the discussion on the theory of eigenvalue problems. This is the reason for the choice of these examples.

It can be seen rather easily from the orthogonality relation (1.30b), which will be given later, that the eigenvalues are real. One of them is $\frac{1}{16}$ with the corresponding eigenfunction G = constant. For a purely subsonic problem, all other eigenvalues are smaller than $\frac{1}{16}$ (cf. e.g., Guderley, 12, p. 8), for purely supersonic problems they are larger than $\frac{1}{16}$, and in the mixed case there exists an infinite number of eigenvalues which are larger than $\frac{1}{16}$, and an infinite number which are smaller than $\frac{1}{16}$. By means of Hilbert's theory of the polar integral equation (cf. e.g., Hamel 15) it can be shown that the system of eigenfunctions is complete.

Let us arrange the eigenvalues according to their magnitude and then denote them by

$$\cdots \lambda_{-k} \cdots \lambda_{-3}, \lambda_{-2}, \lambda_{-1}, \lambda_0, \lambda_1, \lambda_2, \lambda_3 \cdots \lambda_k \cdots .$$

Subscripts with negative signs refer to eigenvalues smaller than $\frac{1}{16}$, subscripts with a positive sign refer to eigenvalues larger than $\frac{1}{16}$, and $\lambda_0 = \frac{1}{16}$. The corresponding eigenfunctions may be denoted by

$$G_{-k} \cdots G_{-3}, G_{-2}, G_{-1}, G_0, G_1, G_2, G_3 \cdots .$$

For the eigenfunctions the following relations of orthogonality exist

$$\int_{c_1}^{c_2} G_h(\xi) G_k(\xi) \frac{\xi}{(1-\xi^3)^{7/6}}\, d\xi = 0 \quad \text{for } h \neq k, \tag{1.30a}$$

$$\int_{c_1}^{c_2} \frac{dG_h}{d\xi} \cdot \frac{dG_k}{d\xi} (1-\xi^3)^{5/6}\, d\xi = 0 \quad \text{for } h \neq k. \tag{1.30b}$$

The eigenfunctions can be normalized

$$\int_{c_1}^{c_2} G_h^2 \frac{\xi}{(1-\xi^3)^{7/6}}\, d\xi = -1 \qquad \text{for positive values of } h, \tag{1.31a}$$

$$\int_{c_1}^{c_2} G_h^2 \frac{\xi}{(1-\xi^3)^{7/6}}\, d\xi = +1 \qquad \text{for negative values of } h. \tag{1.31b}$$

For G_0 the normalization constant may be either positive or negative.

The particular solutions for Ω formed with these eigenfunctions may be denoted by

$$\Omega_{\mathrm{I}h} = \rho^{-1/12+1/3\sqrt{\lambda_h}} \cdot G_h(\xi), \tag{1.32a}$$

$$\Omega_{\mathrm{II}h} = \rho^{-1/12-1/3\sqrt{\lambda_h}} \cdot G_h(\xi), \tag{1.32b}$$

$$\Omega_{\mathrm{III}h} = \rho^{-1/12} G_{-h}(\xi) \cdot \cos\left(\tfrac{1}{3}\sqrt{|\lambda_{-h}|}\log\rho\right), \tag{1.32c}$$

$$\Omega_{\mathrm{IV}h} = \rho^{-1/12} \cdot G_{-h}(\xi) \cdot \sin\left(\tfrac{1}{3}\sqrt{|\lambda_{-h}|}\log\rho\right), \tag{1.32d}$$

for $h = 1, 2 \cdots$;

$$\Omega_{\mathrm{I}0} = 1, \ \Omega_{\mathrm{II}0} = \rho^{-1/6}.$$

From the completeness of the system of functions G_h it follows that a function can be represented by a superposition of the expressions $\Omega_{\mathrm{I}h}$, $\Omega_{\mathrm{II}h}$, $\Omega_{\mathrm{III}h}$, $\Omega_{\mathrm{IV}h}$, $\Omega_{\mathrm{I}0}$, and $\Omega_{\mathrm{II}0}$ if it fulfils the differential Eq. (1.16) everywhere in a region bounded by the two lines $\xi = c_1$ and $\xi = c_2$ and by two lines $\rho =$ constant and if it fulfils the boundary condition $\Omega_\xi = 0$ along the lines $\xi = c_1$ and $\xi = c_2$ (cf. Guderley, 12).

With these particular solutions we can now study some boundary value problems.

10. A Subsonic Boundary Value Problem

In Fig. 11 the boundary consists of the two lines $\xi = c_1$ and $\xi = c_2$ and of a line ρ = constant = 1. Along the lines ξ = constant the condition $\Omega_\xi = 0$ may be prescribed, along the line $\rho = 1$ Ω_ρ may be given arbitrarily as $\Omega_\rho = f(\xi)$. We require the solution to be finite at point 0.

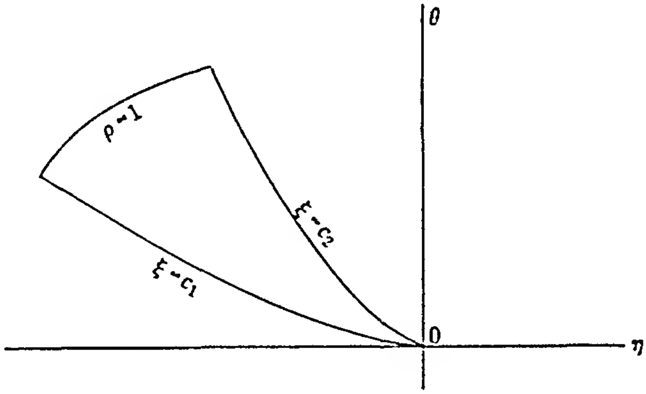

FIG. 11

Then it can be represented by a superposition of only the expressions Ω_{Ih}. In the present example, the particular solutions Ω_{IIIh} and Ω_{IVh} do not exist. So we have

$$\Omega = \sum_{0}^{\infty} a_h \cdot \rho^{-1/12+1/3\sqrt{\lambda_h}} \cdot G_h(\xi), \tag{1.33}$$

where the a_n are arbitrary constants. Hence one finds for $\rho = 1$

$$\Omega_\rho = \sum_{1}^{\infty} a_h\left(-\tfrac{1}{12} + \tfrac{1}{3}\sqrt{\lambda_h}\right) \cdot G_h(\xi).$$

In the last expression the term with G_0 is not present since $\lambda_0 = \frac{1}{16}$. Therefore an arbitrary function $f(\xi)$ can be represented only if f is orthogonal to G_0, i.e., if

$$\int_{c_1}^{c_2} \frac{\xi}{(1-\xi^3)^{5/6}} \cdot f(\xi)d\xi = 0.$$

This condition is equivalent with Eq. (1.18). The coefficients $a_h(h = 1,2 \cdots)$ can be obtained readily by the equations of orthogonality (1.30a). The solution which one obtains in this manner is finite and continuous everywhere.

11. A Supersonic Boundary Value Problem

The boundary value problem of Fig. 12 is patterned according to that of Fig. 11. If one prescribes along the line ρ = constant only the

values of Ω_ρ, then one sees by means of the method of characteristics, which in this case can also be used to construct the solution, that the solution is not fully determined. One needs also the values of Ω. For the representation of the solutions we have now the system of particular solution $\Omega_{\mathrm{III},h}$, $\Omega_{\mathrm{IV}h}$, and $\Omega_{\mathrm{I}0}$. The coefficients can be found rather easily by means of the relations of orthogonality. Again the condition (1.18) imposes a restriction on the values of Ω_ρ. In this solution it is remarkable that all particular solutions tend to infinity as one approaches point O. It follows that the entire solution will tend also to infinity. To show this, one can either assume that the boundary conditions are prescribed in such a manner that only one of the coefficients is different from zero. In this case the solution will certainly tend to infinity.

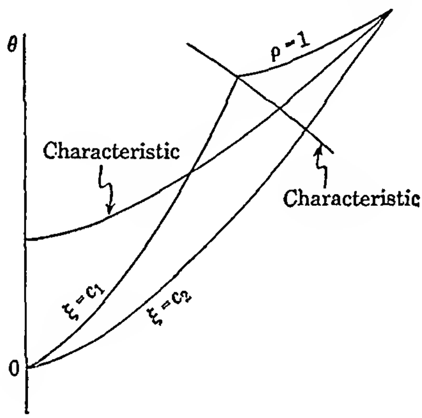

FIG. 12

Another way of reasoning is as follows. If one writes the solution more explicitly as

$$\Omega = \sum_1^\infty [a_{\mathrm{III},h} \cdot \rho^{-1/12} \cdot \cos (\tfrac{1}{3} \sqrt{|\lambda_{-h}|} \log \rho) + a_{\mathrm{IV},h}\rho^{-1/12} \sin (\tfrac{1}{3} \sqrt{|\lambda_{-h}|} \log \rho)]G_{-h} + \text{const.},$$

one can consider the expressions $a_{\mathrm{III}h}\rho^{-1/12} \cos (\frac{1}{3} \sqrt{|\lambda_{-h}|} \log \rho) + a_{\mathrm{IV},h} \cdot \rho^{-1/12} \sin (\frac{1}{3} \sqrt{|\lambda_{-h}|} \log \rho)$ in the sum as coefficients of the functions G_{-h}. These coefficients depend naturally upon ρ. By means of Eqs. (1.30) and (1.31) they can be determined along each line ρ = constant by a Fourier analysis, i.e., by integrals

$$\int_{c_1}^{c_2} \Omega \cdot G_h \frac{\xi}{(1 - \xi^3)^{7/6}} \, d\xi.$$

The integrand is bounded if Ω is bounded and $c_2 = 1 - \epsilon$ with $\epsilon > 0$. Thus the coefficients of the functions G_h will be bounded for any value

of ρ. However the presence of the factor $\rho^{-1/2}$ in Eq. (1.34) shows that they are not bounded. Because of this contradiction, the assumption that Ω is bounded in the entire region is wrong.

One thus finds that in this purely supersonic problem the solution tends to infinity as one approaches point 0. No solution of this problem which is finite at point 0, exists. The example shows that with data prescribed along a closed contour in an arbitrary manner, a solution will exist in general only if a singularity at the sonic point of the contour is admitted. The same phenomenon will be found for mixed boundary value problems.

12. A Mixed Boundary Value Problem

Figure 13 shows a mixed boundary value problem for which the contour does not contain a "gap." The subsonic contour is formed by the

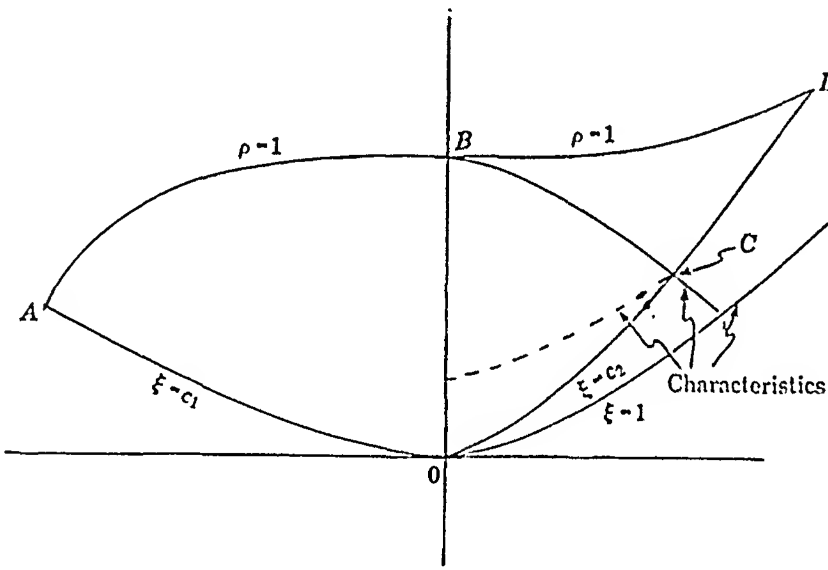

FIG. 13

line OA ($\xi = c_1$) and the line AB ($\rho = 1$). The supersonic contour is formed by the characteristic BC and the line $\xi = c_2 < 1$. No characteristic intersects the supersonic contour more than once.

This problem can be reduced to one for which the data are given along lines ξ = constant and ρ = constant only. For this purpose one prescribes arbitrarily the condition $\Omega_\xi = 0$ along the portion CD of the line $\xi = c_2$. Then from this condition and the data along the characteristic BC one can construct the solution in the region BCD. If one now determines a solution which assumes along BD the values of Ω and

of Ω_ρ obtained by the previous construction, it will agree in the entire region BCD with the solution previously constructed and will therefore assume along the characteristic BC the boundary values originally prescribed. Accordingly the original boundary value problem is equivalent to one, in which $\Omega_\xi = 0$ is prescribed along the lines $\xi = c_1$ and $\xi = c_2$ (from O to D) and Ω_ρ is prescribed along the line ABD and in which furthermore Ω is given along BD. Incidentally, this boundary value problem can be considered as one in which the supersonic contour intersects certain characteristics more than once. In this example, the solution would obviously not be determined if one prescribes only the value of the generalized normal derivative along the contour BD. For the representation of the solution, the functions $\Omega_{\mathrm{I}h}$, $\Omega_{\mathrm{III}h}$, and $\Omega_{\mathrm{IV}h}$ will be used. Expressions $\Omega_{\mathrm{II}h}$ are not admitted analogously to the subsonic problem of Fig. 11. They have at point O a stronger singularity than the functions $\Omega_{\mathrm{III}h}$ and $\Omega_{\mathrm{IV}h}$. So we have

$$\Omega = \sum_1^\infty a_{\mathrm{I}h} \cdot \Omega_{\mathrm{I}h} + \sum_1^\infty a_{\mathrm{III}h} \cdot \Omega_{\mathrm{III}h} + \sum_1^\infty a_{\mathrm{IV}h}\Omega_{\mathrm{IV}h} + \text{const.}$$

Here $a_{\mathrm{I}h}$, $a_{\mathrm{III}h}$, and $a_{\mathrm{IV}h}$ are suitable constants.

The fulfilment of the conditions for Ω_ρ along ABD leads to a Fourier analysis. It yields in a similar manner, as in the previous analysis, the values of $a_{\mathrm{I}h}$ and of the linear combination $(-\frac{1}{12}a_{\mathrm{III}h} + \frac{1}{2}\sqrt{|\lambda_{-h}|} \cdot a_{\mathrm{IV}h})$. This linear combination occurs since $a_{\mathrm{III}h}$ as well as $a_{\mathrm{IV}h}$ contribute to Ω_ρ. The coefficients $a_{\mathrm{III}h}$ can be found by an infinite system of equations which results from the conditions for Ω along BD.

The solution of this system need not be investigated; for if for any value of h the above linear combination of $a_{\mathrm{III}h}$ and $a_{\mathrm{IV}h}$ differs from zero, then the solution cannot be bounded in the vicinity of $\rho = 0$ for the same reason as in the previous section. Hence it follows that unless the boundary conditions are chosen in such a particular manner that all coefficients $a_{\mathrm{III}h}$ and $a_{\mathrm{IV}h}$ are zero, the resulting solution will be singular at point O.

13. General Remarks Concerning These Examples

The purpose of the previous examples was to show what may happen in a potential flow over a given surface, if the surface is changed by a small amount. One obtains a boundary value problem which has the form of the last examples (although in general the boundary will be quite different). We suspected, that if the contour does not possess a gap, as it happens in the flow where a supersonic region is embedded into a subsonic flow, a continuous solution is not possible and that the discontinuity

will appear at one of the points of intersection of the contour with the sonic line.

The examples of a supersonic and of a transonic boundary value problem show exactly this property. A solution for these boundary value problems exists only if one admits particular solutions Ω_{IIIk} and Ω_{IVk}, or if the coefficients of these particular solutions happen to be zero. The presence of these particular solutions gives a flow which is physically impossible; a further discussion would show that one obtains folds in the supersonic region of the physical plane which extend eventually into the subsonic region. One can therefore say with regard to the problem of a slightly disturbed contour that in general no solution exists in the form of a potential flow.

This present investigation reaffirms Frankl's conclusions, but it is more than a stricter derivation of Frankl's results, it shows the mechanism by which the nonexistence of a continuous solution of the problem is caused, i.e., by the occurrence of the particular solutions Ω_{IIIk} and Ω_{IVk}.

One may ask if the above examples are sufficiently general. One might object to the singularity which the contour possesses at point O. That this singularity does not cause the solution to become singular is shown by the example of the purely subsonic flow (Fig. 11). The discussion of more general boundaries is rather difficult. In Section II,6 a simple example which is due to Busemann will be given. It shows the occurrence of singular particular solutions even for a smooth contour.

II. Physical Considerations

1. *Introductory Remark*

The first section of this article brought mainly mathematical investigations, which show that the boundary value problem for the transonic potential flow over a body has in general no solution. In the approach of Busemann-Guderley the impossibility of a potential flow was indicated by the presence of particular solutions with an oscillatory character in the direction of changing values of ρ. They tend to infinity in one of the corners of the supersonic region. In the following it will be shown that in a supersonic region which is embedded in a subsonic flow these oscillatory solutions can be expected for physical reasons.

2. *A Flow Pattern with Waves in the Supersonic Region*

In a potential flow with a local supersonic region (Fig. 14) the contour may be changed locally in such a manner that a singularity of the contour, e.g., a jump of the curvature arises. In Fig. 14 ABC may give the sonic line, and the jump of the curvature may occur at point D. This singu-

larity in the stream line shape will propagate downstream along a characteristic until the characteristic reaches the sonic line. The reflection of such a singularity at the sonic line has been investigated in Guderley (10, p. 10). There it has been shown that the singularity does not vanish but will propagate in a changed form along the characteristic which starts at the point of the sonic line where the original characteristic arrived (point E in Fig. 14). The singularity propagating along this characteristic will in turn be reflected at the surface of the body and then propagate along a characteristic which runs toward the sonic line. One thus obtains a pattern in which the singular Mach wave is reflected from the surface of the body and the sonic line an infinite number of times as one approaches the "exit" corner of the supersonic region.

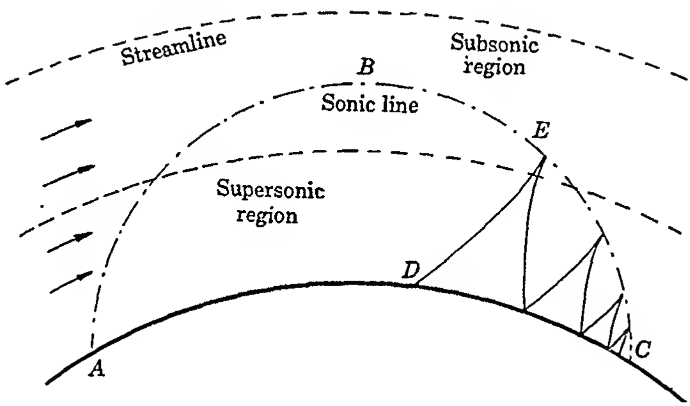

FIG. 14

Whether this flow pattern represents a wavy flow cannot be decided from this description—a mathematical analysis is needed at this point—but at least this flow field suggests a study of waves within such a supersonic region.

Even in the present preliminary ideas about the structure of this flow pattern, one can see an interesting alternative which in its most striking form stems from Busemann (13; see also 11, Introduction). The accumulation of singular waves in the corner of the supersonic region will either be compatible with a potential flow or it will be incompatible and then the potential flow will be changed in some way.

Assume that the first is correct. If one then reverses the flow direction, one will obtain the flow field shown in Fig. 15 where the perturbation propagates toward the other corner of the supersonic region. In a potential flow however, one can reverse all the velocity vectors and therefore Fig. 15 will also represent a solution for the flow over the body

in the original direction. So this assumption leads to the consequence that the solution of the flow problem is not unique.

The other alternative, that the accumulation of singular waves destroys the potential flow at the end of the supersonic region, would save the uniqueness and require the introduction of a new physical effect, probably the introduction of shocks.

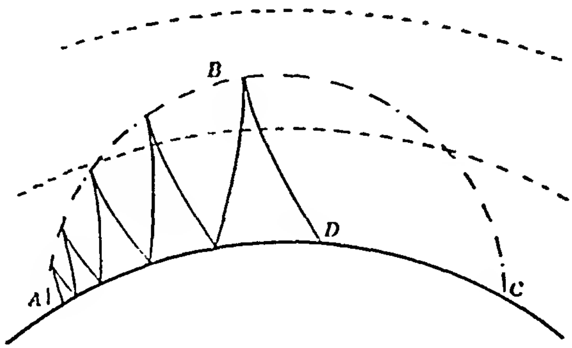

FIG. 15

3. *Perturbations in a Potential Vortex*

An example of a mixed flow in which perturbations can be studied very easily is the potential vortex, i.e., a flow whose potential in the physical plane is given by $\phi = \omega$ where ω denotes the angle in polar coordinates. The stream lines in this case are concentric circles; along the stream lines the velocity is constant. For the inner circles the velocity is supersonic; for the outer circles it is subsonic. Two stream lines may represent the walls; they may either lie at supersonic or at subsonic speeds, or one wall can lie at a supersonic, the other at a subsonic speed. If one considers the flow in only one sheet of the physical plane, then one cannot differentiate between the upstream or the downstream direction. For this reason it will be assumed that the physical plane is covered by an infinite number of Riemann sheets, and the flow field extends through all these sheets (Fig. 16).

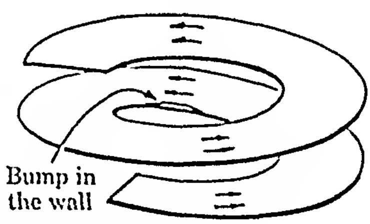

FIG. 16

The map of the flow in the hodograph plane is given by $\phi = \theta$. This flow runs in the physical plane in the counterclockwise direction. The walls may be given by the lines $\eta = \eta_1$ and $\eta = \eta_2$, where η_1 and η_2 are constants. In mapping from the hodograph plane to the physical plane one must use Eq. (1.8). If one changes in this flow one or both walls, then one obtains the boundary value problem of finding a solution of the

differential equation

$$\Omega_{\eta\eta} - \eta\Omega_{\theta\theta} = 0 \tag{1.17}$$

with the boundary conditions

$$\Omega_\eta(\eta_2) = F(\theta).$$

At points at which the wall has been left unchanged F is zero, and at points where the wall has been changed, F is determined by these changes. This is a classical problem. One has a linear homogeneous differential equation with nonhomogeneous boundary conditions. As is well known (see e.g., 9), this problem can be converted into one with homogeneous boundary conditions but with a nonhomogeneous differential equation. In the present case the nonhomogeneous problem can be solved if one has a system of particular solutions of the homogeneous differential equation with homogeneous boundary conditions. Such solutions can be found by the hypothesis

$$\Omega = G(\eta) \cdot e^{\sqrt{\lambda}\cdot\theta},$$

which leads to the differential equations

$$G'' - \eta\lambda G = 0 \tag{2.1}$$

with the boundary conditions

$$G'(\eta_1) = 0, \quad G'(\eta_2) = 0. \tag{2.2}$$

This is an eigenvalue problem for the function G (very similar in character to the eigenvalue problems dealt with in the first part of this paper). For a purely subsonic flow the eigenvalues λ are positive, for a purely supersonic problem they are negative and for a mixed problem there is an infinite number of positive and negative eigenvalues. The eigenfunctions and eigenvalues may be denoted in the same fashion as in the first part. Also the particular solutions Ω may be denoted in the same manner, i.e., we have now

$$\begin{aligned}
\Omega_{\mathrm{I}h} &= e^{-\sqrt{\lambda_h}\theta} \cdot G_h(\eta), \\
\Omega_{\mathrm{II}h} &= e^{+\sqrt{\lambda_h}\theta} \cdot G_h(\eta), \\
\Omega_{\mathrm{III}h} &= \cos\left(\sqrt{|\lambda_{-h}|} \cdot \theta\right) \cdot G_{-h}(\eta), \\
\Omega_{\mathrm{IV}h} &= \sin\left(\sqrt{|\lambda_{-h}|} \cdot \theta\right) \cdot G_{-h}(\eta),
\end{aligned} \tag{2.3}$$

where $h = 1, 2 \cdots$.

The particular solutions $\Omega_{\mathrm{I}h}$ and $\Omega_{\mathrm{II}h}$ formed with the eigenfunctions for positive eigenvalues increase or decrease exponentially when θ goes to positive or negative infinity; the particular solutions for negative eigenvalues oscillate as one proceeds θ in the direction.

Let us assume that only the wall for which $\eta = \eta_2$ is changed and that this change occurs between $\theta = \theta_1$ and $\theta = \theta_2$ where $\theta_1 < \theta_2$. In order to convert the problem with nonhomogeneous boundary conditions into one for which the boundary conditions are homogeneous it is practical to introduce a function γ defined by the equation

$$\gamma'' - \eta\nu \cdot \gamma = 0 \tag{2.4}$$

and the boundary condition $\gamma'(\eta_1) = 0$ and $\gamma(\eta_1) = 1$. This differential equation is identical with Eq. (2.1) with the exception that the constant ν does not coincide with an eigenvalue. Then an expression which fulfils the boundary conditions can be written in the form

$$\Omega = \frac{F(\theta)}{\gamma'(\eta_2)} \cdot \gamma(\eta) + \sum_1^\infty a_h(\theta) \cdot G_h(\eta) + \sum_1^\infty b_h(\theta) \cdot G_{-h}(\eta). \tag{2.5}$$

Here the unknown functions a_h and b_h must be determined in such a manner that the differential Eq. (1.17) is fulfilled. The details have been carried out in Appendix I. One obtains

$$\begin{aligned} a_h = \frac{1}{2\sqrt{\lambda_h}} \cdot \frac{G_h(\eta_2)}{\lambda_h - \nu} \cdot \Big\{ & e^{\sqrt{\lambda_h}\cdot\theta} \cdot \int_{c_1}^{\theta} (\nu \cdot F(\tau) - F''(\tau)) \cdot e^{-\sqrt{\lambda_h}\cdot\tau} d\tau \\ & - e^{-\sqrt{\lambda_h}\cdot\theta} \int_{c_2}^{\theta} (\nu F(\tau) - F''(\tau)) \cdot e^{\sqrt{\lambda_h}\cdot\tau} d\tau \Big\}, \end{aligned} \tag{2.6}$$

$$\begin{aligned} b_h = \frac{1}{\sqrt{|\lambda_{-h}|}} \cdot \frac{G_{-h}(\eta_2)}{\lambda_{-h} - \nu} \Big\{ & -\cos(\sqrt{|\lambda_{-h}|} \cdot \theta) \int_{c_3}^{\theta} (\nu F(\tau) - F''(\tau)) \\ & \cdot \sin(\sqrt{|\lambda_{-h}|}\, \tau) d\tau + \sin(\sqrt{|\lambda_{-h}|} \cdot \theta) \int_{c_4}^{\theta} (\nu F(\tau) - F''(\tau)) \\ & \cdot \cos(\sqrt{|\lambda_{-h}|}\, \tau) d\tau \Big\}. \end{aligned}$$

Now the choice of the limits of integration c_1, c_2, c_3, and c_4 is important. Let us consider first the purely subsonic boundary value problem. Then only particular solutions with positive eigenvalues are present. In a subsonic field one expects the flow at a far distance from the perturbed spot to approach the undisturbed flow. In order to obtain such a flow pattern, one must choose the constants of integration in the following manner: $c_1 = \theta_2$, $c_2 = \theta_1$. Accordingly, upstream of the perturbed spot, only such solutions of the homogeneous differential equation are present which decrease as one goes upstream; downstream of the perturbed spot one has only solutions which decrease as one goes downstream.

For an entirely supersonic flow it is in general impossible to leave the flow upstream and downstream undisturbed simultaneously. In the

present case this is expressed by the fact that for a purely supersonic flow the particular solutions are undamped periodic functions of θ. The natural physical assumption is, that the oncoming flow is free of perturbations while downstream of the perturbed spot no conditions are imposed. Accordingly the solution in the supersonic case requires that $c_3 = \theta_1$, $c_4 = \theta_1$.

In the mixed case, particular solutions of both types are present simultaneously. One will expect the flow to become smooth as one goes in the upstream direction, whereas downstream the smoothest possible flow which does not perturb infinity in the upstream direction will give the desired solution. Thus the choice of the constants will be

$$c_1 = \theta_2; \quad c_2 = c_3 = c_4 = \theta_1. \tag{2.7}$$

These results show that in a mixed flow a perturbation of the wall (either in the subsonic or in the supersonic region) will create a wavy flow pattern (downstream of that perturbation). This pattern although it is felt in the subsonic region will have its largest amplitudes in the supersonic region. These supersonic particular solutions are the ones originally discovered by Taylor (14), whose interpretation however is quite different.

This example is also quite interesting from another point of view. The influence of a wall perturbation in a subsonic or in a supersonic flow is known. In a subsonic flow a perturbation spreads in all directions and at the same time becomes weaker. In the supersonic flow a perturbation spreads only downstream, but it keeps its strength. Now what happens in a mixed case? The present example shows that there are particular solutions which have the character of subsonic perturbations, and particular solutions which have the character of supersonic perturbations. Therefore the mixed flow combines the properties of a subsonic and a supersonic flow. A part of the perturbations propagates only downstream without decreasing in strength, while another part of the perturbation which attenuates in strength travels both upstream and downstream.

This example shows that in a mixed flow a wavy flow pattern can actually be produced by a wall perturbation. The other question of what happens to these oscillations if the supersonic region terminates can naturally not be answered by the present example. As a preliminary step, one may ask what happens if the Mach number at the wall changes.

4. Interpretation of Fig. 13

A physically possible flow in which the Mach number changes along the stream lines is obtained by an interpretation of Fig. 13. One must

find a suitable basic flow which fits the boundaries of Fig. 13. This requires that ψ = constant along the lines $\xi = c_1$ and $\xi = c_2$. Solutions of this character can be found easily if one remembers that, with the transonic simplifications, the differential equations for the stream function and the transformed potential are the same, so that particular solution of Eq. (1.23) written in terms of ψ, can be used. In the present case, a flow which has the lines $\xi = c_1$ and $\xi = c_2$ as stream lines is given by $\psi = f(\xi)$, where $f(\xi)$ is the function G obtained from Eq. (1.25a) for $\lambda = \frac{1}{16}$. This solution represents the flow in a curved channel (Fig. 17); it is similar to the flow in Fig. 16. Lines θ = constant in Fig. 16 correspond here to lines ρ = constant, and lines η = constant to lines ξ = constant. Along the outer stream line ($\xi = c_1$) the velocity is subsonic; along the inner stream line it is supersonic. The sonic line extends along a stream line within the tunnel. The only difference between Figs. 16 and 17 is that in Fig. 17 the Mach number along the stream lines changes. Finally a cross section is reached where one has a parallel sonic flow.

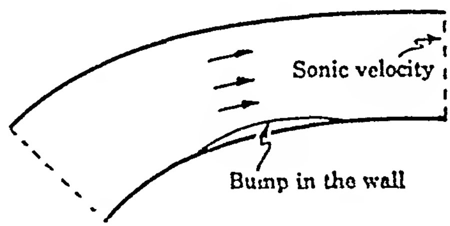

FIG. 17

While in Fig. 13 the region considered is bounded in one direction by a line ρ = constant, which would mean that the flow starts at a certain cross section at a finite distance, we rather assume that the flow field is unlimited in upstream direction and that at a large distance upstream one has the basic flow. Perturbations may be introduced into this flow by a bump along the wall which extends between the values of $\rho = \rho_1$, and $\rho = \rho_2$. Then one obtains according to Eq. (1.28) as boundary conditions for the perturbed flow $\Omega_\xi = F(\rho)$, where $F(\rho)$ is determined by the change of the wall; at points of the walls which have not been changed, it is zero.

Except for the fact that the differential equations are somewhat different, the problem of the potential vortex with a wall perturbation and the present example are exactly alike. So is the solution and the choice of the constants of integration. The particular solutions with $\lambda > \frac{1}{16}$ describe such perturbations which spread out in a subsonic manner in the upstream and downstream directions and die out as one goes to a larger distance from the perturbed spot. The other particular solutions spread only downstream. Here one encounters another difference: when the Mach numbers become closer to one, the strength of the perturbation increases, as has been seen in the discussion of Fig. 13.

If one maps the perturbed flow into the physical plane, one sees that part of the physical plane will be covered by several sheets.

The mathematical analysis cannot indicate in which manner this situation can be remedied, a physical rather than a mathematical concept is needed. The example of the corresponding supersonic flow may serve as a guide. There one can construct the arising flow pattern alternately by the method of characteristics. This construction can take into account the arising of shocks, and thus one obtains a physically possible flow although the mathematical difficulties in the analytical treatment are the same. One will be inclined to believe that also in mixed flow patterns the multiple covered regions can be removed by the admission of shocks.

In the mathematical treatment of this example, the assumption was made that the boundary conditions can be linearized. One might blame this linearization for the presence of folds in the physical plane. A counter example is the purely supersonic flow. There the method of characteristics takes into account the correct boundary conditions. Nevertheless folds in the physical plane will arise unless shocks are admitted.

5. Another Interpretation of Fig. 13

The main interest of the flow pattern discussed previously lies in its close relation to the potential vortex. But it does not illustrate our main problem of how the flow behaves, if the sonic line reaches the wall.

Such a flow can be obtained if one chooses the basic flow in Fig. 13 differently. Again we use the fact that the differential equations for ψ and Ω are the same. With a suitable value of λ in Eq. (1.25a) one can find solutions of the form (1.24) which have $\psi = 0$ along $\xi = c_1$ and along $\xi = c_2$ and for which G does not become zero between these values of ξ. Lines $\psi =$ constant in the $\eta\theta$-plane are shown qualitatively in Fig. 18; Fig. 19 represents the corresponding flow pattern. The dash-dot line indicates the sonic line. At the point where the sonic line hits the contour, one of the higher derivatives is singular. In Fig. 19 it appears strange, that at the sonic point, the wall curvature changes its sign. A solution in the η,θ-plane, according to Fig. 20, can be treated in exactly the same manner as the flow of Fig. 18. Then the sonic point of the contour in the physical plane will still be singular, but at least the curvature of the boundary stream line does not change its sign.

The dotted line in Figs. 18 and 19 shows a line $\rho =$ constant. As in the previous example, the flow may extend to infinity (in this case in every direction). A perturbation may be introduced into this flow by a perturbation of the wall either in the subsonic or in the supersonic region. If one requires that infinity is undisturbed, then the mathematical prob-

lem is exactly the same as in the previous example. Therefore, also here, particular solutions in Ω_{IIIh} and Ω_{IVh} will be present in the expression for the perturbation potential. They will cause physical difficulties for small values of ρ, i.e., close to the sonic point of the contour.

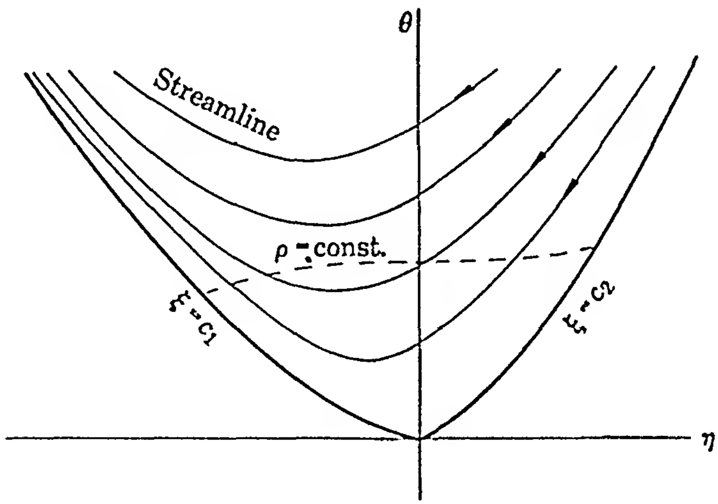

FIG. 18

In this interpretation a comparison with the purely supersonic problem is impossible, since no corresponding basic flow exists. In this discussion the flow represents an exit corner of a supersonic field. If one

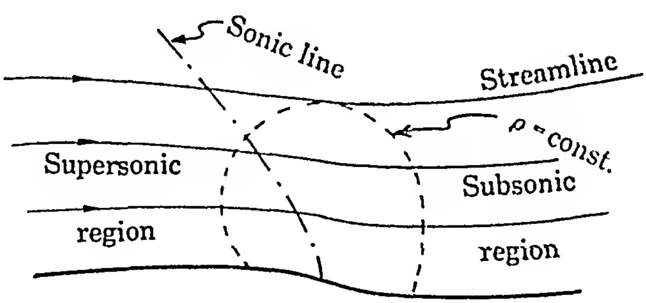

FIG. 19

reverses all velocity vectors, one will obtain an entrance corner. Then no perturbation Ω_{IIIh} and Ω_{IVh} will be admitted for $\rho = 0$. In the solution of the boundary value problem which is quite similar to Eq. (1.39), this means only a change of the limits of integration in the expression with

the particular solution G_{-h}. Then the particular solution with an oscillatory character will propagate to infinity. In this process they become weaker, but not to the same extent as the solution with eigenvalues larger than $\frac{1}{16}$.

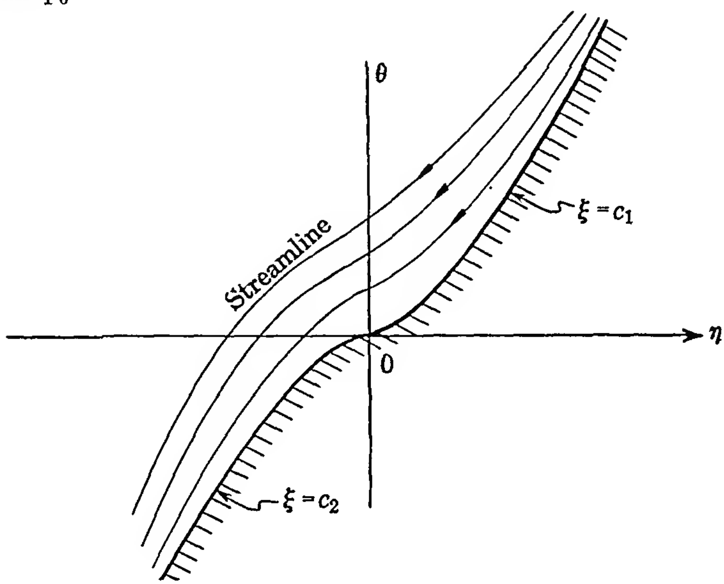

Fig. 20

If one changes in these examples the wall in the subsonic region instead of in the supersonic region, and if this perturbation extends over not too large a range of ρ, then particular solutions Ω_{IIIh} and Ω_{IVh} will be excited here also. This shows that the presence of oscillatory particular solution in the supersonic region does not depend on the occurrence of a singularity of the wall stream line in the supersonic region. It also shows that particular solution Ω_{IIIh} and Ω_{IVh} will be excited even though the perturbed parts of the subsonic contour lie downstream of the sonic point of the contour.

6. *A More General Case*

In the last examples the boundary stream line was singular with respect to one of the higher derivatives at the sonic point of the contour. The problem for which the boundary stream line is regular was treated in the original publications of Busemann and Guderley, under rather general conditions. Since the essential point of the present investigations, i.e., the occurrence of oscillatory particular solutions whose amplitude increases toward the exit corner of the supersonic region, has been made quite obvious by the preceding discussion, it will suffice here to show only one example for which the treatment is particularly simple. This approach is due to Busemann.

The basic flow in the η,θ-plane may be given by $\psi = \eta - \alpha\theta$, where α is an arbitrary constant. Obviously this flow fulfils the differential Eq. (1.11). The boundary stream line may be given by $\eta = \alpha \cdot \theta$. By an analysis, details of which are given in Appendix II, one finds that for small values of θ a system of particular solutions which fulfil the boundary conditions is represented by

$$\Omega = \theta^{-1/4} \cdot \sin\,(2(\tau^*)^{3/2} \cdot \theta^{-1/2}) \cdot G\left(\frac{\eta}{\theta} \cdot \tau^*\right)$$

where τ^* and G are defined in the Appendix II. Also these solutions increase as one approaches the exit corner of the supersonic region. The similarity between this result and the result in the previous examples becomes still stronger, if one expresses the increase of amplitude in terms of the value of η at the points where the lines ρ = const. or θ = const. intersect the wall, then in either case the amplitude behaves like $\eta^{-1/4}$. Actually for small values of c_2 the two kinds of examples can be treated by the same method.

From the mathematical point of view, one can make an objection to Busemann's and Guderley's approach to this problem. The solution is obtained in the form of an expansion with respect to a suitable parameter (in Appendix II, for example, one has an expansion with respect to powers of $\theta^{1/2}$). This expansion fulfils the differential equation and the boundary condition. However one ought to show either that this expansion converges and that the result fulfils the differential equation, or that the deviation of the approximate solution from the exact solution can be made arbitrarily small, if one takes a finite number of terms of this expansion and lets the parameter with respect to which the development has been carried out, tend to zero. As in many problems of applied mathematics this proof has not been given.

7. *Concluding Remarks*

The first part of the article shows that the boundary value problem for the transonic potential flow past a body has in general no solution. First Frankl's argument is given, which contains certain elements of plausibility. Then the problem is attacked by investigating changes in a transonic potential flow due to small deformations of the contour. The type of boundary value problem arising is studied in suitable examples. They show that in general (i.e., unless very strong conditions are imposed on the boundary value problem) this problem does not have a solution which is continuous everywhere. A discussion of the singularities which must be admitted in the hodograph plane would show that the flow pattern thus obtained is physically impossible.

In the second part the particular solutions whose presence indicate the impossibility of a potential flow are interpreted physically. They would correspond to a wavy flow in a physical plane. First, a flow pattern is described (Figs. 14 and 15) which makes the occurrence of a wavy flow in the supersonic region plausible. This example shows also that if a solution in the form of a potential flow could always be found, this solution would not be unique. With this preparation, some boundary value problems are discussed (mostly problems discussed in the first part from the mathematical point of view) in which wavy flow patterns do occur, they indicate that the amplitude of these waves will increase as one approaches the end of the supersonic region.

These examples show that a change of the walls in a potential flow (even of the walls in the subsonic region) will cause the flow in the supersonic region to become wavy. In the vicinity of the perturbed spot, these waves will have the magnitude of the original perturbation. If the perturbation lies in the subsonic region, they will even attenuate as one goes to larger distances from the perturbed spot. However if the local Mach number at the wall in the supersonic region approaches one, the amplitudes will increase until they introduce into the flow field overlapping portions which are naturally impossible.

At this point it would be desirable to show examples or give a theory which indicates that the admission of shocks will remedy this situation. The only examples of the kind which can be obtained easily concern purely supersonic flow patterns. The analytic solutions for these cases are completely analogous to mixed problems. The difficulties which one encounters in the physical plane can be remedied by the admission of shocks. So it is conceivable that the same will happen in a mixed flow.

The investigations do not give an immediate criterion regarding the contours for which potential flows will be possible. To disprove conclusively the surmise that a particular class of contours, e.g., analytic contours will always have a shock-free flow is difficult. In one of the examples it was shown that even though the contour is analytic in the supersonic region, a potential flow does not exist.

Frequently the present investigations have been connected with the idea of stability. But the word stability suggests the behavior of perturbations of the flow field with respect to time. The present investigations consider the change of the contour in a steady flow and ask which other steady flow will arise. They predict that at the end of the supersonic region a difficulty will arise. It must be emphasized that this difficulty does not mean a major change of the flow pattern as a whole; a major deviation from the original flow will be experienced only in the vicinity of the exit corner of the supersonic region. If one considers a

number of contours which deviate from the contour of a potential flow in various degrees, then the area in which major changes of the plane field will occur will be smaller for the smaller deviations.

For any fixed point of a flow field at a distance from the exit corner of the supersonic region a continuous change of the contour will produce a continuous change of the physical conditions.

From the practical point of view, the drag rise with increasing Mach number in the transonic region is one of the characteristic phenomena. One will ask whether the phenomena predicted here can be considered as an indication for that drag rise. In this regard one can say that, although the occurrence of shocks will bring about a drag increase (because of the entropy change), this drag rise will be negligible for weak shocks in comparison to the friction drag. Only if the supersonic region has grown to an appreciable size and if the shocks have a certain strength, will the effect of the shock be important. So this technical question is left unanswered.

That a drag rise must occur at Mach numbers close to 1 is seen from the investigation of flow patterns with exactly the Mach number 1. They show in accordance with the idea that such a flow pattern can be considered as the limiting case of the flow in a Laval nozzle with an infinite width, that the flow behind the body is supersonic and that every body of finite dimensions has a drag different from zero. Hence it is conceivable that for high subsonic Mach numbers the supersonic region will also extend behind the body. Then a shock must be expected according to the consideration in Section I,1. For reasons of continuity one would expect the drag at high subsonic Mach numbers to be different from zero since the drag at a Mach number 1 is different from zero. In a frictionless, two dimensional subsonic flow the presence of a drag requires the change of the entropy, otherwise no momentum loss can be felt at infinity. This is another indication for the presence of shocks in such flow fields.

Frequently the hodograph method has been used in order to give examples for transonic flows. By the nature of the method all these examples will correspond to a potential flow. Thus they cannot give the full picture of what may happen in transonic boundary value problems. But the results of such hodograph investigations are still of interest, for from the practical point of view one is interested in maintaining the potential flow up to as high a Mach number as possible.

The attempt has been made to explain the arising of shocks by an instability of the potential flow, i.e., by the fact that deviations from the original flow grow in the course of time. This implies that a potential flow exists; in other words, such considerations apply only to the excep-

tional cases for which the shape of the contour allows a potential flow. If the results indicate an instability, than the number of physically possible flows would be reduced further.

A similar situation exists with respect to the attempt of explaining the presence of shocks by the influence of the boundary layer. If by an adverse pressure gradient in the supersonic region the boundary has a strong tendency to separate and if by its separation it produces a shock which in turn maintains the separation, this would indicate that flow patterns which, according to the present theory could exist as potential flows, will actually show shocks. But there exist also flow patterns in which shocks must be present, even though the boundary layer is disregarded.

Appendix I

Details of the Treatment of the Potential Vortex

In the main text, an expression which fulfils the boundary conditions has been given in the form

$$\Omega = \frac{F(\theta)}{\gamma'(\eta_2)} \cdot \gamma(\eta) + \sum_1^\infty a_h(\theta) \cdot G_h(\eta) + \sum_1^\infty b_h(\theta) \cdot G_h(\eta),$$

where the G_h fulfils the differential equation.

$$G_h'' - \lambda_h \cdot \eta \cdot G_h = 0 \tag{I.1}$$

with the boundary conditions

$$G_h' = 0 \quad \text{for } \eta = \eta_1 \text{ and } \eta = \eta_2.$$

γ fulfils the differential equation

$$\gamma'' - \nu \cdot \eta \cdot \gamma = 0 \tag{I.2}$$

with the boundary condition $\gamma' = 0$, $\gamma = 1$ for $\eta = \eta_1$. The G_h are eigenfunctions and one has the relations of orthogonality

$$\int_{\eta_1}^{\eta_2} \eta \cdot G_h \cdot G_k \cdot d\eta = 0 \text{ for } h \neq k \text{ (h and k positive or negative).} \tag{I.3}$$

The G_k may be normalized.

In the same manner in which one derives the equation of orthogonality one can obtain

$$\int_{\eta_1}^{\eta_2} \eta \cdot \gamma G_k d\eta = \frac{\gamma'(\eta_2) \cdot G_k(\eta_2)}{\lambda_k - \nu}. \tag{I.4}$$

We now form

$$\Omega_{\eta\eta} = \frac{F(\theta)}{\gamma'(\eta_2)} \cdot \gamma'' + \sum_1^\infty a_h(\theta) \cdot G_h'' + \sum_1^\infty b_h(\theta) \cdot G_{-h}''$$

and

$$\Omega_{\theta\theta} = \frac{d^2F}{d\theta^2} \cdot \frac{1}{\gamma'(\eta_2)} \cdot \gamma + \sum_1^\infty \frac{d^2a_h}{d\theta^2} \cdot G_h + \sum_1^\infty \frac{d^2b_h}{d\theta^2} \cdot G_{-h}.$$

By means of the differential Eqs. (I.1) and (I.2) the expression for $\Omega_{\eta\eta}$ can be changed into

$$\Omega_{\eta\eta} = \frac{F(\theta)}{\gamma'(\eta_2)} \cdot \eta \cdot \nu \cdot \gamma + \sum_1^\infty a_h(\theta) \cdot \eta \cdot \lambda_h \cdot G_h + \sum_1^\infty b_h(\theta)\eta \cdot \lambda_{-h} \cdot G_{-h}.$$

Introducing these expressions into the differential equation

$$\Omega_{\eta\eta} - \eta\Omega_{\theta\theta} = 0$$

one obtains

$$\frac{\nu \cdot F(\theta) - \dfrac{d^2F}{d\theta^2}}{\gamma'(\eta_2)} \cdot \eta \cdot \gamma + \sum_1^\infty (a_h \cdot \lambda_h - a_h'') \cdot G_h + \sum_1^\infty (b_h\lambda_{-h} - b_h'') \cdot G_{-h} = 0.$$

In order to obtain equations for the a_k we multiply this equation with $\eta \cdot G_k$ and integrate with respect to η from η_1 to η_2. Then one obtains with the relations of orthogonality (I.3) the normalization conditions and with Eq. (I.4) the following ordinary differential equation for

$$\frac{\nu \cdot F(\theta) - \dfrac{d^2F}{d\theta^2}}{\lambda_k - \nu} \cdot G_k(\eta_2) + a_k\lambda_k - a_k'' = 0.$$

This is a nonhomogeneous ordinary differential equation. Solutions of the homogeneous part of this differential equation are given by $e^{\pm\sqrt{\lambda_k}\theta}$ (for positive values of h) and by $\cos(\sqrt{|\lambda_{-h}|}\,\theta)$ and $\sin(\sqrt{|\lambda_{-h}|}\,\theta)$ for negative values of h.

The solution of the nonhomogeneous equation can be derived by means of the method of variation of a parameter; with τ as a variable of integration one obtains

$$a_k = \frac{1}{2\sqrt{\lambda_k}} \cdot e^{\sqrt{\lambda_k}\cdot\theta} \int_{c_1}^{\theta} \frac{\left(\nu \cdot F(\tau) - \dfrac{d^2F}{d\theta^2}(\tau)\right) \cdot G_k(\eta_2)}{\lambda_k - \nu} \cdot e^{-\sqrt{\lambda_k}\cdot\tau} d\tau$$
$$- \frac{1}{2\sqrt{\lambda_k}} \cdot e^{-\sqrt{\lambda_k}\cdot\theta} \int_{c_2}^{\theta} \frac{\left(\nu \cdot F(\tau) - \dfrac{d^2F}{d\theta^2}(\tau)\right) \cdot G_k(\eta_2)}{\lambda_k - \nu} \cdot e^{+\sqrt{\lambda_k}\cdot\tau} d\tau.$$

Similarly one finds

$$b_k = -\frac{1}{\sqrt{|\lambda_{-k}|}} \cdot \cos\left(\sqrt{|\lambda_{-k}|} \cdot \theta\right) \int_{c_3}^{\theta} \frac{\left(\nu \cdot F(\tau) - \frac{d^2F}{d\theta^2}(\tau)\right) \cdot G_{-k}(\eta_2)}{\lambda_{-k} - \nu} \cdot \sin\left(\sqrt{|\lambda_{-k}|}\,\tau\right) d\tau + \frac{1}{\sqrt{|\lambda_{-k}|}} \cdot \sin\left(\sqrt{|\lambda_{-k}|} \cdot \theta\right) \int_{c_4}^{\theta} \frac{\left(\nu \cdot F(\tau) - \frac{d^2F}{d\theta^2}(\tau)\right) \cdot G_{-k}(\eta_2)}{\lambda_{-k} - \nu} \cdot \cos\left(\sqrt{|\lambda_{-k}|} \cdot \tau\right) d\tau.$$

APPENDIX II

Verification of Busemann's Solution for the Exit Corner of a Supersonic Region

According to the formulation of the problem in the main text, one must find solutions of the differential equation

$$\Omega_{\eta\eta} - \eta\Omega_{\theta\theta} = 0, \tag{1.17}$$

which fulfil the boundary condition

$$\Omega_\eta + \eta \cdot \frac{d\eta}{d\theta} \cdot \Omega_\theta = 0$$

along the line $\eta = \alpha \cdot \theta$. With this shape of the boundary this condition can be written in the form

$$\Omega_\eta + \alpha^2 \cdot \theta\Omega_\theta = 0. \tag{II.1}$$

In the direction of negative values of η the region may extend to infinity. The solution will be written in the form of an expansion with respect to θ. We introduce a function G which is defined as a solution of the differential equation

$$\frac{d^2G(\tau)}{d\tau^2} + \tau \cdot G(\tau) = 0 \tag{II.2}$$

with the boundary condition $G \to 0$ as $\tau \to -\infty$. This determines the function G except for an arbitrary constant which is of no importance.

The solution may be written in the form

$$\Omega = e^{i(\tau^*)^{3/2} \cdot 2\theta^{-1/2}} \cdot \{\theta^n \cdot G(\tau) + \theta^{n+1/2} \cdot [A \cdot \tau^3 \cdot G(\tau) + B \cdot \tau \cdot G'(\tau) + C \cdot G(\tau)]\}, \tag{II.3}$$

where the argument τ of the function G is given by

$$\tau = \frac{\eta}{\theta} \cdot \tau^* \tag{II.4}$$

τ^*, n, A, B, and C are constants which must be chosen so that each power of θ in the differential equation and the boundary conditions vanishes

separately. The function G is defined in such a manner that the lowest order terms in θ drop out automatically. The next order terms will then give a relation between n, A, and B. Because of the definition of G also the terms with C will drop out in the second order approximation. Therefore the terms of the order of magnitude $\theta^{n+1/2}$ are not determined completely by this analysis. However we are only interested in the lowest order terms.

From Eq. (II.4) one obtains

$$\frac{\partial \tau}{\partial \eta} = \frac{\tau^*}{\theta}, \quad \frac{\partial \tau}{\partial \theta} = -\frac{\tau}{\theta}.$$

Differentiating the solution (II.3) and replacing expressions G'' by G according to Eq. (II.2) one obtains

$$\begin{aligned}
\Omega_\eta &= e^{i\tau^{*3/2}\cdot 2\theta^{-1/2}} \cdot \tau^* \{\theta^{n-1} \cdot G'(\tau) + \theta^{n-0.5}[A(3\tau^2G + \tau^3G') + B(G' - \tau^2G) \\
&\qquad + C \cdot G']\}, \\
\Omega_{\eta\eta} &= e^{i\tau^{*3/2}\cdot 2\theta^{-1/2}} \cdot \tau^{*2} \{\theta^{n-2}(-\tau \cdot G) + \theta^{n-1.5}[A \cdot (6\tau G + 6\tau^2G' - \tau^4G) \\
&\qquad + B(-3\tau G - \tau^2G') - C \cdot \tau \cdot G]\}.
\end{aligned}$$

In the derivatives with respect to θ we neglect terms of order higher than the second:

$$\begin{aligned}
\Omega_\theta &= e^{i\tau^{*3/2}\cdot 2\theta^{-1/2}} \{-i \cdot \tau^{*3/2} \cdot \theta^{n-1.5} \cdot G(\tau) + \theta^{n-1}[-i \cdot \tau^{*3/2}(A \cdot \tau^3G \\
&\qquad + B \cdot \tau \cdot G' + C \cdot G) + n \cdot G - \tau G']\}, \\
\Omega_{\theta\theta} &= e^{i\cdot\tau^{*1.5}\cdot 2\cdot\theta^{-1/2}} \{-\tau^{*3} \cdot \theta^{n-3} \cdot G(\tau) + \theta^{n-2.5}[-\tau^{*3} \cdot (A\tau^3G + B \cdot \tau \cdot G' \\
&\qquad + C \cdot G) - i\tau^{*1.5}((n - \tfrac{3}{2})G - \tau G' + nG - \tau G')]\}.
\end{aligned}$$

If one introduces these expressions into the differential Eq. (1.17) which by the use of Eq. (II.4) can be written for this purpose in the form

$$\Omega_{\eta\eta} - \frac{\tau}{\tau^*} \cdot \theta \cdot \Omega_{\theta\theta} = 0,$$

one finds that the terms in θ^{n-2} drop out, the terms of the next order yield

$$\tau^{*2}\{A(6\tau G + 6\tau^2G') + B(-3\tau G)\} + i \cdot \tau^{*1/2}((2n - \tfrac{3}{2}) \cdot \tau \cdot G - 2\tau^2G').$$

Hence from the terms with τG and τ^2G' respectively

$$\begin{aligned}
6\tau^{*1.5} \cdot A - 3\tau^{*1.5} \cdot B + i(2n - \tfrac{3}{2}) &= 0, \\
6 \cdot \tau^{*1.5} \cdot A \qquad\qquad - 2i &= 0.
\end{aligned}$$

This gives

$$A = \frac{i}{3\tau^{*1.5}} \tag{II.5}$$

$$B = \frac{(2n + \frac{1}{2}) \cdot i}{3 \cdot \tau^{*1.5}}. \tag{II.6}$$

At the boundary the argument τ of G becomes $\tau^* \cdot \alpha$. Inserting the above expressions for Ω_η and Ω_θ into the boundary condition (II.1) one obtains from the terms of the lowest order

$$G' = 0. \tag{II.7}$$

Using this, the terms of the next order yield

$$A \cdot 3\alpha^2 \cdot \tau^{*3} - B \cdot \alpha^2 \cdot \tau^{*3} + \alpha^2 \cdot i\tau^{*3/2} = 0.$$

Inserting the expressions (II.5) and (II.6) one obtains $n = -\frac{1}{4}$. Equation (II.7) can be fulfilled by a suitable choice of the values of τ^*. Let us denote the value of the argument of G for which $G' = 0$ by

$$\tau_n (n = 1,2 \cdot \cdot \cdot);$$

then one obtains $\tau^* = \dfrac{\tau_n}{\alpha^2}$.

References

1. Cole, J. D., Problems in transonic flow, Thesis California Institute of Technology, 1949.
2. Nikolski, A. A., and Taganoff, G. I., Flow of a gas in a local supersonic region and some conditions for the break down of potential flow. Brown University translation A9-T-17, 1948.
3. Busemann, A., The problem of drag at high subsonic speeds, Translation 184, British Ministry of Aircraft Production, 1947.
4. Guderley, G., Considerations on the structure of transonic flow patterns, Wright Field report F-TR-2168-ND.
5. Liepmann, H. W., and Puckett, A. E., *Introduction to Aerodynamics of a Compressible Fluid*, John Wiley & Sons, New York, 1947.
6. Schaefer, M., Auftreten eines Verdichtungsstosses in the Nachbarschaft einer konvexen singularitaetenfreien, Wandkontur, Wasserbau Versuchsanstalt Kochelsee, Archiv Bericht Nr. 44/12b (also Brown University translation).
7. Tricomi, F., On linear differential equations of the second order of mixed type. Brown University translation A9-T-26. Original source: *Atti reale accod. nozl Lincei, Ser. V, Mem. Classe sci. fis. mat. e nat.*, **14**, 134 (1923).
8. Frankl, F. I., On the formation of shocks in subsonic flows with local supersonic velocities, NACA TM 1251, 1950.
9. Courant, R., and Hilbert, D., *Methoden der mathemotischen Physik*, Interscience Publishers, New York. Vol. I, 1931, Vol. II, 1937.
10. Guderley, G., Singularities at the sonic velocity, Wright Field Report, F-TR-1171-ND.
11. Guderley, G., On the transition from a transonic potential flow to a flow with shocks, Wright Field Report F-TR-2160-ND.
12. Guderley, G., Two-dimensional flow patterns with a free stream Mach number close to 1, AF Tech. Report No. 6343.
13. Busemann, A., The drag problem at high subsonic speeds, *J. Aeronaut. Sci.*, **16**, 337–44 (1949).
14. Taylor, G. I., Recent work on the flow of compressible fluids, *J. London Math. Soc.*, volume **5**, 1930.
15. Hamel, G., *Integral Gleichungen*, Springer Verlag, Berlin, 1937, pp. 121–122.

Vortex Systems in Wakes[1]

By L. ROSENHEAD
University of Liverpool, England

I. Object of the Review

The object of this paper is to assess the basic content of many theoretical and experimental papers which have been written about wakes for the range of Reynolds number up to about 2500. It is in this range that systematic arrangements of vortices have been observed in the wakes of many different types of obstacle. Many experimenters have recorded periodicities in the flow above this value, but have not been able to isolate eddies. At still higher values of R the flow becomes completely turbulent, and systematic periodicities have not been recorded. It should be noted, however, that even at relatively low values of R, when eddies are formed, the flow downstream is usually completely turbulent.

The reason for this review is that there has been a renewal of interest in the phenomena associated with relatively low subsonic speeds, both from the point of view of adding to fundamental knowledge and also from its potential value in a number of interesting applications. [See, for example, Steinman (1).]

Two theoretical investigations probably stand out in the minds of those who are interested in this field—that due to Kármán (2,3,4) and that due to Föppl (5). Föppl's paper investigates the stability of a vortex line pair behind a circular cylinder; those with which Kármán is associated investigate the stability of the unsymmetrical double row of vortices at a considerable distance from the body from which the vortices were shed. Föppl's paper, though dealing with a range of Reynolds number lower than that in which the double row appears, was written after the Kármán papers. It is unfortunate however that these investigations, especially the brilliant one of Kármán, have been interpreted in such a way as to suggest that they explain completely the phenomena which they purport to describe. Both were valuable in their time, but both are now open to criticism in the light of new ideas, and it would

[1] This paper was written under Naval Contract N5ori-76-Project 22. It was prepared as a result of discussions with Professor Garrett Birkhoff with whom the author had the pleasure and privilege of working in Harvard University during the summer of 1950.

probably be of value to investigate the whole field anew. This point will be referred to later in this note.

II. General

The papers of Kármán and Föppl have been singled out as being especially significant, but one probably their equal in fundamental importance is that written by Sir William Thomson (6) in 1880 on the vibrations of a columnar vortex. Another important paper is that by Hooker (7) which contains an idea through which it might be possible to reconcile many apparently discordant experimental results. A brief critical survey of the whole field has been given by Jeffreys (8) and a detailed account by Goldstein (9). The present review deals mainly with papers of a theoretical nature, but reference is also made to some experimental investigations where they appear to be relevant. It is believed that the most important papers have been included, but no doubt many others have been omitted. In particular no references have been made to the classical mathematical papers on hollow and annular rectilinear vortices, or to circular vortices; these can be found in Lamb (10).

From the point of view of the experimenter, interest seems to have centered mainly round the two-dimensional Kármán street of vortices, which have been observed in the approximate range of Reynolds number 40 to 2500. The beautiful results which can be obtained and the surprising regularity with which vortices are formed are no doubt responsible for this interest, but I believe that at the present stage further experimentation along these well-worn lines will add little to knowledge. What is badly needed is a quantitative theoretical treatment which will consolidate the facts already available. In addition, a systematic experimental investigation of wakes behind three-dimensional bodies of various shapes might be valuable; some interesting experimental results in this field already exist, but they are rather fragmentary.

III. The Vortex Line Pair

A qualitative description of the phenomena associated with wakes has been given by Goldstein (9). For very small Reynolds numbers the Navier-Stokes equations may be solved by the methods of Stokes or Oseen, as shown by Lamb (11), and by the method of Thom (12). The method of Stokes does not show a wake. That of Oseen shows the broadening out of the streamlines behind a sphere (13,14,15,16), a circular cylinder (17,18,19), and a flat plate (20,21). The numerical method of Thom yields estimates of the drag in very good agreement with experiment and shows simply and clearly the opening out of the streamlines

to form the beginnings of a wake at very small Reynolds numbers; there is an inflow along the central axis of the wake. As the Reynolds number is increased, the streamlines broaden out and form a closed region behind the obstacle; the inflow along the axis increases in magnitude. To compensate for this inflow there is an outflow within the closed region, in the neighborhood of the bounding streamlines. This circulatory motion constitutes a vortex line pair.

The mathematics of an idealized line pair was investigated by Föppl (5). He found that if the vortices are to remain stationary relative to the cylinder they must lie on a curve whose formula was stated; if in addition they were known to be stationary at points on the curve whose coordinates were known, the vortex strengths could be determined from another formula. This second formula indicated that the vortices moved downstream as their strengths increased. In addition it was shown that any position of relative equilibrium was stable for disturbances symmetrical with respect to the axis of the wake, and unstable for antisymmetrical ones (Goldstein, 22). Eventually, therefore, the vortices might be expected to move downstream in an unsymmetrical manner, as the Reynolds number is increased.

It is interesting to examine the basis of the calculation as a result of which the statements about stability were made. All rectilinear vortices were imagined to receive small translational disturbances without distortion of the vortices. This is a special kind of displacement and all that was, and can be, claimed for the investigation is that it describes the reaction of the system to disturbances of the type which were imposed. It is incorrect to interpret the results as indicating stability or instability with respect to disturbances of a very general nature. In fact it is still not known whether the vortex pair is stable with respect to the kind of disturbances which occur under real conditions—the random three-dimensional type of disturbance which has been disclosed by investigations of turbulence. Similar objections apply to almost all known investigations of the stability of vortex systems. Additional factors should be taken into account in any reexamination of accepted conclusions, but these will be referred to later.

In every experimental arrangement in which the characteristics of the vortex pair have been investigated, there appears to be some critical Reynolds number in the region of which the vortices start to move away. This critical value probably depends on the shape of the obstacle, the degree of turbulence in the fluid, and the proximity of the channel walls. Thom (12) has investigated this experimentally, but there is probably material here for analytical investigations which may throw light on turbulence at low Reynolds numbers.

IV. The Double Row of Vortices

The mechanism leading to the formation of vortices and to the motion subsequent to their discharge has been explained qualitatively in terms of boundary layers and vortex layers. The fluid in the wake is separated from that in the main flow by layers of vorticity or surfaces of discontinuity which originate on the body at the positions of separation of flow. At very small values of the Reynolds number the two-dimensional vortex layers, originally on opposite sides of the body, join together downstream. Vorticity diffuses from these layers into the main stream, but is also generated in the boundary layer and is added to the vortex pair. At small Reynolds numbers, when the vortex pair is stationary relative to the body, a state of equilibrium is set up between the rates of generation and diffusion of vorticity. An analytic investigation of this balance might repay study.

As the Reynolds number is increased, vorticity seems to be generated at a rate greater than that at which it diffuses from the existing vortex layers; they therefore become longer in the direction of flow so as to provide a larger area from which vorticity can diffuse. At the same time the strengths of the individual vortices of the vortex pair seem to increase.

The vortex layers are presumed to be unstable on the basis of experimental evidence, for they are seen to break away from the obstacle and to travel downstream. The instability of this system, under realistic assumptions, has still to be investigated, though evidence of a general nature is available from other sources. For example, Helmholtz (23) first remarked on the instability of surfaces of discontinuity, and Rosenhead (24) showed numerically how an initially small sinusoidal disturbance on a surface of discontinuity grows with time, destroys the initial configuration, and creates something similar to a row of isolated vortices. Kaden (25) and Westwater (26) have also shown numerically the rolling up of a surface of discontinuity under different conditions, but an analytic demonstration of this phenomenon is very desirable.

With the discharge of the first two vortices free vortex layers trail downstream. These have been examined experimentally in considerable detail by Fage and Johansen (27). In particular it was noted that the Helmholtz-Kirchhoff-Rayleigh free stream theory considerably underestimates the rate of discharge of vorticity. The variation in the form of the layers from a circular cylinder, as the Reynolds numbers increases from about $10^{3.5}$ to $10^{4.5}$, has been studied by Schiller and Linke (28) and also by Linke (29).

One or other of the trailing sheets of vorticity rolls up into a vortex and is discharged downstream. The asymmetrical system thus set up

produces a fall of pressure directed toward the other side of the body and, after some small interval of time, a quantity of vorticity is discharged from the other side in the form of a vortex. This sets up a reaction in the opposite direction and vortices are discharged alternately from the two sides. Up to the present this stage of the motion has not been investigated mathematically.

Downstream the vortices assume what appears to be a regular pattern; this is usually evident from some four to five diameters behind the body. A periodicity of some kind in the wake seems first to have been observed by Strouhal (30), though not its precise nature. The first description of the double row of vortices behind an obstacle is due to Mallock (31), and the phenomenon was investigated extensively by Bénard in a series of papers (32), and by other French investigators. The vortices appear to arrange themselves in a double row, in which each vortex is opposite the mid-point of the interval between two vortices in the opposite row. This suggests that in every experimental arrangement in which R is a constant the time interval between the discharge of vortices from alternate sides of the obstacle is approximately constant, and that the vortices ultimately travel downstream with some approximately constant velocity. In the lower end of the range of R in which they are observed, the system persists for a considerable distance, this distance growing smaller as R increases. There is, however, an observable periodicity in the wake up to about R equal to about 5×10^5 as indicated by Relf and Simmons (33). In addition Relf and Ower (34) have shown experimentally that where vortices are generated by wires in a wind the frequency of the note emitted is equal to the frequency with which the vortices are generated. Beyond the upper limit the flow appears to be completely turbulent.

Of especial interest is the paper of Kovaznay (35), who investigated the wake behind a circular cylinder by utilizing the "hot-wire technique"; he found that in his experimental arrangement the double row of vortices did not appear below a Reynolds number of 40. He also found that in the range of Reynolds number which he investigated the vortices were not shed directly from the cylinder, but appeared some distance downstream as a consequence of the instability of the laminar wake.

Up to the present no explanation has been given as to why the vortices arrange themselves in an apparently regular pattern so *quickly* after leaving the body. For theoretical purposes Kármán (2,3,4) considered the system far downstream—and assumed the double row to extend to infinity in both directions. The effects of channel walls and diffusion of vorticity were ignored. Kármán (2) investigated the effect of imagining only two of the vortices to be given small translational disturbances

and found that instability resulted unless the spacing ratio (distance between vortices to distance between rows) was 0.36. If, however, all the vortices were given a disturbance according to a stated general law instability resulted unless the spacing ratio was 0.281. Kármán and Rubach (4) did find ratios of 0.28 and 0.3 in special cases, but other investigators (Hooker, 7) have obtained spacing ratios which varied from about 0.25 to 0.53.

In the Kármán-Rubach investigation it was assumed that all the vortices were slightly disturbed. A mathematically imposed disturbance affecting all vortices from $-\infty$ to $+\infty$ must of necessity affect all fluid elements of the system, for the vortices are but lines of fluid elements endowed with rotation. In the investigation the whole system of fluid particles was imagined to be disturbed, the wavelength of the disturbance in the direction of the main stream being $2\pi a/\phi$, so that the vortex whose abscissa relative to the system was originally ra experienced a disturbance whose components are the real parts of the following expressions:

$$x_r = \alpha \exp [i2\pi(ra)/(2\pi a/\phi)] = \alpha \exp [ir\phi],$$
$$y_r = \beta \exp (ir\phi),$$

α and β being functions of the time. The disturbing velocity at any one vortex was then obtained by summing the values due to the other disturbed vortices and by neglecting small quantities higher than those of the first order. The investigation then resolved itself into a determination of whether α and β were circular or exponential functions of the time. Kármán restricted ϕ to the range $0 \leq \phi < 2\pi$ so that the wavelengths of the assumed disturbances were restricted to lie between a and infinity. The effect of disturbances of shorter wavelength, of diffusion of vorticity, of three-dimensional infinitesimal disturbances, and of finite disturbances still remain to be investigated. Kármán's conclusions regarding stability apply only to disturbances of the kind specified and not to the more general types of disturbance which probably occur in normal experimental arrangements.

The type of initial disturbance which is assumed seems to have an important correlation with the deduction regarding stability, for example Schmieden (36) investigated the effect of a disturbance in which initially every alternate vortex in one row is moved the same distance perpendicularly to the row, all the others remaining undisturbed. He also investigated the case in which alternate vortices in each row all have the same displacement, so that the whole street is divided into four rows. Rosenhead (37) investigated the stability of a staggered row of vortices, but Maue (38) and Urano and Munakata (39), assuming a more general form of the displacement, arrived at a somewhat different conclusion.

Other factors which may affect the stability are the proximity of the channel walls and the velocity profile of the stream in which the vortices may be considered to be embedded. The former problem was investigated by Rosenhead (40) and Tomotika (41), the latter by Levy and Hooker (42), but all assume simple two-dimensional infinitesimal displacements.

V. Three-Dimensional Disturbances

One can summarize all the stability investigations mentioned up to this point by saying that, although they are suggestive of what happens in experiment, they are by no means conclusive. There have, however, been two attempts to impose somewhat more realistic disturbances, and these are recorded in the publications of Schlayer (43) and Rosenhead (44). These papers, which really derive from that published by Sir William Thomson (6) in 1880, indicate that the double row is really unstable for a three-dimensional disturbance, the instability being caused by those components whose wavelength along the axis of the street is small. As a consequence of this instability the vortices become increasingly distorted, and the general pattern is destroyed. Unfortunately the value of the conclusions is somewhat vitiated by the fact that diffusion of vorticity was not taken into account. The suggestion of fundamental instability is well supported by the experimental investigation of Rosenhead and Schwabe (45) in which the paths of individual vortices were recorded and plotted.

There is no doubt, however, that for a certain portion of the wake the vortices do assume an approximately regular pattern, but this is probably a transient stage in an intrinsically unstable system. The spacing ratios have been determined by many investigators and have been reviewed by Goldstein (46). The results differ considerably among themselves, and confusion might have been very great had it not been for the important contribution made by Hooker (7), referred to in Section II. He pointed out that visual or photographic observations of vortices usually determine points of zero relative velocity, but what were really needed were determinations of centers of vorticity, after allowance has been made for diffusion of vorticity. Hooker determined the centers of vorticity in his own experiments and found that, for a considerable distance downstream, the spacing ratio was very nearly equal to the one predicted by the Kármán investigation. Eventually, however, the vortices departed from their positions of symmetry.

If the explanation put forward by Hooker does in fact explain the differences between the experimental results which have been obtained, the problem still remains: why does the highly idealized mathematical investigation of Kármán produce a result so close to the experimental one?

VI. Other Problems

Although much is known about the spacing ratio, very little is known about the connection between the width of the double row and the dimensions of the obstacle. The problem of the determination of this relation has still to be investigated.

Another important characteristic of the phenomena which I have attempted to describe is the frequency with which the vortices are shed. This has been investigated experimentally in a series of papers (47) and has been reviewed by Goldstein (48). A mathematical treatment of this phenomena is not yet available.

A formula for the average drag associated with the double row of vortices was determined by Kármán (3), and different methods of deriving it have been given by Synge (49), Pérès (50), and Villat (51). The corresponding formula for a channel has been obtained by Rosenhead (40), Tomotika (52), and Glauert (53). Basically the formulas are given in terms of four unknown quantities, the width of the double row, the spacing ratio, the vortex intensity, and the frequency of discharge of the vortices. Even if one accepts the Kármán value of the spacing ratio as approximately correct and a formula connecting vortex intensity with the other characteristics of the flow, two quantities must still be determined experimentally in each particular case before the drag can be evaluated. In addition very little is known about the periodic part of the drag.

VII. Three-Dimensional Wake

The three-dimensional wake behind bodies, in the range of Reynolds number in which there is a periodic discharge of vorticity, is in some ways similar to the two-dimensional one, but there are interesting differences (see 54,55,56). In the place of the vortex pair, a vortex ring appears. There is no mathematical evidence that its equilibrium position is unstable, but experiment suggests that this is the case. A cylindrical sheet of vorticity trails downstream and, on the basis of observation, is considered to be unstable. Attempts to generalize the Kármán two-dimensional street into three dimensions have been made by Levy and Forsdyke (57). They investigated the possibility of the wake consisting of vortex rings and found that if the rings were inclined to the axis of flow they would drift away from it, and if they were at right angles to the axis they would be unstable. Levy and Forsdyke (58) also investigated the possibility of the wake consisting of a helical vortex but showed that all helical vortices whose pitch was greater than a stated value were unstable. In particular, the rectilinear vortex was found to be unstable, thus confirming the earlier conclusion of Sir William Thomson (6).

Rosenhead (59) was of the opinion that these generalizations of the Kármán street did not occur in nature and that the only possibility was a sequence of irregularly shaped vortex loops discharged downstream with some plane of symmetry whose orientation in space was purely random, its orientation in any particular case being determined by the position of the point on the sheath of discontinuity at which a part of the vortex sheet breaks away due to instability. He suggested that evidence might be provided by photographing the wake simultaneously from two mutually perpendicular directions.

An experiment of this kind was carried out with a circular disk by Stanton and Marshall (56). It was clearly proved that, although photographs from one direction might appear to show the projection of an apparently helical discharge of vorticity, photographs from two mutually perpendicular directions showed the discharge of distorted loops of vorticity arranged with some measure of symmetry. The orientation of the planes of symmetry of the discharge appeared to be random. One of the photographs is reproduced by Goldstein (60).

At higher Reynolds numbers the vortex sheet and vortex loops diffuse very rapidly; a sheath of discontinuity along which corrugations travel in an irregular manner can usually be seen behind the body. At still greater Reynolds numbers, the flow becomes completely turbulent and it is no longer possible to speak of a systematic arrangement of vortices in the wake.

VIII. Conclusion

It is clear from what has been written above that a great deal remains to be investigated before a mathematically satisfactory description can be given of the phenomena of vortex systems in wakes. Most of what has been done is interesting, suggestive and qualitatively correct, but if greater precision is needed, it is necessary to reinvestigate in fine detail much of what has already been done.

References

1. Steinman, D. B., Proc. Third Hydraulics Conference, Iowa, *Univ. Iowa Studies Eng. Bull.*, **31**, 136–164 (1946).
2. Kármán, Th. v., Göttinger Nachrichten, 509–517, 1911.
3. Kármán, Th. v., Göttinger Nachrichten, 547–556, 1912. (See also Sir H. Lamb, Hydrodynamics, pp. 225–229. Cambridge University Press, 1932.)
4. Kármán, Th. v., and Rubach, H. L., *Physik.* A., **13**, 49–59 (1912).
5. Föppl, L., *Sitzber. bayer. Akad. Wiss. München Mathphys. Klasse*, 1–17 (1913).
6. Thomson, Sir W., *Phil. Mag.* (5), **10**, 155–168 (1880); (or Lord Kelvin's collected papers, **4**, 152–165).
7. Hooker, S. G., *Proc. Roy. Soc.* (*London*), A**154**, 67–89 (1936).

8. Jeffreys, H., *Proc. Roy. Soc.* (*London*), **A128**, 376–393 (1930).
9. Goldstein, S., Modern Developments in Fluid Dynamics, Vol. II, Chapter XIII. Oxford University Press, 1938.
10. Lamb, Sir H., Hydrodynamics, Chapter VII. Cambridge University Press, 1932.
11. Lamb, Sir H., Hydrodynamics, pp. 594–616. Cambridge University Press, 1932.
12. Thom, A., *Proc. Roy. Soc.* (*London*), **A141**, 651–669 (1933).
13. Oseen, C. W., *Arkiv Mat. Astron. Fysik,* **6**, (29), (1910).
14. Oseen, C. W., *Arkiv Mat. Astron. Fysik,* **9**, (16), (1913).
15. Oseen, C. W., Vorträge aus dem Gebiete der Hydro- und Aerodynamik, pp. 127–129, Innsbruck, 1922; Berlin, 1924.
16. Goldstein, S., *Proc. Roy. Soc.* (*London*), **A123**, 225–235 (1929).
17. Lamb, Sir H., *Phil. Mag.* (6), **21**, 112–121 (1911).
18. Bairstow, L., Cave, B. M., and Lang, E. D., *Phil. Trans.*, **A223**, 383–432 (1923).
19. Faxén, H., Nova Acta Regiae Societatis Scientiarum Upsaliensis, Volumen extraordinem, pp. 3–55, 1927.
20. Burgers, J. M., *Proc. Koninkl. Akad. Wetenschap. Amsterdam,* **33**, 1–9 (1930).
21. Piercy, N. A. V., and Winny, H. F., *Proc. Roy. Soc.* (*London*), **A140**, 543–561 (1933).
22. Goldstein, S., Modern Developments in Fluid Dynamics, Vol. II, pp. 552–553. Oxford University Press, 1938.
23. Helmholtz, H., *Berlin Monatsber.*, 1868. (See also Sir H. Lamb, Hydrodynamics, p. 374. Cambridge University Press, 1932.)
24. Rosenhead, L., *Proc. Roy. Soc.* (*London*), **A134**, 170–192 (1931).
25. Kaden, H., *Ing.-Archiv,* **2**, 140–168 (1931).
26. Westwater, F. L., *Aeronaut. Research Comm., Rept. and Mem.* 1692, 1936.
27. Fage, A., and Johansen, F. C., *Phil. Mag.* (7) **5**, 417–441 (1928).
28. Schiller, L., and Linke, W., *Z. Flugtech. Motorluftschiffahrt,* **24**, 193–198 (1933).
29. Linke, W., *Physik. Z.*, **32**, 900–914 (1931).
30. Strouhal, V., *Ann. Physik Chem.* (*Wiedemann's Ann.*), **5**, 216–251 (1878).
31. Mallock, A., *Proc. Roy. Soc.* (*London*), **A79**, 262–273 (1907).
32. Bénard, H., *Compt. rend.*, **147**, 839–842, 970–972 (1908); **156**, 1003–1005, 1225–1228 (1913); **182**, 1375–1377, 1523–1525 (1926); **183**, 20–22, 184–186, 379 (1926); **187**, 1028–1030, 1123–1125, 1300 (1928).
33. Relf, E. F., and Simmons, L. F. G., see S. Goldstein, Modern Developments in Fluid Dynamics, Fig. 149, p. 419. Oxford University Press, 1938.
34. Relf, E. F., and Ower, E., *Aeronaut. Research Comm., Rept. and Mem.* 825, 1923.
35. Kovaznay, L., *Proc. Roy. Soc.* (*London*), **A198**, 174–190 (1949).
36. Schmieden, C., *Ing.-Archiv,* **7**, 215–221, 337–341 (1936).
37. Rosenhead, L., *Proc. Camb. Phil. Soc.,* **25**, 132–138 (1929).
38. Maue, A. W., *Z. angew. Math. Mech.*, **20**, 129–137 (1940).
39. Urano, K., and Munakata, K., *Proc. Phys.-Math. Soc. Japan* (3), **24**, 790–799 (1942).
40. Rosenhead, L., *Phil. Trans. Roy. Soc.* (*London*), **A228**, 275–329 (1929).
41. Tomotika, S., *Rept. Aeronaut. Research Inst. Tokyo Imp. Univ.*, **4**, 213–239 (1929).
42. Levy, H., and Hooker, S. G., *Phil. Mag.* (7), **9**, 489–502 (1930).
43. Schlayer, K., *Z. angew. Math. Mech.* **8**, 352–372 (1928).
44. Rosenhead, L., *Proc. Roy. Soc.* (*London*), **A127**, 590–612 (1930).
45. Rosenhead, L., and Schwabe, M., *Proc. Roy. Soc.* (*London*), **A129**, 115–135 (1930).

46. Goldstein, S., Modern Developments in Fluid Dynamics, Vol. II, pp. 568–570. Oxford University Press, 1938.
47. Strouhal, V., *Ann. Physik. Chem.* (*Weidemann's Ann.*), **5**, 216–251 (1878).
Rayleigh, Lord, *Phil. Mag.* (6), **29**, 433–444 (1915); (or *Scientific Papers*, **6**, 315–325).
Relf, E. F., and Ower, E., *Aeronaut. Research Comm., Rept. and Mem.*, 825, 1923.
Richardson, E. G., *Proc. Phys. Soc.* (*London*), **36**, 153–165 (1923).
Tylep, E., *Phil. Mag.* (7), **11**, 849–890 (1931).
Fage, A., and Johansen, F. C., *Phil. Mag.* (7), 417–441 (1928).
Blenk, H., Fuchs, R., Liebers, F., *Luftfahrt-Forsch.*, **12**, 38–41 (1935).
48. Goldstein, S., Modern Developments in Fluid Dynamics, Vol. II, pp. 570–571. Oxford University Press, 1938.
49. Synge, J. L., *Proc. Roy. Irish Acad.*, **37**, 95–109 (1927).
50. Pérès, J., *Compt. rend.*, **189**, 1246–1248 (1929).
51. Villat, H., Mécanique des Fluides, pp. 131–140. Paris, 1930; Leçons sur les tourbillons, pp. 80–109. Paris, 1930.
52. Tomotika, S., *Rept. Aeronaut. Research Inst. Tokyo Imp. Univ.*, **5**, 101–140 (1930).
53. Glauert, H., *Proc. Roy. Soc.* (*London*), **A120**, 34–46 (1928).
54. Eden, C. G., *Aeronaut. Research Comm., Rept. and Mem.*, 58, 1912.
55. Simmons, L. F. G., and Dewey, N. S., *Aeronaut. Research Comm., Rept. and Mem.*, 1334, 1931.
56. Stanton, Sir T. E., and Marshall, D., *Aeronaut. Research Comm., Rept. and Mem.*, 1358, 1932. (See also *Proc. Roy. Soc.* (*London*), **A130**, 295–301 (1930), for a version of the paper without the Appendix.)
57. Levy, H., and Forsdyke, A. G., *Proc. Roy. Soc.* (*London*), **A114**, 594–604 (1927).
58. Levy, H., and Forsdyke, A. G., *Proc. Roy. Soc.* (*London*), **A120**, 670–690 (1928).
59. Rosenhead, L., See Appendix to Stanton, Sir T. E., and Marshall, D., *Aeronaut. Research Comm., Rept. and Mem.*, 1358, 1932.
60. Goldstein, S., Modern Developments in Fluid Dynamics, Vol. II, facing p. 579. Oxford University Press, 1938.

Some Recent Results in the Theory of an Ideal Plastic Body

By HILDA GEIRINGER

Wheaton College Norton, Mass.

This article deals with some more recent aspects of the mathematical theory of a perfectly plastic body. The choice of the material included is very subjective. The main problem considered is contained in Part II, namely an introduction to the theory of the "general and complete" plane problem. By this we mean a plane problem with a general yield condition and correspondingly general relation between stresses and strain rates. Such an extension which only in the last years has found some more systematic attention is suggested by mechanical as well as mathematical considerations. It is well known that in "plane *strain*" both St. Venant's and von Mises's three-dimensional yield conditions lead to the same simple two-dimensional condition (a) $(\sigma_1 - \sigma_2)^2$ = constant, with σ_i principal stresses. On the other hand, a problem of "plane *stress*" leads for these two spatial conditions to plane yield conditions different from each other and from (a). The new problems are more difficult; they are of a type which is no longer "orthogonal" (in a sense which we shall discuss), it is no longer everywhere hyperbolic, but partly also elliptic or parabolic, and since the whole problem is nonlinear, the determination of these regions of different behavior is only possible together with the finding of the solution. It seems natural to try to find mechanically adequate plane yield conditions which might offer a simpler mathematical situation. Our approach is first of all to study general yield conditions or, more precisely, to study the plane problem under assumption of a general yield condition, which, however, must be derived from a physically correct three-dimensional setup. Let us add that another line of research leads likewise to the study of arbitrary yield conditions, namely the plane problem (plane strain), not of ductile metals but of more general materials as considered in soil mechanics.

The indicated approach is followed up in some detail in Part II; all through we consider the complete problem, stresses, *and* deformations. The nonlinear stress equations may be "linearized" in several ways; according to the choice of stress variables, different linear equations in the stress plane are obtained and discussed (Sections II,1,a,d,e and II,2,c). A few rather obvious partial solutions are indicated where one can go much farther; one most important group of partial solutions, the so-called simple waves, are however studied in some detail in II,3; stress and velocity distributions are explicitly determined. In II,2 we give the theory of the characteristics of the complete problem, followed by the discussion of the approximate solution of some initial value problems in case of real characteristics.

In Part III we present a few selected boundary value problems. They are not based on the theory exposed in Part II but on the assumption of plane strain [condition (a)]. Our aim in this part was to illustrate

some specific features of boundary value problems of plasticity theory. In such problems the main difficulty often consists not so much in the integration of a well-defined problem as in the careful definition and setting up of the physical problem (that is, of the boundary conditions in the widest sense). The actual solutions may then in many cases be composed of very simple particular solutions. In the difficult task of setting up the specific problem one would like to complement the physical intuition by appropriate mathematical information, but the latter is very often not available. Unlike the state of affairs in other parts of mechanics (we think of important domains in the theory of elasticity or fluid mechanics) we so-far cannot indicate, in a precise way, general and at the same time typical situations for which we know combinations of boundary data that assure existence and uniqueness of the solution. One specific difficulty of our problem is, of course, connected with the need to take into consideration the boundaries, in general unknown, between the plastic and the elastic (or rigid) material.

To illustrate these points it seemed appropriate to limit ourselves to problems of plane strain, which are mathematically so much simpler than those necessitating the theory of Part II. We may thus the better recognize some of the difficulties mentioned which we wish to emphasize rather than to understate. This last part, just as the others, deals with recent work, mainly by E. H. Lee and W. Prager. All through, our aim was to give not so much a review of some more or less related recent results, but rather a coherent presentation of certain aspects of a mathematical theory. This necessitated various additions and remarks not included in the author's previous papers.[1]

I. Definition and Derivation of a General Plane Problem

1. *Three-Dimensional Problem with Quadratic Yield Condition*

In this introductory chapter our main aim is to formulate a general plane problem for the perfectly plastic isotropic body. In order to be sure that a plane problem is meaningful, one must be able to derive it from a three-dimensional problem. We start with the three-dimensional theory as formulated in 1913, by von Mises (12a), and consider the corresponding plane problem. Then we shall derive a more general plane problem from a more general three-dimensional setup. We do not attempt to sketch the history of the first complete formulation of the three-dimensional problem, for this (which would include an account of

[1] The manuscript of this article was concluded in the fall 1951 and reflects the author's points of view and knowledge of literature of that time.

the ideas of St. Venant (18), Lévy (10), Coulomb, Guest, Tresca (23), Huber, and others) has already had several presentations.

Denote the stress tensor by Σ, the hydrostatic pressure by p, the tensor of strain rate by $\dot{E}$, an unknown function of the space coordinates by k. These are eleven unknown functions of x,y,z: the six components of Σ, $\sigma_{xx} = \sigma_x$, $\sigma_{yy} = \sigma_y$, $\sigma_{zz} = \sigma_z$ (the normal stresses), and $\tau_{xy} = \tau_z$, $\tau_{yz} = \tau_x$, $\tau_{xz} = \tau_y$ (the shearing stresses); the three components v_x,v_y,v_z of the velocity vector $\bar{v}$; the pressure, p; and the function of proportionality, k. From $\bar{v}$ one derives the tensor of strain rate, $\dot{E}$, with components, $\dot{\epsilon}_x = \frac{\partial v_x}{\partial x}, \frac{1}{2}\dot{\gamma}_z = \frac{1}{2}\left(\frac{\partial v_x}{\partial y} + \frac{\partial v_y}{\partial x}\right)$, etc. The eleven corresponding equations of the *perfectly plastic body*, are then the following. First the three equations of motion, (ρ is the density, $\bar{X}$ the vector of external forces):

$$\rho \frac{d\bar{v}}{dt} = \bar{X} + \operatorname{div} \Sigma.$$

If we merely consider a problem of equilibrium, in the absence of acceleration and of external forces, the above reduces to the vector equation

$$\operatorname{div} \Sigma = 0 \tag{1.I}$$

with the three-component equations

$$\frac{\partial \sigma_x}{\partial x} + \frac{\partial \tau_z}{\partial y} + \frac{\partial \tau_y}{\partial z} = 0, \text{ etc.} \tag{1.I$'$}$$

Next there is the yield or plasticity condition, which limits the admissible stresses to a five-dimensional manifold. In the von Mises theory it has the form

$$(\sigma_x - \sigma_y)^2 + (\sigma_y - \sigma_z)^2 + (\sigma_z - \sigma_x)^2 + 6(\tau_x^2 + \tau_y^2 + \tau_z^2) = 2\sigma_0^2 = 8K^2$$

or

$$\begin{aligned} \sigma_x^2 + \sigma_y^2 + \sigma_z^2 - \sigma_x\sigma_y - \sigma_y\sigma_z - \sigma_z\sigma_x \\ + 3(\tau_x^2 + \tau_y^2 + \tau_z^2) - \sigma_0^2 = 0.^2 \quad (Y_1) \end{aligned} \tag{1.II}$$

Here σ_0 is the yield stress in simple tension. We call (1.II) the *quadratic* yield condition. It is seen that the left side of (1.II) is merely a function of the three *principal stresses*, σ_1, σ_2, σ_3, namely,

$$(\sigma_1 - \sigma_2)^2 + (\sigma_2 - \sigma_3)^2 + (\sigma_3 - \sigma_1)^2 - 8K^2 = 0 \tag{1.II$'$}$$

or

$$\sigma_1^2 + \sigma_2^2 + \sigma_3^2 - \sigma_1\sigma_2 - \sigma_1\sigma_3 - \sigma_2\sigma_3 - 4K^2 = 0$$

or, with $2\tau_1 = |\sigma_3 - \sigma_2|$, etc.,

$$\tau_1^2 + \tau_2^2 + \tau_3^2 - 2K^2 = 0. \tag{1.II$''$}$$

[2] If the function to the left is negative, this signifies an elastic range; whereas a positive value cannot be realized in perfectly plastic material.

(The τ_i are called the principal shearing stresses.) Note that if as an abbreviation the left side of the first formula (1.II) is denoted by $q(\sigma_x,\sigma_y,\sigma_z)$ then the so-called octahedral stress, τ_{oct} equals

$$\tau_{oct} = \tfrac{1}{3}\sqrt{q}$$

and (1.II) becomes

$$3\tau_{oct} = \sigma_0\sqrt{2}. \tag{1.II'''}$$

The relation taking the place of Hooke's law, which links the variables of stress with those of strain, is as follows: It is assumed that the tensor, $\dot{E}$, of *strain rate* and the tensor $\Sigma' = \Sigma + pJ$ of *stress deviation* (J denotes the unit matrix) are similar tensors:

$$\Sigma + pJ = k\dot{E}. \tag{1.III} \qquad (V_1)$$

In contrast to viscous flow theory, $k(x,y,z)$ is here a nonnegative unknown function of proportionality. The six components of (1.III) are:

$$\begin{gathered}\sigma_x' = \sigma_x + p = k\dot{\epsilon}_x, \quad \sigma_y' = \sigma_y + p = k\dot{\epsilon}_y, \quad \sigma_z' = \sigma_z + p = k\dot{\epsilon}_z \\ \tau_x = \tfrac{1}{2}k\dot{\gamma}_x, \quad \tau_y = \tfrac{1}{2}k\dot{\gamma}_y, \quad \tau_z = \tfrac{1}{2}k\dot{\gamma}_z.\end{gathered} \tag{1.III'} \qquad (V_2)$$

Finally the "continuity equation" holds which also expresses the assumed incompressibility of the medium:

$$\operatorname{div} \bar{v} = 0 \quad \text{or} \quad \dot{\epsilon}_x + \dot{\epsilon}_y + \dot{\epsilon}_z = 0. \tag{1.IV}$$

This equation is consistent with (1.III) since $\sigma_x' + \sigma_y' + \sigma_z' = 0$. These are $3 + 1 + 6 + 1 = 11$ equations for the above-mentioned eleven unknowns, Σ, $\bar{v}$, k, and the hydrostatic pressure p.

2. *Plane Problem. Quadratic Yield Condition*

We now wish to derive a plane problem from the above three-dimensional one. To do this, we adapt to our problem the concepts of "plane strain" and of "plane stress," well known in elasticity theory. That means we consider two particular solutions of our three-dimensional problem. In *both cases* it is assumed that one of the three principal directions of Σ (consequently also of $\dot{E}$) is parallel to a fixed direction which we take as z-axis. From (1.III) it follows that

$$\dot{\gamma}_x = \dot{\gamma}_y = 0, \quad \tau_x = \tau_y = 0.$$

(a) In *plane strain* it is further assumed that (1) all components of strain and of stress are independent of z and (2) the strain component, $\dot{\epsilon}_z = \dot{\epsilon}_3$ vanishes everywhere. From (1.III) and (1.IV), in connection with the above remarks, the well-known conclusions follow:

$$\begin{gathered}\dot{\epsilon}_x + \dot{\epsilon}_y = 0, \quad \sigma_x + \sigma_y + 2p = 0, \\ \tau_x = \tau_y = 0, \sigma_z + p = 0 \quad \text{or} \quad p = -\tfrac{1}{2}(\sigma_x + \sigma_y), \sigma_z = \tfrac{1}{2}(\sigma_x + \sigma_y),\end{gathered}$$

and (1.II) takes the form:

$$(\sigma_x - \sigma_y)^2 + 4\tau_z^2 = \tfrac{16}{3}K^2 = \tfrac{4}{3}\sigma_0^2.$$

The six Eqs. (1.III) reduce to three of which, on account of $\dot{\epsilon}_x + \dot{\epsilon}_y = 0$, only two are independent. Eliminating k between the Eqs. (1.III) we obtain the well-known *complete* system of plane strain (writing $\tau_z = \tau$, $\gamma_z = \gamma$)

$$\text{(1.1)} \qquad \frac{\partial \sigma_x}{\partial x} + \frac{\partial \tau}{\partial y} = 0, \quad \frac{\partial \tau}{\partial x} + \frac{\partial \sigma_y}{\partial y} = 0,$$

$$\text{(1.2)} \qquad (\sigma_x - \sigma_y)^2 + 4\tau^2 = \tfrac{4}{3}\sigma_0^2 \qquad (\text{y}_1)$$

$$\text{(1.3)} \qquad \dot{\epsilon}_x + \dot{\epsilon}_y = 0, \quad \frac{\dot{\epsilon}_y - \dot{\epsilon}_x}{\gamma} = \frac{\sigma_y - \sigma_x}{2\tau} \qquad (\text{v}_1)$$

for the unknowns σ_x, σ_y, τ, v_x, v_y. The Eqs. (1.1) and (1.2) form a system of three equations for the three unknowns σ_x, σ_y, τ, a well-known and important fact.

It is known that in plane strain St. Venant's three-dimensional yield condition[3] leads to the same condition (1.2), with the only difference that now the value $4k^2 = \sigma_0^2$ appears in place of $16k^2/3 = 4\sigma_0^2/3$.

(b) The formulation of the *complete* problem of *plane stress*, even under the particular yield condition (1.II), is less well known. Here, as before, everywhere

$$\tau_x = \tau_y = 0 \quad \text{or} \quad \sigma_z = \sigma_3,$$

and moreover

$$\sigma_z = \sigma_3 = 0.$$

The remaining components σ_x, σ_y, $\tau_z = \tau$ are independent of z. We get from (1.II)

$$\text{(1.4)} \qquad \sigma_1^2 + \sigma_2^2 - \sigma_1\sigma_2 - 4K^2 = 0$$

or

$$\text{(1.4')} \qquad \sigma_x^2 + \sigma_y^2 - \sigma_x\sigma_y + 3\tau^2 - 4K^2 = 0. \qquad (\text{y}_2)$$

The three Eqs. (1.I) reduce again to the two Eqs. (1.1). From (1.III) and (1.IV) follow

$$\sigma_x + \sigma_y + 3p = 0, \quad p = -\tfrac{1}{3}(\sigma_x + \sigma_y).$$

Substituting this in the first, second, and last Eq. (1.III′) one finds

$$\text{(1.5)} \qquad 2\sigma_x - \sigma_y = 3k\dot{\epsilon}_x, \quad 2\sigma_y - \sigma_x = 3k\dot{\epsilon}_y, \quad 2\tau = K\dot{\gamma} \qquad (\text{v}_2)$$

[3] St. Venant's condition states that during plastic flow the greatest of the three principal shearing stresses has a constant value equal to the yield stress in simple shear.

or, eliminating k,

$$\frac{\dot\epsilon_x - \dot\epsilon_y}{\gamma} = \frac{\sigma_x - \sigma_y}{2\tau}, \quad \frac{\dot\epsilon_x + \dot\epsilon_y}{\gamma} = \frac{\sigma_x + \sigma_y}{6k}. \tag{1.5'} \qquad (v_3)$$

Equations (1.1) and (1.4) form a system of three equations for σ_x, σ_y, τ. Corresponding to each solution of this system there exist certain solutions, v_x, v_y, $k \geqq 0$ of the three Eqs. (1.5). Such a system σ_x, σ_y, τ, v_x, v_y, k forms a solution of the problem of a thin plate of uniform thickness under the action of forces applied to its edge, parallel to the middle plane (the x,y-plane) of the plate, and distributed uniformly over its thickness. There remain three Eqs. (1.III), namely

$$\frac{\partial v_x}{\partial z} + \frac{\partial v_z}{\partial x} = 0, \quad \frac{\partial v_y}{\partial z} + \frac{\partial v_z}{\partial y} = 0, \quad \frac{\partial v_z}{\partial z} = -\frac{\sigma_x + \sigma_y}{3k}.$$

They serve to determine v_z, $\dfrac{\partial v_x}{\partial z}$, $\dfrac{\partial v_y}{\partial z}$.

Let us add two remarks: The set (1.III) of strain stress relations and the yield condition (1.II) are not independent of each other; in an analogous way (1.5) and (1.5′) are related to (1.4). We shall return to this point.

The fact that the two most often used three-dimensional yield conditions of von Mises and of St. Venant reduce in plane strain to the same two-dimensional condition was one of the reasons for the intensive consideration of the problem (1.1), (1.2), (1.3); other reasons were its comparatively simple mathematical nature, and above all, the approximate realization of "plane strain" in important mechanical problems. However, as we just have seen, in "plane stress" von Mises' condition leads no longer to (1.2) and, as is easily seen, no longer to the same plane condition as obtained from St. Venant's three-dimensional assumption. For some reasons still other yield conditions have been proposed. It seems then natural to go one step further and to consider a plane problem where Eqs. (1.1) are supplemented by some arbitrary appropriate yield condition $f(\sigma_x,\sigma_y,\tau) = 0$; as long as this function is not specified the relation of this plane problem (consisting of Eqs. (1.1) and some equation $f = 0$) to a three-dimensional problem need not be considered. Such a problem of three equations and three unknowns is well defined. [It has been studied by Sokolovsky (20a,b), von Mises (12d), Geiringer (2d,e), Neuber (14), Sauer (19), Hodge (6a,b), Hill (5a); we shall report on these contributions in Part II.] If, however, we want to set up a *complete* plane problem we have to consider in addition a strain-stress relation. Our previous strain-stress relations (1.3) as well as (1.5) were derived from the relation (1.III), related to the particular yield condition (1.II).

Obviously, in order to arrive at a complete plane problem with a more general yield condition, we have to consider a more general three-dimensional problem.

3. *General Three-Dimensional Problem*

The relations (1.I) of Section 1 remain unchanged; instead of the quadratic condition (1.II) we now assume a general condition

$$g(\sigma_x,\sigma_y,\sigma_z,\tau_x,\tau_y,\tau_z) = 0.$$

This function must be subjected to several restrictions which will influence the corresponding plane yield condition. First, if we assume an *isotropic* medium we must restrict ourselves to a function g which is independent of the coordinate system; g depends only on the three invariants J_1, J_2, J_3 of the stress tensor, or, otherwise stated, only on the principal stresses, σ_1, σ_2, σ_3, and in a symmetric way. Second we assume that g remains unchanged if Σ is replaced by $\Sigma' = \Sigma + pJ$; hence with $\sigma_x' = \sigma_x + p$, etc.

$$g(\sigma_x,\sigma_y,\sigma_z,\tau_x,\tau_y,\tau_z) = g(\sigma_x',\sigma_y',\sigma_z',\tau_x,\tau_y,\tau_z) = G(\sigma_1,\sigma_2,\sigma_3) = G(\sigma_1',\sigma_2',\sigma_3')$$

with G being a symmetric function of the σ_i. From the last of the above equations it follows that G depends actually only on the differences $(\sigma_1 - \sigma_2)$, etc., or (which is the same) only on

$$\tau_1 = \tfrac{1}{2}(\sigma_2 - \sigma_3), \quad \tau_2 = \tfrac{1}{2}(\sigma_3 - \sigma_1), \quad \tau_3 = \tfrac{1}{2}(\sigma_1 - \sigma_2).$$

Hence, with symmetric G or K,

$$\text{(1.V)} \qquad g(\sigma_x,\sigma_y, \cdots \tau_z) = G(\sigma_1,\sigma_2,\sigma_3) = K(\tau_1,\tau_2,\tau_3) = 0 \qquad (\mathrm{Y}_2)$$

will be the form of a general yield condition for an isotropic perfectly plastic body. It is a consequence of this form that

$$\text{(1.VI)} \qquad \frac{\partial G}{\partial \sigma_1} + \frac{\partial G}{\partial \sigma_2} + \frac{\partial G}{\partial \sigma_3} = \frac{\partial g}{\partial \sigma_x} + \frac{\partial g}{\partial \sigma_y} + \frac{\partial g}{\partial \sigma_z} = 0$$

must hold.

From a function $g(\sigma_x,\sigma_y, \cdots \tau_z)$ the "derivated tensor," Grad g, may be deduced:

$$\text{(1.VII)} \quad \operatorname{Grad} g = \begin{pmatrix} \dfrac{\partial g}{\partial \sigma_x}, & \dfrac{1}{2}\dfrac{\partial g}{\partial \tau_z}, & \dfrac{1}{2}\dfrac{\partial g}{\partial \tau_y} \\ \cdot & \dfrac{\partial g}{\partial \sigma_y} & \dfrac{1}{2}\dfrac{\partial g}{\partial \tau_x} \\ \cdot & \cdot & \dfrac{\partial g}{\partial \sigma_z} \end{pmatrix} = \begin{pmatrix} \dfrac{\partial g}{\partial \sigma_x'}, & \dfrac{1}{2}\dfrac{\partial g}{\partial \tau_z}, & \dfrac{1}{2}\dfrac{\partial g}{\partial \tau_y} \\ \cdot & \dfrac{\partial g}{\partial \sigma_y'} & \dfrac{1}{2}\dfrac{\partial g}{\partial \tau_x} \\ \cdot & \cdot & \dfrac{\partial g}{\partial \sigma_z'} \end{pmatrix}.$$

In other words, g is the "potential" of Grad g. As an example, consider the derivated tensor of the left side of the quadratic condition (1.II); we find

$$\frac{\partial g}{\partial \sigma_x} = 2\sigma_x - \sigma_y - \sigma_z, \quad \frac{1}{2}\frac{\partial g}{\partial \tau_x} = 3\tau_x, \text{ etc.}$$

Comparing these with the components of $\Sigma' = \Sigma + pJ$, appearing in (1.III), with $p = -(\sigma_x + \sigma_y + \sigma_z)/3$, we see that $\sigma_x' = \frac{1}{3}(2\sigma_x - \sigma_y - \sigma_z)$, etc. and that

$$\text{Grad } g = 3\Sigma', \tag{1.VIII}$$

if g is given by (1.II) and p as above. In case of the yield condition (1.II), one may therefore replace (1.III) by $k\dot{E} = \text{Grad } g$.

This last form suggests itself likewise for use in case of a more general yield condition. von Mises (12c) in a study of the plasticity of crystals has proposed a form of strain-stress relation where the yield function serves as "plastic potential" in an equation of the form above. In this setup the link between yield function and strain-stress relation is then conserved. Thus we put in case of condition (1.V):

(1.IX) $$k\dot{E} = \text{Grad } g \qquad (V_3)$$

or, more explicitly

(1.IX′) $$\begin{aligned} k\dot{\epsilon}_x &= \frac{\partial g}{\partial \sigma_x}, & k\dot{\epsilon}_y &= \frac{\partial g}{\partial \sigma_y}, & k\dot{\epsilon}_z &= \frac{\partial g}{\partial \sigma_z} \\ k\dot{\gamma}_x &= \frac{\partial g}{\partial \tau_x}, & k\dot{\gamma}_y &= \frac{\partial g}{\partial \tau_y}, & k\dot{\gamma}_z &= \frac{\partial g}{\partial \tau_z}. \end{aligned} \qquad (V_4)$$

The complete system consists then of (1.I), (1.IV), (1.V), [where g has the property (1.VI)], and (1.IX). In this system the p is already eliminated. There are ten unknowns, the six components of Σ, the three of $\bar{v}$, and k. There are three Eqs. (1.I), one Eq. (1.IV), one Eq. (1.V), and five Eqs. (1.IX). Indeed, of the six Eqs. (1.IX′) only five are independent, since the sum of the first three, on account of (1.VI), leads back to (1.IV).

A further step would be to consider a plastic potential *not identical* with the yield function. The complete system consists then of the equations (1.I), (1.IV), (1.V) *and* of an equation

(1.X) $$k\dot{E} = \text{Grad } h \qquad (V_5)$$

with components

(1.X′) $$\begin{aligned} k\dot{\epsilon}_x &= \frac{\partial h}{\partial \sigma_x}, & k\dot{\epsilon}_y &= \frac{\partial h}{\partial \sigma_y}, & k\dot{\epsilon}_z &= \frac{\partial h}{\partial \sigma_z}, \\ k\dot{\gamma}_x &= \frac{\partial h}{\partial \tau_x}, & k\dot{\gamma}_y &= \frac{\partial h}{\partial \tau_y}, & k\dot{\gamma}_z &= \frac{\partial h}{\partial \tau_z}. \end{aligned} \qquad (V_6)$$

Here h is a function of the stresses such that

$$h(\sigma_x,\sigma_y, \cdots \tau_z) = H(\sigma_1,\sigma_2,\sigma_3) \tag{1.XI}$$

and

$$\frac{\partial h}{\partial \sigma_x} + \frac{\partial h}{\partial \sigma_y} + \frac{\partial h}{\partial \sigma_z} = \frac{\partial H}{\partial \sigma_1} + \frac{\partial H}{\partial \sigma_2} + \frac{\partial H}{\partial \sigma_3} = 0, \tag{1.XI$'$}$$

where H is a symmetric function of the principal stresses. The continuity equation is consistent with (1.X) because of (1.XI′). On account of (1.IV) the system (1.X) contains only five independent equations which together with (1.I), (1.IV), (1.V) form the ten equations of this problem. Often, however, we shall stick to the assumption (distinguished by an extremum property) which identifies yield function and plastic potential.

4. *Plane Problem under General Yield Condition*

We wish to define particular solutions of problem (1.I), (1.IV), (1.V), (1.IX) which correspond to "plane strain" and "plane stress." By deriving our plane problem from a three-dimensional one we make sure that we introduce desirable generality along with necessary restrictions.

Consider first *plane strain*, where, as explained $\dot\epsilon_3 = \dot\epsilon_z = \dfrac{\partial v_z}{\partial z} = 0$, $\dot\gamma_x = \dot\gamma_y = 0$ and all components of strain and of stress independent of z. The following theorem will facilitate our derivation:

In case of an isotropic medium, i.e., in case of a plastic potential, h, which as in (1.V) and (1.XI) depends only on the principal stresses, the tensor Grad h is coaxial with the stress tensor. This is clear for physical reasons. To prove it by a computation we consider $h(\sigma_x,\sigma_y, \cdots \tau_z)$ as a function of the three invariants

$$J_1 = \sigma_x + \sigma_y + \sigma_z, \quad J_2 = (\sigma_x\sigma_y - \tau_z^2) + (\sigma_y\sigma_z - \tau_x^2) + (\sigma_z\sigma_x - \tau_y^2);$$
$$J_3 = \sigma_x\sigma_y\sigma_z + 2\tau_x\tau_y\tau_z - \tau_x^2\sigma_x - \tau_y^2\sigma_y - \tau_z^2\sigma_z.$$

Then from

$$h(\sigma_x,\sigma_y, \cdots \tau_z) = L(J_1,J_2,J_3)$$

with $L_1 = \dfrac{\partial L}{\partial J_1}$, $L_2 = \dfrac{\partial L}{\partial J_2}$, $L_3 = \dfrac{\partial L}{\partial J_3}$, we compute:

$$\frac{\partial h}{\partial \tau_x} = -\tau_x(L_2 + \sigma_x L_3) + \tau_y\tau_z L_3$$
$$\frac{\partial h}{\partial \tau_y} = -\tau_y(L_2 + \sigma_y L_3) + \tau_x\tau_z L_3$$
$$\frac{\partial h}{\partial \tau_z} = -\tau_z(L_2 + \sigma_z L_3) + \tau_y\tau_x L_3$$

The three right sides vanish, if $\tau_x = \tau_y = \tau_z = 0$, i.e., for the principal axes of the stress tensor, which are thus seen to coincide with the principal axes of Grad h.

Now, from the above assumptions about plane strain together with (1.IX′), it follows that

$$\frac{\partial g}{\partial \sigma_z} = 0, \quad \frac{\partial g}{\partial \tau_x} = 0, \quad \frac{\partial g}{\partial \tau_y} = 0, \tag{1.6}$$

or

$$\frac{\partial G}{\partial \sigma_3} = 0. \tag{1.6′}$$

These equations characterize our plane problem. We conclude from the property of Grad h just proved that $\tau_x = \tau_y = 0$, and $\sigma_z = \sigma_3$. From (1.6′) we compute σ_3 in terms of σ_1 and σ_2, and (1.6) is then replaced by

$$\begin{gathered} \tau_x = \tau_y = 0 \\ \sigma_z = l(\sigma_x,\sigma_y,\tau) = p(\sigma_1,\sigma_2) = \sigma_3 \end{gathered} \tag{1.6′}$$

where p is some symmetric function of σ_1 and σ_2; (in the particular problem with quadratic yield condition the corresponding relation is $\sigma_3 = \frac{1}{2}(\sigma_1 + \sigma_2)$). Hence with $G(\sigma_1,\sigma_2,p(\sigma_1,\sigma_2)) = F(\sigma_1\sigma_2)$ the plane yield condition may be written, with a symmetric F, as

$$f(\sigma_x,\sigma_y,\tau) = F(\sigma_1,\sigma_2) = 0. \tag{1.7}$$

Next it is seen that

$$\frac{\partial f}{\partial \sigma_x} + \frac{\partial f}{\partial \sigma_y} = \frac{\partial F}{\partial \sigma_1} + \frac{\partial F}{\partial \sigma_2} = 0.$$

In fact, if we denote by the subscript p, that after differentiation we put $\sigma_3 = p(\sigma_1,\sigma_2)$ then

$$\frac{\partial F}{\partial \sigma_1} + \frac{\partial F}{\partial \sigma_2} = \left[\frac{\partial G}{\partial \sigma_1} + \frac{\partial G}{\partial \sigma_2} + \frac{\partial G}{\partial \sigma_3}\left(\frac{\partial p}{\partial \sigma_1} + \frac{\partial p}{\partial \sigma_2}\right)\right]_p = \left[\frac{\partial G}{\partial \sigma_1} + \frac{\partial G}{\partial \sigma_2}\right]_p = 0$$

on account of (1.6′) and (1.VI).

The three remaining strain-stress relations of the three-dimensional problem reduce therefore to

$$k\dot{\epsilon}_x = \frac{\partial f}{\partial \sigma_x}, \quad k\dot{\epsilon}_y = \frac{\partial f}{\partial \sigma_y}, \quad k\dot{\gamma} = \frac{\partial f}{\partial \tau}, \tag{1.8} \qquad (\mathrm{V}_4)$$

of which only two are independent on account of

$$\dot{\epsilon}_x + \dot{\epsilon}_y = 0, \quad \frac{\partial f}{\partial \sigma_x} + \frac{\partial f}{\partial \sigma_y} = \frac{\partial F}{\partial \sigma_1} + \frac{\partial F}{\partial \sigma_2} = 0; \tag{1.8′}$$

these relations follow from $\dot{\epsilon}_z = 0$, and (1.IV), and from (1.VI) and $\partial g/\partial \sigma_z = 0$ respectively. Our set of equations consists thus of the two Eqs. (1.1), the yield condition (1.7) with the restriction (1.8′), the Eqs. (1.8), of which only two are independent on account of the restriction $\dot{\epsilon}_x + \dot{\epsilon}_y = 0$, hence six equations for the six unknowns $\sigma_x, \sigma_y, \tau, v_x, v_y, k$. If, in (1.8) the function k is eliminated, we obtain

$$\dot{\epsilon}_x : \dot{\epsilon}_y : \dot{\gamma} = \frac{\partial f}{\partial \sigma_x} : \frac{\partial f}{\partial \sigma_y} : \frac{\partial f}{\partial \tau},$$

or the two equations

$$\dot{\epsilon}_x + \dot{\epsilon}_y = \frac{\partial f}{\partial \sigma_x} + \frac{\partial f}{\partial \sigma_y} = 0, \quad \frac{\dot{\epsilon}_x - \dot{\epsilon}_y}{\dot{\gamma}} = \frac{\dfrac{\partial f}{\partial \sigma_x} - \dfrac{\partial f}{\partial \sigma_y}}{\dfrac{\partial f}{\partial \tau}}. \tag{1.9} \qquad (v_5)$$

We shall easily see that this last quotient is equal to cot 2ϑ where ϑ is the angle between the x-axis and the first principal direction. Let us add that on account of (1.8′) the function F can depend only on the difference $(\sigma_1 - \sigma_2)$, hence the yield condition is of the form $A[(\sigma_1 - \sigma_2)] = 0$ where A denotes a function of one variable. Thus the five equations of plane strain under general yield condition are:

$$(1.10) \quad \begin{aligned} &\frac{\partial \sigma_x}{\partial x} + \frac{\partial \tau}{\partial y} = 0, \quad \frac{\partial \tau}{\partial x} + \frac{\partial \sigma_y}{\partial y} = 0 \\ &f(\sigma_x,\sigma_y,\tau) = A[(\sigma_1 - \sigma_2)] = 0 && (y_3) \\ &\dot{\epsilon}_x + \dot{\epsilon}_y = \frac{\partial f}{\partial \sigma_x} + \frac{\partial f}{\partial \sigma_y} = 0, \quad \frac{\dot{\epsilon}_x - \dot{\epsilon}_y}{\dot{\gamma}} = \frac{\dfrac{\partial f}{\partial \sigma_x} - \dfrac{\partial f}{\partial \sigma_y}}{\dfrac{\partial f}{\partial \tau}}. && (v_1) \end{aligned}$$

In addition, there is $\tau_x = \tau_y = 0$, $\sigma_3 = p(\sigma_1,\sigma_2)$ and $v_z =$ constant; thus we have here indeed a particular solution of the general problem of the preceding section. It is seen that the yield condition (y_3) is hardly more general than the classical (y_1), $\tau_{max} =$ constant.

It is finally seen that the above derivations are not much changed if a plastic potential h is used, not identical with the yield function g. In the relations (1.6) and (1.6′), g is replaced by h and the complete system consists of the first three Eqs. (1.10), and the equations

$$\dot{\epsilon}_x : \dot{\epsilon}_y : \dot{\gamma} = \frac{\partial h}{\partial \sigma_x} : \frac{\partial h}{\partial \sigma_y} : \frac{\partial h}{\partial \tau},$$

where $\dfrac{\partial h}{\partial \sigma_x} + \dfrac{\partial h}{\partial \sigma_y} = 0$. If, for example, the special strain relation (1.III) is adopted in connection with a general yield relation (1.V), then von

Mises' yield function (1.II) forms the plastic potential, and we arrive easily at a system of the form (1.10). In fact, as in I,2 we find $\sigma_z = -p = \frac{1}{2}(\sigma_x + \sigma_y) = \frac{1}{2}(\sigma_1 + \sigma_2)$, $\sigma_x' = -\sigma_y' = \frac{1}{2}(\sigma_x - \sigma_y)$, and from $\dot\gamma_x = \dot\gamma_y = 0$, $\tau_x = \tau_y = 0$ follows. If these values are substituted into a general three-dimensional yield condition, one obtains

$$(1.11)\qquad \begin{aligned} 0 &= g\left(\sigma_x, \sigma_y, \frac{\sigma_x + \sigma_y}{2}, 0, 0, \tau\right) \\ &= G\left(\sigma_1, \sigma_2, \frac{\sigma_1 + \sigma_2}{2}\right) \\ &= f(\sigma_x,\sigma_y,\tau) = F(\sigma_1,\sigma_2), \end{aligned}$$

where

$$\frac{\partial F}{\partial \sigma_1} + \frac{\partial F}{\partial \sigma_2} = \frac{\partial G}{\partial \sigma_1} + \frac{\partial G}{\partial \sigma_2} + \frac{\partial G}{\partial \sigma_3}\cdot\frac{1}{2} + \frac{\partial G}{\partial \sigma_3}\cdot\frac{1}{2} = \frac{\partial G}{\partial \sigma_1} + \frac{\partial G}{\partial \sigma_2} + \frac{\partial G}{\partial \sigma_3} = 0.$$

Plane stress. Let us consider a particular solution of the general three-dimensional problem, where

$$\sigma_z = \tau_x = \tau_y = 0, \text{ i.e., } \sigma_3 = 0,$$

and σ_x, σ_y, τ depend on x and y only. Then

$$(1.12)\quad g(\sigma_x,\sigma_y,0,0,0,\tau_z) = f(\sigma_x,\sigma_y,\tau) = G(\sigma_1,\sigma_2,0) = F(\sigma_1,\sigma_2) = 0,$$

where F is symmetric, and there is no further restriction imposed on the yield function $F(\sigma_1,\sigma_2)$. Equations (1.I) reduce to (1.1), and

$$\left[\frac{\partial g}{\partial \sigma_x}(\sigma_x,\sigma_y,\sigma_z,\tau_x,\tau_y,\tau_z)\right]_{\sigma_z=\tau_x=\tau_y=0} = \frac{\partial g(\sigma_x,\sigma_y,0,0,0,\tau)}{\partial \sigma_x} = \frac{\partial f}{\partial \sigma_x},$$

and one arrives as in (1.8) at:

$$(1.13)\qquad k\dot\epsilon_x = \frac{\partial f}{\partial \sigma_x},\quad k\dot\epsilon_y = \frac{\partial f}{\partial \sigma_y},\quad k\dot\gamma = \frac{\partial f}{\partial \tau} \qquad (\mathrm{v}_4)$$

where f is defined by (1.12). The other three Eqs. (1.III′) become, under consideration of the results of p. 206,

$$\begin{aligned} k\dot\gamma_x &= \left(\frac{\partial g}{\partial \tau_x}\right)_{\sigma_z=\tau_x=\tau_y=0} = 0 \\ k\dot\gamma_y &= \left(\frac{\partial g}{\partial \tau_y}\right)_0 = 0 \\ k\dot\epsilon_z &= \left(\frac{\partial g}{\partial \sigma_z}\right)_0 = -\left[\frac{\partial g}{\partial \sigma_x} + \frac{\partial g}{\partial \sigma_y}\right]_0 = -\left[\frac{\partial f}{\partial \sigma_x} + \frac{\partial f}{\partial \sigma_y}\right]. \end{aligned}$$

These are three equations

$$\frac{\partial v_y}{\partial z} + \frac{\partial v_z}{\partial y} = 0,\quad \frac{\partial v_x}{\partial z} + \frac{\partial v_z}{\partial x} = 0,\quad \frac{\partial v_z}{\partial z} = -\frac{1}{k}\left[\frac{\partial f}{\partial \sigma_x} + \frac{\partial f}{\partial \sigma_y}\right]$$

for v_z, $\partial v_x/\partial z$, $\partial v_y/\partial z$. It is seen that, unless $\dot{\epsilon}_z = 0$, the sum

$$\frac{\partial f}{\partial \sigma_x} + \frac{\partial f}{\partial \sigma_y} = \frac{\partial F}{\partial \sigma_1} + \frac{\partial F}{\partial \sigma_2}$$

is *different* from zero.

If k is eliminated from (1.13) one obtains

$$\dot{\epsilon}_x : \dot{\epsilon}_y : \dot{\gamma} = \frac{\partial f}{\partial \sigma_x} : \frac{\partial f}{\partial \sigma_y} : \frac{\partial f}{\partial \tau}.$$

The problem of plane stress is thus defined by the six equations (1.1), (1.12), (1.13), or by the five equations

$$\frac{\partial \sigma_x}{\partial x} + \frac{\partial \tau}{\partial y} = 0, \quad \frac{\partial \tau}{\partial x} + \frac{\partial \sigma_y}{\partial y} = 0$$

$$f(\sigma_x,\sigma_y,\tau) = F(\sigma_1,\sigma_2) = 0 \qquad (y_4)$$

$$\text{(1.14)} \qquad \frac{\dot{\epsilon}_x - \dot{\epsilon}_y}{\dot{\gamma}} = \frac{\dfrac{\partial f}{\partial \sigma_x} - \dfrac{\partial f}{\partial \sigma_y}}{\dfrac{\partial f}{\partial \tau}}, \quad \frac{\dot{\epsilon}_x + \dot{\epsilon}_y}{\dot{\gamma}} = \frac{\dfrac{\partial f}{\partial \sigma_x} + \dfrac{\partial f}{\partial \sigma_y}}{\dfrac{\partial f}{\partial \tau}}.$$

Here the last two equations will appear later in a much more convenient form. The mathematical difference between (1.10) and (1.14) consists only in the fact that in (1.10) the sum

$$\frac{\partial f}{\partial \sigma_x} + \frac{\partial f}{\partial \sigma_y} = i$$

(and consequently $\dot{\epsilon}_x + \dot{\epsilon}_y$), *must be zero identically for all stress values*, whereas no such condition exists in (1.14).

We may now forget all about "plane strain" and "plane stress" and consider as the *general plane problem* the problem (1.14) with *no restriction* on

$$i = \frac{\partial f}{\partial \sigma_x} + \frac{\partial f}{\partial \sigma_y}.$$

For reasons which will appear soon we shall call the particular case where $i = 0$ the *orthogonal* case. The most frequently considered orthogonal case where $f = (\sigma_x - \sigma_y)^2 + 4\tau^2 -$ constant (resulting from both St. Venant's and von Mises' three-dimensional yield condition in case of plane strain), that is, the problem (1.1), (1.2), (1.3) we shall denote as the *special* or *classical* case. We note again: if we consider a plastic potential different from f the first three Eqs. (1.14) remain unaltered, and in the last two equations the three partial derivatives of f are replaced by $\partial h/\partial \sigma_x$, $\partial h/\partial \sigma_y$, $\partial h/\partial \tau$. Each of the two sums $\dfrac{\partial f}{\partial \sigma_x} + \dfrac{\partial f}{\partial \sigma_y}$, and $\dfrac{\partial h}{\partial \sigma_x} + \dfrac{\partial h}{\partial \sigma_y}$ may or may not be identically zero.

It may seem unnecessary to some reader that we have gone through all these derivations in order to arrive at the system (1.14) which might have been written down in analogy to the three-dimensional setup. It seemed, however, preferable to derive the plane problem as a particular solution of the three-dimensional one in order to make sure that the important cases of plane stress and plane strain are taken care of, and that enough generality is achieved, together with necessary restrictions. Also the opportunity of reviewing a few aspects of the three-dimensional situation was welcome. Finally, the relation of the slightly more general "orthogonal" problem (1.10), or problem of plane strain, to the "classical" case (1.1), (1.2), (1.3) could thus be stated.

5. A Generalization of the Plane Problem

Certain problems which cannot be regarded as problems of "plane stress" in the above sense may be considered as states of "generalized plane stress," where the stress and velocity components are averaged over the thickness h of the plate. In formulating this problem, Hill (5a, p. 306 ff.) uses the special yield criterion (1.4). One may, however, consider a general condition as in (1.14).

Consider a plate of small thickness h, under the conditions of "plane stress" ($\sigma_z = \tau_x = \tau_y = 0$, loads applied along edge of plate, etc.) where the thickness h does not remain quite uniform during the deformation; under certain conditions of *small* rate of change the state of stress may still be considered as approximately "plane." Assume that at a certain moment, t_0, the thickness $h(x,y)$ is a given function. Denote by σ_x, σ_y, τ the stress components, averaged over the thickness of the plate; insert these averaged stresses into the yield criterion; this will induce only a small error if the variation of the stresses over the thickness is not considerable. Denote by v_x,v_y the averaged velocity components, and use as before, $\dot{\epsilon}_x = \partial v_x/\partial x$, etc. The system of five equations of this problem is then

$$\frac{\partial}{\partial x}(h\sigma_x) + \frac{\partial}{\partial y}(h\tau) = 0, \quad \frac{\partial}{\partial x}(h\tau) + \frac{\partial}{\partial y}(h\sigma_y) = 0,$$

$$f(\sigma_x,\sigma_y,\tau) = 0, \tag{1.15}$$

$$\dot{\epsilon}_x : \dot{\epsilon}_y : \dot{\gamma} = \frac{\partial f}{\partial \sigma_x} : \frac{\partial f}{\partial \sigma_y} : \frac{\partial f}{\partial \tau}.$$

These are five equations with the usual five unknowns σ_x, σ_y, τ, v_x, v_y. In addition the equation of continuity may serve to compute the *change* of h at the instant $t = t_0$. Denote by dh/dt the "material derivative" of h:

$$\frac{dh}{dt} = \frac{\partial h}{\partial t} + v_x \frac{\partial h}{\partial x} + v_y \frac{\partial h}{\partial y};$$

the rate of strain in the z-direction averaged through the thickness is $\dot{\epsilon}_z = \frac{1}{h}\frac{dh}{dt}$. Hence from (1.IV) the equation of continuity is

$$\frac{dh}{dt} + h(\dot{\epsilon}_x + \dot{\epsilon}_y) = 0$$

or

$$\frac{\partial h}{\partial t} + \frac{\partial}{\partial x}(hv_x) + \frac{\partial}{\partial y}(hv_y) = 0. \tag{1.16}$$

If $h(x,y)$ is known at $t = t_0$ and v_x,v_y have been determined, then (1.16) may serve to determine $[\partial h/\partial t]_{t=t_0}$.

On the other hand, Hodge (6c) considers the system (1.15) with $h(x,y)$ as an *unknown* function of x,y, assuming $(\partial h/\partial t)_{t=t_0} = 0$. This is then a system of six equations with the additional unknown h; in this case the separation into two groups of equations, with the first three equations containing only the stresses is no longer possible, since the unknown h enters into the stress equations. Mathematically, this is a more difficult problem than (1.14) (Hodge, in the quoted paper, computed the characteristics), while the above described problem (1.15), where h is given at $t = t_0$ does not differ much from (1.14) as far as the mathematics is concerned.

II. On the General Plane Problem

We have defined the general complete plane problem of the perfectly plastic isotropic body by means of the Eqs. (1.14). The problem (1.1), (1.2), (1.3) almost exclusively dealt with until recently we called the particular or classical case. [See the books by Nadai (13), Geiringer (2c), Sokolovsky (20c), Hodge (6a), Hill (5a), Prager (16g).] The mathematical theory of this last problem is rather advanced. One knows much less about the general problem (1.14). Some results will be reported in the following. Considering the great difficulties of actual physical problems even if they are based on the "classical" setup, one may wonder whether it makes sense to study an even more general and difficult setup. It is, however, both interesting and useful to consider various yield conditions, to study their influence on the solutions, and to try to compare the results with actual experiences and observations. (The yield condition in plasticity theory corresponds somehow to the pressure-density relation in compressible fluid theory, among which the adiabatic relation is the most important but not the only possible one.) Moreover, as stated in the introduction, the problems of plane stress (thin plate) of ductile metals, as well as the plane problem of nonmetallic materials, lead to the consideration of general yield conditions.

1. *Linearization*

a. Several Linearizations of the Stress Equations. Stress Graph. Consider the first three Eqs. (1.14) of Section I,4, namely

$$\frac{\partial \sigma_x}{\partial x} + \frac{\partial \tau}{\partial y} = 0, \quad \frac{\partial \tau}{\partial x} + \frac{\partial \sigma_y}{\partial y} = 0, \tag{2.1}$$

$$f(\sigma_x,\sigma_y,\tau) = F(\sigma_1,\sigma_2) = 0. \tag{2.2}$$

They constitute a nonlinear system. By means of (2.2) one may eliminate in many ways one of the stress components and thus arrive at two *nonlinear* but *reducible* equations of first order.

We shall mainly use here an approach, advanced by von Mises, together with the introduction of a *stress graph* (12d); this approach seems to offer mathematical advantages. Other linearizations which, on the other hand, are more general in a certain sense, will likewise be discussed.

For reasons of symmetry we use a parametric representation of the yield condition (2.2):

$$F(\sigma_1,\sigma_2) = 0, \quad \sigma_1 = \sigma_1(s), \quad \sigma_2 = \sigma_2(s). \tag{2.3}$$

Let us assume from now on that $\sigma_2 \geqq \sigma_1$. Very often we shall understand by the parameter, s: $s = \frac{1}{2k}(\sigma_1 + \sigma_2)$, where k is a constant, e.g., the constant appearing in the flow condition (1.4). The following formulas are, however, independent of this particular interpretation of k. As in the preceding part we denote by ϑ the angle between the positive x-direction and the first principal direction, which we call the u-direction, the second being denoted as the v-direction. Denote by $\partial/\partial u$ (or more explicitly by $\partial/\partial s_u$) and $\partial/\partial v$ (or $\partial/\partial s_v$) directional derivatives in these directions. As shown by Jenne (7), the equilibrium conditions (2.1) are then equivalent to the system

$$\frac{\partial \sigma_1}{\partial u} = (\sigma_2 - \sigma_1)\frac{\partial \vartheta}{\partial v}, \quad \frac{\partial \sigma_2}{\partial v} = (\sigma_2 - \sigma_1)\frac{\partial \vartheta}{\partial u}. \tag{2.4}$$

Introduce for σ_i the values from (2.3) and put

$$\frac{d\sigma_1}{ds} = \sigma_1', \quad \frac{d\sigma_2}{ds} = \sigma_2'$$

and use the abbreviations

$$\frac{\sigma_2 - \sigma_1}{\sigma_1'} = f(s), \quad \frac{\sigma_2 - \sigma_1}{\sigma_2'} = g(s). \tag{2.5}$$

Then (2.4) yields the *reducible*, planar equations [see (1) for these terms],

$$\frac{\partial s}{\partial u} = f(s)\,\frac{\partial \vartheta}{\partial v}, \quad \frac{\partial s}{\partial v} = g(s)\,\frac{\partial \vartheta}{\partial u}. \tag{2.6}$$

The dependent variables are s and ϑ; together with (2.3) they determine the stress tensor at each point. If in (2.6) dependent and independent variables are interchanged, we arrive at a *linear* system. The plane of the variables s and ϑ, or more particularly, the plane where s and ϑ are polar coordinates is called stress graph by von Mises; however in a more general sense this term might be used for any plane of two stress variables which in our theory determine the stress tensor. At every point where the Jacobian $j = \partial(s,\vartheta)/\partial(u,v)$ is different from zero the dependent and independent variables may be interchanged (solutions, for which $j = 0$, cannot be obtained by this transformation). With

$$\frac{\partial s}{\partial u} = j\,\frac{\partial v}{\partial \vartheta}, \quad \frac{\partial s}{\partial v} = -j\,\frac{\partial u}{\partial \vartheta}, \frac{\partial \vartheta}{\partial u} = -j\,\frac{\partial v}{\partial s}. \quad \frac{\partial \vartheta}{\partial v} = j\,\frac{\partial u}{\partial s} \tag{2.7}$$

we find von Mises' linear equations

$$\frac{\partial v}{\partial \vartheta} = f(s)\,\frac{\partial u}{\partial s}, \quad \frac{\partial u}{\partial \vartheta} = g(s)\,\frac{\partial v}{\partial s}. \tag{2.8}$$

Note that in Eq. (2.6) the derivatives $\partial/\partial u$ and $\partial/\partial v$ are directional derivatives; u and v are not coordinates. Therefore Eqs. (2.8) must be used with some care. We shall return to this point.

If in compressible fluid theory φ and ψ denote potential and stream function, q and ϑ the polar coordinates of the velocity vector, ρ and M density and Mach number (both depend on q only), the basic equations in the hodograph plane are of the same form as (2.8):

$$\frac{\partial \varphi}{\partial \vartheta} = \frac{q}{\rho}\,\frac{\partial \psi}{\partial q}, \quad \frac{\partial \psi}{\partial \vartheta} = -\frac{\rho q}{1 - M^2}\,\frac{\partial \varphi}{\partial q}$$

with q and ϑ corresponding to s and ϑ, the stress graph to the hodograph plane, and the yield condition to the adiabatic condition.

Before going on, let us give equations equivalent to (2.6) in other variables. If we make for s the particular choice $s = \dfrac{1}{2K}(\sigma_1 + \sigma_2)$, using s and ϑ as stress variables, these are almost the same as used by Prager, Hodge, Sokolovsky, and others, namely:

$$\omega = \frac{\sigma_1 + \sigma_2}{4K}, \quad \chi = \frac{\sigma_2 - \sigma_1}{4K}. \tag{2.9}$$

From the well-known formulas

$$\begin{aligned} \sigma_x &= \sigma_1 \cos^2 \vartheta + \sigma_2 \sin^2 \vartheta = \frac{\sigma_1 + \sigma_2}{2} + \frac{1}{2}(\sigma_1 - \sigma_2) \cos 2\vartheta, \\ \sigma_y &= \sigma_1 \sin^2 \vartheta + \sigma_2 \cos^2 \vartheta = \frac{\sigma_1 + \sigma_2}{2} - \frac{1}{2}(\sigma_1 - \sigma_2) \cos 2\vartheta, \\ \tau &= \cos \vartheta \sin \vartheta \cdot (\sigma_1 - \sigma_2) = \frac{\sigma_1 - \sigma_2}{2} \sin 2\vartheta, \end{aligned} \tag{2.10}$$

one obtains

$$\sigma_x = 2K[\omega - \chi \cos 2\vartheta], \quad \sigma_y = 2K[\omega + \chi \cos 2\vartheta] \\ \tau = -2K\chi \sin 2\vartheta. \tag{2.10'}$$

The yield condition (2.2) is then written in the form

$$\chi = h(\omega). \tag{2.11}$$

Eliminating χ, denoting $\dfrac{dh}{d\omega} = \dfrac{d\chi}{d\omega}$ by h' and partial derivatives by subscripts, we find:

$$\begin{aligned} \omega_x(1 - h' \cos 2\vartheta) - \omega_y h' \sin 2\vartheta + 2\vartheta_x h \sin 2\vartheta - 2\vartheta_y h \cos 2\vartheta &= 0 \\ \omega_x h' \sin 2\vartheta - \omega_y(1 + h' \cos 2\vartheta) + 2\vartheta_x h \cos 2\vartheta + 2\vartheta_y h \sin 2\vartheta &= 0. \end{aligned} \tag{2.12}$$

These are two reducible equations for the dependent variables ω and ϑ, taking the place of our Eqs. (2.6). A linearization of (2.12) by means of exchange of variables, of course, is possible. However, system (2.6) and the corresponding system (2.8) are simpler.

b. Yield Conditions. We shall consider some particular cases of the general yield condition (2.2) which have proved to be of interest. First, we consider the "quadratic" condition (1.4) of von Mises, then the St. Venant condition of constant maximum shear, both under the conditions of plane stress, the latter we may call "hexagonal" condition; next, a new condition proposed in 1948 by von Mises, which has considerable mathematical advantages compared to the two others; it may be called parabola condition and should give a good approximation to the von Mises condition [see however (6a, Sec. 59)]; finally some generalizations of these conditions will be considered.

In a $\sigma_1 - \sigma_2$-plane the *quadratic* limit (1.4) is represented by an ellipse. Using for s the value above suggested we have

$$\begin{aligned} &\sigma_1^2 + \sigma_2^2 - \sigma_1\sigma_2 - 4K^2 = 0, \\ &s = \frac{1}{2K}(\sigma_1 + \sigma_2) \quad (-2 \leqq s \leqq +2), \\ &\sigma_1 = K\left[s \pm \sqrt{\frac{4 - s^2}{3}}\right], \quad \sigma_2 = K\left[s \mp \sqrt{\frac{4 - s^2}{3}}\right], \end{aligned} \tag{2.13}$$

where the upper signs apply to the right and the lower to the left side of the ellipse. At the left part, then, $\sigma_2 \geqq \sigma_1$. We note for future use that for the functions f,g in (2.5)

$$f \cdot g = \frac{(\sigma_2 - \sigma_1)^2}{\sigma_1'\sigma_2'} = \frac{(4 - s^2)^2}{3 - s^2}. \tag{2.13'}$$

Sometimes it is useful to consider the variables

$$p = \tfrac{1}{2}(\sigma_1 + \sigma_2), \quad \tau_3 = \tfrac{1}{2}(\sigma_2 - \sigma_1);$$

the equation of the ellipse is then

$$p^2 + 3\tau_3^2 = 4K^2.$$

As the next example consider the *St. Venant condition* in plane stress; it states that $|\tau|_{\max} = \text{constant}$. Hence

$$|\sigma_1 - \sigma_2| \begin{cases} = 2K \quad \text{if } \sigma_1\sigma_2 \leqq 0, \\ = 4K - |\sigma_1 + \sigma_2| \quad \text{if } \sigma_1\sigma_2 \geqq 0. \end{cases} \tag{2.14}$$

Thus $\frac{1}{2} \cdot |\sigma_1 - \sigma_2| = K$ if σ_1 and σ_2 have opposite signs, while otherwise $\sigma_1 = 2K$ or $\sigma_2 = 2K$. This condition is represented geometrically by a

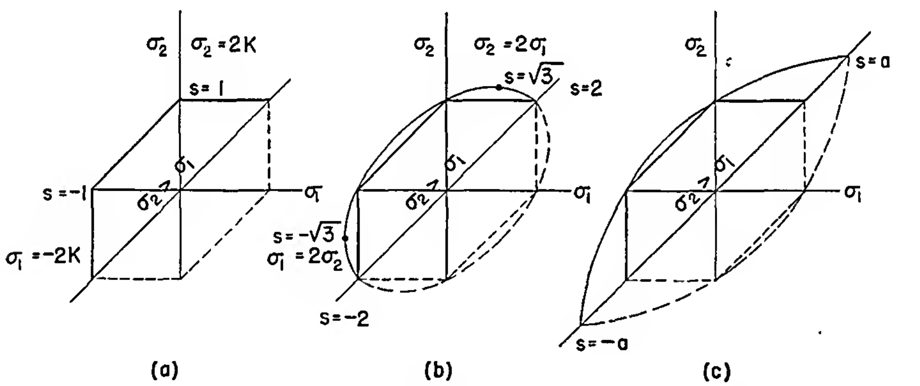

FIG. 1. Yield conditions: (a) Saint Venant condition (b) quadratic condition (c) parabola condition.

hexagon inscribed in the ellipse (2.13). With $s = \dfrac{1}{2K}(\sigma_1 + \sigma_2)$, the *parametric* representation of the 45° line to the left is

$$\sigma_1 = K(s - 1), \quad \sigma_2 = K(s + 1), \quad |s| \leqq 1 \tag{2.15}$$

and

$$fg = 4. \tag{2.15'}$$

For the horizontal and vertical sides to the left

$$\sigma_1 = K[-2 + s + |s|], \quad \sigma_2 = K[2 + s - |s|], \tag{2.15''}$$

and

(2.15‴) $$\frac{\sigma_2 - \sigma_1}{2K} = 2 - |s|, \quad 1 \leqq |s| \leqq 2.$$

Equation (2.15) is also the representation of the yield condition of the "classical" problem $(\sigma_2 - \sigma_1)^2 = 4K^2$.

Now consider the *parabola limit* for which, as we shall see, the stress problem is *hyperbolic throughout* (i.e., the characteristics are real and distinct). In the $\sigma_1 - \sigma_2$-plane this limit is represented by two branches of parabolas passing through four of the corners of St. Venant's hexagon. Their equation is, if we write $a = 1 + \sqrt{2}$,

(2.16) $$\frac{\sigma_2 - \sigma_1}{K} = \pm \frac{1}{a}\left[a^2 - \left(\frac{\sigma_1 + \sigma_2}{2K}\right)^2\right].$$

The upper sign applies to the left, the lower to the right branch. Using always the same s, one obtains the parametric representation of the left branch by (2.17) together with the values of f and g

(2.17) $$\sigma_1 = Ks - \frac{K}{2a}(a^2 - s^2), \quad \sigma_2 = Ks + \frac{K}{2a}(a^2 - s^2). \quad |s| \leqq a.$$

Here

(2.17′) $$f = a - s, \quad g = a + s, \quad fg = a^2 - s^2.$$

Recently P. G. Hodge, Jr., introduced a "generalized Treska condition" (6b). (We would rather call it generalized St. Venant condition.) This uses the 45° lines (2.15) in the second and third quadrant, while instead of (2.15‴)

(2.18) $$\frac{\sigma_2 - \sigma_1}{2K} = (1 + \lambda) - \lambda\left|\frac{\sigma_1 + \sigma_2}{2K}\right|.$$

This reduces to (2.15‴) for $\lambda = 1$. Written in parametric form with $s = \dfrac{\sigma_1 + \sigma_2}{2K}$ as parameter, it reads

(2.18′) $$\sigma_1 = K[s + \lambda|s| - 1 - \lambda], \quad \sigma_2 = K[s - \lambda|s| + 1 + \lambda].$$

For $\lambda < 1$ those lines are between the St. Venant limit (2.15′) and the left branch of von Mises' parabola (2.12) while for $\lambda > 1$ they are inside the St. Venant hexagon.[4] (For details see the above quoted paper by Hodge.)

c. Directions of Maximum Shear and Directions of Vanishing Normal Strain. In the "classical" case there exists a pair of orthogonal axes bisecting the angles of the first and second principal stress directions; they

[4] As the figure shows there is a discontinuity of the derivative similar to that in the St. Venant hexagon which makes it less appropriate for use as a "plastic potential."

coincide with the principal axes of the $\dot{E}$ tensor. With respect to these axes the $\dot{E}$ tensor becomes

$$\dot{E} = \begin{pmatrix} 0 & \frac{1}{2}(\dot{\epsilon}_1 - \dot{\epsilon}_2) \\ \frac{1}{2}(\dot{\epsilon}_1 - \dot{\epsilon}_2) & 0 \end{pmatrix}.$$

For these directions the normal strains are $\frac{1}{2}(\dot{\epsilon}_1 + \dot{\epsilon}_2) = 0$, and the shear has its greatest possible value. They are also the directions of the *characteristics* of the classical problem.

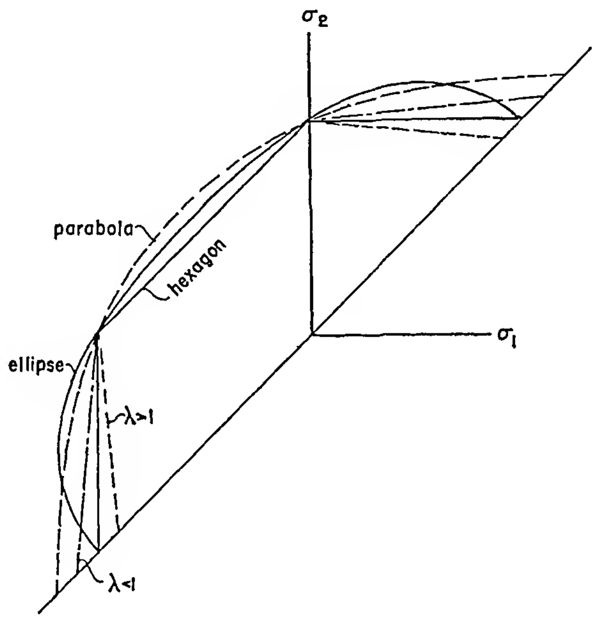

FIG. 2. Generalized Saint Venant conditions.

In the more general case the situation is less simple. The directions of maximum shear and those of vanishing strain do no longer coincide. The former are of course still the 45°-lines, the latter are, as we shall see, the characteristics. Let us give the simple geometric facts.

We first prove that even in this general case the two tensors of stress and of deformation rate have the same directions. In fact, putting $\sigma = \frac{1}{2}(\sigma_1 + \sigma_2)$, $\dot{\epsilon} = \frac{1}{2}(\dot{\epsilon}_1 + \dot{\epsilon}_2)$, we see that *the five tensors*

$$\Sigma, \quad \Sigma' = \Sigma - \sigma J, \qquad \text{Grad}\, f,\ \dot{E}, \quad E' = \dot{E} - \dot{\epsilon} J$$

are coaxial. This is obvious for Σ and Σ', and also for $\dot{E}$ and E', likewise, on account of (1.13) it holds for Grad f and $\dot{E}$; the only not obvious fact is that Σ and Grad f have the same principal directions. This follows now easily by direct computation (see p. 206 for three dimensions). Denote by ϑ' the angle of the first principal direction of Grad f

with the x-axis, write as always $f(\sigma_x,\sigma_y,\tau) = F(\sigma_1,\sigma_2)$, and

$$F_i = \partial F/\partial\sigma_i \quad (i = 1,2);$$

then

$$\tan 2\vartheta' = 2\,\frac{\dfrac{1}{2}\dfrac{\partial f}{\partial\tau}}{\dfrac{\partial f}{\partial\sigma_x} - \dfrac{\partial f}{\partial\sigma_y}} = \frac{(F_1 - F_2)\sin 2\vartheta}{(F_1 - F_2)\cos 2\vartheta} = \tan 2\vartheta.$$

Hence there exists at each point only *one* pair of 45°-directions for the five tensors. With respect to it they are:

$$\Sigma = \begin{pmatrix} \dfrac{\sigma_1 + \sigma_2}{2}, & \dfrac{\sigma_1 - \sigma_2}{2} \\ \dfrac{\sigma_1 - \sigma_2}{2}, & \dfrac{\sigma_1 + \sigma_2}{2} \end{pmatrix}, \qquad \Sigma' = \begin{pmatrix} 0 & \dfrac{\sigma_1 - \sigma_2}{2} \\ \dfrac{\sigma_1 - \sigma_2}{2} & 0 \end{pmatrix},$$

$$\operatorname{Grad} f = \begin{pmatrix} \dfrac{F_1 + F_2}{2} & \dfrac{F_1 - F_2}{2} \\ \dfrac{F_1 - F_2}{2} & \dfrac{F_1 + F_2}{2} \end{pmatrix}, \qquad \dot E = \begin{pmatrix} \dfrac{\dot\epsilon_1 + \dot\epsilon_1}{2} & \dfrac{\dot\epsilon_1 - \dot\epsilon_1}{2} \\ \dfrac{\dot\epsilon_1 - \dot\epsilon_2}{2} & \dfrac{\dot\epsilon_1 + \dot\epsilon_2}{2} \end{pmatrix},$$

$$E' = \begin{pmatrix} 0 & \dfrac{\dot\epsilon_1 - \dot\epsilon_2}{2} \\ \dfrac{\dot\epsilon_1 - \dot\epsilon_2}{2} & 0 \end{pmatrix}.$$

In the classical case E' coincides with $\dot E$ and $\operatorname{Grad} f$ with Σ'. At any rate, however, $\frac{1}{2}(\sigma_1 - \sigma_2)$ is the absolutely greatest possible value of τ_{xy} and $\frac{1}{2}(\dot\epsilon_1 - \dot\epsilon_2)$ of $\dot\gamma_{xy}$. *These 45°-directions are therefore the directions of maximum shear*, but now the normal extension $\frac{1}{2}(\dot\epsilon_1 + \dot\epsilon_2)$ is *not zero;* if one subtracts the "spherical" tensor $\dot\epsilon J$, one obtains the tensor E', with the normal strain equal to zero.

We now show that *there are two directions, symmetric to the first principal direction so that with respect to them the normal strain is zero.* Let us call such a direction a $\bar\nu$-direction, φ its angle with the first principal direction, and k the factor appearing in (1.13). Then by (1.13)

$$k\dot\epsilon_{\nu\nu} = k(\dot\epsilon_1 \cos^2\varphi + \dot\epsilon_2 \sin^2\varphi) = F_1\cos^2\varphi + F_2\sin^2\varphi.$$

This last expression is zero only if

$$\tan^2\varphi = -\frac{F_1}{F_2},$$

a most important relation which we shall find again in (2.50) and (2.59). We see also that $\varphi = \pi/4$ if and only if $F_1 + F_2 = 0$ (orthogonal case). If and only if this holds, the "characteristic" directions which make angles $\pm\varphi$ with the first principal direction coincide with the 45° lines.

By a similar computation we find the shear value corresponding to these directions:

$$k\dot{\gamma} = k(-\dot{\epsilon}_1 \cos\varphi \sin\varphi + \dot{\epsilon}_2 \cos\varphi \sin\varphi) = \frac{F_2 - F_1}{2} \sin 2\varphi,$$

and, since for this φ there is $\sin 2\varphi = \dfrac{2\sqrt{-F_1F_2}}{F_1 - F_2}$, we have

$$k\dot{\gamma} = \sqrt{-F_1F_2} = F_2 \tan\varphi = F_1 \cot\varphi$$

or

$$\dot{\gamma} = \sqrt{-\dot{\epsilon}_1\dot{\epsilon}_2} = \dot{\epsilon}_2 \tan\varphi = \dot{\epsilon}_1 \cot\varphi.$$

One may verify that this $\dot{\gamma}$-value is absolutely *less* than $\frac{1}{2}(\dot{\epsilon}_1 - \dot{\epsilon}_2)$; this follows from $(\dot{\epsilon}_1 + \dot{\epsilon}_2)^2 \geqq 0$. The elementary computations of this section have thus given these results:

There exists always a pair of 45° lines bisecting the angles of the principal axes for which both the shear strain and the shear stress have their extremum. The corresponding normal strain equals $\frac{1}{2}(\dot{\epsilon}_1 + \dot{\epsilon}_2)$, *and similarly for the stresses. If* $\dot{\epsilon}_1 + \dot{\epsilon}_2 \neq 0$, i.e., $F_1 + F_2 \neq 0$, *there exist two nonorthogonal directions making angles* $\pm\varphi$ *with the first principal axis, where* $\tan^2\varphi = -F_1/F_2$; *they are real if* F_1 *and* F_2 *are of opposite sign; for each of these directions the normal strain is zero and the corresponding shear* $\dot{\gamma} = \sqrt{-\dot{\epsilon}_1\dot{\epsilon}_2}$.

d. Differential Equations of the Linearized Problem.[5] In Eqs. (2.6) and (2.8) u and v are not coordinates. We are going to derive from (2.8) certain systems of differential equations for quantities which may serve as coordinates in the physical plane. Let

$$X = x\cos\vartheta + y\sin\vartheta, \quad Y = y\cos\vartheta - x\sin\vartheta. \tag{2.19}$$

According to the definitions of the u- and v-directions we have

$$\begin{aligned} dx &= du\cos\vartheta - dv\sin\vartheta, & du &= dx\cos\vartheta + dy\sin\vartheta,\\ dy &= du\sin\vartheta + dv\cos\vartheta, & dv &= dy\cos\vartheta - dx\sin\vartheta. \end{aligned}$$

Hence from (2.19)

$$\begin{aligned} dX &= dx\cos\vartheta + dy\sin\vartheta + Y d\vartheta = du + Y d\vartheta,\\ dY &= dy\cos\vartheta - dx\sin\vartheta - X d\vartheta = dv - X d\vartheta, \end{aligned}$$

and from these relations

$$\begin{aligned} \frac{\partial X}{\partial\vartheta} &= \frac{\partial u}{\partial\vartheta} + Y, & \frac{\partial Y}{\partial\vartheta} &= \frac{\partial v}{\partial\vartheta} - X,\\ \frac{\partial X}{\partial s} &= \frac{\partial u}{\partial s}, & \frac{\partial Y}{\partial s} &= \frac{\partial v}{\partial s}. \end{aligned}$$

[5] See also Section II, 2c, Eqs. (2.55) and (2.57).

Applying (2.8) we conclude that

$$\frac{\partial X}{\partial \vartheta} - Y = \frac{\partial u}{\partial \vartheta} = g(s)\frac{\partial v}{\partial s} = g(s)\frac{\partial Y}{\partial s},$$
$$\frac{\partial Y}{\partial \vartheta} + X = \frac{\partial v}{\partial \vartheta} = f(s)\frac{\partial u}{\partial s} = f(s)\frac{\partial X}{\partial s}.$$

One obtains thus the following system of linear equations of first order (s,ϑ independent, X, Y dependent variables):

(2.20) $$\frac{\partial X}{\partial \vartheta} = g(s)\frac{\partial Y}{\partial s} + Y, \quad \frac{\partial Y}{\partial \vartheta} = f(s)\frac{\partial X}{\partial s} - X.$$

From (2.20) the equations of second order follow

(2.21) $$\frac{\partial^2 X}{\partial \vartheta^2} - fg\frac{\partial^2 X}{\partial s^2} = -X + \frac{\partial X}{\partial s}(f'g + f - g),$$

(2.22) $$\frac{\partial^2 Y}{\partial \vartheta^2} - fg\frac{\partial^2 Y}{\partial s^2} = -Y + \frac{\partial Y}{\partial s}(g'f + f - g).$$

These equations are hyperbolic or elliptic according as to whether $fg \gtrless 0$ [see (2.5)] i.e., according to $d\sigma_1/d\sigma_2 \gtrless 0$, where $d\sigma_1/d\sigma_2$ follows directly from the yield condition $F(\sigma_1,\sigma_2) = 0$. They are parabolic at points where either fg or its reciprocal value equals zero. If a solution $X(s,\vartheta)$ has been found the corresponding $Y(s,\vartheta)$ follows from (2.20) and the coordinates x,y from (2.19) without further integration; then s and ϑ may be determined in terms of x and y.

To find integrals of (2.21), we may apply classical methods of series expansion or try to adapt modern operator methods to our equations. Because of the linearity of the equations solutions of (2.21) may be superposed; the difficulties encountered in actual problems where the boundary conditions are given in the physical plane, are well known from the analogous situation in fluid mechanics (hodograph plane).

Let us investigate the above condition of hyperbolic or other behavior *for the particular yield conditions* of the preceding section.

(1) *Quadratic condition.* From (2.13) we find

(2.23) $$fg = \frac{(\sigma_2 - \sigma_1)^2}{\sigma_2'\sigma_1'} = \frac{(4 - s^2)^2}{3 - s^2}.$$

It is seen that $fg > 0$ for $s^2 < 3$ while $fg < 0$ for $s^2 > 3$ and $fg \to \infty$ for $s^2 \to 3$. We consider merely the left part of the ellipse ($\sigma_2 > \sigma_1$); on this left part the arc corresponding to $-\sqrt{3} < s < \sqrt{3}$ yields a region with hyperbolic behavior of the equations; to $s = +\sqrt{3}$ and $s = -\sqrt{3}$ correspond the "sonic points"

$$\sigma_2 = 2\sigma_1 = 4K/\sqrt{3} \text{ and } \sigma_1 = 2\sigma_2 = -4K/\sqrt{3};$$

for $\sqrt{3} < |s| < 2$ one has "elliptic" states of stress. In the physical plane the "sonic line" separates the domains of hyperbolic from that of elliptic behavior; its image in the stress graph is the circle about the origin with radius $s = \sqrt{3}$. The parametric representation of the hyperbolic part for $\sigma_2 > \sigma_1$ is

$$\sigma_1 = K\left[s - \sqrt{\frac{4 - s^2}{3}}\right], \quad \sigma_2 = K\left[s + \sqrt{\frac{4 - s^2}{3}}\right], \quad |s| < \sqrt{3}. \tag{2.24}$$

(2) *St. Venant limit.* From (2.15) we see that the 45° line corresponds to the hyperbolic solutions, where

$$fg = 4, \quad |s| < 1. \tag{2.25}$$

The vertical and horizontal lines of the hexagon correspond to parabolic solutions, $fg = 0$.

The generalized St. Venant limit (2.18) *is everywhere hyperbolic* if $\lambda < 1$, and partly hyperbolic, partly elliptic, if $\lambda > 1$, the "sonic points" corresponding to $|s| = 1$.

(3) *For the parabola limit,* (2.16) and (2.17),

$$f = a - s, \quad g = a + s, \quad fg = a^2 - s^2.$$

Here for all s-values, except $s = \pm a$ when $fg = 0$, the problem is *hyperbolic.*

We derive now a second set of linear equations which show even closer analogy to the hydrodynamic situation than (2.20) and (2.21). One may satisfy the first Eq. (2.20) identically by a function $\psi(s,\vartheta)$ such that

$$\frac{\partial\psi}{\partial s} = \frac{X}{g(s)k(s)}, \quad \frac{\partial\psi}{\partial\vartheta} = \frac{Y}{k(s)}, \tag{2.26}$$

where $k(s)$ satisfies the equation

$$g(s)k'(s) + k(s) = 0. \tag{2.26'}$$

Substituting this ψ into the second Eq. (2.20) one finds

$$\frac{\partial^2\psi}{\partial\vartheta^2} - fg\frac{\partial^2\psi}{\partial s^2} = \frac{\partial\psi}{\partial s}(fg' - f - g). \tag{2.27}$$

In the same manner we introduce $\varphi(s,\vartheta)$ by

$$\frac{\partial\varphi}{\partial s} = \frac{Y}{f(s)h(s)}, \quad \frac{\partial\varphi}{\partial\vartheta} = \frac{X}{h(s)}, \tag{2.28}$$

where

$$f(s)h'(s) - h(s) = 0. \tag{2.28'}$$

Then the equation

$$\frac{\partial^2\varphi}{\partial\vartheta^2} - fg\frac{\partial^2\varphi}{\partial s^2} = \frac{\partial\varphi}{\partial s}(gf' + g + f) \tag{2.29}$$

follows in the same manner.[6]

We can apply "separation of variables," e.g., to the first Eq. (2.21). With

$$fg = c(s), \quad f'g + f - g = d(s), \tag{2.30}$$

this equation reads

$$\frac{\partial^2 X}{\partial\vartheta^2} - c\frac{\partial^2 X}{\partial s^2} + X = d\frac{\partial X}{\partial s};$$

with $X = a(s)b(\vartheta)$ we find

$$\frac{b''}{b} - c\frac{a''}{a} + 1 - d\frac{a'}{a} = 0,$$

and conclude in the usual way (λ denoting a constant)

$$b'' = \lambda b, \quad ca'' + da' = a(\lambda + 1). \tag{2.31}$$

In a hyperbolic domain $c > 0$, in an elliptic domain $c < 0$. The Eqs. (2.31) may be followed up for particular yield conditions. In the "classical" case $c = 4$, and $d = 0$; then (2.21) reduces to

$$\frac{\partial^2 X}{\partial\vartheta^2} - 4\frac{\partial^2 X}{\partial s^2} = X,$$

for which the "general solution" can be given. For (2.31) we obtain

$$b'' - \lambda b = 0, \quad 4a'' = a(\lambda + 1),$$

which leads to well-known solutions.

As an other example consider the parabola condition and Eq. (2.27). Putting now

$$\psi(s,\vartheta) = p(s)q(\vartheta), \tag{2.32}$$

we find with $a = 1 + \sqrt{2}$ and λ again denoting some constant,

$$q'' = \lambda q \quad \text{and} \quad (a^2 - s^2)p'' - (a + s)p' - \lambda p = 0. \tag{2.33}$$

Next, introducing new variables u and U by

$$s = a(2u - 1), \quad \frac{dp}{ds} = \frac{1}{2a}\frac{dU}{du}, \quad \frac{d^2p}{ds^2} = \frac{1}{4s^2}\frac{d^2U}{du^2},$$

[6] These equations may be transformed to standard forms (2f, pp. 8, 9, 12).

we find

$$u(1-u)\frac{d^2U}{du^2} - u\frac{dU}{du} - \lambda U = 0 \tag{2.34}$$

which is a hypergeometric equation. Putting $\lambda = -n^2$ and

$$q = C \sin n(\vartheta - \vartheta_0),$$

we can combine $q(\vartheta)$ with solutions of (2.34) to obtain solutions $\psi(s,\vartheta)$ of the form (2.32) which in turn may be superposed.

One could likewise apply more modern operator methods to our linear equations. Such linearizations are of value, just as in aerodynamics. However, the main difficulty of plasticity theory lies in the setting up and solving of complete boundary problems, where in general the boundary conditions are given in the physical plane. Our linearizations point the way for finding particular solutions which may lend themselves to the construction of solutions of actual problems.

e. Sauer's and Neuber's Linearization of the Stress Equations. A very simple and natural choice of stress variables has been made by Neuber (14) and Sauer (19). The yield condition is assumed in the form, also valid for an anisotropic medium:

$$\sigma_y = k(\sigma_x, \tau). \tag{2.35}$$

That is, σ_y is given in terms of σ_x and τ, which are the components of the stress vector corresponding to the x-direction. Then

$$\frac{\partial \sigma_y}{\partial y} = \frac{\partial k}{\partial \sigma_x}\frac{\partial \sigma_x}{\partial y} + \frac{\partial k}{\partial \tau}\frac{\partial \tau}{\partial y},$$

and the Eqs. (2.1) become, with $\dfrac{\partial k}{\partial \sigma_x} = k_1$, $\dfrac{\partial k}{\partial \tau} = k_2$,

$$\begin{aligned} \frac{\partial \sigma_x}{\partial x} + \frac{\partial \tau}{\partial y} &= 0, \\ k_1\frac{\partial \sigma_x}{\partial y} + \frac{\partial \tau}{\partial x} + k_2\frac{\partial \tau}{\partial y} &= 0. \end{aligned} \tag{2.36}$$

Here k_1 and k_2 depend on σ_x and τ only, hence the system (2.36) is reducible. Using again the method of exchange of variables (this approach is different from Sauer's) we have, if the corresponding Jacobian is different from zero,

$$\frac{\partial \sigma_x}{\partial x} : \frac{\partial \sigma_x}{\partial y} : \frac{\partial \tau}{\partial x} : \frac{\partial \tau}{\partial y} = \frac{\partial y}{\partial \tau} : -\frac{\partial x}{\partial \tau} : -\frac{\partial y}{\partial \sigma_x} : \frac{\partial x}{\partial \sigma_x}, \tag{2.37}$$

and obtain the linear system

$$\frac{\partial x}{\partial \sigma_x} + \frac{\partial y}{\partial \tau} = 0, \tag{2.38}$$

$$k_2 \frac{\partial x}{\partial \sigma_x} - k_1 \frac{\partial x}{\partial \tau} - \frac{\partial y}{\partial \sigma_x} = 0.$$

System (2.36) corresponds to our (2.6), and (2.38) to (2.8); Eqs. (2.36) and (2.38) are indeed very simple. However k_1 and k_2 depend in general on both, σ_x and τ, in contrast to (2.8) where the coefficients depend on one variable only; also the representation (2.35) is not symmetric while the usual yield conditions are of a symmetric nature; on the other hand this setup holds also in case of anisotropy. Now put $\sigma_x = v$, $\tau = -u$,[7] then (2.38) becomes

$$\begin{aligned} k_1 \frac{\partial x}{\partial u} + k_2 \frac{\partial x}{\partial v} - \frac{\partial y}{\partial v} &= 0, \\ \frac{\partial x}{\partial v} - \frac{\partial y}{\partial u} &= 0. \end{aligned} \tag{2.38'}$$

From (2.38′) we can derive a differential equation of second order. We satisfy the second Eq. (2.38′) by

$$x = \frac{\partial \psi}{\partial u}, \quad y = \frac{\partial \psi}{\partial v}; \tag{2.39}$$

then the first Eq. (2.38) gives the *linear* equation

$$k_1 \frac{\partial^2 \psi}{\partial u^2} + k_2 \frac{\partial^2 \psi}{\partial u \partial v} - \frac{\partial^2 \psi}{\partial v^2} = 0 \tag{2.40}$$

or

$$\frac{\partial^2 \psi}{\partial \sigma_x^2} + k_2(\sigma_x,\tau) \frac{\partial^2 \psi}{\partial \sigma_x \partial \tau} - k_1(\partial_x,\tau) \frac{\partial^2 \psi}{\partial \tau^2}.$$

The above derivation has been given to show the analogy to the previous procedure, where likewise "exchange of variables" was used. Sauer himself does not use this method, nor does he derive the linear equations of first order (2.38). He directly derives a nonlinear differential equation of second order and then transforms it into a linear equation by means of the *Legendre transformation*. Let us explain this approach.

The first equation (2.1) may be satisfied by means of a "stress potential" $\varphi(x,y)$ where

$$\sigma_x = \frac{\partial \varphi}{\partial y}, \quad \tau = -\frac{\partial \varphi}{\partial x}. \tag{2.41}$$

[7] It is clear that these u and v have *nothing* to do with the u-direction and v-direction used before for the directions of principal stress.

Substituting these into the second Eq. (2.36) one obtains the quasi-linear equation of second order

$$\frac{\partial^2 \varphi}{\partial x^2} + k_2 \frac{\partial^2 \varphi}{\partial x \partial y} - k_1 \frac{\partial^2 \varphi}{\partial y^2} = 0. \tag{2.42}$$

To this we apply the Legendre transformation. Use as before $u = -\tau$, $v = \sigma_x$ and introduce a new dependent variable, ϕ, defined by

$$\begin{aligned} \phi &= ux + vy - \varphi, \\ x &= \frac{\partial \phi}{\partial u}, \quad y = \frac{\partial \phi}{\partial v}, \\ d\phi &= x\,du + y\,dv. \end{aligned} \tag{2.43}$$

Now

$$\frac{\partial^2 \phi}{\partial u^2}\frac{\partial u}{\partial x} + \frac{\partial^2 \phi}{\partial u \partial v}\frac{\partial v}{\partial x} = 1, \quad \frac{\partial^2 \phi}{\partial u^2}\frac{\partial u}{\partial y} + \frac{\partial^2 \phi}{\partial u \partial v}\frac{\partial v}{\partial y} = 0,$$

and two similar relations. With $J = \partial(u,v)/\partial(x,y)$ one has

$$\frac{\partial^2 \varphi}{\partial y^2} = \frac{\partial v}{\partial y} = J\frac{\partial^2 \phi}{\partial u^2}, \quad \frac{\partial^2 \varphi}{\partial x^2} = \frac{\partial u}{\partial x} = J\frac{\partial^2 \phi}{\partial v^2},$$
$$\frac{\partial^2 \varphi}{\partial x \partial y} = \frac{\partial u}{\partial y} = -J\frac{\partial^2 \phi}{\partial u \partial v},$$

and, under the assumption $J \neq 0$, (2.42) is transformed into the linear equation:

$$\frac{\partial^2 \phi}{\partial v^2} - k_2 \frac{\partial^2 \phi}{\partial u \partial v} - k_1 \frac{\partial^2 \phi}{\partial u^2} = 0 \tag{2.44}$$

or

$$\frac{\partial^2 \phi}{\partial \sigma_x^2} + k_2 \frac{\partial^2 \phi}{\partial \sigma_x \partial \tau} - k_1 \frac{\partial^2 \phi}{\partial \tau^2} = 0.$$

This last equation is of course the same as (2.40). It may be compared with our Eqs. (2.21) or (2.27) which seem preferable in case of an isotropic yield condition. The function $k(\sigma_x,\tau)$ and its derivatives, k_1 and k_2 will very often not be simple, in case of symmetric yield conditions. But, at any rate, (2.44) is a very elegant result. It seems however a little better to use instead of k_1 and k_2 the partial derivatives

$$\frac{\partial f}{\partial \sigma_x} = f_1, \quad \frac{\partial f}{\partial \tau} = f_2, \quad \frac{\partial f}{\partial \sigma_y} = f_3$$

of $f(\sigma_x,\sigma_y,\tau) = 0$. Then (2.42) becomes:

$$f_3\varphi_{xx} - f_2\varphi_{yy} + f_1\varphi_{yy} = 0$$

and (2.44)

$$f_3 \frac{\partial^2 \phi}{\partial \sigma_x^2} - f_2 \frac{\partial^2 \phi}{\partial \sigma_x \partial \tau} + f_1 \frac{\partial^2 \phi}{\partial \tau^2} = 0.$$

We shall return to Sauer's approach when we discuss the characteristics of our problem. Then Neuber's work on which Sauer's is partly based will also be reported on.

2. *Characteristics*

a. Characteristics of the Complete Plane Problem. Consider the complete problem (1.14)

$$\frac{\partial \sigma_x}{\partial x} + \frac{\partial \tau}{\partial y} = 0, \quad \frac{\partial \tau}{\partial x} + \frac{\partial \sigma_y}{\partial y} = 0$$

$$f(\sigma_x, \sigma_y, \tau) = 0, \tag{2.45}$$

$$\frac{\dot\epsilon_x - \dot\epsilon_y}{\dot\gamma} = \frac{\dfrac{\partial f}{\partial \sigma_x} - \dfrac{\partial f}{\partial \sigma_y}}{\dfrac{\partial f}{\partial \tau}}, \quad \frac{\dot\epsilon_x + \dot\epsilon_y}{\dot\gamma} = \frac{\dfrac{\partial f}{\partial \sigma_x} + \dfrac{\partial f}{\partial \sigma_y}}{\dfrac{\partial f}{\partial \tau}}.$$

We have previously replaced the first three Eqs. by (2.6) and had, with the notations used before:

$$\frac{\partial s}{\partial u} = f(s)\,\frac{\partial \vartheta}{\partial v}, \quad \frac{\partial s}{\partial v} = g(s)\,\frac{\partial \vartheta}{\partial u}. \tag{2.46}$$

Thus our system (2.45) is equivalent to the system of *four* equations, consisting of the two Eqs. (2.46) and the last two Eqs. (2.45). We shall sometimes distinguish them by the terms "stress equations" and "velocity equations." Together they are four equations with the dependent variables s, ϑ, v_x, v_y and the independent variables x and y, since the directional derivatives in (2.46) can be readily replaced by

$$\frac{\partial}{\partial u} = \frac{\partial}{\partial x}\cos\vartheta + \frac{\partial}{\partial y}\sin\vartheta, \text{ etc.}$$

For a system of any number of planar (by that we mean: "linear in the derivatives") equations of order one with only two independent variables, the formal theory of characteristics is almost as simple as for two such equations with two unknown functions. We want to find the *characteristic directions* and the relations which must hold between derivatives in these directions, the *compatibility relations.* It seems rather obvious that in our case our system of $m = 4$ dependent and $n = 2$ independent variables will resolve, *also with respect to the characteristics,* into two groups of equations. This, however, is not self-evident, and it may be appropriate to start with a derivation of this basic result.

We shall denote uniformly the unknowns by u_k, ($k = 1,2,3,4$) and the independent variables by x and y. Our system is then

$$L_i = a_{ik}\frac{\partial u_k}{\partial x} + b_{ik}\frac{\partial u_k}{\partial y} = c_i \quad (i = 1, \cdots 4), \tag{2.47}$$

where the usual summation convention holds.

In (2.47) all coefficients a_{ik}, b_{ik}, c_i depend on x,y, and on the u_k. (If a and b depend on x and y only and if the c are linear functions of the u, the system is linear.) We want to determine at each point certain "exceptional directions" which are defined as follows:[9] From the four Eqs. (2.47) we derive a linear combination, using constants α_i:

$$\alpha_i a_{ik}\frac{\partial u_k}{\partial x} + \alpha_i b_{ik}\frac{\partial u_k}{\partial y} = c_i\alpha_i. \tag{2.47.a}$$

With $\alpha_i a_{ik} = \gamma_k$, $\alpha_i b_{ik} = \delta_k$ each term to the left $\gamma_k\frac{\partial u_k}{\partial x} + \delta_k\frac{\partial u_k}{\partial y}$ may be interpreted as the derivative of u_k in a certain direction. We wish to determine such α_i that possibly all four u_k are differentiated in the same direction. The direction normal to such a direction we call an exceptional direction; we may then also say we seek such a combination that none of the variables be differentiated in the exceptional direction. (In the case of only two independent variables it is not really necessary to introduce the direction of the normal; one may as well use the direction of the differentiation only, but it is convenient to consider both.) Denote by λ,μ direction numbers of an exceptional direction; then direction (γ_k,δ_k) must be perpendicular on direction (λ,μ), hence

$$\lambda\gamma_k + \mu\delta_k = 0, \quad (k = 1,2,3,4)$$

or

$$\lambda\alpha_i a_{ik} + \mu\alpha_i b_{ik} = 0. \tag{2.47.b}$$

We write Eqs. (2.47.b) as equations for the unknowns α_i.

$$\alpha_i(\lambda a_{ik} + \mu b_{ik}) = 0, \quad (k = 1,2,3,4). \tag{2.47.c}$$

These equations can have a nontrivial solution only if the determinental equation

$$\|\lambda a_{ik} + \mu b_{ik}\| = 0 \tag{2.48}$$

holds. The left side of this equation is a determinant of order four whose general element in the ith column and kth row is $a_{ik}\lambda + b_{ik}\mu$; (2.48) is a homogeneous algebraic equation of degree four for λ/μ with coeffi-

[9] With respect to the theory of characteristics see (9),(12e), and J. Hadamard, Le problème de Cauchy et les équations aux derivées partielles linéaires hyperboliques, Paris, 1932; see also the paper by Symonds (21); of course, much is found in (1b) and (1a). We follow here in general von Mises' ideas which in turn are based on the work of Levi Civita and Hadamard.

cients dependent on the values of the coefficients of the original equations at the point P under consideration. Thus (2.48) defines in general four directions at a point P in the x,y-plane. They need not be real and they may in various ways coincide. Each direction perpendicular to such an exceptional (λ,μ)-direction we term *characteristic.*

We have still to find the combinations of the original equations which have the initially described property (2.47.b), i.e., which contain no differentiation in the exceptional directions. To find them, a root (λ_1,μ_1) is substituted in (2.47.c) and the corresponding α_i are determined. Substitution of these into (2.47.a) yields then the desired combination, or *compatibility relation* along the characteristic; corresponding to a simple root (λ,μ), there is *one* compatibility relation: to an r-fold root correspond r compatibility relations. This last case with $r = 2$ will appear in our plasticity problem.

As indicated before, in case of two independent variables one might use right away the characteristic directions instead of their normals; this amounts to writing for example dy and $-dx$ instead of λ and μ.

Now consider our particular system, that is, the two Eqs. (2.46) and the last two Eqs. (2.45). It is seen that the Eqs. (2.46) contain only $\partial s/\partial x$, $\partial s/\partial y$, $\partial \vartheta/\partial x$, $\partial \vartheta/\partial y$, while the last two contain only $\partial v_x/\partial x$, $\partial v_x/\partial y$, $\partial v_y/\partial x$, $\partial v_y/\partial y$. Hence in this case the determinant (2.48) has the form:

$$\begin{vmatrix} \lambda a_{11} + \mu b_{11}, & \lambda a_{12} + \mu b_{12} & 0 & 0 \\ \lambda a_{21} + \mu b_{21}, & \lambda a_{22} + \mu b_{22} & 0 & 0 \\ 0 & 0 & \lambda a_{33} + \mu b_{33}, & \lambda a_{34} + \mu b_{34} \\ 0 & 0 & \lambda a_{43} + \mu b_{43}, & \lambda a_{44} + \mu b_{44} \end{vmatrix}$$

and this resolves readily into the product of two determinants. It is thus seen that, in order to find all characteristics of our system, it is sufficient to investigate separately those of the "stress equations" and those of the "velocity equations," always together with the corresponding compatibility relations.

b. Characteristics of the Stress Equations. Many of the results of this section are essentially the same as corresponding results of Sokolovsky, von Mises, Hodge, and Hill.[10] Our derivations, based on (2.6) and (2.8) are however simpler, and our results perhaps more complete (see 2,d,e,f).

Consider (2.6) and write the determinant (2.48) with $\lambda = \sin\varphi$, $\mu = -\cos\varphi$ where φ denotes the angle of a characteristic direction with the first principal direction. Then

[10] Hill's book came to my knowledge after publication of (2,d,f) and during the printing of (2,e).

$$\begin{vmatrix} \sin\varphi & f\cos\varphi \\ \cos\varphi & g\sin\varphi \end{vmatrix} = 0 \tag{2.49}$$

must hold. Hence with $\sigma_i' = \dfrac{d\sigma_i}{ds}$ and $F_i = \dfrac{\partial F}{\partial \sigma_i}$ where F is defined in (2.2):

$$\tan^2\varphi = \frac{f}{g} = \frac{\sigma_2'}{\sigma_1'} = -\frac{F_1}{F_2} = -\frac{\dot\epsilon_1}{\dot\epsilon_2} \tag{2.50}$$

$$\tan\varphi = \frac{dv}{du} = \pm\sqrt{\frac{f}{g}} = \pm\sqrt{\frac{d\sigma_2}{d\sigma_1}} \tag{2.50'}$$

(This equation has been found already in another connection in Section II,1,c.)

We have seen before that the hyperbolic points are those where f and g, or $d\sigma_1$ and $d\sigma_2$, have the same sign; then fg is positive, and likewise the

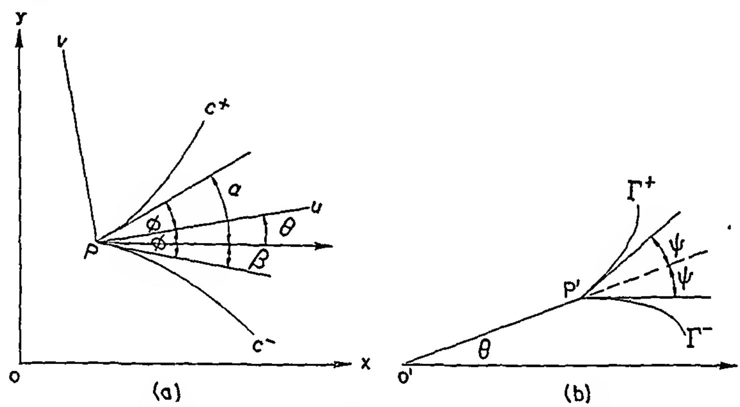

FIG. 3. Characteristics in: (a) physical plane (b) stress plane.

quotient f/g appearing in (2.50). At such a point there are two directions making angles of $+\varphi$ and $-\varphi$ with the first principal direction; we denote by C^+ and C^- the characteristic curves making at each point those angles $+\varphi$ and $-\varphi$ respectively with the first principal direction, and by

$$\alpha = \vartheta + \varphi, \quad \beta = \vartheta - \varphi, \tag{2.51}$$

the angles of such a curve with the x-axis. We have then for the direction coefficient of a characteristic, the upper sign applying to C^+

$$\frac{dy}{dx} = \tan(\vartheta \pm \varphi) = \frac{\tan\vartheta \pm \sqrt{\dfrac{f}{g}}}{1 \mp \tan\vartheta\sqrt{\dfrac{f}{g}}}. \tag{2.50''}$$

The angle φ in (2.50) and (2.50') depends only on s; here (2.51) together with (2.50'') shows clearly how the characteristics depend on the respec-

tive solution under consideration. If such a solution

$$s = s(x,y), \quad \vartheta = \vartheta(x,y)$$

is introduced into (2.50″) this becomes an ordinary differential equation for the determination of the characteristics.

Let us next determine the corresponding compatibility relations. Multiply the first Eq. (2.6) by $\cos\varphi$, the second by $(g/f)^{1/2}\sin\varphi$. In the second Eq. (2.6), multiply the first term by $\sin\varphi$, the second by $(f/g)^{1/2}$ $\cos\varphi$ and add (at a hyperbolic point f/g is nowhere zero or infinite). We obtain

$$\frac{\partial s}{\partial u}\cos\varphi + \frac{\partial s}{\partial v}\sin\varphi = \sqrt{fg}\cdot\left(\frac{\partial\vartheta}{\partial u}\cos\varphi + \frac{\partial\vartheta}{\partial v}\sin\varphi\right);$$

on denoting by $\partial/\partial l^{\pm}$ differentiation in a characteristic direction, the result is

$$\frac{\partial s}{\partial l^+} = \sqrt{fg}\,\frac{\partial\vartheta}{\partial l^+}, \quad \frac{\partial s}{\partial l^-} = \sqrt{fg}\,\frac{\partial\vartheta}{\partial l^-}. \tag{2.52}$$

These are the desired compatibility relations, being relations between the derivatives of the dependent variables along C^+ or C^- respectively. They do not depend on the validity of the transformation (2.7).

The C^+,C^- are the images of *fixed characteristics* in the stress graph; we denote them by Γ^+, and Γ^-. It follows from (2.21) that for these fixed characteristics

$$\frac{d\vartheta}{ds} = \pm\frac{1}{\sqrt{fg}} = \pm\frac{\sqrt{\sigma_1'\sigma_2'}}{\sigma_2 - \sigma_1}. \tag{2.53}$$

This same result is found if the characteristic determinant is computed for Eqs. (2.8), and again the same result is expressed in (2.52). (Note that computing (2.53) in these two ways, once by means of (2.8) and once from (2.52), gives a proof of the fact that the characteristics, Γ, in the stress graph are at the same time the images of the C in the x,y-plane. Note also that a compatibility relation like (2.52) contains in principle the right sides of the given differential equations. In our case, in (2.6), these right sides are zero. On the other hand, the mapping which leads from (2.6) to (2.8) is only possible if the right sides of the equations are zero; in this case the compatibility relations appear in the two forms (2.52) and (2.53).)

We might ask whether some simple relation exists between the directions of the fixed Γ-curves in the stress graphs and the corresponding characteristics in the physical plane, similar to that between the epicycloids and Mach lines in gas dynamics. For our choice of stress variables the answer is negative. Relations between the derivatives are, for example,

$$\tan \varphi = \frac{dv}{du} = \frac{d\vartheta}{ds} \frac{\sigma_2 - \sigma_1}{\sigma_1'}, \quad \text{or} \quad \cot \varphi = \frac{du}{dv} = \frac{d\vartheta}{ds} \frac{\sigma_2 - \sigma_1}{\sigma_2'}.$$

(These are of course again the compatibility relations.) Nevertheless a construction of the C-curves which uses the Γ-curves is possible in our case as for any reducible system (see Section II,2,i) and is almost as simple as the corresponding construction in gas dynamics. A very elegant relation between characteristics and their images in the stress graph exists for the Sauer-Neuber choice of stress variables (Section II,2,e).

Returning to (2.53) we note that the Γ^+ and Γ^- make equal angles $+\psi$ and $-\psi$ with the radius vector in the stress graph, if s and ϑ are polar coordinates, and $\tan \psi = s d\vartheta/ds$. From (2.52) it is also seen that C^+ corresponds to Γ^+, and C^- to Γ^-. The Γ-curves can be found once and for all by quadratures. In fact, introducing according to (2.53)

$$G(s) = \int^s \frac{ds}{\sqrt{fg}}, \tag{2.53'}$$

we have for Γ^+ and Γ^- respectively

$$G(s) - \vartheta = \text{const.}, \quad G(s) + \vartheta = \text{const.} \tag{2.53''}$$

c. Characteristic Coordinates. These last relations suggest the introduction of characteristic coordinates. Let us denote the C^+ and C^- as ξ-lines and η-lines respectively. Since on a ξ-line $\vartheta - G(s)$ and on an η-line $\vartheta + G(s)$ remains constant, we put similar to the procedure in the classical case

$$G(s) + \vartheta = 2\xi, \quad G(s) - \vartheta = 2\eta, \tag{2.54}$$

whence

$$\vartheta = \xi - \eta, \quad G(s) = \xi + \eta. \tag{2.54'}$$

We may likewise use ξ and η as stress variables instead of s and ϑ. (For the following compare, for example, (2c, p. 36 ff.); there the characteristics are denoted as α-lines and β-lines, the orientation is different from the present one, and ϑ denotes the angle between an α-line and the x-axis.) From (2.50'') it follows that

$$\frac{\partial y}{\partial \xi} = \frac{\partial x}{\partial \xi} \tan (\vartheta + \varphi), \quad \frac{\partial y}{\partial \eta} = \frac{\partial x}{\partial \eta} \tan (\vartheta - \varphi). \tag{2.55}$$

Here, as (2.54') shows, s and consequently $\varphi(s)$ depend on $\xi + \eta$, hence $\tan (\vartheta + \varphi)$ and $\tan (\vartheta - \varphi)$ depend on ξ and η, and (2.55) thus constitutes a system of two *linear* partial differential equations with x and y as the dependent, ξ and η as the independent variables. From any solutions of these equations one may then deduce ξ, η (or s, ϑ) as functions of

x,y. From (2.55) one may obtain equations of second order for x alone or for y alone which generalize equations of Oseen known in the classical theory [see (26‴) and (30) in (2c, p. 40)].

The equations corresponding to (2.53″) in the classical case form the starting point for the study of the geometry of the slip line field. Without going into any details, we shall here indicate some immediate consequences. Consider two fixed lines of the same family, say two ξ-lines, $\eta = \eta_0$ and $\eta = \eta_1$, and denote by ξ_L an arbitrary value of ξ; then from (2.54′).

$$\epsilon = \vartheta(\xi_L,\eta_1) - \vartheta(\xi_L,\eta_0) = \xi_L - \eta_1 - (\xi_L - \eta_0) = \eta_0 - \eta_1;$$

thus ϵ depends only on the two fixed ξ-lines and not on the variable η-line. Similarly, interchanging the role of the two families

$$\epsilon' = \vartheta(\xi_1,\eta_L) - \vartheta(\xi_0,\eta_L) = (\xi_1 - \eta_L) - (\xi_0 - \eta_L) = \xi_1 - \xi_0.$$

Thus: *Denote by A and B two fixed curves of one of the two families and by C_L a variable curve of the other family. The angle formed by the two first principal directions at the points of intersection, A_L, B_l is the same for each curve C_k.* A similar relation holds for $G(s)$:

$$\begin{aligned} \epsilon &= G(\xi_l,\eta_0) - G(\xi_l,\eta_1) = \eta_0 - \eta_1, \\ \epsilon' &= G(\xi_1,\eta_l) - G(\xi_0,\eta_L) = \xi_1 - \xi_0. \end{aligned}$$

The difference of the values of $G(s)$ at the points of intersection of the variable curve C_L with two fixed curves, A, B of the other family does not depend on C_k; it is equal to the above introduced angles ϵ or ϵ' respectively.

The simple form of the equations of the classical case which hold, if the radii of curvature are taken as dependent variables and the characteristic coordinates as independent variables, is based on the particular role which those radii of curvature play there. In fact, let ds_ξ, ds_η denote line elements of the ξ- and η-curves respectively; then in that case the derivatives $d\xi/ds_\xi$ and $d\eta/ds_\eta$ along the respective curves, i.e., the local derivatives of the coordinates which play the decisive role in the geometry of curvilinear coordinates, are simply equal to the curvature of the respective characteristics. In our more general situation put $ds_\xi = h_1 d\xi$, $ds_\eta = h_2 d\eta$. We find then from (2.51) and (2.54′), using the relation $\dfrac{d\alpha}{d\xi} = \dfrac{d\vartheta}{d\xi} + \varphi' \dfrac{ds}{d\xi} = 1 + \dfrac{\varphi'}{G'}$ and a similar one for $\dfrac{d\beta}{d\eta}$,

$$h_1 = R_\xi\left(1 + \frac{\varphi'}{G'}\right), \quad h_2 = -R_\eta\left(1 + \frac{\varphi'}{G'}\right),$$

which for $\varphi = \pi/4$ reduce to the above-mentioned simple result. Next, according to the definition of h_1,h_2, we have for a vector $d\bar{r}$ with com-

ponents dx and dy, if $\bar{\xi}^0$, $\bar{\eta}^0$ denote unit vectors in the respective directions,

$$\frac{d\bar{r}}{d\xi} = h_1\bar{\xi}_0, \quad \frac{d\bar{r}}{d\eta} = h_2\bar{\eta}^0,$$

or if, as in (2.51), $\alpha = \vartheta + \varphi$, $\beta = \vartheta - \varphi$

$$\begin{aligned} \frac{\partial x}{\partial \xi} &= h_1 \cos \alpha, \quad \frac{\partial x}{\partial \eta} = h_2 \cos \beta, \\ \frac{\partial y}{\partial \xi} &= h_1 \sin \alpha, \quad \frac{\partial y}{\partial \eta} = h_2 \sin \beta. \end{aligned} \tag{2.56}$$

Here we differentiate the first equation with respect to η, the second with respect to ξ, using the relation

$$\frac{d\alpha}{d\eta} = \frac{d(\vartheta + \varphi)}{d\eta} = -1 + \frac{d\varphi}{d\eta} = -1 + \frac{\varphi'}{G'}$$

and similarly

$$\frac{d\beta}{d\xi} = 1 - \frac{\varphi'}{G'},$$

and then subtract; in the same way we deal with the third and fourth Eq. (2.56); the result is:

$$\begin{aligned} &\frac{\partial h_1}{\partial \eta} \cos \alpha - \frac{\partial h_2}{\partial \xi} \cos \beta + (h_1 \sin \alpha + h_2 \sin \beta)\left(1 - \frac{\varphi'}{G'}\right) = 0, \\ &\frac{\partial h_1}{\partial \eta} \sin \alpha - \frac{\partial h_2}{\partial \xi} \sin \beta - (h_1 \cos \alpha + h_2 \cos \beta)\left(1 - \frac{\varphi'}{G'}\right) = 0. \end{aligned}$$

These may still be simplified. Multiplying the first equation by $\sin \alpha$, the second by $\cos \alpha$ and substracting we eliminate $\partial h_1/\partial\eta$; in an analogous way we eliminate $\partial h_2/\partial\xi$. The final equations are

$$\begin{aligned} \frac{\partial h_2}{\partial \xi} \sin 2\varphi + \left(\frac{\varphi'}{G'} - 1\right)(h_1 + h_2 \cos 2\varphi) &= 0 \\ \frac{\partial h_1}{\partial \eta} \sin 2\varphi + \left(\frac{\varphi'}{G'} - 1\right)(h_1 \cos 2\varphi + h_2) &= 0 \end{aligned} \tag{2.57}$$

which for $\varphi = \pi/4$, $h_1 = R_\xi$, $h_2 = -R_\eta$ reduce to the well-known simple equations for the radii of curvature mentioned above which in the special case form the basis for the integration of the stress equations. Our Eqs. (2.57) are linear for h_1 and h_2 with respect to ξ and η. In the special case the corresponding equations present a definite advantage compared with (2.55); here the advantage is less obvious. If a solution, h_1,h_2 of (2.57) in terms of ξ,η is known we find from (2.56) x,y in terms of ξ,η and deduce from this ξ,η (or s,ϑ) in terms of x,y.

We have thus indicated a few steps and results which generalize the well-known methods and a few of the results of the classical case. Whether this approach in which the stress variables are ξ and η rather than s and ϑ, presents an advantage need not be decided and may depend on the particular problem. We shall again use characteristic coordinates when we consider the velocity problem. For the moment we turn to another aspect of our study of the characteristics.

d. Relation to Family of Mohr Circles. Examples. So far we have defined characteristics by means of the ideas which lead to the characteristic determinant (Section II,2,a). We shall consider now an interesting geometric property of the characteristics which might also be used to define them. Consider the so-called *circle of Mohr* (we speak here only of a *plane* tensor). The stress tensor Σ, or in fact any symmetric tensor,

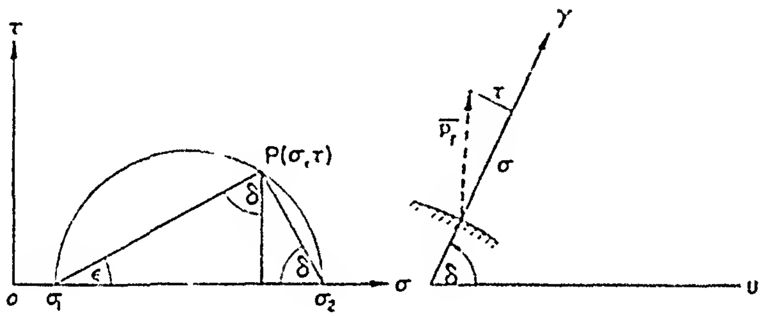

FIG. 4. Mohr's circle.

associates to any direction $\bar{\nu}$ (normal to a surface element) a stress vector $\bar{p}_\nu$, with normal component $p_{\nu\nu} = \sigma$ in the $\bar{\nu}$-direction and shear-stress component, τ, in the direction normal to $\bar{\nu}$. If σ and τ are taken as the abscissa and ordinate of a point representing the stress transmitted across the line element with normal direction $\bar{\nu}$, then the locus of all these points for all $\bar{\nu}$ is a circle with center $\frac{1}{2}(\sigma_1 + \sigma_2)$ and radius $\frac{1}{2}(\sigma_2 - \sigma_1)$. In fact denote by δ the angle between the ν-direction and the first principal direction, then from the well-known formulas

$$\sigma = \frac{\sigma_1 + \sigma_2}{2} + \frac{\sigma_1 - \sigma_2}{2}\cos 2\delta, \quad \tau = \frac{\sigma_2 - \sigma_1}{2}\sin 2\delta \tag{2.58}$$

we have immediately

$$\left(\sigma - \frac{\sigma_1 + \sigma_2}{2}\right)^2 + \tau^2 = \left(\frac{\sigma_2 - \sigma_1}{2}\right)^2, \tag{2.58'}$$

the equation of Mohr's circle. Its main value consists in furnishing directly the angle δ corresponding to each stress vector, i.e., to each point on the circumference of the circle, and vice versa. Let us show that the δ

corresponding in (2.58) to an arbitrary point P is indeed the angle so denoted in the figure. For this last one we have

$$\tan \delta = \frac{\tau}{\sigma_2 - \sigma} = \frac{\sigma - \sigma_1}{\tau} \tag{2.59}$$

or

$$\tan^2 \delta = \frac{\sigma - \sigma_1}{\sigma_2 - \sigma}; \tag{2.59'}$$

from this expression we find $\cos 2\delta$ and $\sin 2\delta$. Substitution in (2.58) shows this to be satisfied identically in σ and τ. The angle ϵ in the figure marks the direction of the line element across which the stress is transmitted. So far this is well known; we have merely presented it in a form adapted to our purpose.

Now we consider the one-dimensional family of Mohr circles which satisfy a given equation, $F(\sigma_1,\sigma_2) = 0$. The corresponding circles have an envelope whose point of contact with any circle may be real or imaginary. In case of a real contact there is on a circle, K, a point of contact with coordinates σ,τ, and corresponding angles δ and ϵ. Now identify F with the yield function of our plasticity problem. Our statement is then that $\epsilon = \varphi$, where φ is the previously introduced angle of a characteristic C_1 with the first principal direction. Or, in a condensed form: *If a one-dimensional family of Mohr circles is defined by means of a yield function, $F(\sigma_1,\sigma_2) = 0$, then the direction corresponding to a real point of contact of any circle K, with the envelope, is a characteristic direction belonging to K in the corresponding plasticity problem.* The case of no real contact corresponds of course to the elliptic case without real characteristics.

A very simple proof of this theorem is the following: We consider as in (2.3), $\sigma_1 = \sigma_1(s)$, $\sigma_2 = \sigma_2(s)$ as representation of $F(\sigma_1,\sigma_2) = 0$, and use s as parameter of our family of circles. Differentiation of (2.58') with respect to s yields

$$\sigma^2 - \sigma(\sigma_1 + \sigma_2) + \sigma_1\sigma_2 + \tau^2 = 0, \tag{2.58'}$$
$$\sigma(\sigma_1' + \sigma_2') = \sigma_1\sigma_2' + \sigma_2\sigma_1'. \tag{2.58''}$$

These define the envelope. From (2.59') we compute $\tan^2 \epsilon = \dfrac{\sigma_2 - \sigma}{\sigma - \sigma_1}$ and find:

$$\tan^2 \epsilon = \frac{\sigma_2 - \sigma}{\sigma - \sigma_1} = \frac{\sigma_2'}{\sigma_1'} = -\frac{F_1}{F_2} = \tan^2 \varphi. \tag{2.60}$$

This last value is identical with (2.50), which proves our statement.

The above proof is independent of and different from a proof of Hill (5,a, p. 295 ff.); according to Hill the first proof of this interesting relation between characteristic directions and points on the envelope of Mohr circles is due to Mandel (11). Hill also

notes that this relation seems to have been known to Prandtl (17a, p. 74). However, in the special case of the yield condition τ_{max} = const., the envelope is a horizontal line, and to the points of contact (the highest point on each circle) corresponds $\delta = \epsilon = \pi/4$; since likewise $\varphi = \pi/4$ the relation is obvious.

In Mohr's theory the envelope of a certain family of circles, "limit circles" ("Grenzspannungskreise"), is considered; the angle δ corresponding to the (σ,τ) at the point of contact with the envelope is the breaking angle. In an interesting note Torre (22) has shown that for this breaking angle Eq. (2.50) holds. The quotient σ_2'/σ_1' in (2.50) is of course computed from this envelope of limit circles, the "limit curve." He does not state the relation between these directions and characteristic directions.

We turn now to the consideration of some *examples.* The Γ curves in the stress graph have been investigated by von Mises for the three yield conditions, quadratic, hexagonal, and parabola conditions (see Section II,1,b). The formulas are in the case of the *quadratic condition:*

$$\frac{d\vartheta}{ds} = \pm \frac{\sqrt{3 - s^2}}{4 - s^2}, \tag{2.61}$$

$$\pm\vartheta = \arctan\left[\frac{s}{\sqrt{3 - s^2}}\right] - \frac{1}{2}\arctan\left[\frac{s}{2\sqrt{3 - s^2}}\right] + \text{const.},$$

and from (2.50)

$$\tan\varphi = \pm \frac{\sqrt{12 - 3s^2} - s}{2\sqrt{3 - s^2}} \tag{2.61'}$$

or

$$\tan^2\varphi = \frac{\sigma_2 - 2\sigma_1}{2\sigma_2 - \sigma_1}.$$

At the "sonic" points $\tan\varphi$ is zero or infinite, $\sigma_2 = 2\sigma_1$ or $\sigma_1 = 2\sigma_2$, $s = \pm\sqrt{3}$, and $\psi = 0$. The hyperbolic part thus extends from $-\sqrt{3} < s < +\sqrt{3}$; the elliptic part is for $\sqrt{3} < |s| < 2$. In the physical plane the "sonic line" separates the domain of hyperbolic from that of elliptic solutions; its image in the stress graph is the circle about the origin with radius $s = \sqrt{3}$.

The Γ-curves in polar coordinates are graphed in (12d). In rectangular coordinates s and ϑ, a Γ-line is monotonously increasing, e.g., from $-\pi/4$ to $+\pi/4$, it is central-symmetric, has inflection points at $s = 0$, $s = \pm\sqrt{2}$, and $d\vartheta/ds = 0$ at $s = \pm\sqrt{3}$.

Hexagonal condition (Tresca, St. Venant). The hyperbolic part is for $|s| < 1$; here $d\vartheta/ds = \pm\frac{1}{2}$; the Γ-characteristics in the hyperbolic area are ordinary spirals $\pm\vartheta = s/2$ + constant or, straight lines in rectangular coordinates s and ϑ. In the parabolic area the unique set of characteristics consists of radii through O'. In the hyperbolic area, $\tan\varphi = \pm 1$, $\alpha = \vartheta + \frac{\pi}{4}$, $\beta = \vartheta - \frac{\pi}{4}$. The characteristics are orthogonal and coincide

with the shear lines, a well-known important fact. We have seen that within our assumption of isotropy this can only happen if

$$F_1 + F_2 = \dot{\epsilon}_1 + \dot{\epsilon}_2 = 0;$$

then the yield condition must be of the form (1.10). This is the most general form of the orthogonal yield condition in case of an isotropic medium. Otherwise, if isotropy is not required, it is easily seen (see Section II,1,e) that the characteristics are orthogonal if the yield condition is of the form $\tau = Q[(\sigma_y - \sigma_x)]$ where Q denotes an arbitrary function of $(\sigma_x - \sigma_y)$.

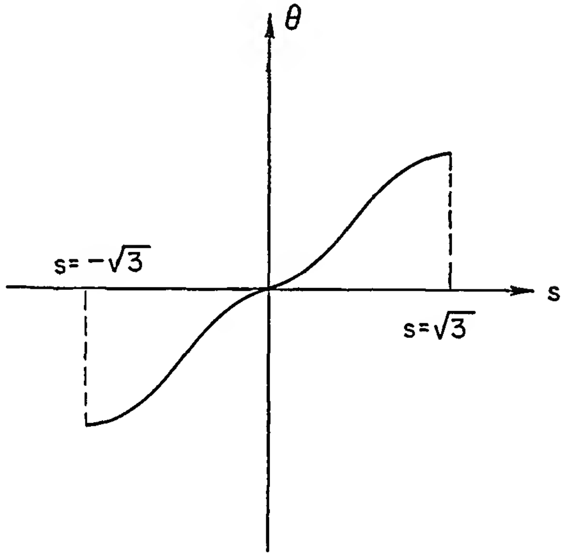

FIG. 5. Quadratic condition. $\vartheta = G(s)$.

Parabola condition. The problem is hyperbolic everywhere with the exception of $s = \pm a$ when $fg = 0$. Here

$$\frac{d\vartheta}{ds} = \pm \frac{1}{\sqrt{a^2 - s^2}}, \tag{2.62}$$

$$\vartheta = \pm \arcsin \frac{s}{a} + \text{const.}$$

These are circles through the origin if interpreted in polar coordinates and sine lines in rectangular coordinates: $s = \pm a \sin(\vartheta - \vartheta_0)$. In this case

$$\tan \varphi = \pm \sqrt{\frac{a - s}{a + s}}. \tag{2.62'}$$

e. A Parallel Reciprocal Relation between the Characteristics and Their Images. Considering Sauer's approach (Section II, 1,e), we find for the

characteristics in the physical plane

$$dy^2 - k_2\,dx\,dy - k_1\,dx^2 = 0,$$
$$(2.63)\qquad \frac{dy}{dx} = \frac{1}{2}\,(k_2 \pm \sqrt{k_2^2 + 4k_1}),$$

or, from (2.38′),

$$-k_1\,dv^2 + k_2\,du\,dv + du^2 = 0$$
$$(2.64)\qquad \frac{du}{dv} = \frac{1}{2}\,(-k_2 \pm \sqrt{k_2^2 + 4k_1}).$$

Hence denoting in (2.63) and (2.64) the direction corresponding to the upper (lower) sign of the root by the subscripts 1 and 2, we see that

$$\left(\frac{dy}{dx}\right)_1 = -\left(\frac{du}{dv}\right)_2, \quad \left(\frac{dy}{dx}\right)_2 = -\left(\frac{du}{dv}\right)_1,$$

or, in terms of the original variables $\sigma_x = v$, $\tau = -u$:

$$(2.65)\qquad \left(\frac{dy}{dx}\right)_1 = \left(\frac{d\tau}{d\sigma_x}\right)_2, \quad \left(\frac{dy}{dx}\right)_2 = \left(\frac{d\tau}{d\sigma_x}\right)_1.$$

Thus the geometric relation between the x,y-plane and the σ_x,τ-plane is very simple and elegant. The direction $(dy/dx)_1$ at a point P in the physical plane is parallel to $(d\tau/d\sigma_x)_2$ in the corresponding point P'. The characteristics in the σ_x,τ-plane are fixed characteristics and can be determined for each particular yield condition from (2.64).

The relations (2.65) follow of course likewise if the characteristic directions dy/dx and $d\tau/d\sigma_x$ are computed from the equations of second order (2.42) and (2.44) respectively. It is easily seen that, if a differential equation

$$(2.42')\qquad a\,\frac{\partial^2\varphi}{\partial x^2} + 2b\,\frac{\partial^2\varphi}{\partial x\,\partial y} + c\,\frac{\partial^2\varphi}{\partial y^2} = 0$$

is transformed by means of the Legendre transformation (2.43) into

$$(2.44')\qquad a\,\frac{\partial^2\phi}{\partial v^2} - 2b\,\frac{\partial^2\phi}{\partial u\,\partial v} + c\,\frac{\partial^2\phi}{\partial u^2} = 0,$$

then the relation of *reciprocal parallelism* holds *always* between the characteristics of (2.42′) and (2.44′) at corresponding points.

Returning to our plasticity problem we see from (2.64) and (2.65) that in the σ_x,τ-plane

$$(2.64')\qquad \left(\frac{d\tau}{d\sigma_x}\right)_1 = \frac{k_2 - \sqrt{k_2^2 + 4k_1}}{2}, \quad \left(\frac{d\tau}{d\sigma_x}\right)_2 = \frac{k_2 + \sqrt{k_2^2 + 4k_1}}{2}.$$

Here the right side is a known function of σ_x and τ. From these relations

follows an elegant result due to Neuber. Remembering (2.35) and $k_1 = \partial k/\partial \sigma_x$, $k_2 = \partial k/\partial \tau$, and using the first Eq. (2.64) we find

$$(2.64'') \qquad -\frac{\partial k}{\partial \sigma_x}\, d\sigma_x^2 - \frac{\partial k}{\partial \tau}\, d\tau\, d\sigma_x + d\tau^2 = d\tau^2 - d\sigma_x\, d\sigma_y = 0.$$

These are two relations, one along each characteristic. Using this last equation, the Neuber-Sauer relations (2.65) of reciprocal parallelism may also be written as

$$(2.65') \quad \left(\frac{dy}{dx}\right)_1 = \left(\frac{d\tau}{d\sigma_x}\right)_2 = \left(\frac{d\sigma_y}{d\tau}\right)_2, \quad \left(\frac{dy}{dx}\right)_2 = \left(\frac{d\tau}{d\sigma_x}\right)_1 = \left(\frac{d\sigma_y}{d\tau}\right)_1.$$

Neuber (14) uses as stress variables $\sigma_x - \sigma_y$ and 2τ (as compared to Sauer's (19) σ_x, τ) and obtains an equally simple construction of the characteristics. (He does not explicitly mention that his u-lines and v-lines are the characteristics.) From (2.65′) with

$$\tan \alpha = (dy/dx)_1, \quad \tan \beta = (dy/dx)_2$$

we have

$$\tan \alpha = \left(\frac{d\sigma_y}{d\tau}\right)_2, \quad \cot \alpha = \left(\frac{d\sigma_x}{d\tau}\right)_2; \quad \tan \beta = \left(\frac{d\sigma_y}{d\tau}\right)_1, \quad \cot \beta = \left(\frac{d\sigma_x}{d\tau}\right)_1;$$

subtraction gives Neuber's results

$$(2.65'') \qquad \cot 2\alpha = \left[\frac{d(\sigma_x - \sigma_y)}{d(2\tau)}\right]_2, \quad \cot 2\beta = \left[\frac{d(\sigma_x - \sigma_y)}{d(2\tau)}\right]_1$$

which allows a very elegant geometric interpretation.

We have mentioned that Sauer's yield condition is not restricted to the isotropic case, i.e., it is not necessarily composed from the invariants $\sigma_x + \sigma_y$ and $\sigma_x\sigma_y - \tau^2$. We see from (2.64′) that the characteristics, both in the x,y-plane and in the stress plane, are *orthogonal* if

$$\left(\frac{d\tau}{d\sigma_x}\right)_1 \cdot \left(\frac{d\tau}{d\sigma_x}\right)_2 = -1,$$

or $k_1 = 1$. This leads to the form

$$(2.66) \qquad \sigma_y - \sigma_x = g(\tau)$$

in contrast to (1.10), where the most general orthogonal yield condition was of the form $A[(\sigma_1 - \sigma_2)] = 0$, or $B[(\sigma_x - \sigma_y)^2 + 4\tau^2] = 0$. If (2.66) holds, we find from (2.65)

$$\frac{d\tau}{d\sigma_x} = \frac{1}{2}\,(g' \mp \sqrt{4 + g'^2}).$$

This shows that the inclination $d\tau/d\sigma_x$ of the characteristics in the stress plane depends only on τ; the characteristics intersect the lines τ = constant at a fixed angle and are therefore parallel and congruent. Further generalizations of the geometric properties of the shear lines in the classical problem follow easily.

We finally mention a further example of a yield condition given by Sauer:

$$\frac{\sigma_1 - \sigma_2}{2} = c_1 - \frac{\sigma_1 + \sigma_2}{2} \quad \text{or} \quad \sigma_x\sigma_y - \tau - c_1(\sigma_x + \sigma_y) + c_1{}^2 = 0.$$

Here the fixed characteristics in the stress plane are straight lines tangent to an ellipse.

f. The Complete Plane Problem. The *stress* Eqs. (2.1) and (2.2) have been studied by various authors previously quoted (Sokolovsky, von Mises, Neuber, Sauer, Geiringer, Hodge, Hill). The *velocity* equations have been considered only quite recently by Hodge (6a, pp. 325–26), Geiringer (2c,g), Hill (5a, p. 305 ff.).

Consider the last two Eqs. (1.14). Using the transformation formulas with $F_i = \partial F/\partial\sigma_i$, $(i = 1,2)$

$$\frac{\partial f}{\partial\sigma_x} = F_1 \cos^2\vartheta + F_2 \sin^2\vartheta, \quad \frac{\partial f}{\partial\sigma_y} = F_1 \sin^2\vartheta + F_2 \cos^2\vartheta,$$
$$\frac{\partial f}{\partial\tau} = (F_1 - F_2)\sin 2\vartheta \tag{2.67}$$

we obtain the three velocity equations of which only two are independent:

$$\frac{\partial v_x}{\partial x}(F_1 \sin^2\vartheta + F_2\cos^2\vartheta) = \frac{\partial v_y}{\partial y}(F_1\cos^2\vartheta + F_2\sin^2\vartheta),$$
$$\frac{\partial v_x}{\partial x}(F_1 - F_2)\sin 2\varphi - \left(\frac{\partial v_x}{\partial y} + \frac{\partial v_y}{\partial x}\right)(F_1\cos^2\vartheta + F_2\sin^2\vartheta) = 0, \tag{2.68}$$
$$\frac{\partial v_y}{\partial y}(F_1 - F_2)\sin 2\vartheta - \left(\frac{\partial v_x}{\partial y} + \frac{\partial v_y}{\partial x}\right)(F_1\sin^2\vartheta + F_2\cos^2\vartheta) = 0.$$

They are simplified by the use of (2.50), $\tan^2\varphi = -F_1/F_2$; add the second and third of Eqs. (2.68); next, subtract the third from the second; finally, by simple computations, with $\alpha = \vartheta + \varphi$, $\beta = \vartheta - \varphi$, the velocity equations are found in the form

$$\frac{\dot\epsilon_x + \dot\epsilon_y}{\dot\gamma} = -\frac{\cos 2\varphi}{\sin 2\vartheta},$$
$$\frac{\dot\epsilon_x - \dot\epsilon_y}{\dot\gamma} = \cot 2\vartheta, \tag{2.69}$$
$$\frac{\dot\epsilon_x}{\dot\epsilon_y} = \tan\alpha\tan\beta.$$

The second of these equations is the same as in the "classical case," because of the coaxiality of the stress tensor and the tensor Grad f (see Section II,1,c). Both the first and the third equation reduce to

$$\dot{\epsilon}_x + \dot{\epsilon}_y = 0$$

if $\varphi = \pi/4$.

The above Eqs. (2.68) can also be transformed by an easy computation into the following form, which will prove useful:

$$\dot{\epsilon}_x : \dot{\epsilon}_y : \dot{\gamma} = \sin\alpha \sin\beta : \cos\alpha \cos\beta : -\sin 2\vartheta. \tag{2.69'}$$

This, in the orthogonal case, reduces to

$$\dot{\epsilon}_x : \dot{\epsilon}_y : \dot{\gamma} = 1 : -1 : \tan 2\vartheta. \tag{2.69''}$$

If the stress problem of the two nonlinear but reducible equations has been solved, i.e., if s and ϑ, and consequently φ and ϑ are known, then any two of the three Eqs. (2.69) form a *linear* system for the two unknowns v_x, v_y. Let us find the characteristics. Denoting by $m = dy/dx$ the angular coefficient of a characteristic, one has

$$(\cos 2\varphi + \cos 2\vartheta)m^2 - 2 \sin 2\vartheta \cdot m + (\cos 2\varphi - \cos 2\vartheta) = 0,$$

and from this, after simplification,

$$m = \frac{dy}{dx} = \frac{\sin 2\vartheta + \sin 2\varphi}{\cos 2\vartheta + \cos 2\varphi} = \tan(\vartheta \pm \varphi) \tag{2.70}$$

or

$$m^+ = \tan\alpha, \quad m^- = \tan\beta.$$

This shows: If in our general problem the plastic potential coincides with the yield condition, then the characteristics of the velocity problem coincide with those of the stress problem. In terms of the complete problem: *At every hyperbolic point, i.e., a point where for the adopted yield condition $F_1F_2 < 0$, there are two doubly counting different characteristics, C^+, C^-. They form the system of characteristics for the complete problem* (1.14). *If we consider "stress problem" and "velocity problem" separately, the first is a reducible problem, while the second one, after the stresses have been found, is linear in the velocities. The C^+ and C^- make with the x-axis the angles $\alpha = \vartheta + \varphi$, and $\beta = \vartheta - \varphi$ where ϑ is the angle between x-axis and first principal direction and φ is defined by* (2.50). Let us also remember that for a characteristic direction the rate of extension is zero (Section II,1,c) at a hyperbolic point. This is seen here again by the third Eq. (2.69).

g. Velocity Plane. Since our Eqs. (2.68) or (2.69) are homogeneous we may exchange dependent and independent variables. From the first and second Eqs. (2.69) we find in the usual way

$$\left(\frac{\partial x}{\partial v_x} - \frac{\partial y}{\partial v_y}\right)\sin 2\vartheta - \left(\frac{\partial x}{\partial v_y} + \frac{\partial y}{\partial v_x}\right)\cos 2\vartheta = 0,$$
$$\left(\frac{\partial x}{\partial v_x} + \frac{\partial y}{\partial v_y}\right)\sin 2\vartheta - \left(\frac{\partial x}{\partial v_y} + \frac{\partial y}{\partial v_x}\right)\cos 2\varphi = 0.$$

Denoting by n the angular coefficient of the characteristics of this system we find the equation for n

$$n^2(\cos 2\varphi - \cos 2\vartheta) + 2n \sin 2\vartheta + (\cos 2\vartheta + \cos 2\varphi) = 0$$

or

$$n = \frac{dv_y}{dv_x} = -\cot(\vartheta \pm \varphi). \tag{2.71}$$

Consider a *velocity plane*, i.e., a plane where v_x, v_y are rectangular coordinates. In hyperbolic points of the velocity plane which are images of

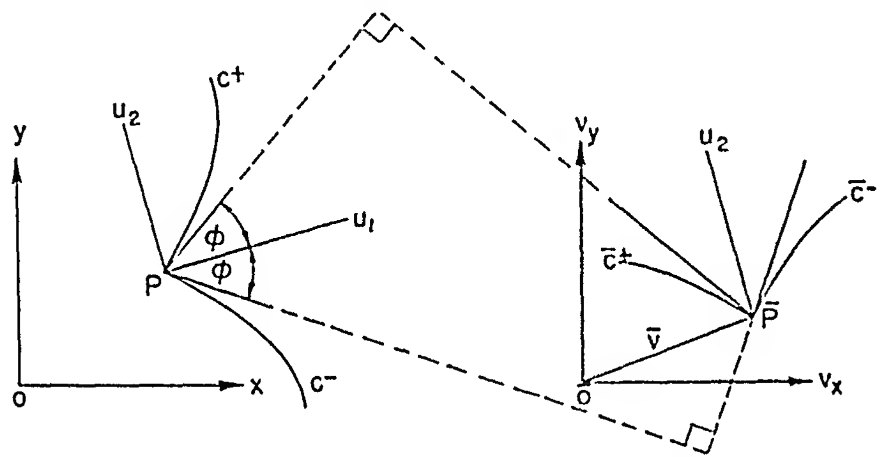

FIG. 6. Physical plane and velocity plane.

hyperbolic points in the physical plane there are two distinct directions n^+ and n^-; consequently there are in a hyperbolic domain of the velocity plane two families of characteristics $\bar{C}^+, \bar{C}^-$, the images of the C^+, C^- respectively and

$$n^+ = -\cot(\vartheta + \varphi), \quad n^- = -\cot(\vartheta - \varphi). \tag{2.71'}$$

Comparing with (2.70) we see that $m^+n^+ = -1$, $m^-n^- = -1$, or $C^+ \perp \bar{C}^+$, $C^- \perp \bar{C}^-$. It is also seen that the $\bar{C}^+$ and $\bar{C}^-$ make equal angles with the second principal direction.

This simple relation between the curves C and $\bar{C}$ reminds us of the relation between Mach lines and their images in the hodograph plane in compressible fluid theory. Here, however, the velocity equations are linear after the stress problem has been solved, and we do not need the velocity plane for purposes of linearization. We shall make use of the simple geometric relation in Section i.

Let us next consider the system of *compatibility relations* of the complete problem. Along each doubly counting characteristic two such relations must hold. One pair has already been found [Section II,2,b, Eqs. (2.52)]. Another pair of relations holds between the derivatives of the velocity components along a characteristic direction. These relations must necessarily express the fact that the rate of extension along a

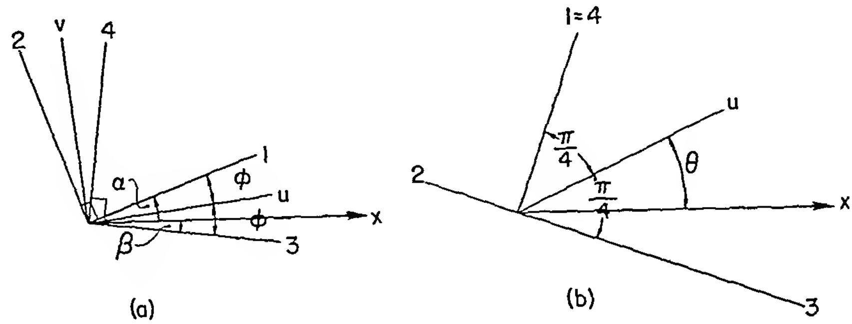

FIG. 7. Characteristic directions and their normals: (a) general case (b) orthogonal case.

characteristic is zero. Here we shall derive them from (2.71). Denote as before, by dl^+,dl^- line elements along a C^+,C^-, respectively. Then from (2.71)

$$\frac{dv_y}{dl^+} = -\frac{dv_x}{dl^+}\cot\alpha, \quad \frac{dv_y}{dl^-} = -\frac{dv_x}{dl^-}\cot\beta. \tag{2.72}$$

These compatibility relations (2.72) may also be written

$$\frac{dv_x}{dl^+}\cos\alpha + \frac{dv_y}{dl^+}\sin\alpha = 0, \quad \frac{dv_x}{dl^-}\cos\beta + \frac{dv_y}{dl^-}\sin\beta = 0.$$

Now denote by 1,2 directions which make angles α and $\alpha + \frac{\pi}{2}$ with the x-axis, by v_1,v_2 components of the vector $\bar{v}$ in these directions,

$$v_1 = v_x\cos\alpha + v_y\sin\alpha, \quad v_2 = v_y\cos\alpha - v_x\sin\alpha. \tag{2.73}$$

By the first eq. of (2.73)

$$\frac{dv_1}{dl^+} = \left(\frac{dv_x}{dl^+}\cos\alpha + \frac{dv_y}{dl^+}\sin\alpha\right) + (v_y\cos\alpha - v_x\sin\alpha)\frac{d\alpha}{dl^+} = v_2\frac{d\alpha}{dl^+}.$$

Introducing in the same way the components v_3,v_4 in directions 3,4 which make angles β and $\beta + \frac{\pi}{2}$ respectively with the x-axis, we find two similar relations [see (2,e)]:

$$\frac{dv_1}{dl^+} = v_2\frac{d\alpha}{dl^+}, \quad \frac{dv_3}{dl^-} = v_4\frac{d\beta}{dl^-} \tag{2.74}$$

or, more briefly

$$\frac{dv_1}{d\alpha} = v_2 \text{ along a } C^+, \quad \frac{dv_3}{d\beta} = v_4 \text{ along a } C^-.$$

In the "classical case," or somewhat more generally, in the orthogonal case, $\varphi = \pi/4$, the directions 1 and 4 coincide, and so does the direction 2 with the negative direction 3. In this case (2.74) reduces to

$$\frac{dv_1}{dl^+} = v_2 \frac{d\alpha}{dl^+}, \quad \frac{dv_2}{dl^-} = -v_1 \frac{d\beta}{dl^-}, \tag{2.75}$$

or, along a C^+ or C^- respectively,

$$\frac{dv_1}{d\alpha} - v_2 = 0, \qquad \frac{dv_2}{d\beta} + v_1 = 0. \tag{2.75'}$$

These relations are well known in the classical case as velocity equations along the slip lines (2a).

In (2.74) there are four different components of $\bar{v}$, of which we may choose two, v_1 and v_3, the components in the characteristic directions, and express the other components in terms of them, using $\alpha - \beta = 2\varphi$, and

$$v_3 = v_1 \cos 2\varphi - v_2 \sin 2\varphi, \quad v_1 = v_3 \cos 2\varphi + v_4 \sin 2\varphi.$$

Hence the relations (2.74) and (2.74′) take the form[11]

$$\frac{dv_1}{d\alpha} = \frac{v_1 \cos 2\varphi - v_3}{\sin 2\varphi} \text{ along } C^+, \quad \frac{dv_3}{d\beta} = \frac{v_1 - v_3 \cos 2\varphi}{\sin 2\varphi} \text{ along } C^- \tag{2.74''}$$

which for $\varphi = \pi/4$, $v_2 = v_3$ reduce to (2.75′). Also, denoting by R^+ and R^- the radii of curvature of C^+ and C^- respectively, Eqs. (2.74) become

$$\frac{dv_1}{dl^+} - \frac{v_2}{R^+} = 0, \quad \frac{dv_3}{dl^-} - \frac{v_4}{R^-} = 0, \tag{2.74'''}$$

and, corresponding to (2.74′′)

$$\frac{dv_1}{dl^+} = \frac{v_1 \cos 2\varphi - v_3}{R^+ \sin 2\varphi}, \quad \frac{dv_3}{dl^-} = \frac{v_1 - v_3 \cos 2\varphi}{R^- \sin 2\varphi}. \tag{2.74$^{\text{IV}}$}$$

We know that the unit extension along a characteristic is zero. But the left sides of (2.74$^{\text{IV}}$) are just the unit extensions, i.e., *the strain rates,* $\dot{\epsilon}_\xi$ *and* $\dot{\epsilon}_\eta$ along the characteristic directions. Hence the relations (2.74) in their various forms express *the fact that* $\dot{\epsilon}_\xi = 0$, $\dot{\epsilon}_\eta = 0$ *along the respective characteristics.*

We consider in this paper the problem (1.14) or (2.45) as the general

[11] The same equations for von Mises' yield condition have been found independently by Hill (5a), p. 306.

plane problem. Let us, however, investigate for a moment the consequences of a formulation where plastic potential and yield function are *not identical.* Denote as before by $f(\sigma_x,\sigma_y,\tau) = F(\sigma_1,\sigma_2)$ the yield function, but by $h(\sigma_x,\sigma_y,\tau) = H(\sigma_1,\sigma_2)$ the plastic potential, then the "stress problem" (Section II,2,a,b) remains unchanged, but the velocity equations are now

$$\frac{\partial h}{\partial \sigma_x}:\frac{\partial h}{\partial \sigma_y}:\frac{\partial h}{\partial \tau} = \dot{\epsilon}_x:\dot{\epsilon}_y:\dot{\gamma}$$

or

$$\text{(2.69*)} \qquad \frac{\dot{\epsilon}_x - \dot{\epsilon}_y}{\dot{\gamma}} = \cot 2\vartheta, \quad \frac{\dot{\epsilon}_x + \dot{\epsilon}_y}{\dot{\gamma}} = -\frac{\cos 2\psi}{\sin 2\vartheta}, \quad \frac{\dot{\epsilon}_x}{\dot{\epsilon}_y} = \tan\gamma\tan\delta,$$

where

$$\text{(2.50*)} \qquad \tan^2\psi = -\frac{H_1}{H_2} = -\frac{\dot{\epsilon}_1}{\dot{\epsilon}_2},$$

$$\text{(2.51*)} \qquad \gamma = \vartheta + \psi, \quad \delta = \vartheta - \psi.$$

The characteristics of (2.69*), K^+,K^- are real if H_1 and H_2 are of opposite sign. At such a point they make the angles γ and δ with the x-axis; we have now no longer coincident characteristics of the "stress" and "velocity" problem. The velocity characteristics are orthogonal if $H_1 + H_2 = \dfrac{\partial h}{\partial \sigma_x} + \dfrac{\partial h}{\partial \sigma_y} = 0$, while the orthogonality of the curves C^+,C^- depends on the vanishing of the sum $F_1 + F_2$. C^+,C^- are mapped onto Γ^+,Γ^- of the stress graph, K^+,K^- onto $\bar{K}^+,\bar{K}^-$ of the velocity plane (Fig. 8).

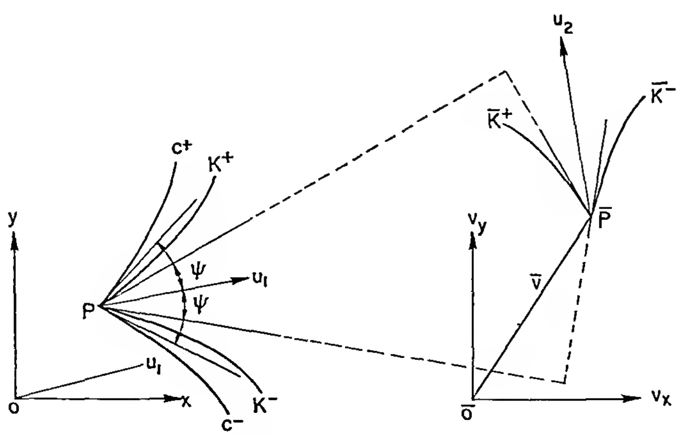

FIG. 8. Physical plane and velocity plane; total hyperbolic point.

The strain rate is zero along a velocity characteristic, and the velocity compatibility conditions hold along them. If both F_1F_2 and H_1H_2 are negative, there are at such a fully hyperbolic point four real and distinct

characteristics, C^+,C^- and K^+,K^-. Various other combinations may arise.

Let us now review the results of Sections II,1,c and II,2,b. In Section II,1,c we have seen that for a characteristic direction the rate of extension is zero. [This is expressed in the compatability relations (2.74).] Consider now the two tensors Grad f, and Grad h, where f and h are yield function and plastic potential respectively. From (2.50) and (2.50*) we see immediately that

$$F_1 \cos^2 \varphi + F_2 \sin^2 \varphi = 0 \qquad \text{and} \qquad H_1 \cos^2 \psi + H_2 \sin^2 \psi = 0.$$

Hence if we denote by ξ and ζ respectively the directions of a stress characteristic C, and of a velocity characteristic K, it is seen that

$$(\text{Grad } f)_{\xi\xi} = 0, \quad (\text{Grad } h)_{\zeta\zeta} = 0. \tag{2.$\overline{50}$}$$

The scalar component of the tensors Grad f, and Grad h, in the respective characteristic direction is zero. From the second of these relations it follows, however, that likewise

$$\dot{E}_{\zeta\zeta} = 0; \tag{2.$\overline{74}$}$$

this means that *the rate of extension in the direction of a velocity characteristic vanishes.*

Finally consider the Mohr circles. We have introduced (p. 236) the family of Mohr circles corresponding to $F(\sigma_1,\sigma_2) = 0$. We may likewise consider the Mohr circles singled out by means of $H(\sigma_1,\sigma_2) = 0$. With the notations of Section II,2,b we had found that $\epsilon = \varphi$, where ϵ is the angle belonging to the point of contact of a circle of the F-family with its envelope. If we denote by η the analogous angle (Fig. 4) for the circles of the family $H(\sigma_1,\sigma_2) = 0$ we see that

$$\epsilon = \varphi, \quad \eta = \psi. \tag{2.60*}$$

Hence, both stress and velocity characteristics may be defined by means of the envelopes of Mohr circles.

These are a few of the parallelisms between the two kinds of characteristics, which are perhaps better understood if $F \neq H$ is assumed. On the other hand, we have also pointed out the important basic *differences* between the respective problems.

h. Initial Value Problems. The special situation where the "stress problem" (2.1), (2.2) is "statically determined" arises if the stresses are uniquely determined by the three Eqs. (2.1), (2.2), and by appropriate stress boundary conditions. In this case, after the stresses have been found, the velocities may be determined by means of the velocity equations and a sufficient number of velocity boundary conditions. The other

case where the stress boundary conditions are not sufficient to determine a stress solution uniquely is more difficult; then the four (or five) equations of the complete problem together with all boundary conditions must be considered more or less simultaneously. Practically, this is often a problem of trial and error: One takes a particular solution of the stress equations which satisfies the given stress boundary condition (and perhaps also a trial choice of a plastic-rigid boundary); then one tries to fit to this a velocity solution which satisfies the remaining boundary conditions (see Part III).

At present we shall formulate certain mathematical problems (see, however, also III,4,5,6). We shall discuss approximate solutions of these problems, particularly such as are based on the consideration of the stress graph and the velocity plane.

First we remember again: if we split the problem into a stress problem, given by (2.1), (2.2), or by (2.6), or by (2.36), etc. and a velocity problem defined, for example, by (2.66), or (2.69), or (2.74), at any rate the first problem is *reducible* and the second one *linear*, inasmuch as the stress problem has been solved beforehand. The reducible character of the stress problem is the reason why here the determination of the characteristics is identical with the finding of the solution, while the (linear) velocity problem actually starts after the characteristics have been found. Another consequence is that, for example, the occurrence of rectilinear characteristics means very much for the stress problem (namely that the state of stress must be constant along such a line) and very little for the velocity problem (see II,3 dealing with simple waves).

Consider now the *stress problem* and, to fix the ideas, think of the Eqs. (2.6) with s and ϑ as dependent variables. Take first the "*Cauchy problem.*" Along an arc K given by $x = x(t)$, $y = y(t)$ (with piecewise continuous derivatives and $\dot{x}^2 + \dot{y}^2 \neq 0$ everywhere along K), values of s and ϑ are given in such a way that the curve has nowhere a characteristic direction; this means that the angle between the curve and the x-axis is nowhere equal either to $\vartheta + \varphi(s)$ or to $\vartheta - \varphi(s)$, where $\varphi(s)$ follows from the respective yield condition [e.g., (2.61′) or (2.62′) for the quadratic or the parabola condition]. These data determine a solution, $s = s(x,y)$, $\vartheta = \vartheta(x,y)$, on both sides in the vicinity of K; on K the solution assumes the prescribed values; this vicinity is wholly contained in the quadrangle formed by the four curves issuing at the ends of K which are characteristics for this solution; and at the points within this quadrangle there is no other solution which takes on the prescribed values and satisfies certain "continuity conditions," for the derivatives.[12]

[12] Existence and uniqueness problems for such reducible systems have been widely considered these last years particularly in connection with problems of gas dynamics

Consider now the *velocity* equations also with respect to the *Cauchy problem*.[13] After $s = s(x,y)$, $\vartheta = \vartheta(x,y)$ are known, the velocity problem is a linear one. Along the previously considered curve K, which by hypothesis has nowhere a characteristic direction, we may now give quite arbitrarily values v_x and v_y, or, in other words, the vector $\bar{v}$ may be prescribed along K. Then a uniquely determined velocity solution exists in the whole characteristic quadrangle determined by K and by the four characteristics issuing at the end points of K. The characteristics in turn are determined by means of the stress solution s, ϑ. (Remember that $\alpha = \vartheta + \varphi(s)$, where α is the angle between a C^+ and the x-axis, and ϑ and s have been found in solving the stress problem.) To summarize: along a curve K values of s and ϑ are prescribed in such a way that the curve nowhere becomes characteristic; along this curve also the velocity vector is arbitrarily prescribed. Then s,ϑ,v_x,v_y are determined within the characteristic quadrangle.

Next consider the *characteristic initial value problem.* In the linear problem of two linear partial differential equations for two unknown functions in two independent variables the characteristics form a net of curves (real or imaginary) completely determined by an ordinary differential equation between the independent variables. In the reducible case with which we are dealing as far as the stress problem is concerned, the situation is quite different. One may, for example, consider an arbitrary curve, C, $y = y(x)$ and *make* it a characteristic, e.g. a C^+, by determining for every x, the $s = s(x)$, $\vartheta = \vartheta(x)$ from the two relations (2.51) and (2.53) (where in case of a C^+ the first relation (2.53) and the positive sign in (2.51) is to be chosen). Equation (2.51) is a relation between the direction of the curve C^+ at the point with abscissa x and the variables s and ϑ at this point; Eq. (2.53) is a relation between ds and $d\vartheta$, or a relation between s and ϑ, but it contains still an arbitrary constant; at any rate it is not possible to prescribe one of the dependent variables, say s, arbitrarily along an assumed curve C, which is to become a characteristic. (This *is* possible in the linear case, where, in turn, C is not arbitrary.)

If on the other hand along an interval of x a function $s = s(x)$ is prescribed arbitrarily, then $y = y(x)$, which determines the shape of the

(for example (1a,c) and (3), Section I and particularly Section II). Our problem in this connection can only be to point out a few of the consequences of these investigations with respect to our particular questions.

[13] It is not our task to formulate here precise existence and uniqueness theorems. We try, however, to describe correctly the main features of the initial value problems which present themselves in our general, nonlinear plasticity problem. In several of the books on our subject the formulations are rather careless; various examples could be quoted.

curve, as well as $\vartheta = \vartheta(x)$, must be derived from (2.51) and (2.53), if the curve is to be a characteristic. Briefly: y,s, and ϑ together must satisfy the above relations (of which one is the condition for a curve to be a characteristic, the other the compatibility relation along this characteristic between the dependent variables); the curve $y(x)$ is then a characteristic. We may also describe the situation as follows: often it is natural in a plasticity problem to know that a curve *is* a characteristic, e.g. a plastic rigid boundary or a boundary of a region for which one has solved a Cauchy problem. Then all one may prescribe along such a curve is *one* value, say s_0, at *one* point; this value will serve to determine the constant in the first relation (2.53″).

For *two intersecting characteristics* we conclude from the preceding remarks: Suppose we know that of two intersecting curves one is a C^+, one a C^-, then *nothing* else can be prescribed arbitrarily: the values s_0 and ϑ_0 at the point of intersection must satisfy four relations which determine them as well as the two constants in (2.53″). All other values s,ϑ along them are likewise determined, and the stresses s and ϑ may be found in a characteristic quadrangle. The stresses being known, the velocity problem is linear with given characteristics and therefore along a characteristic curve one component of $\bar{v}$ may be arbitrarily prescribed; the other follows from the respective velocity compatibility relation. If one and the same component is given along both characteristics, then another component must still be given at *one* point of one of the characteristics. (Also a linear combination of two components may be given along one, and another combination of the same components along the other characteristic.) Reviewing one particularly important situation, we may say: If we know that of two intersecting arcs one, AB, is a characteristic, C^+, the other, AC is a C^-; and if we know in addition v_x (or v_y) along AB, and v_y (or v_x) along AC (expressed slightly more generally, $\bar{v}$ must be known along BAC in a way satisfying the compatibility relations), then a solution of the complete problem, consisting of stresses and velocities and assuming the prescribed values on BAC is determined in the characteristic quadrangle $ABDC$. The characteristics CD,BD depend, however, on the stress solution.

i. Approximate Solutions of Initial Value Problems. In the classical case the usual approximate solution of the stress problem is based on the well-known properties of the slip line field. These must be modified in our more general situation according to (2.53″). We shall discuss here primarily a geometric approach, which for the stress problem imitates the Prandtl-Busemann construction of a characteristic net, well known in gas dynamics, while for the velocity problem our velocity plane seems a useful tool. (Such a type of construction is valid for *any* system of

reducible equations; it becomes a little more simple if, as in the approach of Neuber or of Sauer, particularly simple geometric relations exist between the characteristics in the stress plane and those in the physical plane.) Another procedure consists in *computing* the unknowns from finite difference equations corresponding to the differential relations derived in the preceding pages. We shall return to that very briefly.

Cauchy problem. On the noncharacteristic arc K we know the values of s and ϑ; we may therefore find and graph the image curve K' of K in the stress plane, and K' will certainly not be a characteristic.

Let us make a preliminary remark. We may use for the constructions we are going to explain any stress plane, for example the s,ϑ-plane or the σ_x,τ-plane. But the ξ,η-plane defined by (2.54) is distinguished by the

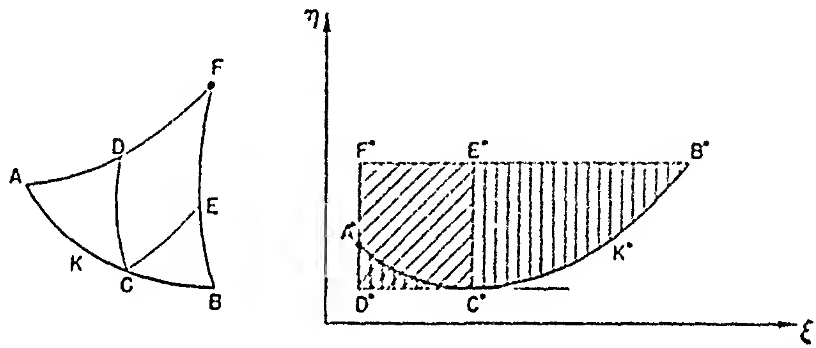

FIG. 9. Cauchy problem with doubly covered characteristic stress plane.

fact that there the characteristics are the coordinate lines η = constant, ξ = constant. It may (or may not) be advantageous to use the ξ,η-plane for the construction; however, the following remark will be particularly simple, if we explain it for this plane. Call K'' the image of K in the ξ,η-plane; it will not be a characteristic, but it may be that it has at one or more points a characteristic direction parallel to the ξ- or η-axis. Then it is necessary to subdivide K'' into arcs which have the ξ- or η-direction at most at the end points. To fix the ideas, consider a curve $A''B''$ which is horizontal at C'' and let $A''C''$ as well as $B''C''$ be monotonous. Then by the procedure to be described we determine in the physical plane the nets of characteristics in the triangles ADC and CEB, where AD,DC,CE,EB are the respective characteristics through A, C, and B. It is still necessary to solve the characteristic initial value problem parting from the characteristics CD and CE. If a solution exists in ACF, we shall find it in this way, notwithstanding the fact that the tangent at C'' has characteristic direction. In the ξ,η-plane (or the s,ϑ-plane) there will be in general a doubly covered region like $A''C''D''$ in our figure. This occurrence is well known in the hodograph plane and need not

prevent existence of a unique solution in ABF. On the other hand it may be that no solution exists in ABF; then the characteristic CE (or CD) will cut into the triangle ADC (or BCE). [If we want the solution in ABF, care is needed in selecting the correct triangle $A''C''D''$ corresponding to ACD (the one below $A''C''$ in the figure).]

If we use the s,ϑ-plane the characteristic directions defined by (2.53) now play of course the role which the directions parallel to the axes played in the ξ,η-plane. These are brief indications of circumstances to be considered; they are not specific to our problem, however.

Now let us describe the procedure. On K we choose a set of points $P_1, P_2, \cdots P_n$. In the stress graph we locate on K' the corresponding points $P_1', P_2', \cdots P_n'$. Through all points P_i' we draw the known fixed Γ-characteristics, which belong to the chosen yield condition. They form a first group of meshes next to K', and determine a row of points $Q_1', \cdots Q_{n-1}'$. Through the points P_i, $(i = 1,2, \cdots n)$, where we know the values of s_i and ϑ_i, we draw straight line segments in the directions $\alpha_i = \vartheta_i + \varphi(s_i)$ and $\beta_i = \vartheta_i - \varphi(s_i)$ and obtain a second row of points $Q_i, (i = 1, \cdots (n-1))$, which correspond to the Q_i'. Hence we know (approximately) the s- and ϑ-values for the Q_i. In this way we may continue. The procedure may be refined in various respects. This construction is based on the net of fixed characteristics in the stress graph.

Moreover, in the Cauchy problem, v_x and v_y are given along K. This is a linear problem; so we draw in the velocity plane which has the rectangular coordinates, v_x, v_y the curve $\bar{K}$, the image of K. On $\bar{K}$ we mark the points $\bar{P}_i$ corresponding to the previously chosen P_i. We assume that the lattice of C-characteristics has been drawn already; now the C^+ at P is perpendicular to the $\bar{C}^+$ at $\bar{P}$ and the same is true for the C^-. Hence through the $\bar{P}_i$ we draw straight line segments in the respective perpendicular directions and find the row of points $\bar{Q}_i$ $(i = 1, \cdots (n-1))$. Since these correspond to the Q_i in the physical plane, we know now the velocity at the Q_i. Continuing in this way we find eventually a net in the velocity plane and the coordinates of each lattice point of this net give the velocity at the corresponding point in the physical plane.

Characteristic initial value problem. Consider two intersecting characteristics, C^+, C^- in the x,y-plane. In the way explained in detail in the preceding section we find the s- and ϑ-values along them, in particular s_0, ϑ_0 at the point of intersection. Next consider m points $P_{01}, P_{02}, \cdots P_{0m}$ on C^+ and n points $P_{10}, P_{20}, \cdots P_{n0}$ on C^-; draw through each P_{i0} a segment of the corresponding C^+ characteristic, and through each P_{0j} a segment of the corresponding C^-. The segments through P_{10} and P_{01} intersect at P_{11}. The corresponding values of s_{11}

and ϑ_{11} follow from the stress graph. We then draw a segment of the C^+ and of the C^- through P_{11} and find P_{21} and P_{12}; their images in the stress graph furnish the corresponding s and ϑ. In this way we continue until we have found (simultaneously) the net in the physical plane and the s,ϑ values at each point in the quadrangle.

Now the velocity problem: suppose we give v_x along the initial curve C^- and v_y along the C^+ and, consequently, know both at P_{00}. In the velocity plane we therefore know $\bar{P}_{00}$; we draw segments of a $\bar{C}^+$ and $\bar{C}^-$ in the prescribed directions through $\bar{P}_{00}$, in such a way that we continue the segment of the $\bar{C}^+$ through $\bar{P}_{00}$ until we reach the abscissa $v_x(P_{10})$. There we locate the point $\bar{P}_{10}$ and find in the same way $\bar{P}_{01}$. These furnish in turn $v_y(1,0)$ and $v_x(0,1)$. In the same way we construct the whole arc $\bar{C}^-$ and the arc $\bar{C}^+$, the images of the given C^+ and C^-, and on them the points $\bar{P}_{10} \cdots \bar{P}_{n0}$ and $\bar{P}_{01}, \cdots \bar{P}_{0m}$. These points furnish the respective $v_y(P_{i0})$ and $v_x(P_{0j})$. Next, we draw in the velocity plane a segment of a $\bar{C}^+$ through $\bar{P}_{10}$ and one of a $\bar{C}^-$ through $\bar{P}_{01}$. They intersect at $\bar{P}_{11}$. The characteristics through $\bar{P}_{11}$ and $\bar{P}_{20}$ intersect at $\bar{P}_{21}$, and these through $\bar{P}_{11}$ and $\bar{P}_{02}$ at $\bar{P}_{12}$. We so obtain the respective velocity values at P_{21} and P_{12}. In this way, always using the orthogonality with respect to the net in the x,y-plane, we find step by step a net in the velocity plane; the coordinates of the nodal points give the velocities at the corresponding points.

We finish this section with a remark on the approximate *numerical* solution of the velocity problem, once the stress problem has been solved e.g., by means of (2.53″). Knowing $s(x,y)$, $\vartheta(x,y)$ we know α,φ, and ϑ at such a point. We may then use the finite difference equivalent of (2.71) or (2.74′) or (2.74″), the choice depending on what exactly the initial data are. If, for example, v_x,v_y are given along a non-characteristic curve, (2.71) seems appropriate; if v_1 is given along a C^+ and v_3 along a C^-, we find v_3 and v_1 respectively through (2.74′) or (2.74″), and then solve a characteristic initial value problem step by step by means of the same equations. We shall omit details.

j. Plastic Rigid Boundary. Lee (8,b) has proved that in the classical case a boundary between plastic and rigid material must be a slip line. In the general case lines of maximum shear strain and characteristics are not identical. We shall prove that, with certain restrictions in the general case, the boundary must be a characteristic.

Assume that

$$\frac{\partial f}{\partial \sigma_x} + \frac{\partial f}{\partial \sigma_y} = \frac{\partial F}{\partial \sigma_1} + \frac{\partial F}{\partial \sigma_2}$$

is not identically zero. Consider a segment AB of the plastic rigid boundary and suppose that the rigid material is at rest. We shall

use a system of orthogonal curvilinear coordinates, ξ,η, in which AB is embedded such that along AB the coordinate η is constant.[14] Consider a point P, on AB, denote by v_ξ, v_η velocity components in these directions for the plastic material, by s_ξ, s_η arc lengths along the ξ-line and the η-line, increasing with increasing ξ and η and by R_ξ, R_η radii of curvature of the coordinate lines, positive in the directions of positive η and ξ

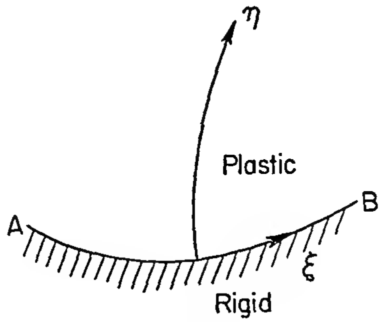

FIG. 10. Plastic-rigid boundary.

respectively. We need the strain rate component in the ξ- and η-direction. Let us give a formal derivation. Compute $\partial v_x/\partial x$, denote the angle between x and ξ by α and let then $\alpha \to 0$. We have

$$v_x = v_\xi \cos\alpha - v_\eta \sin\alpha, \quad v_y = v_\xi \sin\alpha + v_y \cos\alpha,$$

$$\frac{\partial}{\partial x} = \frac{\partial}{\partial s_\xi}\cos\alpha - \frac{\partial}{\partial s_\eta}\sin\alpha, \quad \frac{\partial}{\partial y} = \frac{\partial}{\partial s_\xi}\sin\alpha + \frac{\partial}{\partial s_\eta}\cos\alpha,$$

$$\begin{aligned}\dot\epsilon_x = \frac{\partial v_x}{\partial x} &= \cos\alpha\,\frac{\partial v_x}{\partial s_\xi} - \sin\alpha\,\frac{\partial v_x}{\partial s_\eta}\\ &= \cos\alpha\left[\frac{\partial v_\xi}{\partial s_\xi}\cos\alpha - \frac{\partial v_\eta}{\partial s_\xi}\sin\alpha - (v_\xi\sin\alpha + v_\eta\cos\alpha)\frac{d\alpha}{ds_\xi}\right]\\ &\quad - \sin\alpha\left[\frac{\partial v_\xi}{\partial s_\eta}\cos\alpha - \frac{\partial v_\eta}{\partial s_\eta}\sin\alpha - (v_\xi\sin\alpha + v_\eta\cos\alpha)\frac{d\alpha}{ds_\eta}\right].\end{aligned}$$

For $\alpha \to 0$, $\dot\epsilon_x \to \dot\epsilon_\xi$ and the result is

$$\dot\epsilon_\xi = \frac{\partial v_\xi}{\partial s_\eta} - v_\eta\frac{d\alpha}{ds_\xi} = \frac{\partial v_\xi}{\partial s_\xi} - \frac{v_\eta}{R_\xi}.$$

(This expression coincides with the left side of (2.74‴).) In a similar way the other strain rate components may be computed and the result is

$$\text{(2.76)}\quad \dot\epsilon_\xi = \frac{\partial v_\xi}{\partial s_\xi} - \frac{v_\eta}{R_\xi}, \quad \dot\epsilon_\eta = \frac{\partial v_\eta}{\partial s_\eta} - \frac{v_\xi}{R_\eta}, \quad \dot\gamma = \frac{\partial v_\xi}{\partial s_\eta} + \frac{\partial v_\eta}{\partial s_\xi} + \frac{v_\xi}{R_\xi} + \frac{v_\eta}{R_\eta}.$$

We assume that R_ξ and R_η are different from zero.

[14] The notation differs from that in Section II,2,c where ξ and η were curvilinear coordinates with the nonorthogonal characteristics as coordinate net. The ξ,η of the present section correspond rather to "1" and "2" of Section II,2,g.

Since the rigid material is at rest, the normal component v_η, must vanish along AB. As to v_ξ, assume first that it be *discontinuous* across AB, that means that v_ξ *is not zero* in the plastic material adjacent to AB. Then:

$$\dot{\epsilon}_\xi = \frac{\partial v_\xi}{\partial s_\xi}, \quad \dot{\epsilon}_\eta = \frac{\partial v_\eta}{\partial s_\eta} - \frac{v_\xi}{R_\eta}, \quad \dot{\gamma} = \frac{\partial v_\xi}{\partial s_\eta} + \frac{v_\xi}{R_\xi}. \tag{2.76'}$$

At points where $v_\xi \neq 0$, $\partial v_\xi / \partial s_\eta$ tends towards infinity;[15] all other terms on the right sides of (2.76′) are finite. Now take x and y tangential to the ξ- and η-line at P; then both $\dot{\epsilon}_x/\dot{\gamma}$ and $\dot{\epsilon}_y/\dot{\gamma}$ tend toward zero; consider the velocity equations in the form (2.69′)

$$\dot{\epsilon}_x : \dot{\epsilon}_y : \dot{\gamma} = \sin\alpha \sin\beta : \cos\alpha \cos\beta : -\sin 2\vartheta, \tag{2.69'}$$

where α is the angle that the C^+ at P makes with the x-direction, and similarly for β. At P both $\sin\alpha \sin\beta$, and $\cos\alpha \cos\beta$ must vanish. If, for example, $\sin\beta = 0$, $\beta = 0$, $\cos\beta = 1$, it follows that $\cos\alpha = 0$, $|\alpha| = \pi/2$. This means that the ξ-direction, that is the plastic boundary, has at P the C^--direction. Hence at every point this boundary has a characteristic direction. Thus the boundary AB is either a characteristic, or an envelope of characteristics. Let us first assume that AB is a characteristic, say a C^- characteristic; then $\beta = 0$. We have seen, moreover, that $\alpha = \pm\pi/2$; this means that, at P, $C^+ \perp C^-$, $\varphi = \pi/4$, or in other words, $F_1 + F_2 = 0$, $\dot{\epsilon}_1 + \dot{\epsilon}_2 = 0$ at every point P of AB.[16] We are, however, considering a yield condition where, by hypothesis, $F_1 + F_2$ is not *identically* zero. On the other hand, there will in general exist a particular value of the parameter s for which $\tan\varphi = 1$, hence $F_1 + F_2 = 0$. (In the quadratic yield condition this happens for $s = 0$, in the parabola condition for $s = 0$ likewise; in the first case $F_1 + F_2 = \sigma_1 + \sigma_2$, and for $s = 0$ we have $\sigma_1 = -2K/\sqrt{3}$, $\sigma_2 = 2K/\sqrt{3}$.) Hence the same value of s must belong to all points of AB; since this line is a characteristic, it follows from (2.53″) that the value of ϑ is also the same all along AB, or in other words, the stress tensor is constant along AB, and if β is the angle which the characteristic makes with the x-axis then along AB this $\beta = \vartheta - \pi/4$ is constant, and AB is *necessarily rectilinear*.[17] This last

[15] This is not mathematically rigorous; the following conclusions are based on this intuitive reasoning, however.

[16] It is seen immediately by considering the Mohr circle of the tensor $\dot{E}$ that an infinite $\dot{\gamma}_{xy}$ is compatible with finite $\dot{\epsilon}_x$ and $\dot{\epsilon}_y$ only if $\dot{\epsilon}_1 + \dot{\epsilon}_2 = 0$. If on the other hand one $\dot{\gamma}$ at a point is very large, almost all $\dot{\gamma}$'s at this point are of the same order of magnitude (as seen from the Mohr circle); hence arguments which are so often found, saying that a direction of infinite shear must necessarily be that of maximum shear, i.e., the 45° direction, are not conclusive.

[17] This rather surprising result seems to be related to $f = h$ (yield function equal to plastic potential).

conclusion holds only if AB is a characteristic. It might be an envelope of characteristics; then the constant in (2.53″) varies from point to point, and so does the ϑ-value, hence the above conclusion is no longer valid.

Next assume $v_\xi = 0$ in the plastic material adjacent to AB. Then from (2.76)

$$\dot\epsilon_\xi = 0, \quad \dot\epsilon_\eta = \frac{\partial v_\eta}{\partial s_\eta}, \quad \dot\gamma = \frac{\partial v_\xi}{\partial s_\eta}. \tag{2.76''}$$

If in (2.76″) the two derivatives, $\partial v_\eta/\partial s_\eta$, $\partial v_\xi/\partial s_\eta$ are different from zero, we see from (2.69′) that $\sin\alpha \sin\beta = 0$, hence either α or β or both are zero, and it follows again that AB has everywhere a *characteristic direction*. If however one of the two derivatives vanishes along AB (or part of it) we have a similar conclusion as at the beginning. In fact, if $\partial v_\eta/\partial s_\eta = 0$, then $\dot\epsilon_\xi = 0$, $\dot\epsilon_\eta = 0$, $\dot\epsilon_\xi + \dot\epsilon_\eta = F_1 + F_2 = 0$ and we conclude as before that AB (or that part of AB) is rectilinear, unless it is an envelope of characteristics. If $\dot\epsilon_\xi = \dot\gamma = 0$, $\dot\epsilon_\eta \neq 0$ then either α or β is equal to zero, $\sin 2\vartheta = 0$, and consequently both s and ϑ must have some fixed value; in fact, if $\alpha = 0$, $\vartheta = 0$, then $\beta = 0$, $\varphi = 0$, or if $\alpha = 0$, $\vartheta = \pi/2$, $\beta = \pi$, $\varphi = -\pi/2$ and we conclude again that AB *must be rectilinear.* The case where *all* four derivatives vanish remains undetermined.

Let us consider the *orthogonal case.* Equations (2.69′) are replaced by

$$\dot\epsilon_x : \dot\epsilon_y : \dot\gamma = 1 : -1 : 2\tan 2\vartheta. \tag{2.69''}$$

If now along AB (or a part of it) $v_\eta = 0$, $v_\xi \neq 0$ we conclude as before that $\dot\gamma \to \infty$, and now from (2.69″), $\vartheta = \pm\pi/4$, and since, in fact, identically $\varphi = \pi/4$, either $\alpha = 0$ or $\beta = 0$ along AB. Hence AB is a characteristic or an envelope of characteristics. Since also $v_\eta = 0$ along AB, and since $\dot\epsilon_\xi = 0$, *it follows that* v_ξ, the amount of the jump, *is constant along* AB. Hence in this case $\partial v_\xi/\partial s_\xi = 0$, $\partial v_\eta/\partial s_\xi = 0$, $\partial v_\xi/\partial s_\eta \to \infty$, $\partial v_\eta/\partial s_\eta = v_\xi/R_\eta$. Finally, if $v_\xi = 0$ along AB, then $\dot\epsilon_\xi = 0$, and from $\dot\epsilon_\xi + \dot\epsilon_\eta = 0$ also $\dot\epsilon_\eta = 0$, hence also $\partial v_\eta/\partial s_\eta = 0$ and $\dot\gamma$ reduces to $\partial v_\xi/\partial s_\eta$ (which we assume different from zero, lest all derivatives vanish). We conclude again that $\vartheta = \pm\pi/4$, and since $\varphi = \pi/4$ this only shows anew that AB is a characteristic.

Let us review the whole situation: *The boundary between a plastic region and a rigid domain* (which we assume at rest), *must be a characteristic or an envelope of characteristics. Along it the normal component of velocity must be continuous, and the tangential component has a constant value.*

In the general case of a yield condition for which the invariant $F_1 + F_2$ is not identically zero, a curved boundary is only possible if the tangential component $v_\xi = 0$ (i.e., likewise continuous across AB), and if neither

$\partial v_\xi/\partial s_\eta$ nor $\partial v_\eta/\partial s_\eta$ vanishes. Otherwise the boundary is either an envelope of characteristics or rectilinear, carrying some constant value of the stress tensor. In the orthogonal case where the above invariant is identically zero the continuity or discontinuity of the tangential component does not determine the shape of this boundary.

3. *Simple Waves*

a. Definition and General Properties. Just as in compressible fluid theory simple waves[18] play a most important role in the building up of solutions to boundary value problems in plasticity (see Part III).

Let us first consider the stress problem of simple waves. Consider the relation between physical plane and stress graph. In general a finite region of the physical plane is mapped onto a finite area of the stress plane and any element of area, $dx\,dy$, is transformed into an element of area A in the stress plane. On the other hand, the most extreme degenerate case is that of a uniform stress tensor, Σ, in all points of some region, i.e., s-constant, ϑ-constant; then the entire domain of that stress distribution corresponds to one point in the stress graph. In between lies the case, now to be considered, where an area, R, in the physical plane, is mapped onto a single arc, Γ, in the stress graph. This type of solution is called simple wave.

The curve Γ in the stress graph cannot be arbitrary. In fact, we know that the characteristics C in the physical plane are always mapped onto characteristics Γ in the stress graph. Consider a point P; one of the characteristic line elements at P may be mapped into P', but not both of them, for then the whole area $dx\,dy$ at P would correspond to a single point. Hence Γ must have everywhere characteristic direction. If this curve is a Γ^+ we speak of a "forward wave," if it is a Γ^-, of a "backward wave." In both kinds of waves each curve of the other set of characteristics (each C^- in a forward wave, each C^+ in a backward wave) is mapped into a single point of Γ, since the image must lie on Γ and on a line having the other characteristic direction (different from that of Γ); consequently for each characteristic of this second set, both s and ϑ, and therefore also $\varphi(s)$, are constant; hence all these characteristics must be straight lines. Thus we arrive at the following description:

A simple wave is a stress distribution for which one set of characteristics in the x,y-plane consists of straight lines along which both s and ϑ (hence Σ) have constant values; the whole simple wave region is the

[18] A substantial part of Courant and Friedrichs' work (1a) deals with simple waves; they also use the term consistently. The terms "Prandtl-Meyer solution," "fan" and "lost solution" are sometimes used by other authors to denote a simple wave.

image of one characteristic, Γ, in the stress graph. In a forward wave (image of a Γ^+), $\vartheta - G(s)$ is constant everywhere in R [see (2.53′) and (2.53″)] and in a backward wave, $\vartheta + G(s)$ is constant for all x,y in the wave region R; in the first case the straight lines are the C^-, in the second case the C^+; all characteristics of the other, non-rectilinear family in R, the "cross characteristics" are mapped onto Γ. The Jacobian of the mapping vanishes everywhere in R. (Therefore simple wave solutions cannot be obtained from the linear problem (2.8), hence the term "lost solutions.") If Γ degenerates into a point both families are rectilinear and the state of stress is constant in R. The concept of a simple wave is linked to the fact that the stress equations are reducible.

A basic property of simple waves is the following. The *region adjacent to a domain of constant stress is always a simple wave region.* This is seen in the following way [see (1a)]. Consider a region D in the physical plane which contains a piece S of a characteristic, C^+, on which s and ϑ are constant. Through each point of D passes a characteristic, C^-. Consider the subregion, $\bar{D}$, of all points of D for which the characteristic C^- intersects S. We see easily that the state in $\bar{D}$ is a simple wave. In fact, the image of S in the stress graph is a point. The images of all characteristics, C^-, in $\bar{D}$ must therefore lie on a characteristic Γ^- through this point. But through this point passes only one characteristic, Γ^-, and thus by our definition the stress pattern in D is a simple wave. Now consider a region of constant state. The line separating such a region from a neighboring one where the state is not constant is a section, S, of a characteristic; consequently the adjacent region is a simple wave region. It is this property of simple waves which is particularly important in building up solutions of boundary problems.

A simple wave can transform any uniform state, $\vartheta = \vartheta_1$, $s = s_1$ into an other state, $\vartheta = \vartheta_2$, $s = s_2$ provided that either $\vartheta + G(s)$ or $\vartheta - G(s)$ has the same value in both states. By combining a forward wave and a backward wave and inserting a uniform state between, *any* final state, ϑ_2, s_2 can be reached in various ways.

Simple waves in gas dynamics have been studied and used extensively by Courant and Friedrichs (1a) and in fact by most authors in this field. They appear likewise in the theory of the orthogonal case as degenerate solutions. In the more general theory which is our subject in this article they have been mainly introduced and studied by Geiringer (2d,e,f). The definitions and several basic properties are of course the same in whatever theory.

b. Simple Waves: Continued. An individual simple wave may be specified in many ways. We may, for example, give *a certain characteristic, say Γ_0^-, in the stress graph and in the physical plane a set of straight*

lines as the C^+. If the given straight lines all have a point in common, i.e., if the envelope degenerates into a point, we speak of a *centered wave.*

The stress distribution for any simple wave, centered or not, follows easily: If a specific yield condition is chosen, then the functions $\varphi(s)$ and $F(s)$ in (2.50) and (2.53′) are given functions of s (see the previous examples). If Γ_0^- is given on one hand, and if on the other hand we introduce the angle δ which a C^+ makes with the x-axis, we have the two equations

$$\vartheta + G(s) = \text{const.}, \quad \vartheta + \varphi(s) = \delta, \tag{2.77}$$

where the constant in the first equation and the δ in the second are known. Hence ϑ and s follow for each C^+. We shall consider examples later.

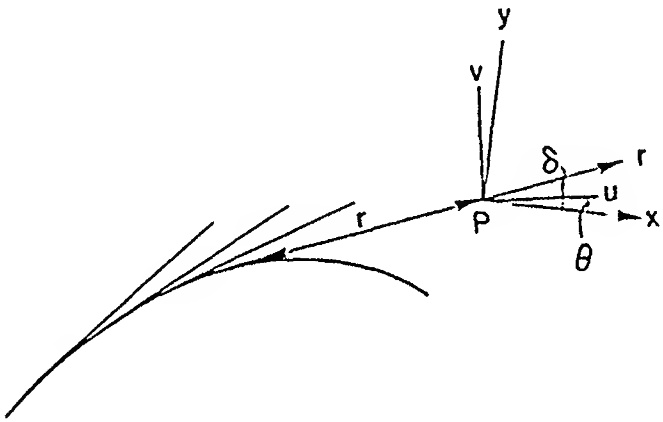

FIG. 11. Straight characteristics.

Let us show that *a solution of our Eqs. (2.6) of which we know that the state of stress is constant along each straight line of a given one-dimensional set of lines must be a simple wave.* Denote by δ the angle formed by each of the given straight lines with the x-direction. Since σ_1, σ_2, and ϑ remain constant along each straight line of the set we have

$$\frac{\partial}{\partial u} = \sin(\vartheta - \delta)\frac{d}{r\,d\delta}, \quad \frac{\partial}{\partial v} = \cos(\vartheta - \delta)\frac{d}{r\,d\delta},$$

and (2.4) yields

$$\begin{aligned} \sin(\vartheta - \delta)\frac{d\sigma_1}{ds} &= (\sigma_2 - \sigma_1)\cos(\vartheta - \delta)\frac{d\vartheta}{ds}, \\ \cos(\vartheta - \delta)\frac{d\sigma_2}{ds} &= (\sigma_2 - \sigma_1)\sin(\vartheta - \delta)\frac{d\vartheta}{ds}. \end{aligned} \tag{2.78}$$

By division we obtain

$$\tan^2(\vartheta - \delta) = \frac{d\sigma_2}{d\sigma_1} \tag{2.79}$$

as in (2.50); hence the straight lines are characteristics. In a hyperbolic region $d\sigma_2/d\sigma_1 > 0$. Next we multiply the first equation (2.78) by $\cos(\vartheta - \delta)$, the second by $\sin(\vartheta - \delta)$ and add:

$$\frac{d(\sigma_1 + \sigma_2)}{d\vartheta} = \frac{\sigma_2 - \sigma_1}{\sin(\vartheta - \delta)\cos(\vartheta - \delta)}. \tag{2.80}$$

From (2.79) and (2.78) we now find our Eq. (2.53). In fact

$$d\vartheta = \frac{d(\sigma_1 + \sigma_2)}{\sigma_2 - \sigma_1}\sin(\vartheta - \delta)\cos(\vartheta - \delta)$$
$$= \frac{d(\sigma_1 + \sigma_2)}{\sigma_2 - \sigma_1}\frac{\sqrt{d\sigma_2 d\sigma_1}}{d\sigma_2 + d\sigma_1} = \frac{\sqrt{d\sigma_2\, d\sigma_1}}{\sigma_2 - \sigma_1},$$

and with $d\sigma_i/ds = \sigma_i'$

$$\frac{d\vartheta}{ds} = \frac{\sqrt{\sigma_1'\sigma_2'}}{\sigma_2 - \sigma_1} = \frac{1}{\sqrt{fg}}. \tag{2.80'}$$

Hence the compatibility condition (2.53) holds; by (2.79) and (2.80′) our statement is proved.

We have seen that so far the relation between the angle δ and the stress distribution (given by ϑ, s, or by $\vartheta, \sigma_1, \sigma_2$) does not depend on the type of the given set of straight lines. For example, it makes no difference for the preceding considerations whether the wave is centered or not. To each δ we can determine by (2.77) the corresponding stress tensor. If, however, we want to find *cross characteristics* and *lines of principal stress* we have to consider the given set of straight lines. Let it be given in the form:

$$y = \gamma x + h(\gamma) \tag{2.81}$$

where the parameter γ equals $\tan \delta$.[19] Assuming that these lines are C^+ characteristics we have $\gamma = \tan(\vartheta + \varphi)$, when ϑ and φ are given functions of s for each given yield condition. Hence γ is a given function of s. The differential equation of the cross characteristics is $dy/dx = \tan(\vartheta - \varphi)$ and since both ϑ and φ depend in a given way on s, and s on γ, we have

$$\frac{dy}{dx} = \tan(\vartheta - \varphi) = k(\gamma). \tag{2.82}$$

From (2.81) we derive

$$dy = x\, d\gamma + \gamma\, dx + h'(\gamma).$$

Substituting this in (2.82) one obtains

$$\frac{dx}{d\gamma} = \frac{x + h'(\gamma)}{k(\gamma) - \gamma} \tag{2.83}$$

[19] This γ has of course nothing to do with the angle γ used occasionally to denote the direction of a velocity characteristic.

and this is a linear differential equation of first order for $x = x(\gamma)$, which can be solved by means of quadratures; thus $x = x(\gamma)$ together with (2.81) provides a parametric representation of the cross characteristics (see also Section II,3,d).

For the *lines of principal stress* the procedure is the same except that $dy/dx = \tan\vartheta$ is used instead of (2.82), while the relation between s and γ remains the same as just before. In case of a centered wave $h(\gamma) = 0$.

c. Examples of Simple Waves. Consider the *quadratic yield condition* where, according to (2.59′),

$$\pm\vartheta = \arctan\frac{s}{\sqrt{3 - s^2}} - \frac{1}{2}\frac{s}{2\sqrt{3 - s^2}} + \text{const.} = G(s) + \text{const.},$$

and consider a forward wave, the image of

(2.84) $$\vartheta = G(s).$$

The C^- are straight lines making the angle $\delta = \vartheta - \varphi$ with the x-axis and, as $\sigma_2 > \sigma_1$, $\tan\varphi$ is given by (2.60) with positive sign. Hence

$$\delta = \vartheta - \varphi = \arctan\frac{s}{\sqrt{3 - s^2}} - \frac{1}{2}\arctan\frac{s}{2\sqrt{3 - s^2}} - \arctan\frac{\sqrt{12 - 3s^2} - s}{2\sqrt{3 - s^2}}.$$

To simplify we introduce

(2.85) $$t = \frac{s}{+\sqrt{3 - s^2}}, \quad s^2 = \frac{3t^2}{1 + t^2}.$$

Thence

$$\delta = \arctan t - \frac{1}{2}\arctan\frac{t}{2} - \arctan\left[\frac{1}{2}\sqrt{4 + t^2} - t\right].$$

As can be seen easily

$$\arctan\left[\frac{1}{2}\sqrt{4 + t^2} - t\right] = \frac{\pi}{4} - \frac{1}{2}\arctan\frac{t}{2}.$$

Thus we obtain the simple result

(2.86) $$\delta = \vartheta - \varphi = \arctan t - \frac{\pi}{4}, \quad t = \tan\left(\delta + \frac{\pi}{4}\right).$$

Reintroducing s, we have s and ϑ in terms of δ:

(2.87) $$s = \sqrt{3}\sin\left(\delta + \frac{\pi}{4}\right), \quad \vartheta = G(s).$$

As s goes from $-\sqrt{3}$ to zero to $+\sqrt{3}$, t goes from $-\infty$, to zero to $+\infty$, ϑ from $-\pi/4$, to zero to $+\pi/4$, and δ from $-3\pi/4$ to $+\pi/4$ (see Fig. 5).

Hence in a "complete wave" δ turns by 180°. In actual problems only parts of a simple wave appear in a solution (in a physical problem the envelope may be approached, but never crossed).

We obtain slightly simpler formulas by considering the wave which is mapped onto

$$\vartheta = G(s) + \frac{\pi}{4} = \arctan t - \frac{1}{2} \arctan \frac{t}{2} + \frac{\pi}{4}, \tag{2.84'}$$

where ϑ goes from 0 to $\pi/2$, as s goes from $-\sqrt{3}$ to $+\sqrt{3}$. Instead of (2.86) and (2.87) we have

$$\delta = \arctan t, \quad t = \tan \delta, \quad \vartheta = \delta + \frac{\pi}{4} - \frac{1}{2} \arctan \left(\frac{\tan \delta}{2}\right) \tag{2.86'}$$

or

$$s = \sqrt{3} \sin \delta, \quad \vartheta = G(s) - \frac{\pi}{4}, \tag{2.87'}$$

and the complete wave varies from $-\pi/2$ to $+\pi/2$.

The image of the Γ^- characteristic

$$\vartheta = -G(s) + \frac{\pi}{4} = \frac{\pi}{4} - \arctan t + \frac{1}{2} \arctan \frac{t}{2} \tag{2.84''}$$

is a wave where, as before,

$$\varphi = \arctan \left[\frac{1}{2} \sqrt{4 + t^2} - t\right] = \frac{\pi}{4} - \frac{1}{2} \arctan \frac{t}{2}.$$

Here

$$\begin{aligned} \delta = \vartheta + \varphi &= -\arctan t + \frac{1}{2} \arctan \frac{t}{2} + \frac{\pi}{4} - \frac{1}{2} \arctan \frac{t}{2} + \frac{\pi}{4} \\ &= \frac{\pi}{2} - \arctan t. \end{aligned} \tag{2.86''}$$

From these equations

$$t = \cot \delta, \quad 2 \tan \delta = \tan 2\varphi. \tag{2.87''}$$

We see that in a forward wave, as δ increases, the mean pressure s as well as ϑ increase in a monotonous way. In a backward wave the opposite holds true.

Next we compute *cross characteristics*, e.g., for the backward wave $\vartheta = -G(s)$, $\delta = \pi/4 - \arctan t$. With notations as in the preceding section we have

$$\gamma = \tan \delta = \tan \left(\frac{\pi}{4} - \arctan t\right) = \frac{1 - t}{1 + t}, \quad t = \frac{1 - \gamma}{1 + \gamma}.$$

Denoting as before by $\beta = \vartheta - \varphi$ the angle formed by a C^- with the x-axis, we have

$$\beta = \frac{1}{2} \arctan \frac{t}{2} - \arctan t - \arctan \left[\frac{1}{2} \sqrt{4 + t^2} - t \right]$$
$$= \arctan \frac{t}{2} - \arctan t - \frac{\pi}{4},$$
$$\tan \beta = - \frac{t^2 + t + 1}{t^2 - t + 2} = - \frac{\gamma^2 + \gamma + 2}{2\gamma^2 + \gamma + 1} = k(\gamma).$$

We may then continue as explained, p. 260.

Let us complete the computation for the particular case of a centered wave where $h(\gamma) = 0$, $\gamma = y/x$ [see (2.81)]. The differential equation of the cross characteristics then becomes

$$\tan \beta = \frac{dy}{dx} = - \frac{y^2 + xy + 2x^2}{2y^2 + xy + x^2}, \tag{2.88}$$

which gives

$$r^2(x + y)^2 = \text{const}.$$

or, in polar coordinates,

$$r^2 \cos \left(\frac{\pi}{4} - \delta \right) = \text{const}. \tag{2.89}$$

We conclude our study of the quadratic condition by deriving a property of the stress tensor; at each point of the wave we use a coordinate

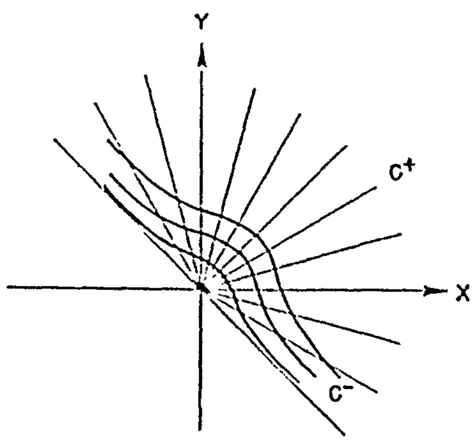

FIG. 12. Quadratic limit; complete centered wave; straight characteristics and cross characteristics.

system, x',y' where x' is the direction of the rectilinear characteristic, y' the direction perpendicular to it. The stress tensor is then given by $\sigma_{x'x'}$, $\sigma_{y'y'}$, $\tau_{x'y'}$. Denote by φ the angle between the x'-direction and the first principal direction and put $\sigma_{x'x'} = \sigma$, $\sigma_{y'y'} = \bar{\sigma}$, $\tau_{x'y'} = \tau$. We have

$$\sigma = \sigma_1 \cos^2 \varphi + \sigma_2 \sin^2 \varphi, \quad \tau = (\sigma_2 - \sigma_1) \sin \varphi \cos \varphi. \tag{2.90}$$

Using primes to denote derivatives, we find from (2.13)

$$\sigma_1' = K\left[1 + \frac{s}{\sqrt{12 - 3s^2}}\right], \quad \sigma_2' = K\left[1 - \frac{s}{\sqrt{12 - 3s^2}}\right],$$

and using (2.60) and (2.13)

$$\cos^2 \varphi = \frac{\sigma_1'}{2K}, \quad \sin^2 \varphi = \frac{\sigma_2'}{2K},$$

$$\begin{aligned} \sigma &= \frac{1}{2K}[\sigma_1\sigma_1' + \sigma_2\sigma_2'] = \frac{1}{4K}\frac{d}{ds}(\sigma_1^2 + \sigma_2^2) = \frac{1}{4K}\frac{d}{ds}(\sigma_1\sigma_2), \\ \sigma &= \frac{1}{4K}\frac{d}{ds}\left[\frac{4K^2}{3}(s^2 - 1)\right] = \frac{2K}{3}s, \quad \tau = \frac{2K}{3}\sqrt{3 - s^2}, \end{aligned} \tag{2.91}$$

$$\sigma^2 + \tau^2 = \frac{4K^2}{3}. \tag{2.91'}$$

Also

$$\begin{aligned} \bar{\sigma} &= \sigma_1 \sin^2 \varphi + \sigma_2 \cos^2 \varphi \\ &= \frac{1}{2K}(\sigma_1\sigma_2' + \sigma_2\sigma_1') = \frac{1}{2K}\frac{d}{ds}(\sigma_1\sigma_2) = 2\sigma. \end{aligned} \tag{2.92}$$

With the quadratic yield condition we obtain for the stress tensor in a simple wave region:

$$\sigma^2 + \tau^2 = \tfrac{4}{3}K^2, \quad \bar{\sigma} = 2\sigma, \tag{2.93}$$

and, with $t = \tan \delta$,

$$\sigma = \frac{2K}{\sqrt{3}} \sin \delta, \quad \tau = \frac{2K}{\sqrt{3}} \cos \delta, \quad \bar{\sigma} = 2\sigma. \tag{2.93'}$$

This gives the stress tensor in terms of the angle δ.

Parabola limit. Using in turn (2.17), (2.61), (2.62), and $s/a = t$, we consider the image of the Γ^--characteristic

$$\vartheta = -\arcsin t = \arccos t - \frac{\pi}{2}. \tag{2.94}$$

From

$$\tan \varphi = \sqrt{\frac{a - s}{a + s}} = \sqrt{\frac{1 - t}{1 + t}} = \tan\left(\frac{\pi}{4} + \frac{\vartheta}{2}\right) \tag{2.95}$$

we conclude that

$$\varphi = \frac{1}{2}\left(\vartheta + \frac{\pi}{2}\right), \quad \delta = \varphi + \vartheta = \frac{3\vartheta}{2} + \frac{\pi}{4}.$$

Thus

$$\vartheta = \frac{2}{3}\left(\delta - \frac{\pi}{4}\right), \quad s = a \cos\left(\vartheta + \frac{\pi}{2}\right) = a \cos \frac{\pi + 2\delta}{3}. \tag{2.96}$$

Here the maximum interval for ϑ equals 180° and for δ it is 270°; as ϑ goes from $\pi/2$ through 0 to $-\pi/2$, δ goes from π through 0 to $-\pi/2$.

We compute the *cross characteristics* for (2.94) assuming a *centered wave*. If β is the angle between a cross characteristic and the x-axis as

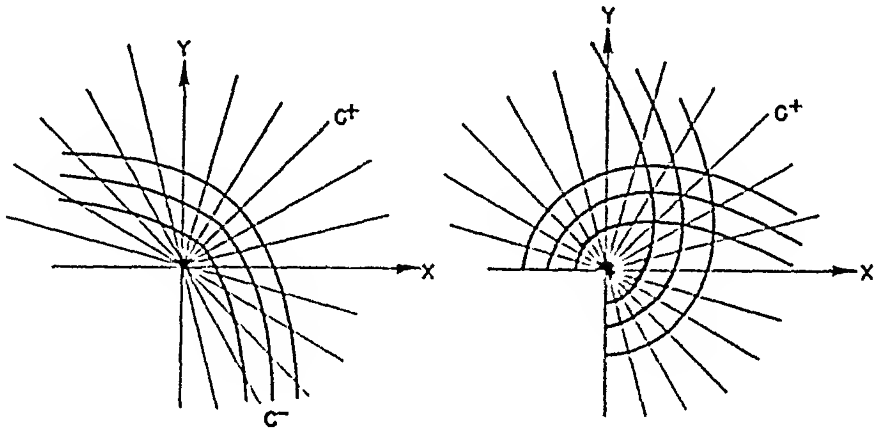

FIG. 13. (a) Parabola limit; straight characteristics and cross characteristics. (b) Parabola limit; lines of principal stress.

before, then $\beta = \delta - 2\varphi$, and we obtain from (2.96), using polar coordinates r and δ,

$$r\frac{d\delta}{dr} = -\tan\varphi = -\tan\left(\frac{\pi}{2} + \vartheta\right) = -\tan\left(\frac{2\delta + \pi}{3}\right), \tag{2.97}$$

and integrated

$$r = r_0\left[\sin\left(\frac{2\delta + \pi}{3}\right)\right]^{-\frac{3}{2}}. \tag{2.98}$$

We finally determine for the same example the *principal stress lines*. For the u-lines (the lines making the angle ϑ with the x-direction) we have

$$\frac{r d\delta}{dr} = -\tan(\delta - \vartheta) = -\tan\left(\frac{\delta}{3} + \frac{\pi}{6}\right) \tag{2.99}$$

or, integrated,

$$r = r_0\left[\sin\left(\frac{2\delta + \pi}{6}\right)\right]^{-3}, \tag{2.100}$$

and for the v-lines

$$r = r_0\left[\cos\left(\frac{2\delta + \pi}{6}\right)\right]^{-3}. \tag{2.100'}$$

These examples may suffice.

d. Velocities. Firstly one may ask whether there exists a simple wave solution of the velocity Eqs. (2.69). The answer is negative because

these equations are linear and not reducible. Consider also the reducible equations, p. 24, which result from (2.68) by interchanging dependent and independent variables. Do these admit a simple wave solution? The answer is again negative, since a whole straight line in the v_x,v_y-plane would have to correspond to one point (x,y) in the physical plane; this means that many different velocities would correspond to the same point, which makes no sense.

Hence our present problem consists merely in *finding the velocity distribution corresponding to the simple waves just investigated.* Let us consider a simple wave determined, for example (for a particular yield condition), by a set of straight lines C^+ and by a constant which singles out the particular $\Gamma_0^-: \vartheta + G(s) = c$, whose image is the simple wave. The velocity problem is linear and has the same characteristics as the stress problem. A velocity distribution may be determined by giving, e.g., along a noncharacteristic curve K which crosses the C^+, both components v_x and v_y.

Let us first settle a special question. We know that along each straight characteristic s and ϑ have constant values; it seems natural to ask whether a velocity distribution exists *such that v_x and v_y are likewise constant along each straight characteristic.* In other words, is it possible to prescribe along a noncharacteristic curve K such initial values v_x and v_y that along each straight C^+ the velocity vector remains constant? Obviously, the initial distribution along K cannot be arbitrary in this case. In fact, consider the image $\bar{K}$ of K in the velocity plane; since to each C^+ corresponds only one point on $\bar{K}$, this $\bar{K}$ is the image of the whole simple wave region, hence also of all C^-. Therefore along $\bar{K}$ the relation

$$\frac{dv_y}{dv_x} = -\cot(\vartheta - \varphi) \tag{2.71}$$

must hold. More explicitly: Through every point of K passes a C^+ hence an angle α belongs to it, and to each α corresponds an s and ϑ, hence also an angle $\beta = \vartheta - \varphi$, and consequently also a value of $\cot(\vartheta - \varphi)$, say, $\cot(\vartheta - \varphi) = H(\alpha)$. K may be given in terms of some parameter, say α, and v_x,v_y along K are likewise functions of α, as $x = x(\alpha)$, $y = y(\alpha)$, $v_x = v_x(\alpha)$, $v_y = v_y(\alpha)$. Then, with primes denoting differentiation with respect to α, one has $v_x'/v_y' = H(\alpha)$ along K. If this condition holds at a point $\alpha = \alpha_1$, on K, it holds the same along the whole C^+ through this point.

If, on the other hand, the prescribed velocity distribution is such that the above condition holds, a corresponding solution of the velocity Eqs. (2.69) exists. To see this, consider (2.69). Since the velocity distribution remains constant along the C^+ which makes the angle α with

the x-axis, we have at a point P of this line

$$\frac{\partial}{\partial x} = -\frac{1}{r}\sin\alpha\frac{d}{d\alpha}, \quad \frac{\partial}{\partial y} = \frac{1}{r}\cos\alpha\frac{d}{d\alpha},$$

and from the third Eq. (2.69)

$$-\frac{1}{r}\sin\alpha\frac{dv_x}{d\alpha} = \frac{1}{r}\frac{dv_y}{d\alpha}\cos\alpha\tan\alpha\tan\beta,$$

which yields the preceding (2.71). Also from the second Eq. (2.69)

$$-\frac{1}{r}\sin\alpha\frac{dv_x}{d\alpha} - \frac{1}{r}\cos\alpha\frac{dv_y}{d\alpha} = \cot 2\vartheta\left(\frac{1}{r}\cos\alpha\frac{dv_x}{d\alpha} - \frac{1}{r}\sin\alpha\frac{dv_y}{d\alpha}\right)$$

we obtain, as $\alpha + \beta = 2\vartheta$,

$$\frac{dv_x}{dv_y} = \frac{\sin\alpha\cos 2\vartheta - \cos\alpha\sin 2\vartheta}{\cos\alpha\cos 2\vartheta + \sin\alpha\sin 2\vartheta} = \frac{\sin(\alpha - 2\vartheta)}{\cos(\alpha - 2\vartheta)} = -\cot\beta,$$

hence again (2.71). We have thus the result: *It is possible to have a solution where the velocity vector is constant along each rectilinear characteristic if and only if the restriction (2.71) holds along the noncharacteristic initial curve K and consequently everywhere in the domain of the solution.* That means that only one of the two velocity components can be given arbitrarily along K. Thus there exist (simple wave) solutions which carry along their rectilinear characteristics not only constant values of the stress tensor but also constant values of the velocity vector. This remark may be useful in applications.

e. *Explicit Determination of the Velocity Distribution.* In the preceding sections, II,3,b,c we have shown how to obtain the stress distribution everywhere in a simple wave. Let us now consider the determination of the velocity distribution; also this problem can be solved explicitly. We must now choose velocity components and a coordinate system. In certain problems it is practical to consider components v_1 and v_2, where $v_1 = v_r$ is in direction of the straight lines, while v_2 is perpendicular to v_1. Accordingly a coordinate system is used, where the straight lines and their orthogonal trajectories are coordinate lines; as coordinates one takes r and α, where α is the angle of the straight C^+ passing through a point P, and r the directed distance of P along that C^+ to one fixed orthogonal trajectory, T_0, (2c); these are orthogonal coordinates.

A more natural though not orthogonal system of coordinate lines is given by the characteristics themselves, (2g). We take the straight lines C^+ as the ξ-lines, (η = constant), the cross characteristics C^- as the η-lines(ξ = constant). The equation of the cross characteristics is then of the form $f_1(x,y,\xi) = 0$, and that of the straight lines of the form

$f_2(x,y,\eta) = 0$; or also $\xi(x,y) =$ constant, $\eta(x,y) =$ constant, respectively. Along each cross characteristics ξ has a constant value while η varies along it and ξ varies along each straight line, along which η is constant. Since all cross characteristics intersect a C^+ at the same angle, we may take this angle for η, or any of the three angles α, or β, or φ, each remaining constant along a C^+. To define a ξ we choose, for example, an appropriate C^+ with equation $\alpha = \alpha_0$ and on it a point O, and take for ξ the distance OP', where P' is the point of intersection of the cross characteristic ξ with this straight line (Fig. 14). The coordinates ξ,η are thus defined for any point P in the wave region. (It is clear that the characteristic coordinates introduced in Section II,2,c cannot be used here since

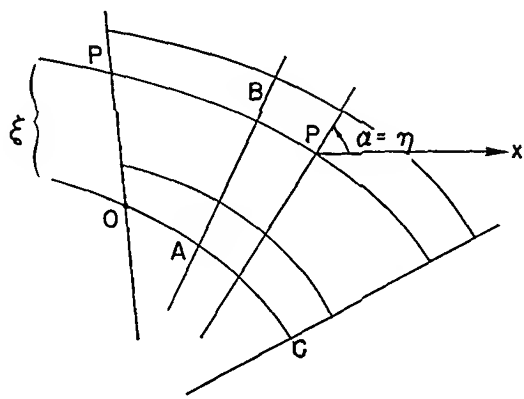

FIG. 14. Characteristic coordinates in simple wave.

the ξ defined by (2.54) would now have a constant value all through the wave region, and along a straight C^+ both ξ and η defined there would be constant.)

As components of $\bar{v}$ we consider now the projections v_1 and v_3 in direction of the C^+ or C^- respectively. The first Eq. (2.74‴) shows now immediately that $dv_1/dl^+ \to 0$. *The component of $\bar{v}$ in direction of a straight C^+ does not change along it.*

$$\frac{dv_1}{d\xi} = 0. \tag{2.101}$$

Next consider the second Eq. (2.74″), valid along a C^-:

$$\frac{\partial v_3}{\partial \beta} = \frac{v_1 - v_3 \cos 2\varphi}{\sin 2\varphi}. \tag{2.102}$$

Since neither φ nor v_1 change along a straight C^+, we see that $\dfrac{\partial v_3}{\partial \beta} + v_3 \cot 2\varphi$ does not change along it. Writing from now on v instead of v_3,

we may state: *Not only* v_1 *but also* $\frac{\partial v}{\partial \beta} + v \cot 2\varphi$ *remains constant along a straight* C^+. The constant value of this expression is of course $v_1/\sin 2\varphi$. This is expressed in the equation of second order

$$\frac{\partial^2 v}{\partial \xi \partial \beta} + \frac{\partial v}{\partial \xi} \cot 2\varphi = 0, \tag{2.103}$$

which for $\varphi = 45°$ (special case) reduces to the known $\partial^2 v/\partial \xi \partial \beta = 0$.

To integrate (2.102) we observe that if v_1 is given along some curve intersecting the C^+, then v_1 is known everywhere; we use $\eta = \alpha$ as independent variable; then we have $\beta = \beta(\alpha)$, $\varphi = \varphi(\alpha)$, $v_1 = v_1(\alpha)$, and (2.102) takes the form

$$\frac{\partial v}{\partial \alpha}\frac{d\alpha}{d\beta} + v \cot 2\varphi - \frac{v_1}{\sin 2\varphi} = 0. \tag{2.102'}$$

Putting

$$\cot 2\varphi \cdot \frac{d\beta}{d\alpha} = a(\alpha), \quad \frac{v_1}{\sin 2\varphi} \cdot \frac{d\beta}{d\alpha} = b(\alpha),$$

we have the linear equation

$$\frac{\partial v}{\partial \alpha} + av - b = 0$$

with the integral

$$v(\xi,\alpha)e^{\int_{\alpha_0}^{\alpha} a\,d\alpha} = \int_{\alpha_0}^{\alpha} b e^{\int_{\alpha_0}^{\alpha} a\,d\alpha}\, d\alpha + \psi(\xi). \tag{2.104}$$

Here ψ is the value of v in terms of ξ for $\alpha = \alpha_0$, that is, $\psi = v(\xi,\alpha_0)$.

Consider a *Cauchy problem*. Along a non characteristic curve K with equation $\xi = \xi(\alpha)$ both v_1 and v_3 are given: $v_1 = g(\alpha)$, $v_3 = v = h(\alpha)$. First we know v_1 along each C^+ intersecting K. The arbitrary function in (2.104) is then determined by the condition that along K, that is, for $\xi = \xi(\alpha)$, $v(\xi,\alpha)$ should reduce to $h(\alpha)$. As a concrete example consider the simple wave, image of

$$\vartheta = -G(s) + \frac{\pi}{4}; \quad G(s) = \arctan \frac{s}{\sqrt{3 - s^2}} - \frac{1}{2}\arctan \frac{s}{2\sqrt{3 - s^2}},$$

or, with $s/\sqrt{3 - s^2} = t$,

$$\varphi = \arctan\left[\frac{1}{2}\sqrt{4 + t^2} - t\right] = \frac{\pi}{4} - \frac{1}{2}\arctan\frac{t}{2},$$

$$\alpha = \vartheta + \varphi = \frac{\pi}{2} - \arctan t,$$

$$\beta = \vartheta - \varphi = \arctan\frac{t}{2} - \arctan t.$$

Then

$$\cot \alpha = t, \quad \tan \beta = -t/(2 + t^2), \quad \tan 2\varphi = 2 \tan \alpha$$

and $a(\alpha)$ and $b(\alpha)$ follow, etc.

In a *characteristic initial value problem* we assume, for example, that v_1 is given along an arc AC of a C^-; we simply assume that it is the C^- given by $\xi = 0$; A then coincides with the point O from which on we count the ξ; also v is given along a piece OB of the straight characteristic $\alpha = \alpha_0$. This problem is particularly simple: Firstly we know again v_1 on each C^+ which intersects OC; and v is given by (2.104) where $\psi(\xi)$ is to be replaced by $v(\xi,\alpha_0) \equiv v_0(\xi)$. Finally, if v is given along OC and along OB, the value of v_1 at O is determined by (2.102), and we know v_1 on OB. In the same way we find v_1 everywhere on OC, hence it is known in the corresponding wave region. If we again denote the v-values along OB by $v(\xi,\alpha_0) = v_0(\xi)$, the $\psi(\xi)$ in (2.104) is equal to $v_0(\xi)$.

We can thus determine stresses and velocities in a simple wave region corresponding to given initial data. Such solutions may be used in the construction of solutions of actual physical problems.

III. Examples of Complete Problems

In the preceding pages we have mentioned repeatedly that one of the great difficulties in plasticity problems is the formulation of actual boundary value problems, where according to the physical nature of the problem the data consist partly of stresses, partly of velocities (see also the Introduction). The convenient resolving of the complete problem in a stress problem and a velocity problem is possible only if we know enough, physically justified, stress conditions to allow the determination of the stresses independent of the velocities. Otherwise particular stress solutions may be given, but the stress solution is not uniquely determined, and if one particular solution is adopted, perhaps for reasons of simplicity, it may then not be possible to satisfy the other physically necessary boundary conditions. Some of the older work has been critically examined from this point of view, particularly by Lee (in 8b and other papers), and Hill (5a), and in the last years a great many problems have been carefully studied and solved [see literature and actual solutions in (5a), (6a), (16g)].

We shall present here a few selected problems in detail. We have chosen, however, problems of plane strain, i.e., problems based on the "special" theory; the main reason for this choice is the much greater simplicity of these problems which allows one to concentrate on the specific features of the "boundary value problem," and to avoid additional difficulties of a more mathematical nature. We shall consider some work of Lee and Prager which seems to us very appropriate for a

discussion of the principles. Problems are considered where a rigid plastic type of analysis may be adopted as an approximation, i.e., elastic material will be considered as rigid.

We begin with the consideration of the problem of a wedge subjected to a uniformly distributed pressure p over a portion of one flank, and follow investigations of Lee. This problem will also necessitate the study of stress discontinuities, a simple and important idea, introduced by Prager.

1. Stress Discontinuities

The simplest example of such a discontinuity occurs according to Prager in the bending of a plastic rigid sheet under conditions of plane strain. The development of the stress distribution can be followed from elastic bending until large plastic strains occur. Figure 15(a) shows the

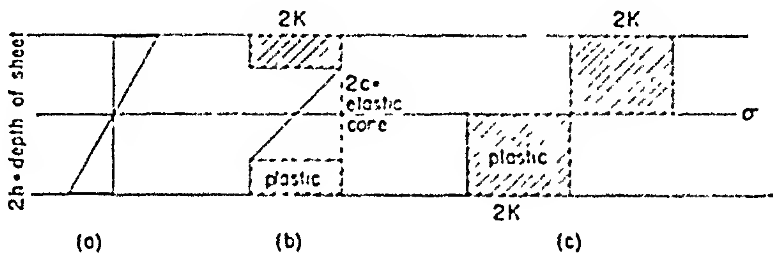

Fig. 15. Stresses in bent slab.

linear elastic stress distribution; the longitudinal stress, σ, is of opposite sign on the two sides of the neutral axis and the bending is totally elastic. As the torque increases (Fig. 15b), the central strip of elastic material shrinks and the elements close to the surface flow plastically. As the bending moment increases further, the elastic core shrinks to a membrane (Fig. 15c), the longitudinal stress on the tension side is everywhere of amount $2K$, while on the compression side it is $-2K$; this means that there is a discontinuity of amount $4K$ along the neutral axis. Here we have the largest possible amount of change in stress at a discontinuity surface (5a, p. 157), (8a).

Now consider the general features of stress discontinuities under conditions of plane strain. If y is the direction of the curve of discontinuity, the equilibrium conditions require only that across that curve σ_x and τ remain continuous, while σ_y may change across the curve, as it is not differentiated in the x-direction. In general, the components σ_n, normal to the curve of discontinuity and τ, parallel to this curve must be the same on both sides of the curve, that means, the stress vector, corresponding to the line element must not change (its components are σ_n and τ) while σ_t acting parallel to the curve need not be the same on both

sides (Fig. 16). The amount $\sigma_t^{(1)} - \sigma_t^{(2)}$ of the tangential stress discontinuity is restricted by the condition that the material on both sides of the line be plastic. If σ_n and τ are regarded as given, the values of $\sigma = \sigma_t^{(1)}$, and $\sigma = \sigma_t^{(2)}$ must satisfy the yield criterion of plane strain

$$(\sigma - \sigma_n)^2 + 4\tau^2 = 4K^2, \tag{3.1}$$

or

$$\sigma = \sigma_n \pm 2\sqrt{K^2 - \tau^2}. \tag{3.2}$$

The tangential stress may therefore have one of two values

$$\sigma_t^{(1)} = \sigma_n + 2\sqrt{K^2 - \tau^2},$$

$\sigma_t^{(2)} = \sigma_n - 2\sqrt{K^2 - \tau^2}$. The discontinuity is of amount $4\sqrt{K^2 + \tau^2}$; the corresponding jump in pressure, $p = \frac{1}{2}(\sigma_n + \sigma_t)$ is $2\sqrt{K^2 - \tau^2}$. In

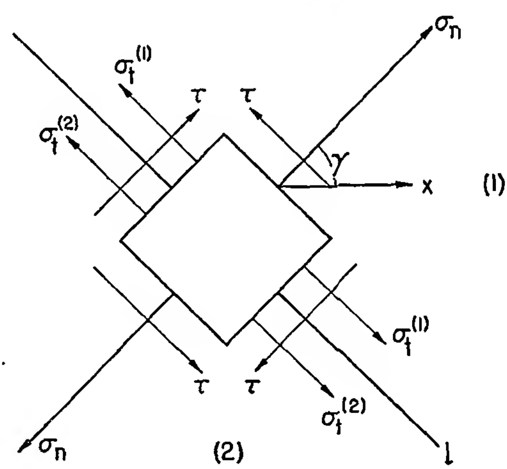

FIG. 16. Discontinuous stresses in plane strain.

an actual medium one may think of the discontinuity as of a narrow transition region through which σ_n and τ remain essentially constant, while σ_t changes rapidly from $\sigma_t^{(1)}$ to $\sigma_t^{(2)}$, and $\sigma_t^{(2)} \leqq \sigma_t \leqq \sigma_t^{(1)}$. The equality signs do not hold since otherwise the corresponding part of the transition region would simply add to the plastic region; hence we have in the transition region $(\sigma_t - \sigma_n)^2 + 4\tau^2 < 4K^2$. This leads to the concept of a discontinuity zone consisting of a very thin elastic membrane between two plastic regions (Lee and Prager, see also p. 277 ff.).

Let us express the jump conditions across a discontinuity line in terms of the variables s and ϑ (5a), (16e). Denote by γ the angle which the normal to the discontinuity line makes with the x-axis, and by ϑ, as always, the angle between the x-axis and the first principal direction, by $\delta = \gamma - \vartheta$ the angle of this normal with the first principal direction.

Then

$$\sigma_n = \frac{\sigma_1 + \sigma_2}{2} + \frac{\sigma_1 - \sigma_2}{2} \cos 2\delta,$$

$$\sigma_t = \frac{\sigma_1 + \sigma_2}{2} - \frac{\sigma_1 - \sigma_2}{2} \cos 2\delta,$$

$$\tau = \frac{\sigma_1 - \sigma_2}{2} \sin 2\delta.$$

or, with $K = \frac{1}{2}(\sigma_1 - \sigma_2)$,

$$s = \frac{1}{2K}(\sigma_1 + \sigma_2)$$

(3.3)
$$\begin{aligned} \sigma_n &= Ks + K \cos 2\delta, \\ \sigma_t &= Ks - K \cos 2\delta, \\ \tau &= \quad\;\; - K \sin 2\delta. \end{aligned}$$

If σ_n and τ are to be continuous, the jumps in s and ϑ must satisfy the equations

(3.4)
$$\begin{aligned} s_2 - s_1 + \cos 2\delta_2 - \cos 2\delta_1 &= 0, \\ \sin 2\delta_2 - \sin 2\delta_1 &= 0. \end{aligned}$$

These equations yield

(3.5)
$$\begin{aligned} \delta_1 + \delta_2 &= \frac{\pi}{2}, \\ s_2 &= s_1 + 2 \cos 2\delta_1. \end{aligned}$$

In plane strain the slip lines coincide with the characteristics and with the 45°-lines; we introduce now $\theta = \vartheta + \frac{\pi}{4}$, the angle which a C^+, a first slip line, makes with the x-axis (in Part II this angle was denoted by α, now we shall need the letter α for other purposes). Then Eq. (3.5) yields

(3.5′)
$$\begin{aligned} \theta_2 &= 2\gamma - \theta_1, \\ s_2 &= s_1 + 2 \sin 2(\theta_1 - \gamma). \end{aligned}$$

At a point of a line of discontinuity there are now four slip line directions C_1^+, C_2^+ and C_1^-, C_2^- and $C_1^+ \perp C_1^-$, $C_2^+ \perp C_2^-$. The first Eq. (3.5′) shows that at any point of a discontinuity line the tangent t to this line bisects the angle of the tangents to C_1^+, C_2^+ and likewise to C_1^-, C_2^- at this point. It is also seen from (3.5′) that the discontinuity line bisects the angle between $\sigma_1^{(1)}$ (first principal direction to the right) and $\sigma_2^{(2)}$ (second principal direction to the left) as well as that between $\sigma_1^{(2)}$ and $\sigma_2^{(1)}$. From (3.5′) we further find

(3.6)
$$s_2 - s_1 = -2 \sin (\theta_2 - \theta_1).$$

This shows that the change of $s/2$ across the discontinuity line equals the sine of the angle between C_1^+ and C_2^+, or between C_1^- and C_2^-.

Let us consider the Mohr circles of two states of stress $\Sigma^{(1)}$ and $\Sigma^{(2)}$ to the two sides of a discontinuity. They have one stress vector (σ_n,τ) in common; in both tensors this vector corresponds to the same normal direction, n. Figure 18 shows the directions of the two pairs of principal axes, compatible with one common stress vector; likewise the angles δ_1 and

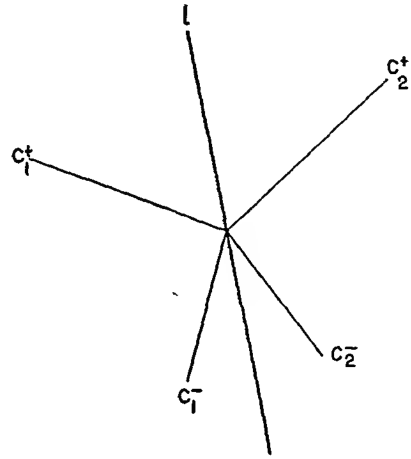

FIG. 17. Discontinuity line.

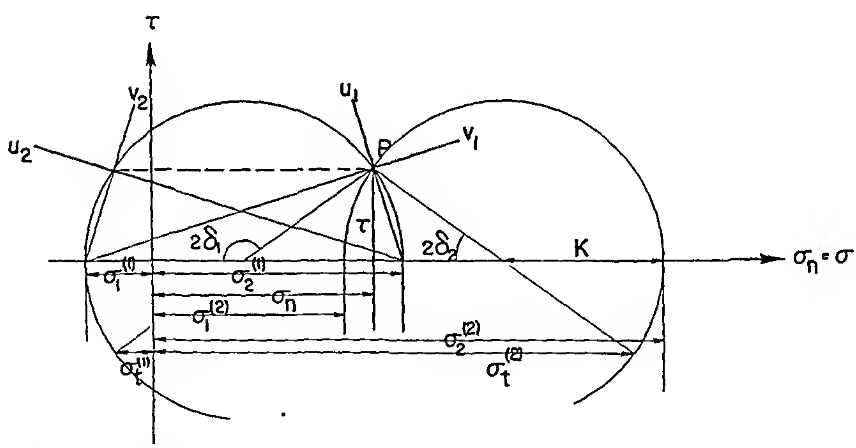

FIG. 18. Mohr circles of two stress tensors having one stress vector in common (stress discontinuity).

δ_2 (see Section II,2,d) as well as the lengths $\sigma_1^{(1)},\sigma_1^{(2)},\sigma_2^{(1)},\sigma_2^{(2)}$ are seen. From this figure we read, among other relations,

$$2\sigma = \frac{\sigma_1^{(1)} + \sigma_2^{(1)}}{2} + \frac{\sigma_1^{(2)} + \sigma_2^{(2)}}{2}, \tag{3.7}$$

$$2\sigma = \sigma_2^{(1)} + \sigma_1^{(2)} = \sigma_1^{(1)} + \sigma_2^{(2)};$$

$$\begin{aligned} \sigma_1^{(1)} + \sigma_1^{(2)} &= 2\sigma - 2K, \\ \sigma_2^{(1)} + \sigma_2^{(2)} &= 2\sigma + 2K. \end{aligned} \tag{3.8}$$

The *curvatures* of the shear lines change abruptly across a discontinuity. The geometry of the shear lines in the classical case is well known [see, for example, (2c, p. 33 ff.) or (5a, p. 136 ff.)]. Denote by ds_ξ, ds_η the arc elements, by R_ξ, R_η the radii of curvature of a first and second slip line respectively (this notation is now used instead of C^+, C^-; we shall denote the characteristics also as ξ-lines and η-lines; θ stands for $\vartheta + \varphi = \vartheta + \frac{\pi}{4}\Big)$. R_ξ and R_η are defined by $R_\xi = d\theta/ds_\xi$, $R_\eta = d\theta/ds_\eta$; ϵ is the acute angle formed by a ξ-direction with a direction which we shall later identify with the direction of a discontinuity line; $\partial/\partial l$ denotes differentiation in this direction. Then

$$\frac{\partial\theta}{\partial l} = \frac{\partial\theta}{\partial s_\xi}\cos\epsilon + \frac{\partial\theta}{\partial s_\eta}\sin\epsilon = \frac{\cos\epsilon}{R_\xi} + \frac{\sin\epsilon}{R_\eta}. \tag{3.9}$$

Next it is known and follows also from our general formulas (Section II,2,b) that $s/2 - \theta$ is constant along a ξ-line and $s/2 + \theta$ along an η-line. From this and the above definition of the radii of curvature one derives easily

$$\frac{\partial}{\partial l}\left(\frac{s}{2}\right) = \frac{\cos\epsilon}{R_\xi} - \frac{\sin\epsilon}{R_\eta}, \tag{3.9'}$$

and from (3.9) and (3.9′), with R and S instead of R_ξ and R_η,

$$\begin{aligned} \frac{1}{R} &= \frac{1}{2\cos\epsilon}\frac{\partial}{\partial l}\left(\frac{s}{2} + \theta\right), \\ \frac{1}{S} &= -\frac{1}{2\sin\epsilon}\frac{\partial}{\partial l}\left(\frac{s}{2} - \theta\right). \end{aligned} \tag{3.10}$$

Now we identify ϵ with the acute angle between a ξ-direction and the tangent to the discontinuity line. Then the corresponding angle on the other side is $-\epsilon$, and we obtain for the radii of curvature on both sides

$$\frac{1}{R_2} = \frac{1}{2\cos\epsilon}\frac{\partial}{\partial l}\left(\frac{s_2}{2} + \theta_2\right), \quad \frac{1}{S_2} = -\frac{1}{2\sin\epsilon}\frac{\partial}{\partial l}\left(\frac{s_2}{2} - \theta_2\right),$$
$$\frac{1}{R_1} = \frac{1}{2\cos\epsilon}\frac{\partial}{\partial l}\left(\frac{s_1}{2} + \theta_1\right), \quad \frac{1}{S_1} = \frac{1}{2\sin\epsilon}\frac{\partial}{\partial l}\left(\frac{s_1}{2} - \theta_1\right),$$

and

$$\begin{aligned} \frac{1}{R_2} - \frac{1}{R_1} &= \frac{1}{2\cos\epsilon}\frac{\partial}{\partial l}\left[\frac{s_2 - s_1}{2} + (\theta_2 - \theta_1)\right], \\ \frac{1}{S_2} + \frac{1}{S_1} &= \frac{1}{2\sin\epsilon}\frac{\partial}{\partial l}\left[\frac{s_1 - s_2}{2} + (\theta_2 - \theta_1)\right]. \end{aligned}$$

Now using (3.6) and $\theta_1 - \theta_2 = 2\epsilon$ we obtain

$$\begin{aligned} \frac{1}{R_2} - \frac{1}{R_1} &= -2 \sin \epsilon \tan \epsilon \frac{d\epsilon}{dl}, \\ \frac{1}{S_2} + \frac{1}{S_1} &= -2 \cos \epsilon \cot \epsilon \frac{d\epsilon}{dl}. \end{aligned} \tag{3.11}$$

These formulas give the jumps in the curvature of the slip lines in terms of the variation of ϵ along the discontinuity line (5a, p. 159; and 16e).

2. Velocities at the Discontinuity Surface

Consider an element of the discontinuity line which has the y-direction; then σ_y is the stress component that may have a jump. From Mohr's circles or from the formulas we know that

$$\sigma_y^{(1)} - \sigma_x = -(\sigma_y^{(2)} - \sigma_x). \tag{3.12}$$

On the other hand we obtain from the basic relation $\dot{E} = \lambda \Sigma'$

$$\dot{\epsilon}_y^{(1)} = \lambda^{(1)} \frac{\sigma_y^{(1)} - \sigma_x}{2}, \quad \dot{\epsilon}_y^{(2)} = \lambda^{(2)} \frac{\sigma_y^{(2)} - \sigma_x}{2}.$$

From (3.12) together with $\dot{\epsilon}_y^{(1)} = \dot{\epsilon}_y^{(2)}$ we conclude (since $\sigma_y^{(1)} - \sigma_x$ cannot vanish unless $\sigma_y^{(1)} = \sigma_x$, $\sigma_y^{(2)} = \sigma_x$, $\sigma_y^{(1)} = \sigma_y^{(2)}$) that $\lambda^{(1)} = -\lambda^{(2)}$; since negative λ-values are excluded, it follows that at *every discontinuity point*

$$\lambda = 0, \quad \dot{\epsilon}_x = \dot{\epsilon}_y = \dot{\gamma} = 0, \quad \text{or} \quad \dot{E} = 0, \tag{3.13}$$

where $\dot{E}$ is the strain rate tensor.

We assume now that the discontinuity line be straight; let it have the y-direction. Then along it v_y is constant and v_x a function of y, e.g., $v_x = f(y)$. Also $\dfrac{\partial v_x}{\partial y} + \dfrac{\partial v_y}{\partial x} = 0$, hence $\dfrac{\partial v_y}{\partial x} = -f'(y)$. (These various conditions constitute only *one* independent boundary condition along the discontinuity line. If $\dot{\epsilon}_y = 0$, we would conclude *from the differential equations* $\dot{\epsilon}_y/\sigma_y' = \dot{\epsilon}_x/\sigma_x' = \dot{\gamma}/2\tau$, which are valid everywhere and in the limit also along the discontinuity line, that there $\dot{\epsilon}_x = 0$ and $\dot{\gamma} = 0$ must hold.) It follows from the preceding considerations that a velocity discontinuity across our discontinuity line of stress is not possible, in fact the normal velocity v_x must be continuous, and if v_y were discontinuous, this would mean $\dfrac{\partial v_y}{\partial x} \to \infty$ and $\dot{\gamma} \to \infty$, while $\dot{\gamma} = 0$ at the discontinuity line.

In case of a discontinuity *curve* $\dot{E} = 0$ must hold at every point. That this is a possible postulate is seen by the example of a uniform

velocity distribution adjacent to the curve. However, if we denote by ds_t the arc element of the discontinuity curve and by R_t the radius of curvature, we see from $\dot{\epsilon}_{tt} = \frac{\partial v_t}{\partial s_t} - \frac{v_n}{R_t}$ that, since $\dot{\epsilon}_{tt} = 0$, $\frac{\partial v_t}{\partial s_t}$ and v_n are either both zero or both different from zero; the assumption $v_t = 0$ (or constant) along the discontinuity line while $v_n \neq 0$, which was admissible earlier in the case of a straight discontinuity line, is not admissible now since now R_t is finite and v_n/R_t does not tend to zero for $v_n \neq 0$. Prager very rightly states that curved discontinuity lines are not yet sufficiently explored.

Thus the essential conditions along a discontinuity line are: (1) The stress vector $\bar{p}_n$ with components σ_n and τ is continuous across the line. (2) The component σ_t may jump, subject to the condition

$$\sigma_t^{(1)} + \sigma_t^{(2)} = 2\sigma_n.$$

(3) The strain rate tensor, $\dot{E}$, must vanish for each point of the line; only velocity distributions compatible with this condition are admissible. These properties describe, in our opinion, the discontinuity line in a sufficient way (other properties follow from them; see the preceding section).

Prager (16c) and Lee (8a) have suggested a physical interpretation of the discontinuity line from which it follows in particular that $v_y = 0$, $v_z = f(y)$ along a straight discontinuity line of y-direction. (We just derived this from $\dot{E} = 0$.) According to these authors one may think of the discontinuity surface as of a thin elastic plate (whose thickness is of the order of the elastic displacements); through this thickness σ_t changes continuously from $\sigma_t^{(1)}$ to $\sigma_t^{(2)}$ while σ_n and τ remain unchanged. In this case all strains are small. The longitudinal strains are small and induce small strains $\dot{\epsilon}_t$ in the adjacent plastic material; hence in a plastic rigid material $\dot{\epsilon}_t = 0$ in the plastic medium to both sides. We are thus led to visualize the thin plate (or the filament if we think of the trace in the x,y-plane) as *inextensible* in the tangential direction. The longitudinal displacements in the filament are likewise of elastic order of magnitude, and the same holds for the induced displacements in the plastic material. On the other hand, in this elastic thin plate *finite bending* is possible, hence *finite normal displacements*, without contradicting the elastic strains which are small in *any* direction; in fact, small elastic bending strains are compatible with finite displacements in the normal direction, inducing finite displacements in the adjacent plastic medium. Thus the picture is that of an *elastic, inextensible, flexible, thin plate*, or a corresponding filament. (We repeat however, that on account of $\dot{E} = 0$, vanishing or even constant tangential velocities (displacements) are compatible with finite

normal velocities only in case of a *straight* discontinuity line. In case of a curved filament with $v_n \neq 0$ we must think of tangential displacements which *vary* along the line in such a way that $\partial v_t/\partial s_t \neq 0$.) From the mathematical point of view it is a problem of differential geometry to describe curves with such velocity distributions along them that everywhere $\dot{E} = 0$.

3. *Wedge with Pressure on One Face: Stress Distribution*

Already in his first paper on stress discontinuities Prager mentioned as a simple example of a problem where in the stress solution a discontinuity line appears the straight-sided wedge subject to uniform normal pressure along a portion of one side. Consider a wedge of perfectly plastic material with vertex angle $2\beta_0 < \pi/2$. Uniform pressure along AB determines a region of constant state ABE; the pressure-free boundary BE determines a region BDE of different but likewise uniform state. Since these regions overlap in $BCFD$, a multivalent stress field would result which is unacceptable. Prager and Lee have determined a complete solution of this problem which features a stress discontinuity line. In the following we shall discuss this solution.

The above-mentioned difficulty arises only if $\beta_0 < \pi/4$. If $\beta_0 \geqq \pi/4$, a continuous stress solution exists given by Prandtl (17a,b). In Fig. 19(b) the triangles ABC and BDE are regions of constant state. In ABC the principal stresses are $-p_0$ normal to AB, and $2K - p_0$ parallel to AB. In BDE they are zero normal to BE, and $-2K$ parallel to it. The region BCD is a centered simple wave ("fan") where the slip lines are radii and circles. To find the value of p_0 that can produce the plastic flow of $ACDE$, we use the constancy of $(s/2 - \theta)$ along a first slip line. From $\left(\frac{s}{2} - \theta\right)_{\text{left}} = \left(\frac{s}{2} - \theta\right)_{\text{right}}$ and $\theta_{\text{left}} = -\theta_{\text{right}}$ we find

$$\theta_{\text{right}} = \theta = \beta_0 - \frac{\pi}{4}$$

and

$$p_0 = 2K\left(1 + 2\beta_0 - \frac{\pi}{2}\right). \tag{3.14}$$

This pattern applies only if $\beta_0 > \pi/4$. If $\beta_0 = \pi/4$, the fan disappears, and for $\beta_0 < \pi/4$ we find the above described inconsistency. Prager showed, however, that in this case a solution with a discontinuity line can be found which satisfies all equilibrium and jump conditions. On account of the first jump condition (3.5′) the discontinuity line bisects the wedge angle; if the subscripts 1 and 2 refer to regions left and right of this line

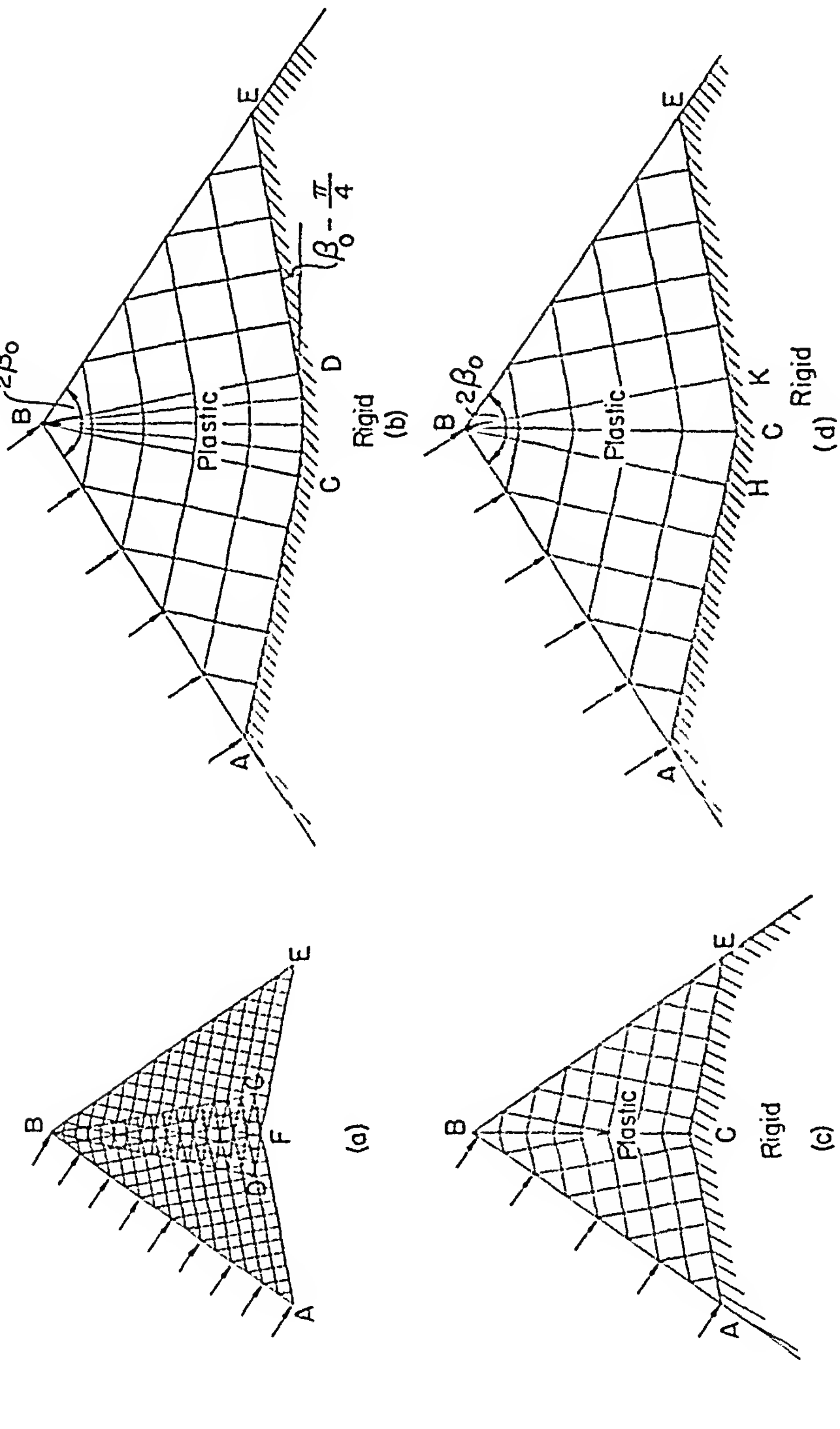

FIG. 19. Stress patterns for wedge with uniform pressure on one face.

we have

$$\theta_1 = -\beta_0 - \frac{\pi}{4}, \quad \frac{s_1}{2} = \frac{1}{2}\left(1 - \frac{p_0'}{k}\right), \tag{3.15}$$
$$\theta_2 = \beta_0 + \frac{\pi}{4}, \quad \frac{s_2}{2} = -\frac{1}{2},$$

(of course s_1 and s_2 are the same as before s_{left} and s_{right}) and from the jump conditions (3.6) we find the pressure necessary for plastic flow p_0':

$$p_0' = 2k(1 - \cos 2\beta_0). \tag{3.16}$$

For $\beta_0 = \pi/2$ both (3.14) and (3.16) reduce to $p_0 = p_0' = 2k$.

On the other hand, as far as stresses are concerned it is seen that a *discontinuous* stress solution of the same type as that which we just described exists also for $\frac{\pi}{4} < \beta_0 < \frac{\pi}{2}$ (see Fig. 19d) with p_0' given by (3.16). It is easily seen that for this range of wedge angle, the p_0' given by (3.16) is less than the p_0 given by (3.14). As far as stresses are considered, both Fig. 19(b) and (d) provide a solution. Hencky (4) and Prandtl (17c) have advanced the principle that in case of alternative solutions the correct one may be that requiring the minimum force. However this question must be decided on the basis of the *complete* solution; we shall see that a complete solution satisfying appropriate velocity conditions can be given on the basis of (b) only. In other words in this wedge problem with the obtuse angle stress *and* velocity boundary conditions must be considered in order to decide between the particular solutions represented by the stress fields (b) and (d).

4. Complete Solution

Following Lee we shall now determine the velocity solution corresponding to Fig. 19(c). Since stress and velocity characteristics coincide and the plastic rigid boundary is a (velocity) characteristic, the characteristics AC,EC form the plastic rigid boundary. Along this boundary the normal component of velocity is zero (for the rigid material at rest). Along the discontinuity line BC it follows from our previous results that $\dot{\epsilon}_y = 0$, $v_y =$ constant and since $v_y = 0$ at C, it follows that $v_y = 0$ along BC. Along AB we prescribe *one* component of velocity, e.g., the normal component. We shall see that these data are just sufficient for the determination of the velocity distribution. Thus along each of the lines BA, AC, CE, CB *one* velocity component is given. Although Lee's solution is clear, simple, and in every way satisfactory, we shall analyze the problem in a slightly more detailed way in order to point out some general features.

In the region ACD we have for two linear differential equations of first order a "mixed" boundary value problem of a type we denote by "3": One unknown is given on the characteristic AC, one on the non-characteristic AD. This determines both unknowns in ACD. (A few remarks on this type of problem will follow; see also p. 286.) In CDF we have again this "mixed" problem, since one variable is known on CF and one on CD (actually both are known on CD on account of the compatibility relation, but this counts for one datum since along a characteristic

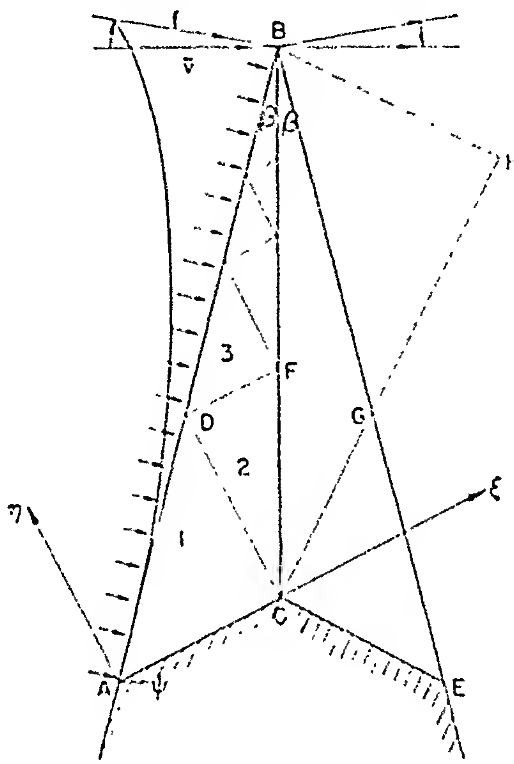

FIG. 20. Wedge under one-sided pressure.

the unknowns are always linked). In the next domain adjacent to DF we have again the same type of problem, one value on DF, one along a piece of DB, and so it goes on through smaller and smaller domains. Assume now for the moment that in this way, using an infinite series and necessary convergence considerations, the velocity at B is found. We still need the distribution to the right.

In our particular problem the distribution to the right can be derived from that to the left by means of symmetry considerations (they are not so obvious since the *data* of the problem are not symmetric). Let us assume, however, this were not so, and try to go on systematically: We know now along BC, which is not a characteristic, *both* unknowns, hence we have a Cauchy problem which gives both unknowns in BCG. Finally,

in GCE there is a characteristic problem since we know one value each on the characteristics CG and CE. (Remarks of Hodge (6a) concerning the velocity distribution to the right are erroneous.)

Now, before continuing, a word on the "mixed" problem. This "mixed" or "third" problem, used in building up our solution to the left, may be formulated as follows. Consider a piece B_1P of a characteristic C, and a piece of a noncharacteristic curve R, in the angular space between the two characteristics C and C_1. We consider two linear equations of first order and call the unknowns here for the moment u_1 and u_2. Then [see (15) and particularly (3)], the following data assure existence and uniqueness of the solution in P_1PP_2: (1) u_1 (or u_2) given on

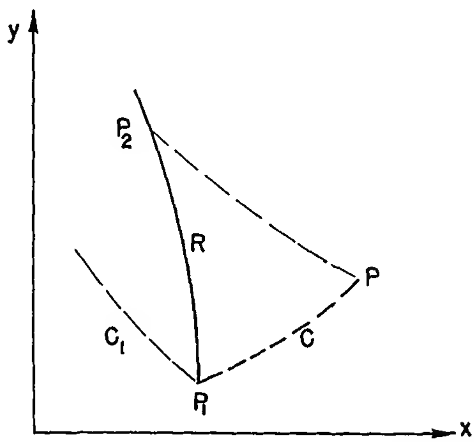

FIG. 21. "Third" or "mixed" initial value problem.

R; u_2 (or u_1) given on C; (2) u_1 and u_2 given on R and C, and u_2 or u_1 on one point of C. In a more general way, a combination $au_1 + bu_2$ may be given on R and another combination $u_1 + cu_2$ on C where $b - ac \neq 0$. Such are in fact the data that are given in our wedge problem in the domains where we solve a mixed problem.

Let us next show why the analogous way of building up a solution of the velocity problem does not work for the wedge with $\beta_0 \geqq \pi/4$. Assume the same data (Fig. 19) and the same procedure. In AHB we have the "third" problem, since the normal component is known on AB and on AH. In BHC the solution is determined by a "second" or characteristic problem, since we know one value on BH, one on HC; there is no way to take into account further data like $v_y = 0$ on BC. Hence, if the normal velocity is prescribed on AB, a solution with discontinuity line does not exist. On the other hand, if we begin with the domain BHC and use $v_n = 0$ on HC and $v_y = 0$ on BC the solution in BHC is determined; and then, in BAH, it is again determined by "problem two."

However, under the particular conditions of our problem this solution would obviously be zero everywhere in ABC, and in particular on AB; this does not represent a problem of plastic flow. Also, since on BC both components are zero, in CBK and finally in BKE the velocity would vanish.

5. Complete Solution: Continued

We call now the shear lines ξ-lines and η-lines; following Lee we use a coordinate system with A as origin (see Fig. 22), and denote by u and v

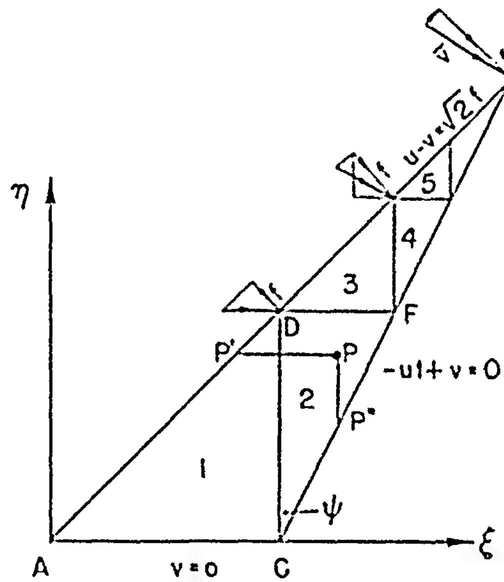

FIG. 22. Velocity solution for wedge (Fig. 20).

components of v in the ξ- and η-direction respectively. Then since the shear lines are straight, our basic Eqs. (2.74) reduce to

(3.17)
$$\frac{\partial u}{\partial \xi} = 0, \qquad \frac{\partial v}{\partial \eta} = 0;$$

hence

(3.18)
$$u = u(\eta), \quad v = v(\xi)$$

everywhere. Along AC the normal component $v = 0$, since below AC the material is rigid; since v does not change with η, its zero value holds all through ACD, and if we denote by v_1 the value in ACD,

(3.19)
$$v_1 = 0$$

follows. The line AB, inclined at 45° to the ξ-axis, has the equation $\xi = \eta$; and putting $\xi = \eta = \zeta$ we give v_n along AB as

(3.20)
$$v_n = f(\zeta) = \frac{1}{\sqrt{2}}[u(\zeta) - v(\zeta)].$$

Let ψ denote the angle between BC and CD; $\psi = \frac{\pi}{4} - \beta_0$, and CB has the equation

$$\eta = \cot \psi \cdot (\xi - 1); \tag{3.21}$$

and since the normal component v_n along BC is $v_n = u \sin \psi + v \cos \psi$, there is, with $t = \tan \psi$ along BC,

$$ut + v = 0. \tag{3.22}$$

Thus for ABC the boundary conditions are: $v = 0$ on AC, (3.20) on AB, and (3.22) on BC. Now the values of $u(\xi,\eta)$ and $v(\xi,\eta)$ at an arbitrary point P are found, on account of (3.18), by means of the projection of P to the left onto AB, which is P', and by means of the projection down onto CB, which is P''; then the u-value at P equals that at P', while the v-value at P equals the v-value at P''. This defines a recurrence procedure where P is first taken in the domain "2," then in the domain "3," and so on, the "initial values" of the recurrence being furnished by the known value $v_1 = 0$ in ACD. Thus considering the equations of AB and BC which are respectively $\xi = \eta$ and $\eta = \frac{\xi - 1}{t}$, our solution is given by the recurrence formulas valid for $n = 1,2, \cdots$

$$\begin{aligned} u_{2n-1} &= u_{2n}, \quad v_{2n-2} = v_{2n-1}, \qquad (n = 1,2, \cdots) \\ u_{2n-1}(\eta) &= \sqrt{2}\, f(\eta) + v_{2n-2}(\eta), \\ v_{2n}(\xi) &= -tu_{2n-1}(\xi), \end{aligned} \tag{3.23}$$

and by the initial condition, where we introduce a value $v_0 = 0$:

$$v_1 = v_0 = 0. \tag{3.23'}$$

Thus for example

$$u_1 = u_2 = \sqrt{2}\, f(\eta), \quad v_2 = v_3 = -tu_1\left(\frac{\xi - 1}{t}\right) = -t\sqrt{2}\, f\left(\frac{\xi - 1}{t}\right), \text{ etc.}$$

$$u_3 = u_4 = \sqrt{2}\, f(\eta) - t\sqrt{2}\, f\left(\frac{\eta - 1}{t}\right), \text{ etc.}$$

If we go on, the expressions for u and v have more and more terms and are of the form

(3.24)

$$u = \sqrt{2}\, f(\eta) - t\left[\sqrt{2}\, f\left(\frac{\eta - 1}{t}\right) - t\left\{\sqrt{2}\, f\left(\frac{\frac{\eta - 1}{t} - 1}{t}\right) \cdots\right\}\right]$$

$$v = -t\left[\sqrt{2}\, f\left(\frac{\xi - 1}{t}\right) - t\left\{\sqrt{2}\, f\left(\frac{\frac{\xi - 1}{t} - 1}{t}\right) \cdots\right\}\right].$$

the velocities in BCG are found. Finally, we know the values on the characteristics CE and GC. But in this domain we have, as in domain 1 of Fig. 21 to the left, $u' = \sqrt{2}\,f'$, $v' = 0$; hence the solution is again symmetric to that in domain 1 in the same way as just before.

Since $\dot{E} = \lambda \Sigma'$ and $\lambda \geqq 0$, it follows from $\tau_{\xi\eta} \geqq 0$ that everywhere $\dot{\gamma}_{\xi\eta} \geqq 0$; hence we should have

$$\frac{\partial u}{\partial \eta} + \frac{\partial v}{\partial \xi} \geqq 0. \tag{3.26}$$

Let us determine the restrictions which this imposes on the function $f(\zeta)$. The left side of (3.26) equals

$$\frac{1}{\sqrt{2}}\left(\frac{\partial u}{\partial \eta} + \frac{\partial v}{\partial \xi}\right) = \left[f'(\eta) - f'\left(\frac{\xi - 1}{t}\right)\right] - \left[f'\left(\frac{\eta - 1}{t}\right) - f'\left(\frac{\frac{\xi - 1}{t} - 1}{t}\right)\right] + \cdots. \tag{3.27}$$

If each term in brackets is positive, this is an alternating series with terms decreasing toward zero, hence converging and with positive sum. Since in ABC there is $\eta \geqq (\xi - 1)/t$, this will happen if f' is increasing with increasing argument or *if f'' is positive.*

Let us finish by mentioning a mathematical difficulty arising in problems of the type considered. Assume instead of the triangle ABC of our problem a quadrangle $AB'BC$ where AC and BB' are characteristic directions. We assume that one of the unknowns is given on AC, on AB, on CB. Then the values of both unknowns are determined in the quadrangle by means of a finite number of steps solving problem three in the domains 1,2,3,4, problem two in domain 5, and finally in 6 again problem three. If we now let B coincide with B', we have the same situation as in the wedge problem of this section, where one unknown was given on the boundary of a triangular region and *infinitely* many steps were needed to obtain the solution.

However, the boundary value problem with the triangular boundary can also be considered in another way. Besides the problems "one," "two," "three" (Cauchy problem, characteristic problem, mixed problem), there exists a problem "four" (see indications in (15) and (1a)), which we did not mention so far for lack of precise information. In this problem values of u_1 and u_2 (unknowns in a system of two linear partial differential equations of first order of the type considered p. 228) are given *on two arcs of curves which are both not characteristic;* first one has now to distinguish whether (a) these arcs are both in the same angle of characteristics or (b) each in one of two different angles. [Courant and Friedrichs (1a, p. 84) distinguish these cases by the terms "time like" and "space like."] It is easy to see that in the second case *two* data on one of the arcs and *one* on the other are not too much (knowing, for example, u_1 and u_2 on AB we have a Cauchy problem in BAD, then we solve problem three in BDC). Or in other words, if in the situation (b) one unknown only is given along each branch, there are still infinitely many solutions. In the other case (a), if *two* data are given, say, on AB and *one* on BC, this is too much since the

example of the wedge; again we consider conditions of plane strain. First it is clear, as we explained in this article and as we stressed repeatedly in previous publications, that a complete problem must consider all stress and velocity conditions, or, more precisely, a complete solution must satisfy: (1) the stress and velocity equations in the plastic region; (2) the stress and velocity boundary conditions. We have proved (Section II,2,i) that the plastic rigid boundary must be characteristic (this fact whose formal proof for plane strain is due to Lee was more or less known and used in many applications). In general the plastic rigid boundary is not known beforehand, but its determination forms part of the required solution. Since we know boundary conditions which are to be satisfied along this plastic rigid boundary, it plays the role of a free boundary. (Of course, sometimes the determination of this boundary curve is very simple, as in the wedge problem.) Velocity boundary conditions along it require that the velocities must be compatible with rigid body motion; this implies that if we assume the rigid body at rest, the normal velocity along the plastic rigid boundary must be zero while the tangential velocity may be discontinuous, hence different from zero. Thus in addition to (1) and (2) the complete solution calls for (3) determination of plastic rigid boundaries and consideration of velocity compatibility conditions along them.

There remain two points to which Lee and others have called attention in recent years, and which have not been sufficiently considered in previous work. First, we have mentioned *velocity* conditions along the plastic rigid boundaries; but the influence of the rigid regions must also be considered inasmuch as it must be possible to extend the plastic *stress* distributions into the rigid regions. Finally, it is obvious that the function λ in the basic relation $\dot{E} = \lambda \Sigma'$ must *not* be *negative;* this ought to be checked before accepting a solution. All this will become clearer if we consider examples. We add for the moment: (4) Satisfactory extension of the stress field into the rigid regions to insure that the maximum value of shear stress K is nowhere exceeded. (5) Check of the sign of λ.

Moreover we repeat: (a) In case of plane strain, where yield function and plastic potential equal each other and are equal to $(\sigma_1 - \sigma_2)^2 - 4K^2$, both stress equations and velocity equations are hyperbolic, with coinciding characteristics; but the first are *reducible,* the latter *linear* (after any particular solution of the stress equations has been introduced into the velocity equations). (b) If the stress boundary conditions alone do not determine a unique stress solution, then infinitely many stress fields (each a particular solution of the stress equations) satisfy the stress equations and the given stress boundary conditions; if we then select a stress field, it may not be the one for which the abundant other conditions can be

symmetry reasons, hence the shear lines should intersect it at 45°; this they do not do. In other words, it is impossible that planes, both subject to the maximum shear traction K as in Fig. 26 (top), do not meet at right angles. Thus this solution cannot be considered satisfactory. A satisfactory extension of the plastic field is only possible if the angle of the small wedge is 90°; then there is a uniform and continuous stress distribution in this wedge with maximum shear K throughout, extending the

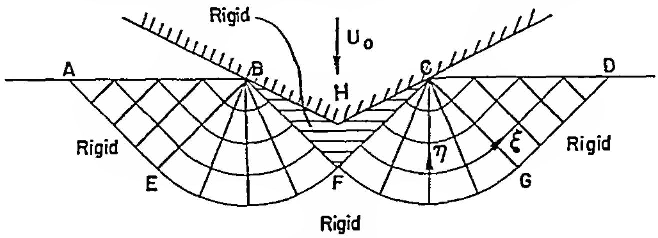

FIG. 27. Straight sided indenter.

plastic region in a satisfactory way below F. Difficulties arise likewise if the small wedge is obtuse angled.

Figure 27 shows an acceptable solution: a field with a rigid region $BHCF$, a "false nose," which performs the penetration; this rigid region extends between the surface of the indenter and the orthogonal slip lines BF and FC. In $BHCF$ the stress field is uniform with maximum shear throughout. The rigid region $BFCH$ transmits the vertical velocity U_0

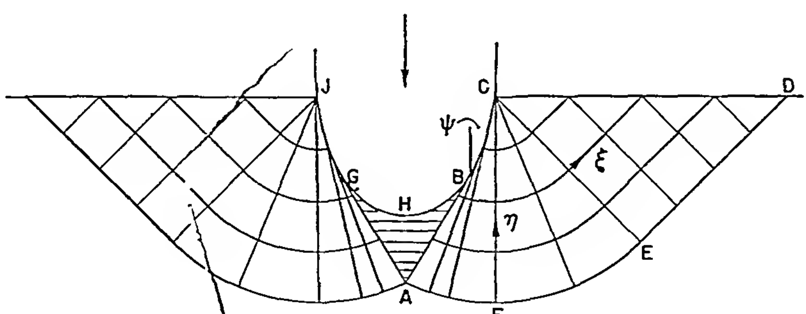

FIG. 28. Curved indenter.

of the indenter; in $FCGD$ we have $v = 0$ because of the rigid region below FGD and the rectilinear slip lines in the η-direction, while $u = U_0/\sqrt{2}$ (here, as before, u and v are velocity components in the ξ- and η-directions respectively).

As a *further example* which shows the necessity of *checking the sign of* λ we consider an example, similar to the preceding, namely the indentation of plastic material through cylindrical punch. The slip line field, given by Prandtl, shows again a "false nose." On the curved profile a point B is chosen so that the tangent to the curve cuts the

In this conception regions of *contained* plastic flow, where the stresses have reached the yield limit but the deformation is restrained by surrounding elastic material, are likewise considered as rigid since there the strains are of elastic order of magnitude. On the other hand, in problems where *only contained* plastic flow appears, it is possibly not adequate to neglect elastic strains; in this case an elastic plastic type of material is to be assumed. We may use in this case too in the plastic regions the Levy-Mises strain relations (exclusively used in this article); then, as a consequence of the boundary conditions the resulting velocities will be zero. One may however prefer to use the Prandtl-Reuss equations rather than the Levy-Mises equations in problems dealing with contained plastic and elastic strain. We mention in this connection the remarkable contributions of quite recent date by Prager and other authors on contained plastic flow and "limit analysis," which have already been incorporated in the new interesting book of Prager and Hodge (16g). We also refer once more to Hill's outstanding work (5a) and the wealth of original papers quoted there.

May we repeat that the choice of material in the present article is, naturally, very subjective. The article contains some material not included in other books on the subject; on the other hand the amount of material, modern and interesting, that is missing far exceeds the amount of material included.

References

1. (a) Courant, R., and Friedrichs, K., *Supersonic Flow and Shock Waves.* Interscience Publishers, New York, 1948.
   (b) Courant, R., and Hilbert, D., Methoden der Mathematischen Physik, Vol. II. S. Springer, Berlin, 1937.
   (c) Courant, R., and Lax, On nonlinear partial differential equations with two independent variables, *Commun. Pure Applied Math.*, **2**, 255–273 (1950).
2. (a) Geiringer, H. Pollaczek, Beitrag zum vollstaendigen ebenen Plastizitaetsproblem. *III Intern. Congr. Techn. Mech.*, **2**, Stockholm, 1930.
   (b) Geiringer, H., and Prager, W., Mechanik isotroper Koerper im plastischen Zustand, *Ergebn. exakt. Naturw.*, **13**, 310–363 (1934).
   (c) Geiringer, H., Fondéments mathématiques de la théorie des corps plastiques isotropes, *Mémor. Sci. Math.*, **86**, Gauthier Villars, Paris, 1937.
   (d) Geiringer, H., (i) Linear differential equations of the plane stress problem of a perfect plastic body, (ii) Simple wave solutions for the plane stress problem, etc., *Bull. Am. Math. Soc.*, **56**, 38–39 (1950).
   (e) Geiringer, H., Simple waves in the complete general problem of plasticity theory, *Proc. Natl. Acad. Sci. U.S.*, **37**, 214–220 (1951).
   (f) Geiringer, H., On the plane problem of a perfectly plastic body, *Quart. Applied Math.*, **9**, 295–308 (1951); (see also: Techn. Rept. 55, Providence, 1950).
   (g) Geiringer, H., On the general plane problem of a perfectly plastic body. *Proc. First Natl. Congr. Applied Mech.*, Chicago, July, 1951.

(c) Nadai, A., *Theory of Flow and Fracture of Solids*, Vol. I, McGraw-Hill, New York, 1950.
14. Neuber, H., Allgemeine Loesung des ebenen Plastizitaetsproblems fuer beliebiges isotropes und anisotropes Fliessgesetz, *Z. angew. Math. Mech.*, **28**, 253–257 (1948).
15. Picard, E., *Leçons sur quelques types simples d'équations aux dérivées partielles, etc.*, Gauthier Villars, Paris, 1927.
16. (a) Prager, W., Mécanique des solides isotropes au déla du domaine élastique, *Mémor. Sci. Math.*, **87**, Gauthier Villars, Paris, 1937.
(b) Prager, W., On Hencky-Prandtl lines, *Rev. faculté sci. univ. Istanbul*, **A4**, 22–24 (1938).
(c) Prager, W., Theory of Plasticity, mimeographed lecture notes, Brown University, Providence, 1942.
(d) Prager, W., Problem types in the theory of perfectly plastic material, *J. Aeronaut. Sci.*, **15**, 337–341 (1948).
(e) Prager, W., *Discontinuous Solutions in the Theory of Plasticity*, Courant Anniversary Volume, New York, 1948, pp. 289–299.
(f) Prager, W., On the boundary value problems of the mathematical theory of plasticity, *Proc. Intern. Congr. Math.*, Harvard, 1950.
(g) Prager, W., Hodge, G. P., Jr., *Theory of Perfectly Plastic Solids*, Wiley, New York, 1951.
17. (a) Prandtl, L., Ueber die Haerte plastischer Koerper, Goettinger Nachrichten, 74–84 (1920).
(b) Prandtl, L., Ueber die Eindringungsfestigkeit plastischer Baustoffe und die Festigkeit von Schneiden, *Z. angew. Math. Mech.*, **1**, 15–20 (1921).
(c) Prandtl, L., Anwendungsbeispiele zu einem Henckyschen Satz ueber das plastische Gleichgewicht, *Z. angew. Math. Mech.*, **3**, 401–406 (1923).
(d) Prandtl, L., Spannungsverteilung in plastischen Koerpern, *Proc. Intern. Congr. Applied Mech.*, Delft, 1925.
18. (a) de St. Venant, B., Mémoire sur l'établissement des équations différentielles des mouvements intérieurs opérés dans les corps solides ductiles au délà des limites où l'élasticité pourrait les rammener à leurs premiers états, *Compt. rend.*, **70**, 473–480 (1870).
(b) de St. Venant, B., Mémoire sur l'établissement des équations différentielles des mouvements intérieurs opérés dans les corps solides, etc., *J. math. math. pures appl.*, **II**, 16 (1871).
19. Sauer, R., Ueber die Gleitkurvennetze der ebenen plastischen Spannungsverteilung bei beliebigem Fliessgesetz. *Z. angew. Math. Mech.*, **29**, 274–279 (1949).
20. (a) Sokolovsky, V. V., Plastic plane stressed state according to Saint Venant, *Compt. rend. acad. Sci. U.R.R.S.*, **51**, 431–434 (1946).
(b) Sokolovsky, V. V., Plastic plane stressed state according to Mises, *Compt. rend. acad. sci. U.R.S.S.*, **51**, 175–178 (1946).
(c) Sokolovsky, V. V., Theory of Plasticity (Russian with English summaries), *Acad. Sci. U.S.S.R.*, Moscow, 1947.
21. Symonds, P. S., On the general equations of problems of axial symmetry in the theory of plasticity, *Quart. Applied Math.*, **6**, 448–452 (1949).
22. Torre, C., Ueber die physikalische Bedeutung der Mohrschen Huellkurve, *Z. angew. Math. Mech.*, **31**, 275–277 (1951).
23. Tresca, H., Mémoire sur l'écoulement des corps solides, *Mém. pres. par div. sav.*, **18**, 733–799 (1868); **20** (1872).

Non-Autonomous Systems

By ALBERT I. BELLIN

Harvard University[1]

Page

I. Introduction

In Volume I of this series, Minorsky (*15*) presented a review of methods for studying nonlinear equations of the second order. We shall consider the equation

$$\ddot{x} = F(x,\dot{x},t) \tag{1}$$

where the t dependence of F is explicit. We call this a non-autonomous equation in contrast to an autonomous equation $\ddot{x} = F(x,\dot{x})$. Discussions of (1), including the equations of Mathieu, Hill, van der Pol, and Duffing are found in (*1*), (*2*), (*9*), (*13*), (*14*), (*19*), and (*20*). Here we confine ourselves to a survey of more recent work. The coverage is not exhaustive; rather our purpose is to portray the present state of the field and to present several representative and significant contributions.

For the most part, the papers are concerned with the existence and stability of periodic solutions when $F(x,\dot{x},t)$ is nonlinear and is periodic in t. In cases of practical interest it is usually not possible to find exact solutions to (1). What is generally called a solution for a nonlinear system is only valid to a particular order of magnitude. Such quantitative results have been limited almost exclusively to slightly nonlinear systems. However, even for badly nonlinear systems it is possible to gain considerable insight into the solution by determining certain gross characteristics. The principal methods of analysis continue to be perturbation schemes or expansions in small parameters for slightly nonlinear systems and topological arguments for studying overall properties

[1] Now with Office of Naval Research.

of general systems. The topological results are particularly useful for engineering applications where a knowledge of such properties as the number and stability of periodic solutions for a system may reduce, or even preclude, a numerical analysis.

In 1943 Lefschetz (*10*) stated sufficiency conditions for the periodic solution of a class of forced, damped systems. More recently, John (*7,8*) has derived general properties for the periodic motion of forced, conservative systems. The work of Levinson (*12*) is of special interest since it is a unified treatment of a very general class of equations. The above four papers are among the few that are applicable to badly nonlinear systems. Bellman's report (*2*) is concerned with boundedness, stability, and asymptotic properties of equations that include (1) and contains an extensive bibliography, particularly for linear, non-autonomous systems. In a number of papers, Cartwright (*3,4*) with Littlewood (*6*) have investigated the equation

$$\ddot{x} - k(1 - x^2)\dot{x} + x = pk\lambda \cos (\lambda t + \alpha)$$

for k small and large. A review of the work of Cartwright and co-workers is contained in (*5*).

The papers of Reuter (*17*), Levenson (*11*), and Obi (*16*) apply to slightly nonlinear equations. The first investigates the subharmonic solutions for a system with an unsymmetrical restoring force, linear damping, and sinusoidal forcing. The second is a classification of solutions for the conservative Duffing equation. Obi's study of the subharmonics for the equation

$$\ddot{x} + a^2x = \epsilon\phi_1(t) + k\phi_2(t) + \epsilon\phi_3(x,\dot{x}) + k\phi_4(x,\dot{x}) + \phi_5(x,\dot{x},k,\epsilon,t)$$

is a rigorous extension of Cartwright's and Reuter's analyses. Schwesinger's paper (*18*) is a simplified, engineering approach to forced nonlinear systems. In presenting some of the above work in this brief compilation, it has been necessary to give certain results without including the complete proofs.

II. The Topological Transformation

We consider the non-autonomous equation (1) where $F(x,\dot{x},t)$ is analytic[2] in x, $\dot{x}$, and t and periodic in t with least period L. If $y = \dot{x}$ is introduced, (1) has a unique solution

$$x = x(x_0,y_0,t_0,t)$$

for the initial values $x(t_0) = x_0$ and $y(t_0) = y_0$. In discussing the behavior of this solution, it is convenient to introduce a three-dimensional phase

[2] For some of the results that follow, weaker conditions than analyticity may be assumed.

From the stated assumptions it follows (*12*) that T is a continuous, one-to-one, order preserving transformation. That is, points on a closed curve are mapped onto a closed curve so that the sense of direction of the points is maintained. Let $C(t_0)$ be a simple closed curve in the x,y plane with area $A(t_0) = \int_{C(t_0)} dx_0 dy_0$ at time t_0. As time progresses, points that were on $C(t_0)$ make up the curve $C(t)$ in accordance with $x(x_0,y_0,t_0,t)$, $y(x_0,y_0,t_0,t)$. The area within $C(t)$ is given by

$$A(t) = \int_{C(t_0)} J\left(\frac{x,y}{x_0,y_0}\right) dx_0 dy_0 \tag{7}$$

where the Jacobian J is a function of time. Differentiating J with respect to t, we get

$$\frac{d}{dt} J\left(\frac{x,y}{x_0,y_0}\right) = \frac{\partial F}{\partial y} J\left(\frac{x,y}{x_0,y_0}\right). \tag{8}$$

Since J is unity at $t = t_0$, we integrate (8) to obtain

$$J\left(\frac{x,y}{x_0,y_0}\right) = \exp \int_{t_0}^{t} \frac{\partial F}{\partial y}\, dt$$

We also see that $J > 0$. If $\exp \int_{t_0}^{t_0+nL} \frac{\partial F}{\partial y}\, dt < 1$ for all x and y, the area within $C(t_0 + rnL)$ goes to zero as $r \to \infty$ with integer values. In the limit, C becomes a point, a line, or perhaps several intersecting lines.

III. Stability of Periodic Solutions

Equation (7) gives some information concerning the stability of a periodic solution. Let a subharmonic of order n be represented by P^* at $t = t_0$. We call this solution stable if, given an arbitrarily small, simple closed curve K that encloses P^*, another simple closed curve $C(t_0)$ containing K can be found such that $C(t_0 + rnL)$ lies entirely within K as $r \to \infty$ with integer values. We define a solution to be unstable if, given an arbitrarily small, simple closed curve K that encloses P^*, it is impossible to find another simple closed curve $C(t_0)$ within K and enclosing P^* such that $C(t_0 + rnL)$ lies entirely within K as $r \to \infty$ with integer values. Let the coordinates of P^* be x^* and y^* at $t = t_0$. The coordinates of points P_0 in the neighborhood of P^* at $t = t_0$ are

$$x_0 = x^* + u_0, \quad y_0 = y^* + v_0,$$

while the coordinates of $T^n P_0$ are

$$x_n = x^* + u_n, \quad y_n = y^* + v_n.$$

If the P_0 are sufficiently close to P^*, u_n and v_n may be expanded in u_0 and v_0. Retaining only the first order terms

$$u_n = au_0 + bv_0, \quad v_n = cu_0 + dv_0, \tag{9}$$

the Jacobian becomes $J[(x,y)/(x_0,y_0)] = ad - bc$ where $ad - bc > 0$. However, if $J_{t_0+nL} > 1$ the area enclosed by $C(t_0 + nL)$ is greater than the area within $C(t_0)$, and the periodic solution is unstable.

More detailed criteria for the stability of a periodic solution are obtained by examining the linear transformation (9) directly. We first seek those u_0' and v_0' such that

$$\frac{u_n'}{u_0'} = \frac{v_n'}{v_0'} = \rho. \tag{10}$$

Combining Eqs. (9) and (10), we find that ρ must be a root of the equation

$$(a - \rho)(d - \rho) - bc = 0. \tag{11}$$

We then define A,B,C,D by the following:

$$\frac{C}{A} = \frac{\rho_1 - a}{b} = \frac{c}{\rho_1 - d}, \qquad \frac{D}{B} = \frac{\rho_2 - a}{b} = \frac{c}{\rho_2 - d}, \tag{12}$$
$$A^2 + C^2 = 1, \quad B^2 + D^2 = 1,$$

and introduce new coordinates by the relations

$$u = A\xi + B\eta, \quad v = C\xi + D\eta. \tag{13}$$

From Eqs. (9), (12), and (13) it follows that

$$\begin{aligned} u_0 &= A\xi_0 + B\eta_0, \quad v_0 = C\xi_0 + D\eta_0; \\ u_n &= \rho_1 A\xi_0 + \rho_2 B\eta_0, \quad v_n = \rho_1 C\xi_0 + \rho_2 D\eta_0. \end{aligned} \tag{14}$$

Also, the coordinates of the point T^{rn} are given by

$$u_{rn} = \rho_1^r A\xi_0 + \rho_2^r B\eta_0, \quad v_{rn} = \rho_1^r C\xi_0 + \rho_2^r D\eta_0. \tag{15}$$

If the roots of (11) are real, the above has a simple geometric interpretation. The line $v/u = C/A$ represents the ξ axis and $v/u = D/B$ gives the η axis. A,B,C,D are the appropriate direction cosines between u,v and ξ,η. We see from (14) and (15) that points originally on either the ξ or η axes are mapped onto the same axis upon repeated transformations T^n. If $\rho_1 > 1$ points on the ξ axis are mapped away from the fixed point (Fig. 1a). If $0 < \rho_1 < 1$, points on the ξ axis are mapped toward the fixed point as in Fig. 1b. For $\rho_1 < -1$ the situation is shown in Fig. 1c. Figure 1d is for $-1 < \rho_1 < 0$. Figures 1a and 1c represent unstable fixed points.

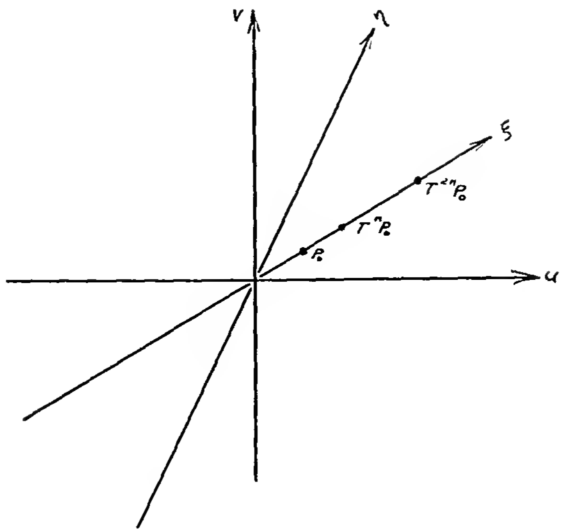

FIG. 1a

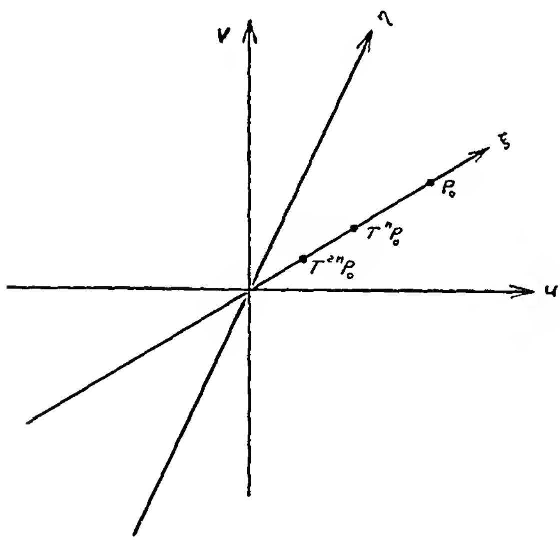

FIG. 1b

The distances from P_0 and $T^{rn}P_0$ to the fixed point are

$$u_0^2 + v_0^2 = (A^2 + C^2)\xi_0^2 + 2(AB + CD)\xi_0\eta_0 + (B^2 + D^2)\eta_0^2$$
$$u_{rn}^2 + v_{rn}^2 = \rho_1^{2r}(A^2 + C^2)\xi_0^2 + 2\rho_1^r\rho_2^r(AB + CD)\xi_0\eta_0 + \rho_2^{2r}(B^2 + D^2)\eta_0^2.$$

If the roots of (11) are complex, then ρ_2,B,D,η are complex conjugates of ρ_1,A,C,ξ respectively. In addition, if $|\rho_1| > 1$, then $u_{rn}^2 + v_{rn}^2 > u_0^2 + v_0^2$ for all P_0 when r is sufficiently great. This again represents an unstable

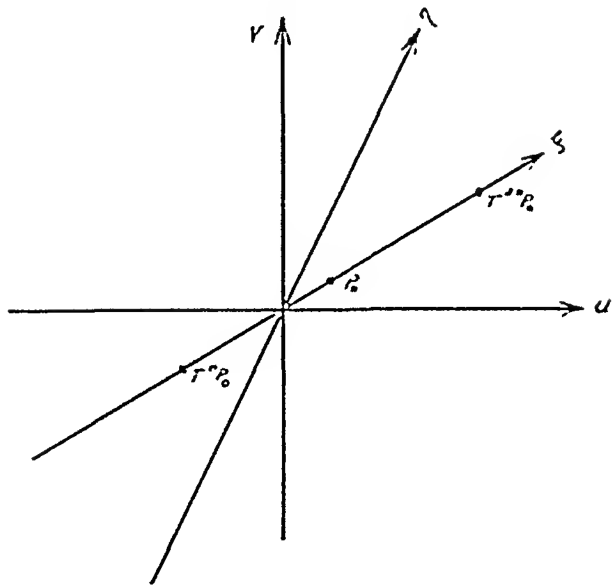

Fig. 1c

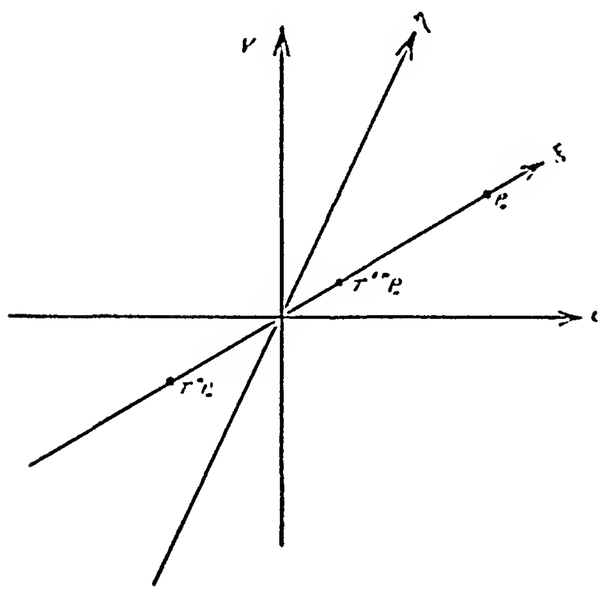

Fig. 1d

fixed point. However, the fixed point is stable if $|\rho_1| < 1$ since $u_{rn}^2 + v_{rn}^2 < u_0^2 + v_0^2$ for all P_0 when r is sufficiently great.

IV. Indices of Fixed Points

To define the index of a simple closed curve under the transformation T^n, we first generate a vector field by drawing an arrow from each point P_0 to the corresponding point T^nP_0. The index of the curve is equal to

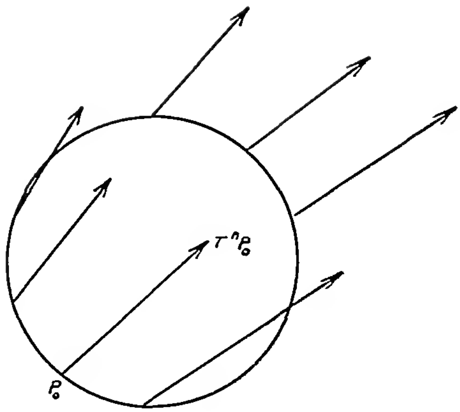

FIG. 2a

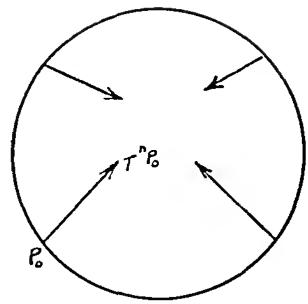

FIG. 2b

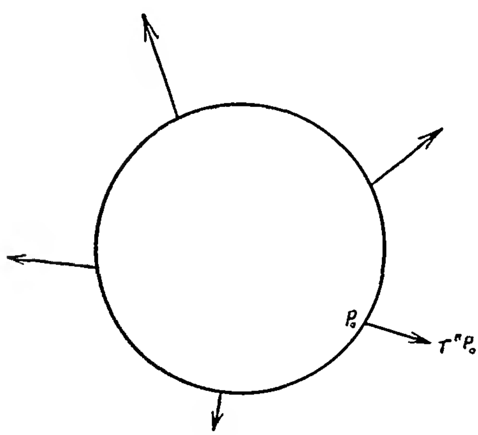

FIG. 2c

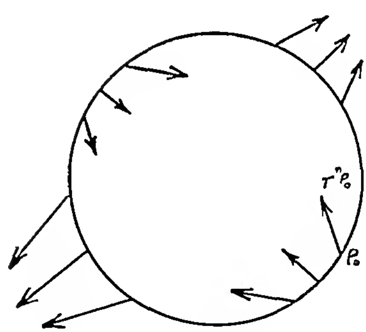

FIG. 2d

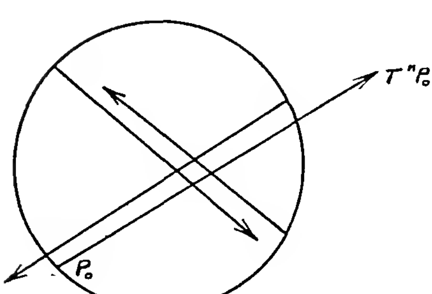

FIG. 2e

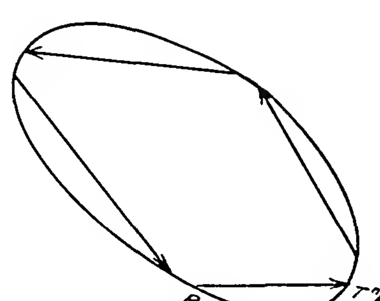

FIG. 2f

the number of counterclockwise revolutions made by the vector as one proceeds around the curve in a counterclockwise direction.

If the curve does not include a point fixed under T^n (Fig. 2a), the index is zero. If a stable point fixed under T^n is included by the curve (Fig. 2b), the index is $+1$. In Figs. 2c, 2d, and 2e the curves enclose unstable points fixed under T^n but of different types. The fixed points are called completely unstable, directly unstable or a direct col, and inversely unstable or an inverse col respectively. The respective indices are $+1$, -1, $+1$. The curve in Fig. 2f encloses a center or an undetermined point fixed under T^n, a point that is neither stable nor unstable and has an index $+1$. The indices of all simple closed curves that

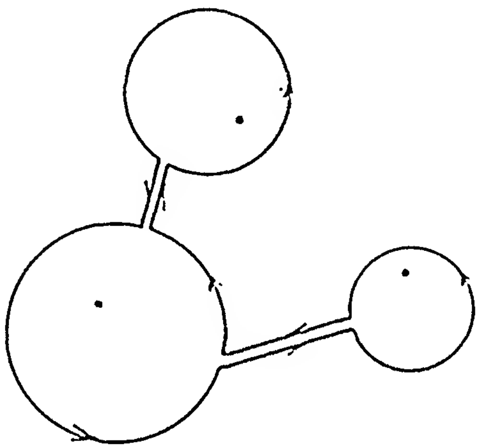

FIG. 3

enclose the same, single fixed point are identical; therefore, the index may be associated with the point. From Fig. 3 we see that the index of a curve that contains several points fixed under T^n is equal to the sum of the indices of the individual fixed points since the contributions along the double paths are cancelled. If $B(n)$ is the number of stable, completely unstable, inversely unstable, and undetermined points fixed under T^n and $D(n)$ is the number of directly, unstable points within K, then

$$B(n) - D(n) = i_K(n) \tag{16}$$

where $i_K(n)$ is the index of K for T^n.

To summarize, we relate the roots of (11) to the type of fixed point:

$$|\rho_1| < 1,\ |\rho_2| < 1 \rightarrow \text{stable, index } +1$$
$$|\rho_1| > 1,\ |\rho_2| > 1 \rightarrow \text{completely unstable, index } +1$$
$$\rho_1 > 1 > \rho_2 > 0 \rightarrow \text{directly unstable, index } -1$$
$$0 > \rho_1 > -1 > \rho_2 \rightarrow \text{inversely unstable, index } +1.$$

When $|\rho_1| = |\rho_2| = 1$, higher order effects may have to be investigated in order to determine the character of the fixed point.

V. Systems of Class D

As defined by Levinson (*12*), a system of class D has the property

$$\limsup_{t \to \infty} x^2(t) + y^2(t) < R^2.$$

Such systems are dissipative for large displacements and large velocities. For each system of class D:

(i) There exists a closed domain I such that the domain is mapped into itself by the transformation T. This does not imply that all points in I are fixed under T; it simply means that for every point P that is in I, both TP and $T^{-1}P$ are in I also.

(ii) For every point P that is outside of I, T^rP approaches I as $r \to \infty$ with integer values.

(iii) Also, every system has at least one point that is fixed under T. Thus, there is at least one harmonic solution.

The general proofs of (i), (ii), and (iii) make use of established topological theorems that are beyond our present scope. However, the statements should be "intuitively agreeable." For example, since a circle of large radius is mapped into a region within the circle by T, we might expect that upon repeated transformations the curve approaches the frontier of a region I. Also, if a region I is mapped into itself by a continuous one-to-one mapping, it "seems clear" that at least one point in I must remain fixed.

The behavior of the transformation at a great distance from the origin, is suggestive of a stable fixed point. Similar to a stable fixed point, the index of a curve that encloses all points fixed under T for a system that belongs to class D is $+1$. For these systems (16) becomes

$$B(n) = 1 + D(n) \tag{17}$$

where all points fixed under T^n are included in $B(n)$ or $D(n)$.

If P_0 represents a subharmonic solution of order n at $t = t_0$, then $P_0, TP_0, \cdots, T^{n-1}P_0$ are distinct fixed points of order n. Thus, there cannot be less than n subharmonics of order n and the number of subharmonics must be of the form Nn where N is an integer. Levinson shows that N must be an even integer and that $\frac{1}{2}Nn$ of the subharmonics are directly unstable. To prove this we let $C(n)$ represent the number of stable, completely unstable, indirectly unstable, and undetermined subharmonic solutions of order n and $E(n)$ the number of directly unstable subharmonics of order n. Corresponding to each of these solutions is a

fixed point of order n. However, for each subharmonic of order n_1, where n_1 is a factor of n, and for each harmonic solution there corresponds another point that is fixed under T^n. Factoring n into powers of distinct primes we get

$$n = p_1^{r_1} p_2^{r_2} \cdots p_m^{r_m}.$$

Equation (17) becomes

$$(18) \quad \sum_{j_1=0}^{r_1} \sum_{j_2=0}^{r_2} \cdots \sum_{j_m=0}^{r_m} [C(p_1^{j_1} \cdots p_m^{j_m}) - E(p_1^{j_1} \cdots p_m^{j_m})] = 1.$$

For points fixed under T^{n/p_1}, Eq. (17) is given by

$$(19) \quad \sum_{j_1=0}^{r_1-1} \sum_{j_2=0}^{r_2} \cdots \sum_{j_m=0}^{r_m} [C(p_1^{j_1} \cdots p_m^{j_m}) - E(p_1^{j_1} \cdots p_m^{j_m})] = 1.$$

Subtracting Eq. (19) from (18), we get

$$(20) \quad \sum_{j_2=0}^{r_2} \sum_{j_3=0}^{r_3} \cdots \sum_{j_m=0}^{r_m} [C(p_1^{r_1} p_2^{j_2} \cdots p_m^{j_m}) - E(p_1^{r_1} p_2^{j_2} \cdots p_m^{j_m})] = 0.$$

If we write Eq. (17) for points fixed under T^{n/p_2} and then for points fixed under T^{n/p_1p_2} and subtract the second from the first, we get

$$(21) \quad \sum_{j_2=0}^{r_2-1} \sum_{j_3=0}^{r_3} \cdots \sum_{j_m=0}^{r_m} [C(p_1^{r_1} p_2^{j_2} \cdots p_m^{j_m}) - E(p_1^{r_1} p_2^{j_2} \cdots p_m^{j_m})] = 0.$$

Subtracting (21) from (20) gives

$$\sum_{j_3=0}^{r_3} \cdots \sum_{j_m=0}^{r_m} [C(p_1^{r_1} p_2^{r_2} p_3^{j_3} \cdots p_m^{j_m}) - E(p_1^{r_1} p_2^{r_2} p_3^{j_3} \cdots p_m^{j_m})] = 0.$$

Continuing the procedure, we find

$$C(p_1^{r_1} \cdots p_m^{r_m}) - E(p_1^{r_1} \cdots p_m^{r_m}) = 0$$

or

$$(22) \qquad C(n) = E(n).$$

If P_0 is a fixed point of order n, then $TP_0, T^2P_0, \cdots T^{n-1}P_0$ are distinct fixed points of order n also. Call TP_0 the point P_0'. We now consider the following small, simple closed curves: $K, K', C(t_0), C(t_0 + L)$. The curve K' encloses P_0' and K encloses P where K is mapped into K' by T. $C(t_0)$ encloses K. Then $C(t_0 + L)$ encloses K' since the trans-

formation T is continuous and one-to-one. If P_0 is a stable fixed point of order $n, C(t_0 + rnL)$ lies entirely within K' and, therefore, $C(t_0 + rnL + L)$ lies entirely within K' as $r \to \infty$ with integer values of r. Thus TP_0 is also a stable fixed point, and similarly for $T^2P_0, T^3P_0, \cdots, T^{n-1}P_0$. Consequently, if there exists one stable fixed point of order n, there exist at least n and the total number is an integer multiple of n. In the same way, it can be shown that

$$E(n) = kn \tag{23}$$

where k is an integer. Since the total number $S(n)$ of subharmonics of order n is given by

$$S(n) = C(n) + E(n), \tag{24}$$

we complete the proof by combining Eqs. (22), (23), and (24) and getting

$$S(n) = 2kn.$$

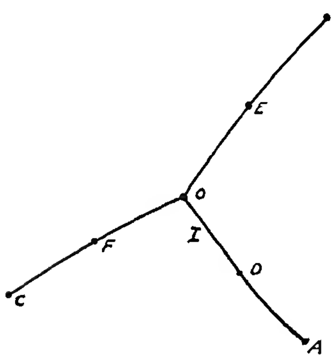

FIG. 4

As an example, for $n = 3$ there must be at least six subharmonics and, of these, at least three directly unstable ones. Also, there must be at least seven points fixed under T^3, i.e., the six subharmonics and at least one harmonic. In addition there will be a region I that is mapped into itself by T^3. Figure 4 shows the case for $n = 3$ where O is a stable harmonic; A,B,C are stable subharmonics; D,E,F are directly unstable subharmonics, and I has zero area. In this case,

$$TA = B, \quad TB = C, \quad TC = A$$
$$T^3D = T^2E = TF = D.$$

Before the results of Levinson may be applied to any particular equation, it must be shown that the equation belongs to class D. Following the proof of Lefschetz (*10*) we shall show that for the equation

$$\ddot{x} + g'(x)\dot{x} + f(x) = e(t) \tag{25}$$

$C(t_0 + L)$ is contained within $C(t_0)$ for $C(t_0)$ sufficiently large. The given conditions are:

(i) $e'(t), f'(x), g'(x)$ exist.

(ii) $e(t)$ has a period L although for the present proof, this condition is not used.

(iii) $f(x)/x \to +\infty$ when $|x| \to \infty$.

she shows that $|x| < B$, $|\dot{x}| < B(k+1)$ for $t > t_0(x_0,y_0)$ where B is a positive constant independent of x_0,y_0, and k. The conditions are that $h(x,k)$ and $p(t,k)$ be continuous functions of x and t respectively and that $f(x,k)$ satisfy a Lipschitz condition in x. Also

(i) $h(x,k) \geq b_1 > 0$ for $|x| \geq 1$; $h(x,k) \geq -b_2$ for all x.

(ii) $f(x,k)$ sign $x \geq b_3 > 0$ for $|x| \geq 1$; $|f(x,k)| \leq r(\xi)$ where r is independent of k for $|x| \leq \xi$.

(iii) $|p(t,k)| \leq B$; $\left|\int_0^t p(t,k)dt\right| < B$.

The b_i are positive constants independent of x_0,y_0,k,t. Cartwright's conditions include the van der Pol equation while those of Lefschetz do not.

VI. The Equation: $\ddot{x} + f(x) = Fg(\sin \omega t)$

The previous results are quite general in that the equation may be badly nonlinear. The analysis by John (7) of the equation

$$\ddot{x} + f(x) = Fg(\sin \omega t) \tag{29}$$

is another notable contribution that is not limited to small nonlinearities. The function $f(x)$ is analytic, monotonically increasing, $f(0) = 0$ and $\lim\limits_{|x|\to\infty} |f(x)| > F$. The forcing function $g(z)$ is an odd, analytic function for $|z| \leq 1$ where $g'(z) > 0$ and $g(1) = 1$. It follows that g is a maximum when $t = \pi/2\omega$. F and ω are positive constants. The existence and stability of solutions for (29) are studied simply on the basis of the above conditions. Since the development is too lengthy for our presentation, conclusions will be presented without proof. The results are a qualitative extension of those found for the slightly nonlinear Duffing equation

$$\ddot{x} + \alpha^2 x + \beta x^3 = F \sin \omega t. \tag{30}$$

The harmonic solution of (30) is usually presented as a plot of amplitude $|M|$ versus ω for various F.

In John's nomenclature, a "simple" solution comes to rest only twice during a period of $2\pi/\omega$. Solutions are of the first or second kind according to $x(-\pi/2\omega) >$ or $< x(\pi/2\omega)$ respectively. The term "in phase" is applied in a special sense to denote solutions with extreme values at $\pm\pi/2\omega$. The solutions for (30) are simple, in phase and of the first kind in I and of the second kind in II (see Figs. 5a and 5b).

Equation (29) has oscillatory solutions about $x = 0$ for all values of t. In the above nomenclature, for a given $M = x(-\pi/2\omega) > 0$, a unique harmonic solution of the first type exists and is in phase. That is, (29) may have several harmonic solutions for a given F and ω, but

Figures 5a and 5b represent cases of Eqs. (31) and (32) respectively. For symmetric systems of (29) that are soft, $\omega = \Omega(M)$ is a decreasing function for harmonic solutions of the first type; e.g., AB in Fig. 5b. Finally, a simple harmonic of the first type with amplitude M is unstable if $-d\Omega/dM > 0$. For example, points on CD in Fig. 5a represent unstable solutions. Thus, the general equation (29) displays many of the properties shown in Figs. 5a and 5b for a special case. The above has been extended somewhat by John in (*8*).

VII. The Equation: $\ddot{x} + a^2x = \phi(x,\dot{x},k,\epsilon,t)$

The existence of subharmonic solutions for the equation

$$\ddot{x} + k\dot{x} + (1 - \epsilon + \tfrac{4}{3}\epsilon x^2)x = \tfrac{1}{3}\epsilon a \cos 3t$$

has been discussed by Cartwright and Littlewood. Their results were generalized by Obi (*16*) in his analysis of the equation

$$\ddot{x} + a^2x = \phi(x,\dot{x},k,\epsilon,t). \tag{33}$$

Obi considers Eq. (33) where ϕ is analytic in all variables, is periodic in t with period L, and has the form

$$\phi = \epsilon\phi_1(t) + k\phi_2(t) + \epsilon\phi_3(x,\dot{x}) + k\phi_4(x,\dot{x}) + \phi_5(x,\dot{x},k,\epsilon,t).$$

ϕ_5 is at least of second order in the small quantities ϵ and k. The existence of subharmonics is determined as a function of ϵ and k, the allowable range of the parameter k being dependent upon ϵ. Following Obi, we seek only bounded periodic solutions of the first kind, i.e., subharmonics that exist for a range of small ϵ and for which $k = 0$ when $\epsilon \to 0$ and $0 < |\alpha| < \infty$ where

$$x = \alpha, \quad \dot{x} = 0 \tag{34}$$

at $t = \beta$. When $\epsilon = k = 0$, the solution of (33) is

$$x = \alpha \cos a(t - \beta). \tag{35}$$

In order that (35) be the limiting solution of a subharmonic of order n, it is necessary that

$$a = \frac{r}{n}\frac{2\pi}{L} \tag{36}$$

where r is an integer. Introducing the integers $m,p,$ and q, we rewrite (36) in the form $a = (p/q)(2\pi/L)$ in which $r = mp$, $n = mq$, and unity is the only common factor of p and q.

We may expand the solution $x(\alpha,\beta,k,\epsilon,t)$ in a double power series in the small parameters ϵ and k,

(37) $$x = \sum_{r=0}^{\infty} \sum_{s=0}^{\infty} \epsilon^r k^s x_{rs}(\alpha,\beta,t)$$

and substitute (37) into the differential equation. Equating each of the coefficients of $\epsilon^r k^s$ in (33) to zero yields a set of differential equation which determine the x_{rs}. From (34) and (37), the initial conditions are

$$x_{00}(\alpha,\beta,\beta) = \alpha$$

$\dot{x}_{00}(\alpha,\beta,\beta) = 0$, $x_{rs}(\alpha,\beta,\beta) = 0$ and $\dot{x}_{rs}(\alpha,\beta,\beta) = 0$ for all r and s not both equal to zero. Solving these equations, we find in particular, that $x_{01},x_{10},\dot{x}_{01}$ and $\dot{x}_{10}$ evaluated at $t = \beta + mqL$ are independent of β, proportional to m, and odd functions of α. In order that (37) represent a subharmonic of order n, it must satisfy

(38) $$x(\alpha,\beta,k,\epsilon,\beta + mqL) - \alpha = 0, \quad \dot{x}(\alpha,\beta,k,\epsilon,\beta + mqL) = 0.$$

Introducing

$$x_{01}(\alpha,\beta,\beta + mqL) = m\xi_{01}(\alpha), \quad x_{10}(\alpha,\beta,\beta + mqL) = m\xi_{10}(\alpha),$$
$$\dot{x}_{01}(\alpha,\beta,\beta + mqL) = m\eta_{01}(\alpha), \quad \dot{x}_{10}(\alpha,\beta,\beta + mqL) = m\eta_{10}(\alpha),$$

and substituting (37) into (38), we find

(39) $$\epsilon m\xi_{10}(\alpha) + km\xi_{01}(\alpha) + \sum_{r=0}^{\infty} \sum_{s=0}^{\infty} \epsilon^r k^s x_{rs}(\alpha,\beta,\beta + mqL) = 0,$$

(40) $$\epsilon m\eta_{10}(\alpha) + km\eta_{01}(\alpha) + \sum_{r=0}^{\infty} \sum_{s=0}^{\infty} \epsilon^r k^s \dot{x}_{rs}(\alpha,\beta,\beta + mqL) = 0$$

for $r + s > 1$.

For very small ϵ and k, it is necessary that

(41) $$\begin{vmatrix} \xi_{10}(\alpha) & \xi_{01}(\alpha) \\ \eta_{10}(\alpha) & \eta_{01}(\alpha) \end{vmatrix} = 0.$$

If a bounded periodic solution of the first kind exists, Eq. (41) must have at least one pair of non-zero real roots $\pm\alpha_0$. Consider the case where α_0 is a simple root and where $\xi_{01}(\alpha_0)$ and $\xi_{10}(\alpha_0)$ are not both zero. Then, from (39) or (40) we get

(42) $$k = \epsilon k_1(\alpha) + \sum_{r=2}^{\infty} \epsilon^r k_r(\alpha,\beta,m),$$

where $k_1 = -\xi_{10}/\xi_{01}$ if $\xi_{01} \neq 0$ or $k_1 = -\eta_{10}/\eta_{01}$ if $\eta_{01} \neq 0$. Eliminating k from (39) or (40) with Eq. (42), we find

(43) $$\epsilon m H_1(\alpha) + \sum_{r=2}^{\infty} \epsilon^r H_r(\alpha,\beta,m) = 0.$$

Solving (43) for α,

$$\alpha = \alpha_0 + \sum_{r=1}^{\infty} \epsilon^r \alpha_r(\beta, m), \tag{44}$$

and (42) becomes

$$k = \epsilon K_1(\alpha_0) + \sum_{r=2}^{\infty} \epsilon^r K_r(\beta, m). \tag{45}$$

It is clear that α_r and K_r are periodic with period L in β.

The values of α and k given by (44) and (45) guarantee a bounded periodic solution of the first kind for a given β and an integer value of m. Since α_0 is independent of m, a solution exists in the neighborhood of α_0 for any integer m. In particular, the solution that is determined by setting $m = 1$ is a subharmonic of order q. Of course, we may consider the period of this solution to be any integer multiple of qL, and it will still satisfy (38). Thus

$$\alpha_r(\beta, 1) = \alpha_r(\beta, m), \quad K_r(\beta, 1) = K_r(\beta, m),$$

and it is unnecessary for us to investigate cases where $m \neq 1$.

If the K_r are independent of β, then to each ϵ there corresponds one k. For this case, (33) will have a subharmonic solution, i.e., a bounded periodic solution of the first kind only for the special pairs of values ϵ and k given by (45) and for the combination of α and β determined by (44).

Let us consider the case where $K_\sigma(\beta)$ is the first term in (45) that is dependent upon β. Equation (45) becomes

$$k = \epsilon K_1(\alpha_0) + \sum_{r=2}^{\sigma-1} \epsilon^r K_r + M\epsilon^\sigma, \tag{46}$$

where

$$M = \sum_{r=\sigma}^{\infty} \epsilon^{r-\sigma} K_r(\beta).$$

Call a_i the stationary values of $K_\sigma(\beta)$ where $a_1 \leq a_2 \leq \cdots \leq a_u$. If values of k and ϵ are given and if

$$a_1 < \frac{1}{\epsilon^\sigma}\left[k - \epsilon K_1(\alpha_0) - \sum_{r=2}^{\sigma-1} \epsilon^r K^r\right] = \mu < a_u$$

then (46) defines β. For small ϵ the stationary values of M are essentially the a_1. We see that, if $a_s < \mu < a_{s+1}$, there are an even number, $2n_s$, of values of β in the interval 0 to L that permit a bounded periodic solution of the first kind.

Thus, Obi's analysis shows that bounded periodic solutions of the first kind exist for sufficiently small ϵ and for the corresponding α in the neighborhood of a simple real root α_0 of (41) if k is in the range where $a_1 < \mu < a_u$. For such a value of k there are $2n$, different β_i in the interval $0 < \beta < L$. Since each β_i gives rise to a subharmonic of order n, we find additional subharmonics of order n by taking solutions with the initial conditions

$$x(\beta) = x(\alpha,\beta_i,k,\epsilon,\beta_i + rL), \quad \dot{x}(\beta) = \dot{x}(\alpha,\beta_i,k,\epsilon,\beta_i + rL)$$

for $i = 1, 2, \cdots, 2n$, and $r = 1, 2, \cdots, n-1$. Therefore, if k is in an allowable range, there will be $2nn$, subharmonics of order n. This, of course, is in agreement with the results of Levinson.

In his paper, Obi applies the above method to several equations. Among them are the following.

$$(47) \qquad \ddot{x} + k\dot{x} + x(1 - \epsilon a + \epsilon x^2) = \epsilon b \cos \rho t + \epsilon k\psi(x,\dot{x},k,\epsilon,t). \qquad \text{I}$$

Necessary conditions for the existence of subharmonic solutions to Eq. (47) are

(a) $a > 0$
(b) If $\rho \neq 3$ and $\rho \neq 5$, then $k = O(\epsilon^4)$
(c) If $\rho = 5$, then $k = \mu\epsilon^2$ where $\mu^2 \leq \dfrac{7^2a^3b^2}{2^{12}3^2}$. For this case, the subharmonics are approximately given by

$$x = \sqrt{\tfrac{4}{3}a} \cos \left(t - \beta_r + \tfrac{2}{5}s\pi\right)$$

where $r = 1,2$; $s = 0,1,2,3,4$ and the β are roots of

$$\mu = [7(\tfrac{4}{3}a)^{3/2}b/8^2] \sin 5\beta$$

for $0 \leq \beta < \frac{2}{5}\pi$.
(d) If $\rho = 3$, then $k = \mu\epsilon^2$ where $|\mu| \leq 3ab/256$. The subharmonics are approximately

$$x = \sqrt{\tfrac{4}{3}a} \cos \left(t - \beta_r + \tfrac{2}{3}s\pi\right)$$

where $r = 1,2$; $s = 0,1,2$, and the β are roots of

$$|\mu| = (3\sqrt{\tfrac{4}{3}a}\, b/32) \sin 3\beta$$

for $0 \leq \beta \leq \frac{2}{3}\pi$.

$$(48) \qquad \ddot{x} + \epsilon(x^2 - 1)\dot{x} + x(1 + k) = \epsilon b \cos \rho t + \epsilon k\psi(x,\dot{x},k,\epsilon,t). \qquad \text{II}$$

Equation (48) has subharmonics if the following conditions are satisfied:
(a) If $\rho \neq 3$ and $\rho \neq 5$, then $k = \frac{1}{8}\epsilon^2 + O(\epsilon^4)$.

(b) If $\rho = 5$, then $k = \frac{1}{8}\epsilon^2 + \mu\epsilon^3$ where $|\mu| \leq |b|/384$ and the subharmonics are approximately

$$x = 2 \cos (t - \beta_r + \tfrac{2}{5}s\pi)$$

for $r = 1,2$; $s = 0,1,2,3,4$ and the β are roots of

$$\mu = -(b/384) \cos 5\beta$$

and $0 \leq \beta < \frac{2}{5}\pi$.

(c) If $\rho = 3$, then $k = \mu\epsilon^2$ where $|16\mu - 2| \leq |b|$. The subharmonics are approximately

$$x = 2 \cos (t - \beta_r + \tfrac{2}{3}s\pi)$$

for $r = 1,2$; $s = 0,1,2$ and the β roots of

$$16\mu = 2 - b \sin 3\beta$$

with $0 \leq \beta < \frac{2}{3}\pi$.

VIII. The Equation: $\ddot{x} + k\dot{x} + \omega^2 x(1 + \alpha x) = 3v \cos 2t$

Prior to Obi's work, Reuter (*17*) applied Poincaré's method to study the existence and stability of subharmonics for a special case of (1). He considers the equation

$$\ddot{x} + \lambda\epsilon^2\dot{x} + (1 + \epsilon x)(1 + \mu\epsilon^2)x = 3\epsilon v \cos 2t \tag{49}$$

where $\lambda > 0$, $v > 0$ and μ are of order unity and $|\epsilon| \ll |$. Following Reuter, we expand the solution of (49) in a power series in ϵ

$$x(t) = x_0(t) + \epsilon x_1(t) + \epsilon^2 x_2(t) + \cdots . \tag{50}$$

Substituting (50) into the differential equation and equating coefficients of ϵ^r to zero, we solve for the $x_r(t)$. Taking

$$x(0) = a, \quad \dot{x}(0) = b \tag{51}$$

as initial conditions, we seek $a(\epsilon)$ and $b(\epsilon)$ such that the solutions are subharmonics of order 2 and reduce to the form $x = a \cos t + b \sin t$ as $\epsilon \to 0$, where a and b are not both equal to zero. It follows from (51) that $x_0(0) = a$, $\dot{x}_0(0) = b$, $x_r(0) = 0$ and $\dot{x}_r(0) = 0$ for $r > 0$. We find

$$\begin{aligned} x_0(2\pi) &= a, \quad \dot{x}_0(2\pi) = b; \qquad x_1(2\pi) = 0, \quad \dot{x}_1(2\pi) = 0; \\ x_2(2\pi) &= \pi[-\lambda a + (\mu + v)b - \tfrac{5}{6}b(a^2 + b^2)] \\ \dot{x}_2(2\pi) &= \pi[-\lambda b - (\mu - v)a + \tfrac{5}{6}a(a^2 + b^2)]. \end{aligned}$$

Introducing

$$x_r(2\pi) = P_r(a,b), \quad \dot{x}_r(2\pi) = Q_r(a,b)$$

into the necessary conditions

$$x(2\pi) - x(0) = 0, \quad \dot{x}(2\pi) - \dot{x}(0) = 0 \tag{52}$$

Eqs. (52) become

$$\epsilon^2[P_2(a,b) + \epsilon P_3(a,b) + \cdots] = 0 \qquad \epsilon^2[Q_2(a,b) + \epsilon Q_3(a,b) + \cdots] = 0. \tag{53}$$

We define a_0 and b_0 by the relations $P_2(a_0,b_0) = 0$, $Q_2(a_0,b_0) = 0$, and find

$$\frac{a_0}{b_0} = \frac{1}{\lambda}(\nu \pm \sqrt{\nu^2 - \lambda^2}), \quad a_0^2 + b_0^2 = \tfrac{6}{5}(\mu \mp \sqrt{\nu^2 - \lambda^2}). \tag{54}$$

To determine a and b, we introduce the small quantities ξ and η, where $a = a_0 + \xi$, $b = b_0 + \eta$ and bring (53) into the form

$$\begin{aligned} \pi\epsilon^2[A(\epsilon) + \xi C(\epsilon) + \eta E(\epsilon) + \cdots] &= 0, \\ \pi\epsilon^2[B(\epsilon) + \xi D(\epsilon) + \eta F(\epsilon) + \cdots] &= 0, \end{aligned} \tag{55}$$

where $A(0) = 0$, $B(0) = 0$, $C(0) = -\lambda - \tfrac{5}{3}a_0b_0$

$$\begin{aligned} D(0) &= -\mu + \nu + \tfrac{5}{2}a_0^2 + \tfrac{5}{6}b_0^2, \\ E(0) &= \mu + \nu - \tfrac{5}{6}a_0^2 - \tfrac{5}{2}b_0^2, \\ F(0) &= -\lambda + \tfrac{5}{3}a_0b_0. \end{aligned} \tag{56}$$

For sufficiently small ξ and η, i.e., for sufficiently small ϵ, Eqs. (55) have a solution if the determinant of the linear terms if unequal to zero. In the limit, therefore, it is necessary that

$$\Delta = \begin{vmatrix} C(0) & E(0) \\ D(0) & F(0) \end{vmatrix} = 4\sqrt{\nu^2 - \lambda^2}\,(\sqrt{\nu^2 - \lambda^2} \mp \mu) \neq 0 \tag{57}$$

Equation (57) imposes the restriction $\nu \neq \lambda$ while Eqs. (54) require

$$\nu > \lambda \tag{58}$$

and

$$\mu > -\sqrt{\nu^2 - \lambda^2}. \tag{59}$$

If, in addition to (58) and (59) $\mu \leq \sqrt{\nu^2 - \lambda^2}$, there are two solutions a_0,b_0 and $-a_0,-b_0$, that correspond to the lower signs. However, if in addition to (58) $\mu > \sqrt{\nu^2 - \lambda^2}$ there are four solutions of (54), two for each pair of signs.

Consider the motion for perturbed initial conditions

$$x(0) = a + \phi, \quad \dot{x}(0) = b + \psi$$

and write

$$x(2\pi) = a + \phi', \quad \dot{x}(2\pi) = b + \psi',$$

where a and b are appropriate for a subharmonic and ϕ,ϕ',ψ,ψ' are small. In place of (55) we have

$$\begin{aligned}\phi' - \phi &= \pi\epsilon^2[A(\epsilon) + (\xi + \phi)C(\epsilon) + (\eta + \psi)E(\epsilon) + \cdots],\\ \psi' - \psi &= \pi\epsilon^2[B(\epsilon) + (\xi + \phi)D(\epsilon) + (\eta + \psi)F(\epsilon) + \cdots].\end{aligned}$$

For small ϵ, the stability depends upon the roots of the equation

$$\begin{vmatrix} 1 + \pi\epsilon^2 C(0) - \rho & \pi\epsilon^2 E(0) \\ \pi\epsilon^2 D(0) & 1 + \pi\epsilon^2 F(0) - \rho \end{vmatrix} = 0.$$

Making use of (56) we find

$$\rho_{1,2} = 1 + \pi\epsilon^2(-\lambda \pm \sqrt{\lambda^2 - \Delta}). \tag{60}$$

When only two subharmonics exist, $|\mu| < \sqrt{v^2 - \lambda^2}$. Then $\Delta > 0$, $|\rho_{1,2}| < 1$ and the solutions are stable. In the case of four subharmonics, $\mu > \sqrt{v^2 - \lambda^2}$ and we find one pair of stable solutions and one pair of unstable solutions corresponding to the lower and upper signs in Δ respectively. The stable subharmonics are of the node or focus type depending on $\lambda^2 >$ or $< \Delta$, where we take the lower sign in Δ.

In order that a harmonic solution of (49) exist, it is necessary that $a_0 = b_0 = 0$. The leading $\phi_i(t)$ with a harmonic term is

$$\phi_1(t) = -v \cos 2t$$

also, $\phi_2(t) = 0$. Since the harmonic is included in the solutions of period 2π, the conditions for its existence and stability are contained in the above analysis. However, equations (54) are no longer applicable and Δ is now $\lambda^2 + \mu^2 - v^2$; $\rho_{1,2}$ is still given by (60). A stable harmonic exists if $\Delta > 0$, i.e., if $\lambda > v$ or if $\lambda < v$ and $|\mu| > \sqrt{v^2 - \lambda^2}$. If $\Delta < 0$, then $\lambda < v$ and $|\mu| < \sqrt{v^2 - \lambda^2}$ and the harmonic is directly unstable. Here again the stable solution is a node or focus depending on $\lambda^2 >$ or $< \Delta$.

We transform (49) into

$$\ddot{z} + k\dot{z} + \omega^2 z(1 + \alpha z) = 3v \cos 2t$$

by introducing $z = x/\epsilon$, $k = \lambda\epsilon^2 > 0$, $\omega^2 = 1 + \mu\epsilon^2$, $\alpha = \epsilon^2$, $v > 0$. With these symbols, the results of Reuter's analysis are listed in the accompanying table.

Conditions	Type of Solution	Form of Solution
$k < \nu\alpha$	1 directly unstable harmonic	(a)
$\lvert\omega^2 - 1\rvert < \sqrt{\nu^2\alpha^2 - k^2}$	2 stable subharmonics $\begin{cases}\text{node if } k^2 > u\\ \text{focus if } k^2 < u\end{cases}$	(b), (c)
$k < \nu\alpha$ $\lvert\omega^2 - 1\rvert > \sqrt{\nu^2\alpha^2 - k^2}$	1 stable harmonic $\begin{cases}\text{node if } k^2 > r\\ \text{focus if } k^2 < r\end{cases}$	(a)
$k < \nu\alpha$	2 stable subharmonics $\begin{cases}\text{node if } k^2 > u\\ \text{focus if } k^2 < u\end{cases}$	(b), (c)
$\omega^2 - 1 > \sqrt{\nu^2\alpha^2 - k^2}$	2 unstable subharmonics	(b), (d)
$k \geq \nu\alpha$	1 stable harmonic $\begin{cases}\text{node if } k^2 > r\\ \text{focus if } k^2 < r\end{cases}$	(a)

(a) $z = -\nu \cos 2t + O(\alpha)$

(b) $z_{1,2} = p \cos (t - \theta) + A \cos t + B \sin t - \frac{1}{4}\alpha p^2 - \nu \cos 2t - \frac{1}{4}\alpha p^2 \cos (2t + 2\theta) + O(\sqrt{\alpha})$

(c) $p^2 = \frac{4}{3}\alpha^{-2}(\omega^2 - 1 + \sqrt{\nu^2\alpha^2 - k^2});\ \tan \theta_{1,2} = \frac{1}{k}(\nu\alpha + \sqrt{\nu^2\alpha^2 - k^2})$

(d) $p^2 = \frac{4}{3}\alpha^{-2}(\omega^2 - 1 - \sqrt{\nu^2\alpha^2 - k^2}),\ \tan \theta_{1,2} = \frac{1}{k}(\nu\alpha - \sqrt{\nu^2\alpha^2 - k^2})$

$u = 4\sqrt{\nu^2\alpha^2 - k^2}(\sqrt{\nu^2\alpha^2 - k^2} + \omega^2 - 1);\ r = (\omega^2 - 1)^2 + (k^2 - \nu^2\alpha^2)$

Figures 6a, 6b, 6c, and 6d show the approximate dependence of the amplitudes upon the parameters of the system. It is seen that the stable solutions are discontinuous with respect to certain parameters. For example, when $\omega > 1$ and only ν is varied, the amplitude changes abruptly and the solution changes from a harmonic to a subharmonic as ν increases across the value k/α.

The transformation T^2 for Eq. (49) is defined by

$$A - a = \epsilon^2[P_2(a,b) + \epsilon P_3(a,b) + \cdots] \tag{61}$$
$$B - b = E^2[Q_2(a,b) + \epsilon Q_3(a,b) + \cdots]$$

where a,b and A,B are the coordinates of the original and transformed points respectively. Here a and b represent an arbitrary point and not necessarily a fixed point. For sufficiently small ϵ, we may study the behavior of T^2 by considering the equation

$$\frac{db}{da} = \frac{Q_2(a,b)}{P_2(a,b)}. \tag{62}$$

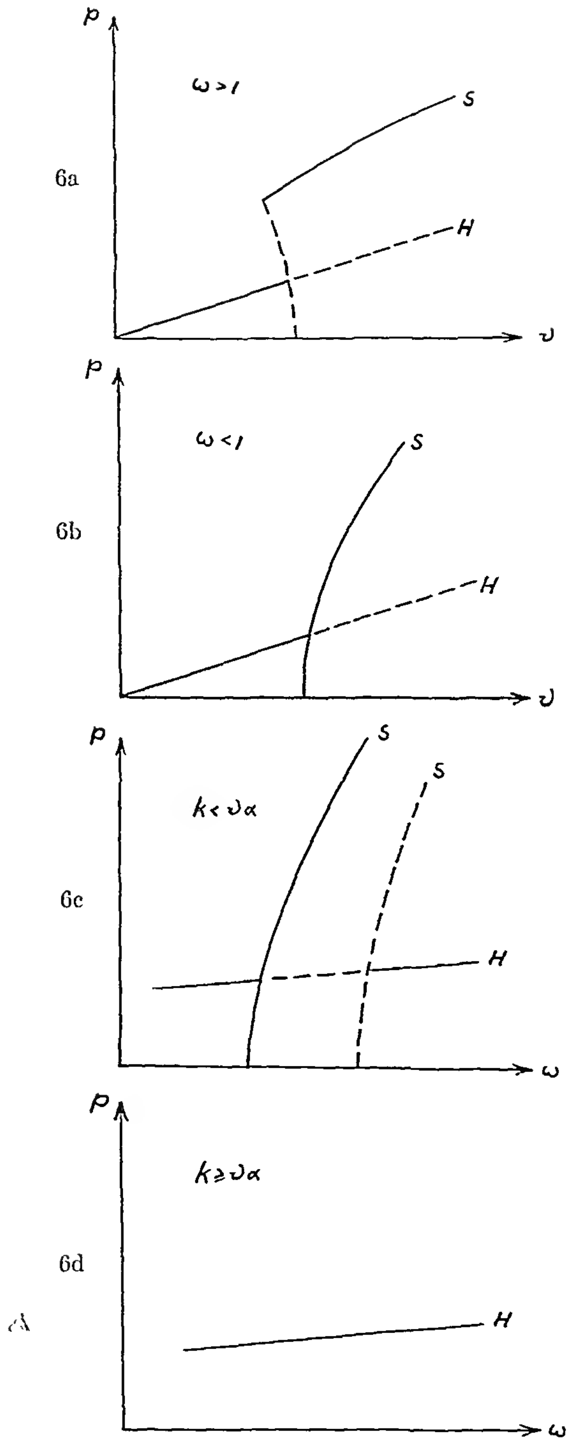

FIG. 6

H Harmonic ------ Unstable

S Subharmonic ———— Stable

In Fig. 7 are plots of $P_2 = 0$ and $Q_2 = 0$. The dotted curves represent solutions of (62). The parameters for the solution in Fig. 7 are such that there exists one stable focus harmonic, two stable focus subharmonics, and two directly unstable subharmonics. It should be kept in mind that

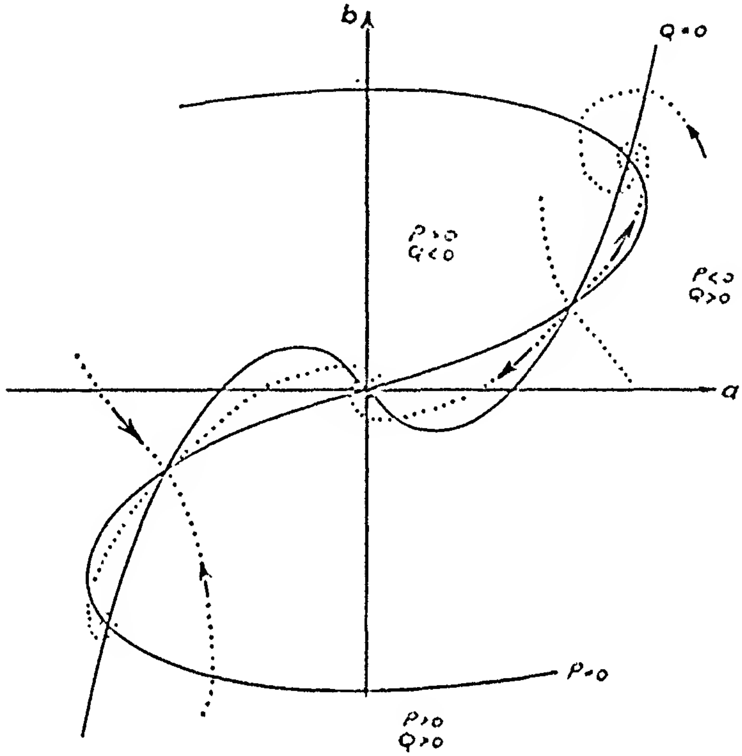

FIG. 7

the representative point for (49) does not move continuously along a curve in the a,b plane under repeated applications of T^2, but moves in increments as given by (61).

References

1. ANDRONOW, A. A., and CHAIKIN, C. E., Theory of Oscillations, translation by S. Lefschetz, Princeton University Press, Princeton, 1949.
2. BELLMAN, R., A Survey of the Theory of the Boundedness, Stability, and Asymptotic Behavior of Solutions of Linear and Nonlinear Differential and Difference Equations, Office of Naval Research Report NAVEXOS P-596, 1949.
3. CARTWRIGHT, M. L., Forced Oscillations in Nearly Sinusoidal Systems, *J. Inst. Elec. Engrs.*, **95**, 88–96 (1948).
4. ——— On Nonlinear Differential Equations of the Second Order: III, *Proc. Cambridge Phil. Soc.*, **45**, 495–501 (1949).
5. ——— Forced Oscillations in Nonlinear Systems, *Annals of Math. Studies*, No. 20, pp. 149–241, Princeton University Press, Princeton, 1950.
6. ——— and LITTLEWOOD, J. E., Nonlinear Differential Equations of the Second Order, *J. London Math. Soc.*, **20**, 180–89 (1945).

7. JOHN, F., On Simple Harmonic Vibrations of a System with Nonlinear Characteristics, Studies in Nonlinear Vibration Theory, pp. 104–92, New York University, N. Y., 1946.
8. ——— On Harmonic Vibrations Out of Phase with the Exciting Force, *Comm. Applied Math.*, **1**, 341–59 (1948).
9. KRYLOFF, N., and BOGOLIUBOFF, N., Introduction to Nonlinear Mechanics, translation by S. Lefschetz, *Annals of Math. Studies*, No. 11, Princeton University Press, Princeton, 1947.
10. LEFSCHETZ, S., Existence of Periodic Solutions for Certain Differential Equations, *Proc. Natl. Acad. Sci.* U.S., **29**, 29–32 (1943).
11. LEVENSON, M. E., Harmonic and Subharmonic Response for the Duffing Equation, *J. Applied Phys.*, **21**, 283–43 (1950).
12. LEVINSON, N., Transformation Theory of Nonlinear Differential Equations of the Second Order, *Annals of Math.*, **45**, 723–37 (1944).
13. MCLACHLAN, N. W., Ordinary Nonlinear Differential Equations, Oxford University Press, London, 1950.
14. MINORSKY, N., Introduction to Nonlinear Mechanics, J. W. Edwards, Ann Arbor, 1947.
15. ——— Modern Trends in Nonlinear Mechanics, *Advances in Applied Mechanics*, **1**, 41–103 (1948).
16. OBI, C., Subharmonic Solutions of Nonlinear Differential Equations of the Second Order, *J. London Math. Soc.*, **25**, 217–26 (1950).
17. REUTER, G. E. H., Subharmonics in a Nonlinear System with Unsymmetrical Restoring Force, *Quart. J. Mech. Applied Math.*, **2**, 198–207 (1949).
18. SCHWESINGER, G., On One-Term Approximation of Forced Non-Harmonic Vibrations, *J. Applied Mech.*, **17**, 202–8 (1950).
19. STOKER, J. J., Nonlinear Vibrations, Interscience, New York, 1950.
20. TIMOSHENKO, S., Vibration Problems in Engineering, D. Van Nostrand, New York, 1937.